Cleared May 22nd, 1978
Clearing Authority: Air Force Avionics Laboratory

DESIGN, FABRICATION, AND GROUND TESTING OF THE F-4 BERYLLIUM RUDDER

J.M. Finn, L.C. Koch, and D.E. Muehlberger

MCDONNELL COMPANY

This document is subject to special export controls and each transmittal to foreign governments or foreign nationals may be made only with prior approval of the Structures Division (FDTS), Flight Dynamics Laboratory, Wright-Patterson Air Force Base, Ohio 45433.

Air Force Flight Dynamics Laboratory
Research and Technology Division
Air Force Systems Command
Wright-Patterson Air Force Base, Ohio

*** Export controls have been removed ***

Approved for Public Release

FOREWORD

This report, prepared by the McDonnell Company, St. Louis, Missouri, covers the work performed under Air Force Contract AF33(615)-2974, Task No. 136806, Project No. 1368, "Structural Design Concepts." The program was administered under the direction of the Air Force Flight Dynamics Laboratory, Research and Technology Division, by Mr. F. E. Barnett (FDTS), Project Engineer.

This study, which began in June 1965 and was concluded in January 1967, represents the efforts of McDonnell Company personnel of the Strength, Weights, Structural Dynamics, Guidance and Control Dynamics, Materials and Processes, Producibility, Advanced Material Fabrication, and Structural Test Departments. The study was conducted by the McDonnell Structural Research Group which was responsible for all structural design and analysis performed under this contract, and for coordination of the activities of all other participating departments. This final report concludes the work on Contract AF33(615)-2974.

The manuscript was released by the authors in March 1967 for publication as a technical report.

This technical report has been reviewed and is approved.

Keith I. Collier
Chief, Applied Mechanics Branch
Structures Division

ABSTRACT

The program described in this report was performed for the advancement of structural beryllium technology through the design, fabrication, test and evaluation of a load-carrying aircraft component to demonstrate a potential for increased capability and efficiency through use of beryllium. The component selected for the performance of this program was the rudder of the McDonnell F-4 aircraft. The beryllium rudder was designed, analyzed, fabricated, and successfully ground tested to the same loading conditions and criteria that apply to the production aluminum rudder. An extensive element test program was conducted to obtain material properties and design data not previously available, and formulate design criteria for beryllium structures. The beryllium rudder weighs 37.59 lbs. (17.05 kg) as compared to 63.03 lbs. (28.59 kg) for the production aluminum rudder and is completely interchangeable with it.

Upon completion of fabrication, the beryllium rudder was installed on an F-4 vertical fin and aft fuselage assembly and subjected to one fatigue test and three static tests. Prior to conducting the static tests, the beryllium rudder upper balance weight support structure was successfully fatigue tested for 50,000 cycles under a fully reversed loading corresponding to 40 g's on the balance weight. The static tests were:

(1) 150% of design limit load on the rudder, for the condition which produces the maximum rudder load and torque that can be sustained without overpowering the actuator.

(2) 150% of design limit load on the rudder and fin, for the rolling pull-out flight condition which produces maximum vertical tail bending.

(3) 250% of design limit load on the rudder for condition (1) above. In a corresponding test during the F-4 development program, the production rudder sustained 225% of the same limit load without failure. In test (3) a failure of the lower closure rib occurred at 205% of design limit load but the rudder was still capable of carrying 250% of design limit load with no further damage. The successful completion of this program demonstrated that complex beryllium structural assemblies can be fabricated within the current state-of-the-art to a predictable strength, and qualified the beryllium rudder for flight testing on the F-4 aircraft.

(Distribution of this abstract is unlimited.)

TABLE OF CONTENTS

SECTION PAGE

I INTRODUCTION. 1

II MATERIAL PROPERTIES, DESIGN DATA AND CORROSION PROTECTION PROCESS 6

1. Introduction. 6
2. Beryllium Material Properties 7
   - 2.1 Chemical Composition 7
   - 2.2 Physical Properties. 8
   - 2.3 Mechanical Properties. 8
3. Design Data 12
   - 3.1 Allowable Static Tension Stresses. 12
   - 3.2 Fatigue Strength of Beryllium Sheet. 12
   - 3.3 Initial Buckling Strength of Beryllium Shear Panels. . 15
   - 3.4 Post-Buckling Strength of Beryllium Shear Panels . . . 15
   - 3.5 Initial Compression Buckling Strength of Flat Panels . 17
   - 3.6 Allowable Crippling Stresses 19
     - 3.6.1 Crippling of Stiffening Elements. 19
     - 3.6.2 Crippling of Stiffened Flat Panels with Constant Skin Thickness 21
     - 3.6.3 Crippling of Panels with Chemically Milled Lands 24
   - 3.7 Analysis of Beryllium Lugs 25
   - 3.8 Joint Design Criteria. 25
     - 3.8.1 Fastener Shear Critical 28
     - 3.8.2 Sheet Bearing Critical. 28
     - 3.8.3 Sheet Tension Critical. 28
     - 3.8.4 Adhesive Bonded Joints. 29
4. Beryllium Rudder Corrosion Protection Process 30
   - 4.1 General Requirements 30
     - 4.1.1 Finishing Sequence. 30
     - 4.1.2 Treatment of Cut or Machined Surfaces 30
     - 4.1.3 Protection During Fabrication and Storage 30
     - 4.1.4 Metal Wool Precautions. 31
   - 4.2 Inorganic Treatment of Beryllium 31
     - 4.2.1 General 31
     - 4.2.2 Exceptions. 31

TABLE OF CONTENTS (CONTD)

SECTION PAGE

4.3 Organic Treatment of Beryllium 32

4.3.1 Internal Surfaces 32
4.3.2 Exterior Surfaces 32
4.3.3 Dissimilar Metal Protection 32
4.3.4 Fasteners: Interior Surfaces 33
4.3.5 Fasteners: Exterior Surfaces 33
4.3.6 Sealing 33

III RUDDER DESIGN AND ANALYSIS. 34

1. Introduction. 34
2. Design Considerations 37
3. Design Conditions 41
4. Strength Analysis 49
5. Structural Dynamics Analysis. 55
6. Control Dynamics Analysis 57
7. Rudder Mass Balance 59
8. Rudder Moment of Inertia. 61
9. Rudder Weight 64

IV ELEMENT TEST PROGRAM. 66

1. Introduction. 66
2. Material Acceptance Tests 68
3. Metal-to-Metal Bond Tests 71
4. Bonded Honeycomb Panel Tests. 76
5. Effect of Stress Concentrations and Interference Fit Fasteners 85
6. Joint Tests 99
7. Panel Shear Tests 105
8. Spliced Panel Shear Tests 111
9. Lug Tests 115
10. Corrosion Tests 119

10.1 Group 1 121
10.2 Group 2 131

11. Stress-Strain Tests 135
12. Rudder Composite Section Tests. 146

12.1 Test No. 1: Chordwise Bending. 148
12.2 Test No. 2: Torque 151
12.3 Test No. 3: Spanwise Bending 151
12.4 Test No. 4: Combined Loading 151

13. Crack Repair Evaluation Tests 155

TABLE OF CONTENTS (CONTD)

SECTION PAGE

V BERYLLIUM RUDDER FABRICATION AND ASSEMBLY 158

1. Introduction. 158
2. General Shop Practices. 159
3. Sawing Beryllium. 161
4. Machining Beryllium 163
5. Drilling Beryllium. 166
6. Countersinking Beryllium. 170
7. Forming Beryllium 171

    7.1 Equipment. 171
    7.2 Form Dies. 171
    7.3 Forming Procedure. 174
    7.4 Post Forming Cleaning. 175

8. Chemical Milling of Beryllium 176
9. Adhesive Bonding. 178
10. Inspection. 182
11. Rudder Assembly 183

VI RUDDER TEST PROGRAM 192

1. Introduction. 192
2. Test 1: Fatigue Test of Upper Balance Weight Support Structure 194

    2.1 Test Set-Up. 194
    2.2 Test Procedure and Results 197

3. Test 2: Rudder Ultimate Static Test With Maximum Airload at 30% Chord. 199

    3.1 Test Set-Up. 199
    3.2 Test Procedure and Results 205

4. Test 3: Rudder Ultimate Static Test With Maximum Loading on Vertical Tail. 216

    4.1 Test Set-Up. 216
    4.2 Test Procedure and Results 216

5. Test 4: Same as Test 2, With Loading Carried Beyond Ultimate. 234

    5.1 Test Procedure and Results 234

VII REFERENCES. 244

APPENDIX - DETAIL DRAWINGS. 245

ILLUSTRATIONS

FIGURE PAGE

1. F-4 Beryllium Rudder 3

2. Effect of Temperature on Specific Heat, Thermal Conductivity, and Coefficient of Expansion of Beryllium. . . 9

3. Effect of Temperature on Tensile, Bearing, and Shear Strength of Beryllium Sheet 11

4. Effect of Temperature and Stress Concentration on Ultimate Tensile Strength of Beryllium Sheet. 13

5. Fatigue Strength of Hot Rolled, Stress Relieved, Ground and Etched Beryllium Sheet 14

6. Design Curves for Initial and Post-Buckling Shear Strength of Flat Beryllium Panels 16

7. Design Curves for Initial Compression Buckling Strength of Flat, Unstiffened Beryllium Panels 18

8. Nondimensional Crippling Design Curves for Beryllium 20

9. Effective Width of Stiffened Sheet 22

10. Stiffened Panel Configurations 23

11. Beryllium Lug Design Chart 26

12. Beryllium Rudder Structure Schematic 35

13. F-4 Beryllium Rudder Structural Configuration. 38

14. F-4 Aluminum Rudder Structural Configuration 39

15. Ultimate Running Load. 43

16. Condition I Ultimate Shear and Moment 44

17. Condition II Ultimate Shear and Moment. 45

18. Condition III Ultimate Shear and Moment 46

19. Ultimate Torque. 47

20. Panel Flutter Criteria 48

21. Cover Skin Thickness Requirements. 50

ILLUSTRATIONS (CONTD)

FIGURE PAGE

22. Ultimate Shear Flows 51

23. Beryllium Rudder Rib and Spar Cross-Sections 52

24. Rudder Bending and Torsional Stiffnesses 54

25. Stability of Rudder With Upper Damper Removed. 56

26. Beryllium Rudder Power Cylinder Stability. 58

27. Mass Balancing of Beryllium Rudder 60

28. Spring Oscillation System for Determining Beryllium Rudder Moment of Inertia 62

29. Material Acceptance Test Set-Up. 69

30. Bonded Lap Shear and Flatwise Tension Tests. 72

31. Cold Temperature (-65°F) Test Set-Up 73

32. Bonded Honeycomb Panel Core Shear Test 77

33. Bonded Honeycomb Panel Edgewise Compression Test 78

34. Core to Edge Member Shear Test 79

35. Stress Concentration and Interference Fit Fastener Test Specimen Configurations. 86

36. Tension-Tension Fatigue Test Set-Up. 87

37. Fatigue Test Results: Specimens With Drilled Holes. 90

38. Fatigue Test Results: Specimens With Countersunk Cherry Rivets 91

39. Fatigue Test Results: Specimens With Drilled and Countersunk Holes. 92

40. Fatigue Test Results: Specimens With Countersunk Solid Rivets 93

41. Tension-Tension Fatigue Test Failed Specimens. 94

42. Fatigue Strength of Notched Sheet: Beryllium, Aluminum and Titanium 95

43. Fatigue Strength-to-Weight Efficiency of Notched Material: Beryllium, Aluminum and Titanium 96

ILLUSTRATIONS (CONTD)

FIGURE		PAGE
44.	Static Tension Test Failed Specimens	98
45.	Spliced Joint Test Specimen Configurations	100
46.	Spliced Joint Tension Test Set-Up.	101
47.	Spliced Beryllium Joint Test Failed Specimens.	104
48.	Panel Shear Test Set-Up.	106
49.	Loading Jig and Failed Shear Panel	109
50.	Panel Shear Test Failed Specimens.	110
51.	Spliced Panel Shear Test Specimen Configurations	112
52.	Spliced Panel Shear Test Failed Specimens.	114
53.	Failed Beryllium Lug Specimens	117
54.	Corrosion Test Specimens	120
55.	Group 1 Corrosion Test Specimens Before 500 Hours Exposure.	122
56.	Group 1 Corrosion Test Specimens After 500 Hours Exposure .	123
57.	Backs of Group 1 Corrosion Specimens After 500 Hours Exposure	124
58.	Effect of Anodize on Beryllium Surface Finish.	129
59.	Surface Coated Tension Test Failed Specimens	130
60.	Group 2 Corrosion Test Specimens Before 500 Hours Exposure.	132
61.	Group 2 Corrosion Test Specimens After 500 Hours Exposure .	133
62.	Stress-Strain Test Specimen Configurations	136
63.	Tension Stress-Strain Test Set-Up (500°F).	137
64.	Compression Stress-Strain Test Set-Up.	138
65.	Tension Stress-Strain Curves: -65°F	140
66.	Tension Stress-Strain Curves: Room Temperature.	141
67.	Tension Stress-Strain Curves: 500°F	142

ILLUSTRATIONS (CONTD)

FIGURE PAGE

68. Compression Stress-Strain Curves: -65°F 143

69. Compression Stress-Strain Curves: Room Temperature. 144

70. Compression Stress-Strain Curves: 500°F 145

71. Relative Sizes of Rudder Composite Section and F-4 Rudder. . . 147

72. Rudder Composite Section Test Set-Up 149

73. Rudder Composite Section Test Loads. 150

74. Loads in Rudder Composite Section at Failure 152

75. Rudder Composite Section Static Test Failure 153

76. Beryllium Facility 160

77. Set-Up for Sawing Beryllium Sheet. 162

78. Machining Beryllium. 164

79. Tools Used to Machine, Drill and Countersink Beryllium 165

80. Tornetic Driller Used for Drilling Beryllium 167

81. Mated Hot Forming Dies for Beryllium Rudder Ribs 172

82. Mated Hot Forming Die for Rib with Closed Angle Flanges. . . . 173

83. Beryllium Rudder Front Torque Box Cover Skins. 177

84. Rudder Trailing Edge Assembly Structural Details 179

85. Rudder Trailing Edge Assembly and Bonding Fixture. 180

86. Beryllium Rudder Bonded Trailing Edge Assembly 181

87. Pre-Fit Assembly of Beryllium Rudder in Assembly Fixture . . . 184

88. Locating Fastener Holes in Rudder Front Torque Box 185

89. Rudder Front Torque Box Detail Parts 187

90. Rivet Installation Along Front Spar of Beryllium Rudder. . . . 188

91. Beryllium Rib with Broken Flange and Repair Splice 189

92. Final Assembly of Beryllium Rudder 190

ILLUSTRATIONS (CONTD)

FIGURE PAGE

93. Completed Beryllium Rudder Assembly 191

94. Set-Up for Balance Weight Support Structure Fatigue Test. . . 195

95. Torsion Spring Installation 196

96. Rivet Failure During Fatigue Test 198

97. Set-Up for Static Tests of Beryllium Rudder 200

98. Aft Fuselage Support Fixture for Beryllium Rudder Static Tests 201

99. Beryllium Rudder With Tension Pads Installed. 202

100. Beryllium Rudder Strain Gage Locations. 203

101. Beryllium Rudder Deflection Point Locations 204

102. Rudder Tension Pad Layout and Ultimate Loads for Test 2 . . . 206

103. Comparison of Test and Design Loads: Design Condition I. . . 207

104. Front Spar Strains: Test 2 208

105. Rear Spar and Trailing Edge Strains: Test 2. 209

106. Forward Cover Skin Strains: Test 2 210

107. Front Spar Deflections: Test 2 211

108. Rear Spar Deflections: Test 2. 212

109. Trailing Edge Deflections: Test 2. 213

110. Hinge Deflections: Test 2. 214

111. Rudder Deflections: Design Condition I 215

112. Vertical Fin Tension Pad Layout and Ultimate Loads for Test 3. 217

113. Rudder Tension Pad Layout and Ultimate Loads for Test 3 . . . 218

114. Beryllium Rudder Prior to Loading 220

115. Beryllium Rudder With Condition III Ultimate Loads Applied. . 221

116. Comparison of Fin Test and Design Loads: Design Condition III 222

ILLUSTRATIONS (CONTD)

FIGURE PAGE

117. Comparison of Rudder Test and Design Loads: Design Condition III. 223

118. Front Spar Strains: Test 3. 224

119. Rear Spar and Trailing Edge Strains: Test 3 225

120. Forward Cover Skin Strains: Test 3. 226

121. Front Spar Deflections: Test 3. 227

122. Rear Spar Deflections: Test 3 228

123. Trailing Edge Deflections: Test 3 229

124. Hinge Deflections: Test 3 230

125. Rudder Deflections: Design Condition III. 231

126. Deflected Hinge Line: Design Condition III. 232

127. Crack in Trailing Edge Lower Closure Rib of Beryllium Rudder . 235

128. Front Spar Strains: Test 4. 237

129. Rear Spar and Trailing Edge Strains: Test 4 238

130. Forward Cover Skin Strains: Test 4. 239

131. Front Spar Deflections: Test 4. 240

132. Rear Spar Deflections: Test 4 241

133. Trailing Edge Deflections: Test 4 242

134. Hinge Deflections: Test 4 243

TABLES

TABLE PAGE

1. Chemical Analysis of Beryllium Sheet 7
2. Summary of Beryllium Properties at Room Temperature. 8
3. Properties of Beryllium Sheet Used for Element Test Specimens and Rudder 10
4. Design Shear Stresses for Bonded Beryllium Lap Joints. . . . 29
5. Weight Summary for Beryllium and Aluminum Rudders. 65
6. Element Test Program 67
7. Material Acceptance Tension Test Results 70
8. Bonded Lap Shear Test Results. 74
9. Bonded Metal-To-Metal Flatwise Tension Test Results. 75
10. Bonded Honeycomb Panel Flatwise Tension Test Results 80
11. Bonded Honeycomb Panel Core Shear Test Results 81
12. Bonded Honeycomb Panel Edgewise Compression Test Results . . 83
13. Core to Edge Member Shear Test Results 84
14. Tension-Tension Fatigue Test Results 89
15. Static Tension Test Results. 97
16. Spliced Joint Tension Test Results 102
17. Flat Panel Shear Test Results. 108
18. Spliced Panel Shear Test Results 113
19. Beryllium Lug Test Results 118
20. Tension Test Results of Surface Treated Specimens. 128
21. Tension and Compression Stress-Strain Test Results 139
22. Tension Test Results of Slotted Beryllium Coupons With and Without Bonded Doublers. 156
23. Control Settings for Drilling Beryllium. 166

SYMBOLS

A	Area of cross-section
a	Length of the unloaded edge of a panel in uniaxial compression; long dimension of a panel in shear
b	Width of an element; width of a stiffened panel; short dimension of a panel in shear; length of the loaded edge of a panel in uniaxial compression
b_f	Width of stiffener flange element
b_w	Height of stiffener web element
c	Fixity coefficient for columns; distance from neutral axis to extreme fiber; subscript "compression"
cr	Subscript "critical"
D	Diameter
d	Depth or height
E	Modulus of elasticity in tension
e	Elongation in percent (this factor being a measure of the ductility of the material and being based on a tension test; unit deformation or strain); eccentricity; minimum distance from a hole center line to edge of sheet
E_c	Modulus of elasticity in compression
F	Allowable stress; Fahrenheit
f	Calculated stress
F_{bru}	Ultimate bearing stress
F_{cc}	Allowable crushing or crippling stress (upper limit of column stress for local failure
F_{cy}	Compressive yield stress at which permanent strain equals 0.002 (from tests of standard specimens)
F_s	Allowable shear stress
$F_{s_{cr}}$	Critical shear stress for buckling of rectangular panels
F_{su}	Ultimate stress in pure shear (average shearing stress over the cross-section)

SYMBOLS (CONTD)

f_t	Calculated tensile stress
F_{tu}	Ultimate tensile stress (from tests of standard specimen)
F_{ty}	Tensile yield stress at which permanent strain equals 0.002 (from tests of standard specimens)
G	Modulus of rigidity
I	Moment of inertia
J	Polar moment of inertia
K	A constant, generally empirical; thermal conductivity
K_T	Stress concentration factor
ksi	KIPS (1000 pounds) per square inch
M	Applied moment (usually a bending moment)
N	Cycles to failure in fatigue
P	Applied load, pounds
P_a	Allowable load
psi	Pounds per square inch
R	Radius; ratio of minimum stress to maximum stress
s	Subscript "shear"
sk	Subscript "skin"
st	Subscript "stiffener"
t	Thickness
W	Width of a lug
μ	Poisson's ratio
η	Plasticity reduction factor

CONVERSION OF U. S. CUSTOMARY UNITS TO Sl UNITS

The International System of Units (Sl) was adopted by the Eleventh General Conference on Weights and Measures, Paris, October 1960. Conversion factors for the units used in this report are given in the following table:

Quantity	U.S. Customary Units	Conversion Factor (*)	Sl Unit
Mass	lb. oz.	453.6 28.3	grams (g)
Stress	ksi	6.895×10^{6}	newtons/meter^{2} (N/m^{2})
Length	in.	0.0254	meters (m)
Temperature	(°F + 460)	5/9	degrees Kelvin (°K)
Volume	gal. pint	3.785×10^{-3} 4.732×10^{-4}	meters^{3} (m^{3})
Frequency	cps	1.0	hertz (Hz)
Moment	in. - lb.	0.113	meter-newtons (m-N)
Moment of Inertia	lb. - in.^{2}	0.2926	gram-meters^{2} (g-m^{2})
Force	lb.	4.448	newtons (N)

* Multiply value given in U. S. Customary Units by conversion factor to obtain equivalent value in Sl Units.

Prefixes to indicate multiple of units are as follows:

Prefix	Multiple
mega (M)	10^{6}
kilo (k)	10^{3}
deci (d)	10^{-1}
centi (c)	10^{-2}
milli (m)	10^{-3}

SECTION I

INTRODUCTION

The program reported herein is for the advancement of structural beryllium technology through the design, fabrication, test and evaluation of a typical load-carrying aircraft component, suitable for flight testing, which demonstrates a potential for increased capability and efficiency through the utilization of beryllium. The program provides structural design information compatible with available material properties, production and component fabrication techniques, and demonstrates the structural integrity of beryllium flight structures.

It was felt that the objectives of this program would be best achieved if the structural component to be evaluated would be a portion of a current aircraft on flying status. Under these conditions, the advantages of beryllium utilization could be appraised in a most direct and timely manner relative to: (a) optimization of detail parts, as well as of the complete component, (b) effects of such component optimization on the aircraft as a whole, and (c) reliability of a beryllium component in actual flight environment, in the event of a future flight test program. Thus, a direct comparison between the "berylliumized" component and its production non-beryllium counterpart would be available in a minimum of time, thereby providing an early assessment of potential benefits that could accrue to a complete aircraft through the advancement of structural beryllium technology.

Based on the above considerations, the rudder on the McDonnell F-4 aircraft was selected for implementation of this program. First, the rudder is a typical sheet metal assembly, which permits a thorough evaluation of structural and manufacturing problems associated with that type of structure, as well as an appreciable weight optimization of most of its structural elements. Second, being a mass-balanced control surface, the reduced structural weight and increased stiffness of the rudder achieved through the use of beryllium permit a decrease in balance weights and the elimination of one (upper) of the two flutter dampers. These changes result in a simplification of the rudder structure and an overall weight reduction of the rudder assembly from the current production weight of 63.03 lbs. (28.59 kg) to 37.59 lbs. (17.05 kg). Third, the F-4 aircraft can fly and land without a rudder, so that an eventual flight test program could be conducted under fail-safe conditions. Figure 1 shows the beryllium rudder.

In Section II, physical and mechanical properties of beryllium sheet and pertinent design data are presented. This information was obtained from the data of element tests performed in this program and in Reference 2 work, and from published literature. Included in Section II is a description of the corrosion protection process developed in this program for intended use on a flight test beryllium rudder.

In Section III, the design and analysis of the beryllium rudder are discussed. This discussion includes the design requirements and considerations which defined the rudder basic configuration and influenced the selection of detail component shapes and sizes. Loading conditions established for the F-4 aircraft and used in designing the beryllium rudder are described, and the results of the strength, structural dynamics, control dynamics, and weight analyses presented. Also included in this section is a description of the rudder mass balancing and of the procedure for determining the rudder moment of inertia.

The results of the element test program are discussed in Section IV. A variety of tests were conducted to verify material properties, to obtain

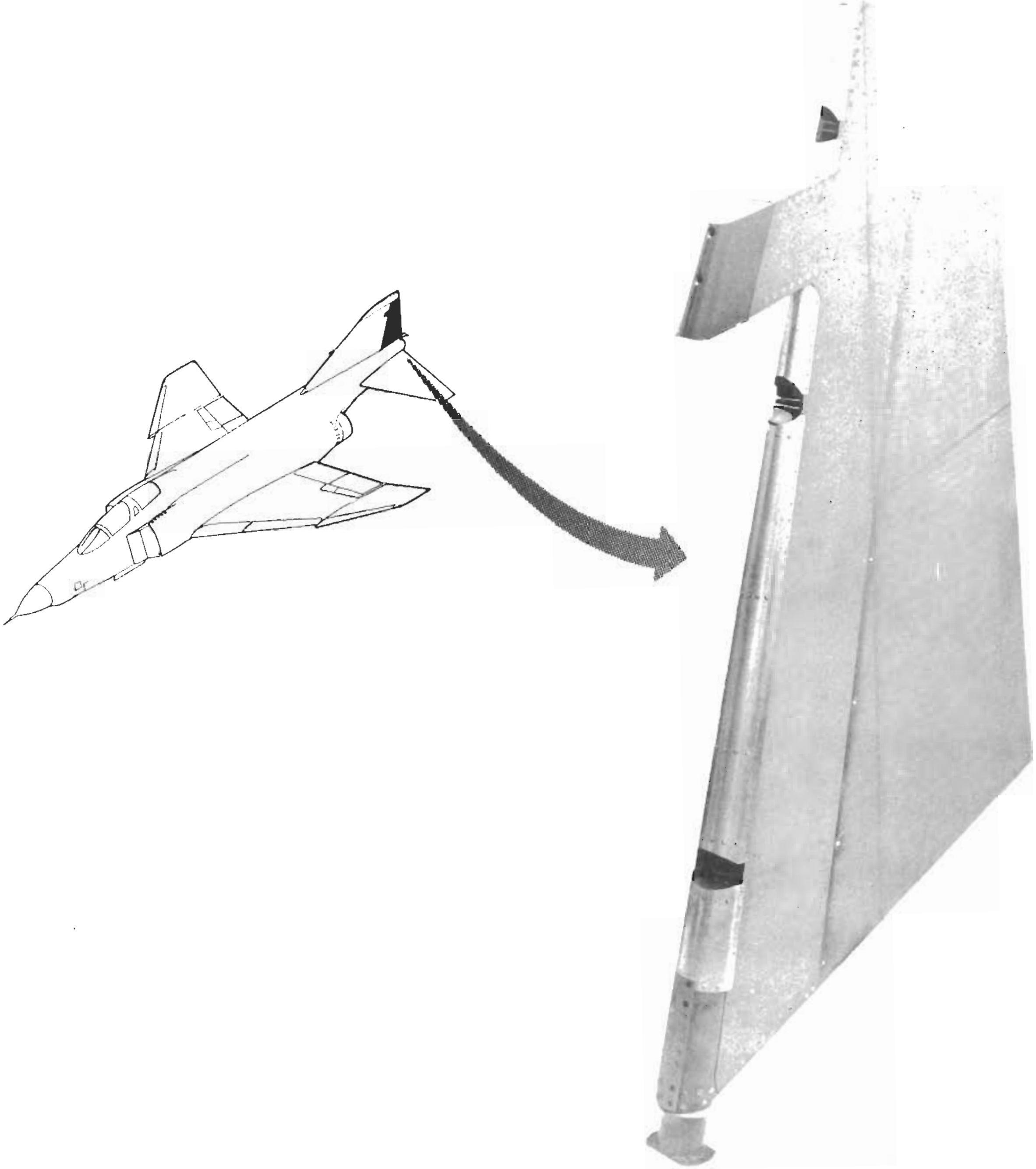

Figure 1 – F–4 Beryllium Rudder

design data, and to evaluate certain structural details of the rudder. The tests reported herein are listed below:

- Material Acceptance Tests
- Metal-to-Metal Bond Tests
- Bonded Honeycomb Panel Tests
- Effects of Stress Concentrations and Interference Fit Fasteners
- Joint Tests
- Panel Shear Tests
- Spliced Panel Shear Tests
- Lug Tests
- Corrosion Tests
- Stress-Strain Tests
- Rudder Composite Section
- Crack Repair Evaluation Tests

These tests demonstrate that beryllium can be joined to itself and other materials using conventional methods and materials, with a predictable high strength capability, that stress concentrations in the form of filled and unfilled fastener holes reduce the static and fatigue strengths of beryllium, that the fatigue strength of beryllium with drilled fastener holes is improved by the installation of interference fit fasteners, that the post buckling strength of beryllium sheet is less than that of high strength aluminum for the specified test conditions, and that corrosion protection of beryllium can be achieved without degradation of mechanical properties.

Equipment and procedures used in sawing, machining, drilling, countersinking, forming, chemical milling, adhesive bonding, inspection, and assembly of the beryllium rudder structural elements are described in Section V. Some problems encountered in fabrication and assembly are described and solutions presented. The knowledge and experience acquired in the beryllium wing-box program (Reference 2) greatly facilitated the manufacturing effort for this program.

Tests were conducted on the beryllium rudder to verify its structural adequacy and qualify it for flight use on the F-4 aircraft. A description of these tests and a discussion of the test results are presented in Section VI. The rudder was first fatigue tested to 50,000 cycles of ± 40 g's on the upper balance weight. Upon successful completion of this test the rudder was then static tested to design ultimate (150% of limit) load for two separate loading conditions: (1) Design Condition I - maximum rudder airload producing maximum rudder torque and (2) Design Condition III - maximum tail (vertical fin plus rudder) loading producing maximum shear and bending in the rudder. These tests were also successfully completed demonstrating that primary load carrying beryllium structures can be fabricated with predictable strength capability, and establishing that the rudder is structurally qualified for flight test use. Following Condition III test, the rudder was again subjected to Condition I loading with the total load allowed to increase beyond 150% of limit load, to provide a direct comparison with the production aluminum rudder which had sustained 225% of this limit load without failure. When the total applied load reached 205% of limit, a crack occurred in the rudder tailing edge lower closure rib, at the rear spar. However, the load did not fall off, and was increased to 250% of limit, after which the test was discontinued. Thus, after an extremely rigorous test program, the beryllium rudder was still capable of carrying more load than had ever been applied to the production rudder for the specified test condition.

SECTION II

MATERIAL PROPERTIES, DESIGN DATA AND CORROSION PROTECTION PROCESS

1. Introduction

The F-4 production rudder is a typical stiffened-skin aircraft structure subjected during its service life to steady and alternating loads, thermal inputs, and corrosive environment. In fabricating the beryllium version of this assembly, commercially available hot cross-rolled, stress relieved, ground and etched beryllium sheet was used for all spars, ribs, doublers and cover skins. Subsection 2 provides the mechanical properties and chemical composition of this material, as certified by the producers, and describes the specification to which it was purchased. Also presented are physical properties of beryllium material and variations in physical and mechanical properties with temperature.

Subsection 3 presents design data on beryllium cross-rolled sheet including the information obtained in Reference 2 program. Subsection 4 describes the beryllium rudder corrosion protection process developed in this program.

2. Beryllium Material Properties

The chemical composition and the physical and mechanical properties of the beryllium sheet used in this program are presented and discussed in the following paragraphs. These data were obtained from the material producers, published literature, and element tests performed during this program. All material was purchased to the requirements of McDonnell Material Specification MMS-191 and is representative of the current, commercially available, beryllium sheet.

2.1 Chemical Composition - The chemical composition of the beryllium sheet used in this program, as certified by the material producers, is given in Table 1 along with the requirements of McDonnell Material Specification MMS-191.

TABLE 1
CHEMICAL ANALYSIS OF BERYLLIUM SHEET

Lot No.	Be (%)	BeO (%)	Fe (%)	Si (%)	Al (%)	Mg (%)	C (%)	Other (%)
2452	98.50	1.70	0.120	0.030	0.090	0.020	0.130	< 0.04
2938	98.60	1.69	0.140	0.040	0.090	0.010	0.100	< 0.04
3516	98.21	1.70	0.140	0.040	0.110	0.008	0.130	< 0.04
3379	98.68	1.77	0.120	0.040	0.110	0.020	0.130	< 0.04
3422	98.59	1.90	0.150	0.050	0.130	0.020	0.130	< 0.04
3318	98.57	1.57	0.160	0.040	0.100	0.010	0.110	< 0.04
3890	98.30	1.93	0.130	0.020	0.090	0.020	0.100	< 0.04
3900	98.30	2.00	0.130	0.030	0.100	0.020	0.130	< 0.04
3939	98.30	1.68	0.120	0.030	0.090	0.020	0.120	< 0.04
3957	98.30	1.94	0.130	0.030	0.100	0.020	0.100	< 0.04
013J	98.30	2.00	0.073	0.076	0.066	0.031	0.063	< 0.04
109H	98.38	1.73	0.168	0.052	0.050	0.008	0.106	< 0.04
804H	98.46	1.49	0.092	0.056	0.070	0.008	0.100	< 0.04
H349	98.17	1.99	0.095	0.069	0.068	0.062	0.131	< 0.04
MMS-191 (2)	98.00 (min.)	2.00 (max.)	0.200 (max.)	0.120 (max.)	0.200 (max.)	0.080 (max.)	0.150 (max.)	0.04 (max.)

Notes:
1. Hot rolled, stress relieved, ground and etched beryllium sheet.
(2) Required per McDonnell Material Specification MMS-191.

2.2 Physical Properties - The physical properties presented herein are applicable to hot-rolled, stress relieved, ground and etched beryllium sheet with a BeO content of 1.75%. The room temperature physical properties are summarized in Table 2. The effects of temperature on specific heat, coefficient of thermal conductivity, and coefficient of expansion are shown in Figure 2. The effect of BeO content on the coefficient of expansion is also shown in Figure 2.

TABLE 2
SUMMARY OF BERYLLIUM PHYSICAL PROPERTIES AT ROOM TEMPERATURE

Density (lb/in.^{3})	0.067
Specific gravity	1.85
Atomic number	4
Atomic weight	9.02
Atomic diameter (A)	2.221
Reflectivity, white light (%)	55
Specific heat, (BTU/lb/^{0}F)	0.445
Latent heat of fusion (BTU/lb)	470
Melting point (^{0}F)	2340
Thermal conductivity, (BTU/ft^2/ft/hr)	104
Thermal expansion, room temperature (in./in./^{0}F)	6×10^{-6}
Electrical conductivity (% of copper)	35 to 45
Resistivity (μohm-in.^{2}/in.)	1.6

2.3 Mechanical Properties - The mechanical properties of hot-rolled, stress relieved, ground and etched beryllium sheet are essentially the same in the longitudinal and transverse grain directions. The longitudinal grain direction is defined as the direction of the last rolling operation. The specified guaranteed minimum mechanical properties at room temperature are:

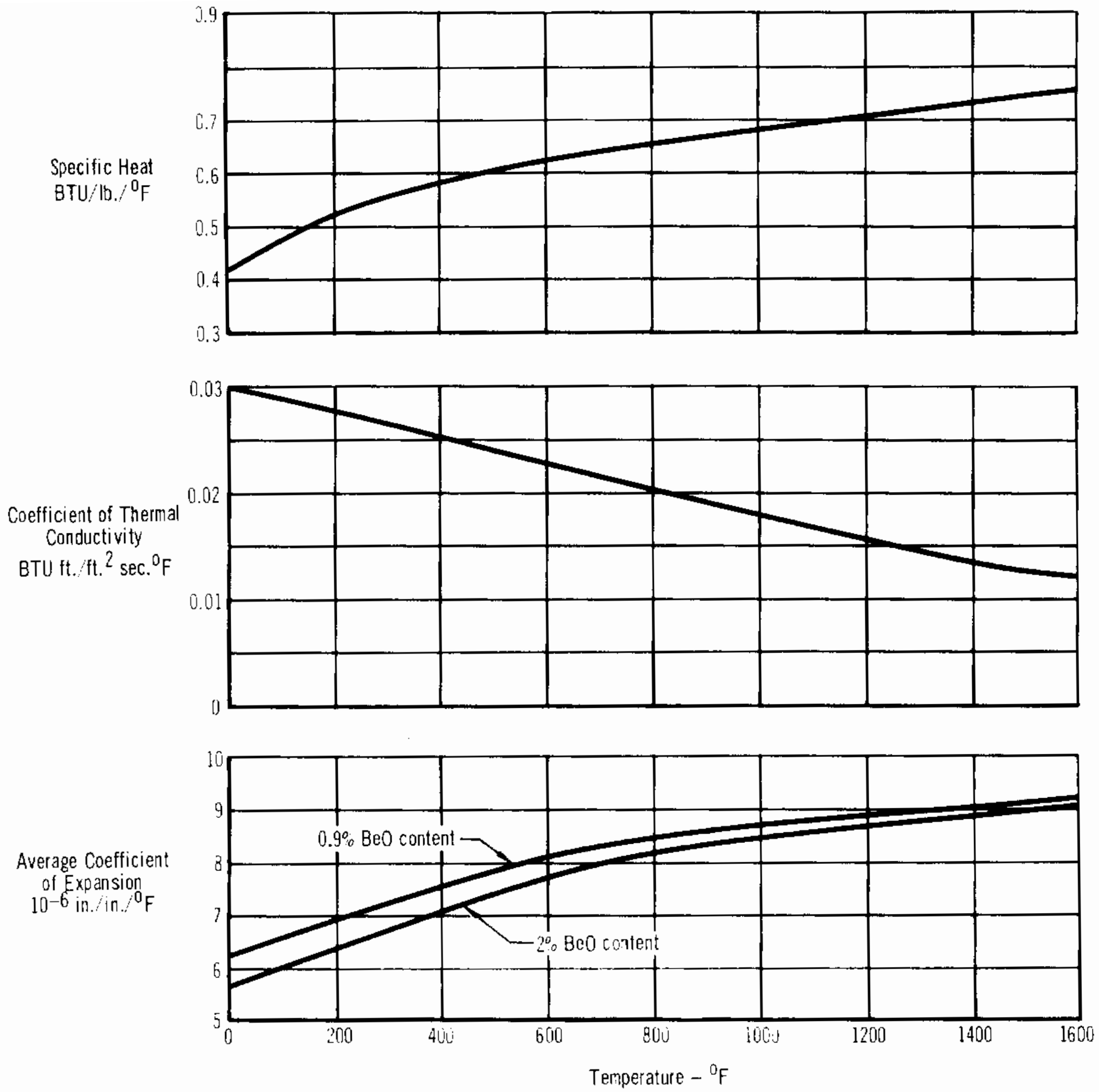

Figure 2 – Effect of Temperature on Specific Heat, Thermal Conductivity, and Coefficient of Expansion of Beryllium

$$F_{tu} = 70 \text{ ksi } (483 \text{ MN/m}^2)$$

$$F_{ty} = 50 \text{ ksi } (345 \text{ MN/m}^2)$$

$$e = 5\% \text{ in } 1.0 \text{ inch } (2.54 \text{ cm})$$

Table 3 gives the mechanical properties of all beryllium sheets purchased for use in this program.

TABLE 3
PROPERTIES OF BERYLLIUM SHEET USED FOR ELEMENT TEST SPECIMENS AND RUDDER

Sheet No.	Lot or Heat	Longitudinal			Transverse		
		F_{tu} (ksi)	F_{ty} (ksi)	e (%)	F_{tu} (ksi)	F_{ty} (ksi)	e (%)
996B	2452	77.2	51.2	27.0	75.3	51.8	20.0
1026A	2938	79.2	54.6	14.0	70.8	55.4	5.0
1026B	2938	79.2	54.6	14.0	70.8	55.4	5.0
1072B	3516	84.2	60.2	15.0	82.2	60.1	18.0
1040A	3379	83.2	58.9	27.5	81.9	56.5	21.0
1048B1	3379	81.6	57.0	22.5	77.7	55.6	29.0
1062B	3422	79.4	59.7	15.0	75.2	58.1	11.0
1053A	3422	79.2	55.1	28.0	78.6	56.5	21.0
1034B	3318	78.5	52.5	19.0	79.4	56.5	27.0
1187C	3890	83.0	60.5	20.0	80.8	61.2	17.0
1197A	3900	74.2	52.3	11.0	76.9	60.7	17.0
1210A2	3939	87.1	64.4	17.0	85.1	60.6	15.0
1211A2	3939	84.0	60.1	17.0	77.1	55.6	6.0
1219A	3957	84.0	58.2	24.0	80.2	58.4	19.0
HR385	013J	74.5	51.0	24.0	72.4	52.1	19.0
HR228-1	109H	74.4	57.3	25.0	73.5	58.5	27.0
HR380	804H	81.5	55.1	22.0	75.4	55.4	14.0
HR382	804H	83.8	58.7	24.0	84.9	60.1	19.0
H-349	-	76.0	53.2	24.0	-	-	-

Figure 3 gives typical values of F_{tu} and F_{ty} vs. temperature, as determined in Reference 2 program. For design, minimum guaranteed mechanical properties should be used rather than typical values. Accordingly, the typical values of F_{tu} at all temperatures have been reduced by the ratio of the typical F_{tu} to the minimum F_{tu} at room temperature, as indicated in Figure 3. Design F_{ty} was obtained by reducing the typical F_{ty} by the ratio of typical F_{ty} to the minimum F_{ty} at room temperature. Figure 3 also shows the effect of temperature on F_{bru} and F_{su} as reported in Reference 3.

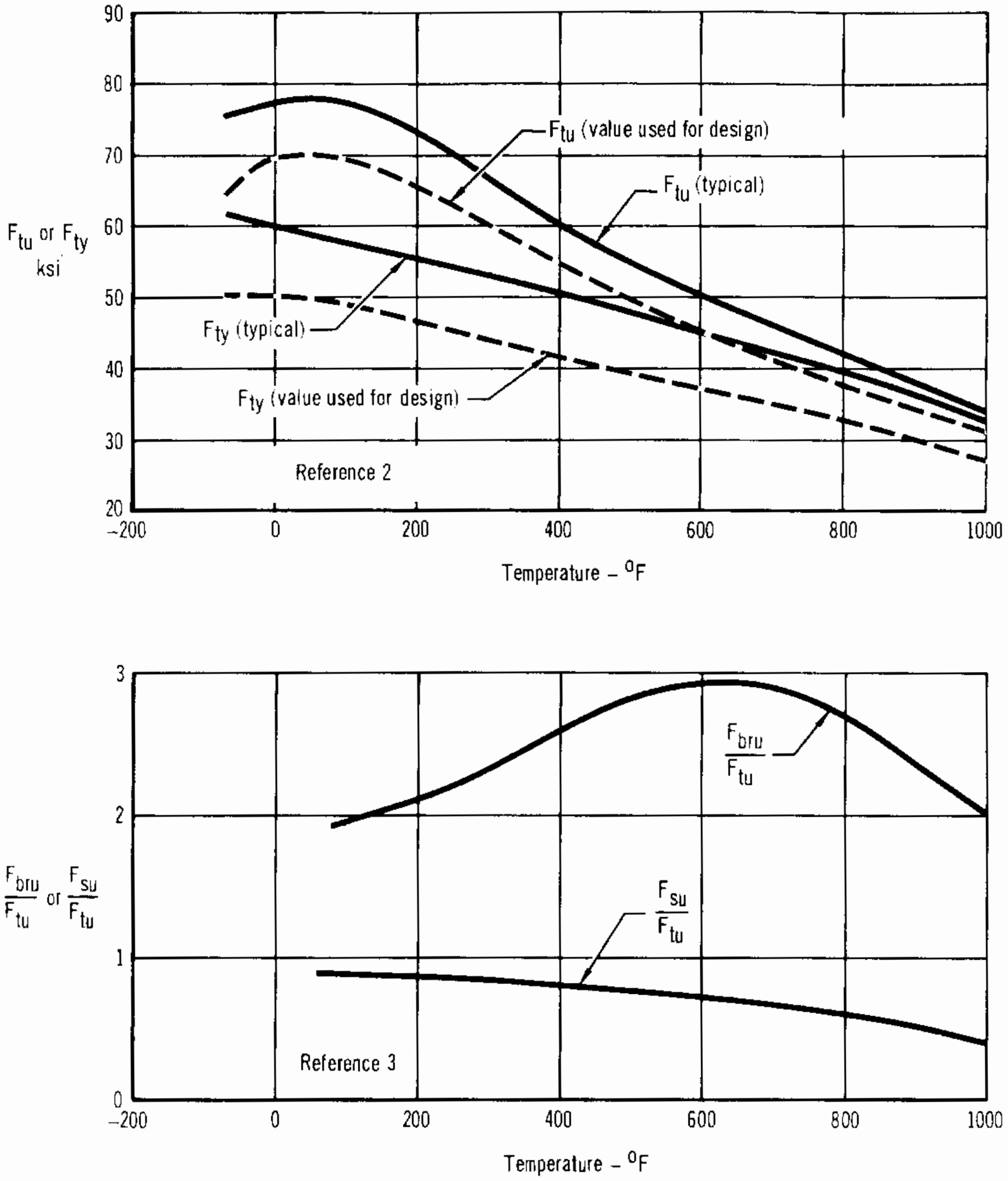

Figure 3 – Effect of Temperature on Tensile, Bearing, and Shear Strength of Beryllium Sheet

3. Design Data

In the following paragraphs, design data and methods of analysis for structural components fabricated of beryllium sheet material are presented. This information was used in the analysis of the beryllium wing-box specimens fabricated and tested in Reference 2 program and in the analysis of the beryllium rudder fabricated and tested in this program. The test results obtained in both programs verify the adequacy of the presented design data and methods of analysis for the accurate prediction of the strength of beryllium structural components.

3.1 Allowable Static Tension Stresses - The effect of temperature on the ultimate tension strength of unnotched beryllium sheet is given in Figure 3. These data can be used for design only when the beryllium component is loaded in uniaxial tension and no stress concentration exists. These conditions seldom prevail in an actual aerospace structural component. Beryllium has been found to be quite notch sensitive at operating temperatures below 400°F (478°K). Figure 4 shows the effects of stress concentration (K_T) and temperature on the ratio of notched to unnotched strength of beryllium sheet. The notched tension strength should be used to size tension members with stress concentrations when the notched strength is less than the unnotched strength. It is apparent from Figure 4 that, for efficient design, stress concentrations must be minimized in beryllium components loaded in tension.

3.2 Fatigue Strength of Beryllium Sheet - Tests of notched and unnotched tensile specimens indicate that beryllium sheet has exceptionally good resistance to the initiation of fatigue cracks in the temperature range from room temperature to 500°F (533°K). Figure 5 provides the results of fatigue tests conducted both in this and in Reference 2 programs.

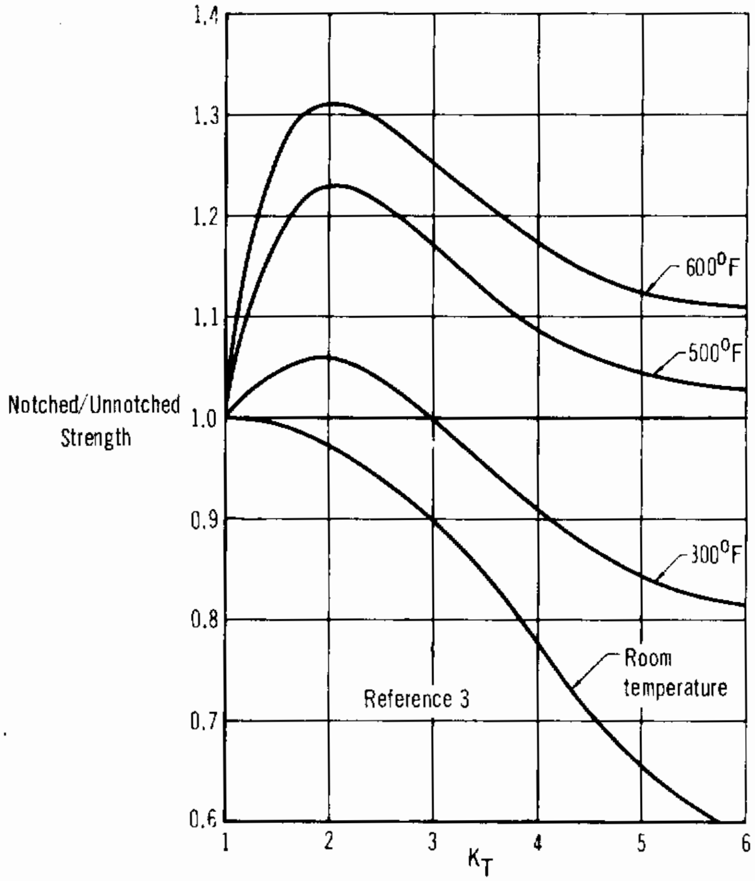

Figure 4 – Effect of Temperature and Stress Concentration on Ultimate Tensile Strength of Beryllium Sheet

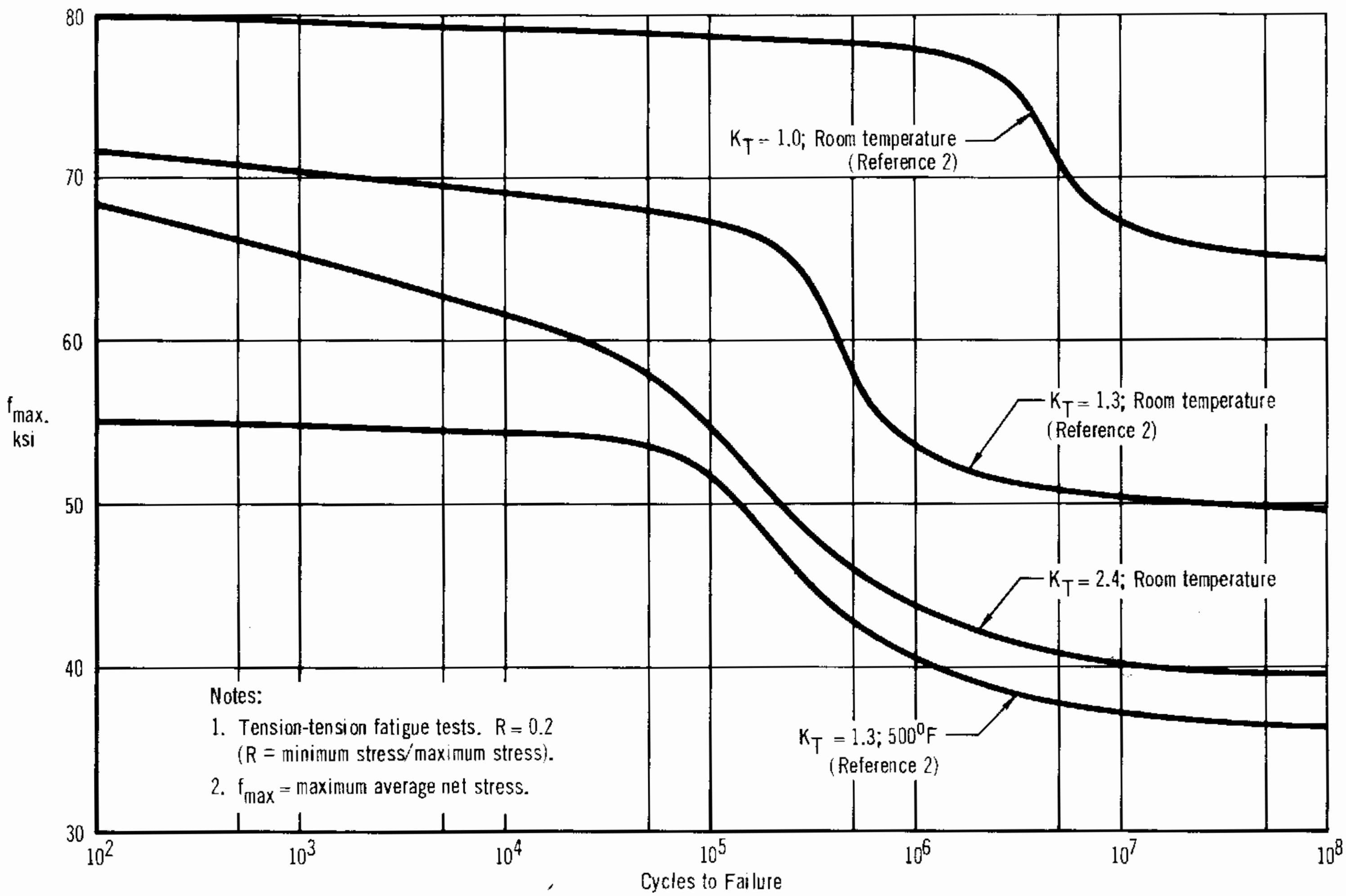

Figure 5 – Fatigue Strength of Hot Rolled, Stress Relieved, Ground and Etched Beryllium Sheet

A surface notched test specimen was used in the fatigue tests conducted in Reference 2 program. The surface notch was produced by chemically milling a groove in the specimen gage area. This configuration was intended to be representative of the condition existing at the edge of a chemically milled land. The resulting stress concentration is relatively low ($K_T = 1.3$).

The fatigue test specimens used in this program had either drilled holes or drilled and countersunk holes in the gage area with hole filling fasteners (CR 2248-4 aluminum cherry rivets and NAS 1097 AD4 solid aluminum rivets) installed in some of the test specimens to determine the effects of the induced tension stresses. These tests (described in detail in Section IV) showed that stress concentrations in the form of filled and unfilled fastener holes reduce the static and fatigue strengths of beryllium, and that fatigue strength is improved and static strength not affected by the installation of the hole filling fasteners in beryllium when compared to specimens with empty holes.

3.3 Initial Buckling Strength of Beryllium Shear Panels - The initial buckling strength of flat, unstiffened panels loaded in shear can be predicted with the equation:

$$\frac{F_{s_{cr}}}{\eta} = \frac{\pi^2 K_s E}{12(1-\mu^2)} \left(\frac{t}{b}\right)^2$$

Figure 6 provides design curves for the prediction of the initial buckling stress of flat beryllium panels loaded in shear at room temperature and at 500°F (533°K). These curves were developed using the method given in Reference 4 except that $F_{su} = .8 F_{tu}$ was assumed on the basis of available beryllium test data following the Reference 2 approach.

3.4 Post-Buckling Strength of Beryllium Shear Panels - The post-buckling (ultimate) strength of flat, unstiffened shear webs fabricated from 2024-T3 and 7075-T6 aluminum may be predicted using the method developed in Reference 5.

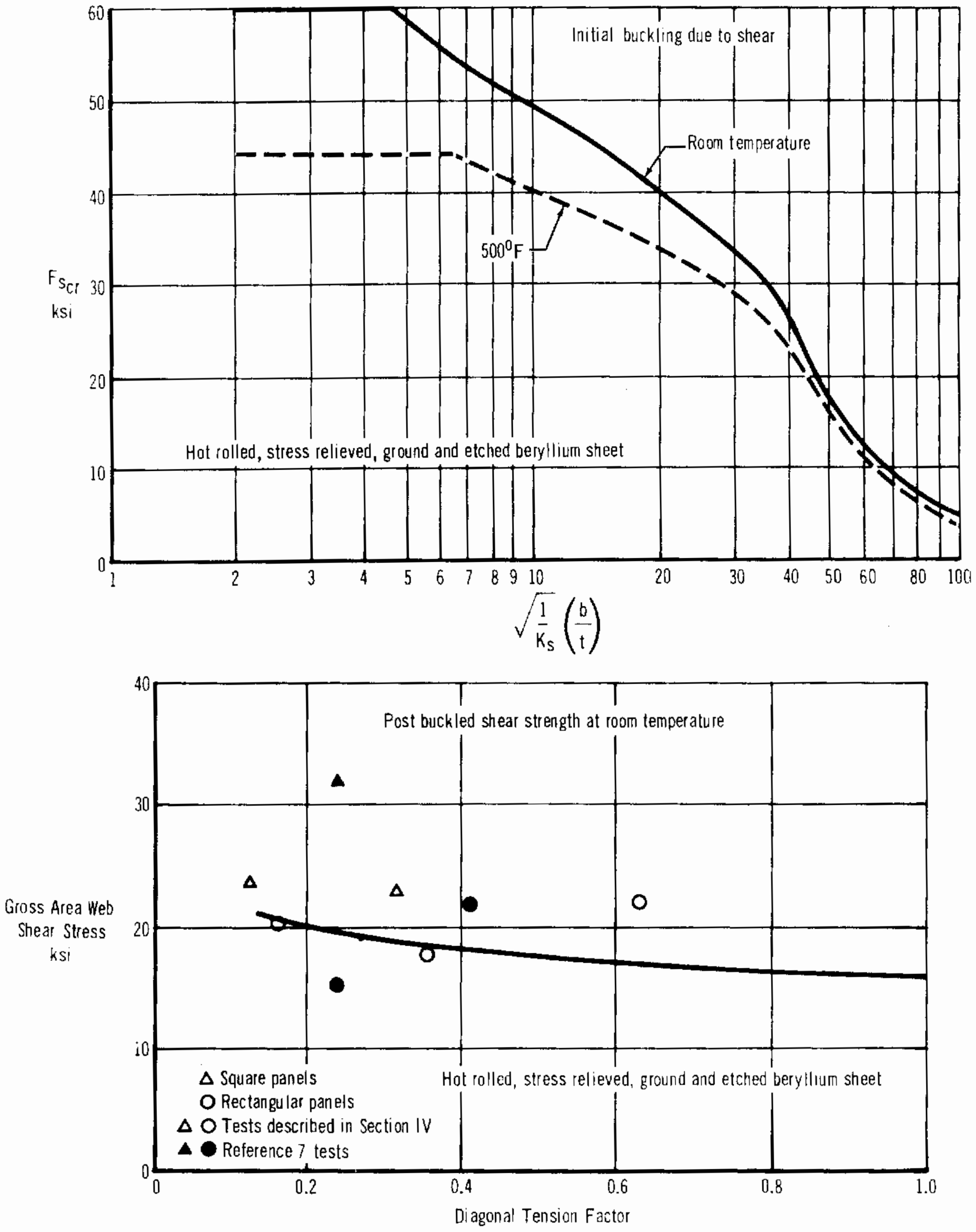

Figure 6 – Design Curves for Initial and Post-Buckling Shear Strength of Flat Beryllium Panels

Reference 6 shows that the shear post-buckling strength of other materials, at any temperature, can be closely approximated by multiplying the post-buckling strength data of the 2024-T3 material by the ratio of the ultimate tensile stress (at temperature) of the new material to that of the 2024-T3 material at room temperature. The results of tests performed in this program and described in Section IV show that this procedure is not suitable for prediction of the post-buckled shear strength of beryllium panels; tests of flat unstiffened shear panels in a cantilever type jig clearly showed that the post-buckled shear strength of beryllium panels was significantly below that of the identical 7178-T6 aluminum panels tested under identical conditions. Tests reported in Reference 7 tend to verify this conclusion. Based on the tests described in Section IV, the design curve shown in Figure 6 was developed for prediction of the post-buckled shear strength of flat, unstiffened beryllium panels.

3.5 Initial Compression Buckling Strength of Flat Panels - Figure 7 shows design curves for prediction of the initial compression buckling stress of flat, unstiffened beryllium panels at room temperature and at 500°F (533°K). These curves were developed by the method of Reference 8 and are in agreement, in the elastic range, with similar design curves given in Reference 7. The curves in Figure 6 predict lower compression buckling stresses in the plastic range than Reference 7 curves because the plasticity reduction factor (η) used in the development of the former was based on typical stress-strain curves for currently available beryllium sheet. Reference 7 curves were based on stress-strain data typical of beryllium sheet available in 1962; this sheet had a slightly higher yield strength (F_{ty}) than the currently available sheet.

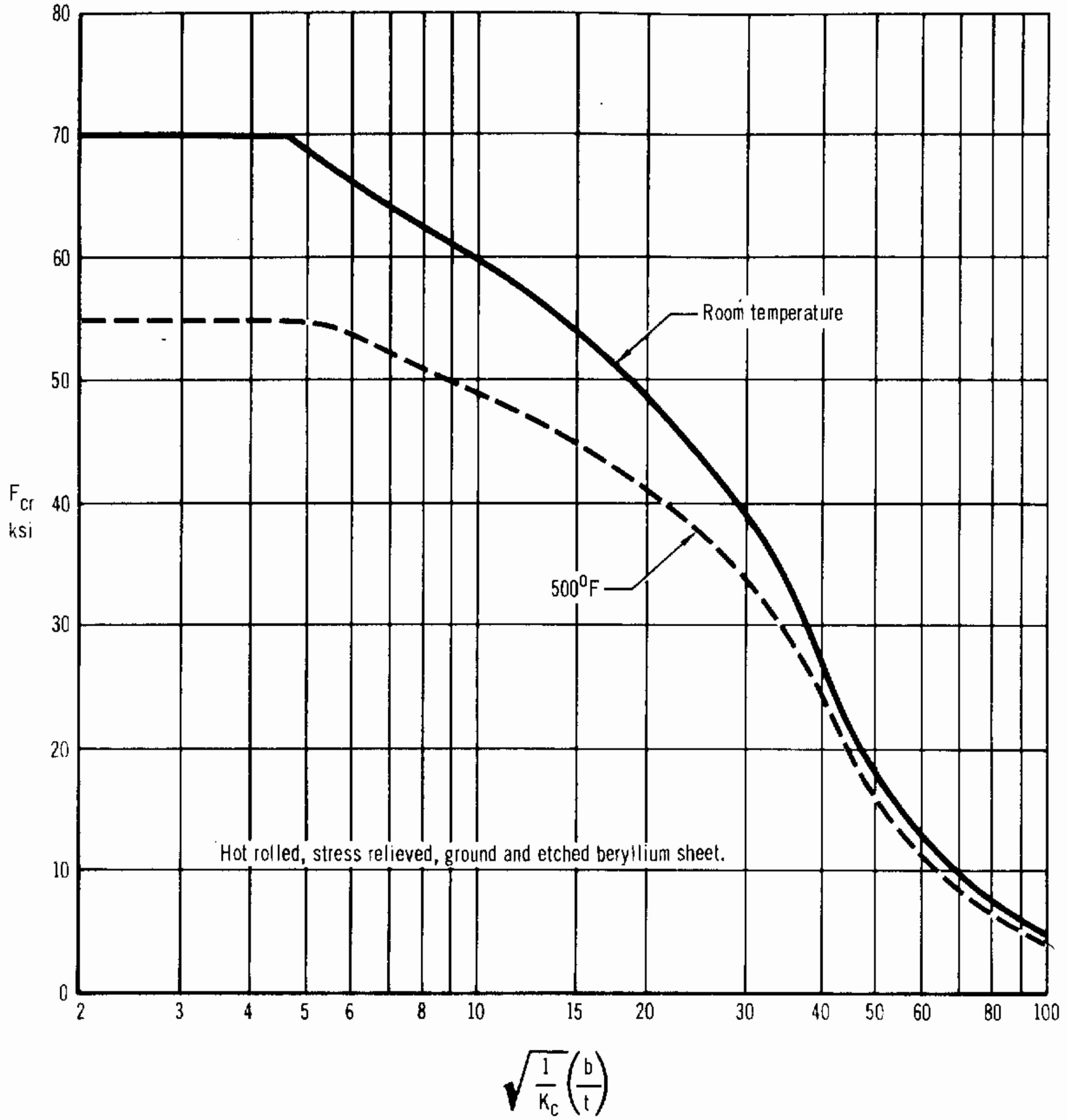

Figure 7 – Design Curves for Initial Compression Buckling Strength of Flat, Unstiffened Beryllium Panels

3.6 Allowable Crippling Stresses - As a result of the tests performed in Reference 2 program, design curves and methods of analysis have been developed for prediction of the crippling strength of stiffening members and stiffened flat panels fabricated of beryllium sheet material. The design curves and methods of analysis given in the following paragraphs were found to give accurate strength predictions for beryllium structures in the temperature range from -65° (219°K) to 500°F (533°K).

3.6.1 Crippling of Stiffening Elements - Virtually any stiffening member (angles, channels, Z-sections, etc.) that can be fabricated from beryllium sheet consists of no-edge-free and/or one-edge-free elements. Nondimensional design curves for determining the crippling stress of no-edge-free and one-edge-free beryllium stiffener elements are given in Figure 8. These design curves may be used for strength predictions at any temperature from -65°F (219°K) to 500°F (533°K) at which beryllium material properties F_{tu}, F_{cy}, and E are known. The following precedure is used to determine the average crippling stress of the stiffener ($F_{cc_{st}}$) and the allowable (ultimate) load of the member.

- Knowing the stiffener geometry and material properties, calculate the average crippling stress ($F_{cc_{st}}$) of the stiffener from the equation:

$$F_{cc_{st}} = \frac{A_1 F_{cc_1} + A_2 F_{cc_2} + \ldots\ldots\ldots A_n F_{cc_n}}{A_1 + A_2 + \ldots . A_n}$$

  A_1, A_2, ... A_n are the actual areas of stiffener elements.

  F_{cc_1}, F_{cc_2}, ... F_{cc_n} are the crippling stresses as determined from Figure 8 for stiffener elements 1, 2, ... n.

- The allowable compression load for the stiffener is:

  $P_a = F_{cc_{st}} A_{st}$

  where $A_{st} = A_1 + A_2 + \ldots A_n$

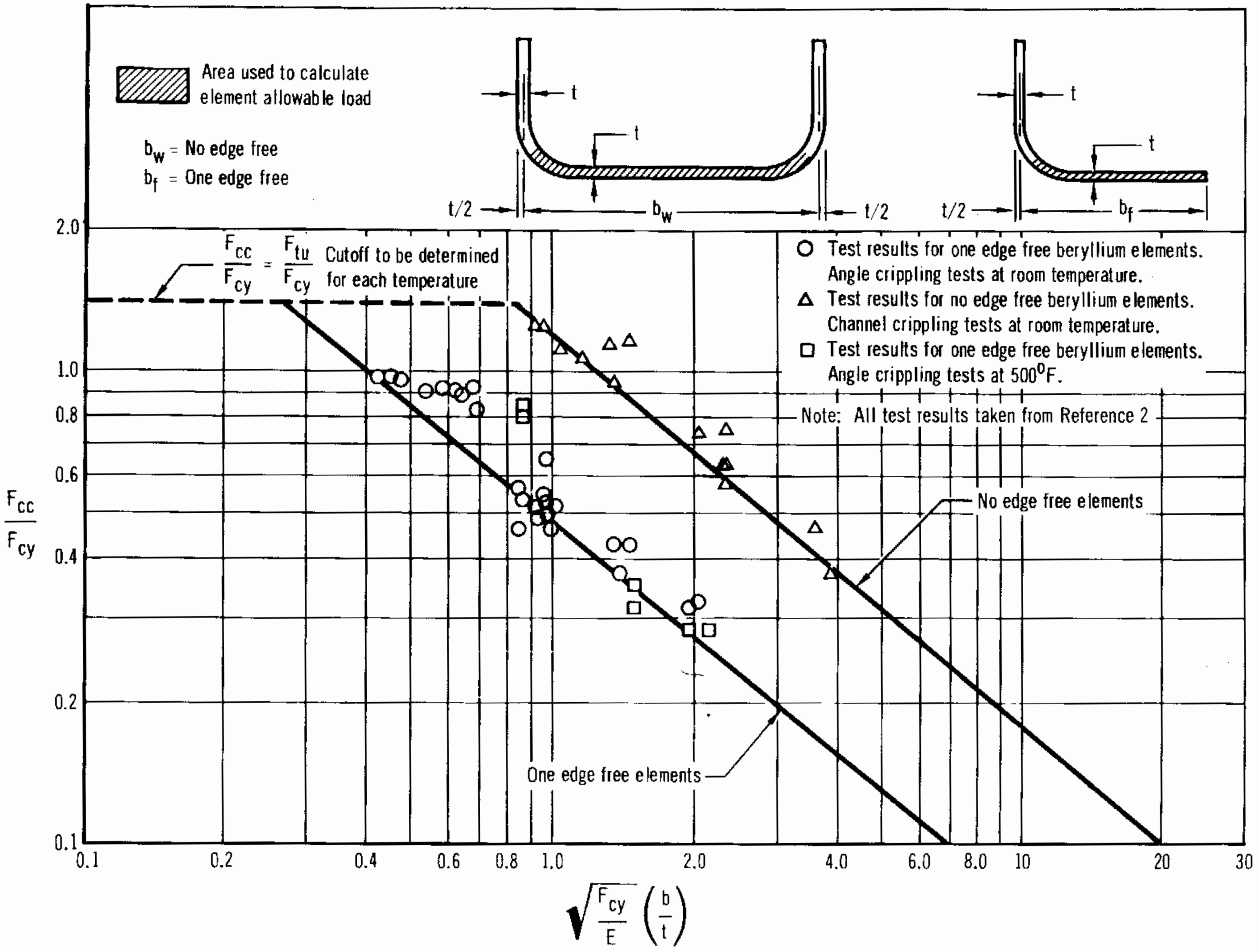

Figure 8 – Nondimensional Crippling Design Curves for Beryllium

3.6.2 Crippling of Stiffened Flat Panels with Constant Skin Thickness -

The total load carried by a stiffened panel is equal to the sum of the loads carried by the stiffeners and by the skin. The crippling strength of the stiffener can be predicted from the design chart, Figure 8. The load carried by the skin can be approximated by use of an "effective width" of skin acting at the stiffener stress. The design chart for determining the "effective width" of skin (taken from Reference 9) is presented in Figure 9. The method used to calculate the crippling strength of panels having skin of constant thickness (like Configuration I shown in Figure 10) is presented below:

- Calculate the average crippling stress for each stiffener as described previously.
- Enter the design chart, Figure 9, for determining the "effective width" of skin acting at the stringer stress. With the stiffener stress, F_{cc}, read the value $2w_e/t$.

  Note: $(\eta E)_{skin} / \sqrt{(\eta E)_{stiff.}} = \sqrt{(\eta E)_{skin}}$ when both the skin and stiffener are of the same material and are at the same temperature. "w_e" is the effective width of skin on either side of the stiffener acting at the same stress as the stiffener. "t' is the skin thickness. If "w_e" is greater than half the stiffener spacing (b) i.e., if effective widths overlap, use $w_e = b/2$.
- Calculate the load carried by the effective skin:

  $$P_{sk} = F_{cc_{st}} \; 2w_e t$$
- The crippling strength of the stringer and its effective skin is:

  $$P = P_{st} + P_{sk}$$
- The total load carried by a panel with a number of stiffeners is:

  $$P_{total} = \Sigma P$$

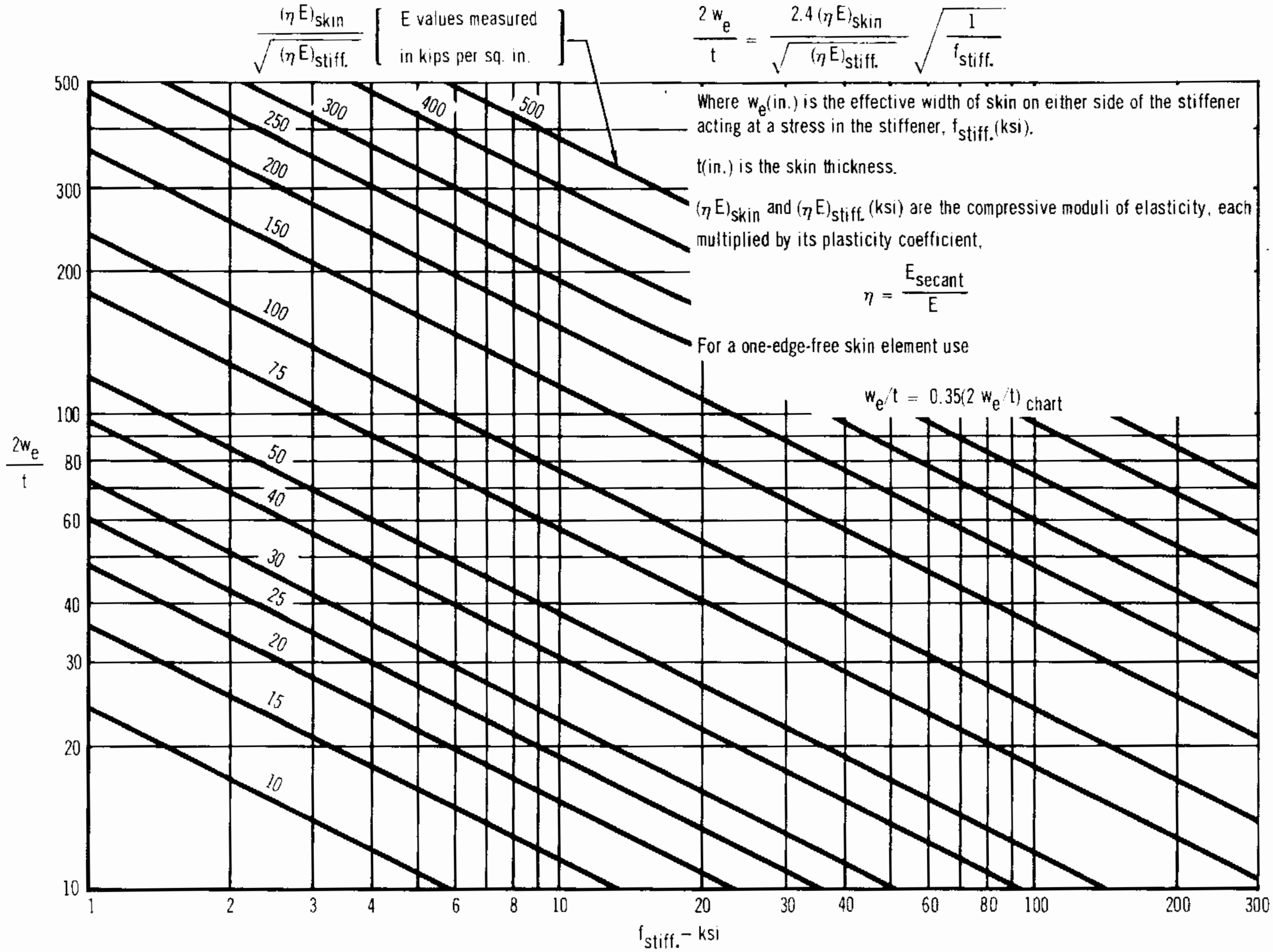

$$\frac{2\,w_e}{t} = \frac{2.4\,(\eta E)_{skin}}{\sqrt{(\eta E)_{stiff.}}}\sqrt{\frac{1}{f_{stiff.}}}$$

Where w_e(in.) is the effective width of skin on either side of the stiffener acting at a stress in the stiffener, $f_{stiff.}$(ksi).

t(in.) is the skin thickness.

$(\eta E)_{skin}$ and $(\eta E)_{stiff.}$ (ksi) are the compressive moduli of elasticity, each multiplied by its plasticity coefficient,

$$\eta = \frac{E_{secant}}{E}$$

For a one-edge-free skin element use

$w_e/t = 0.35(2\,w_e/t)$ chart

Figure 9 – Effective Width of Stiffened Sheet

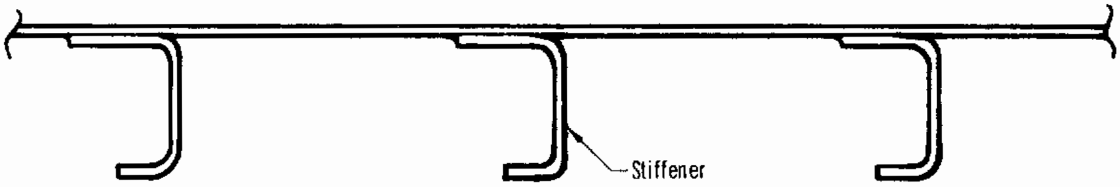

Configuration I
Stiffened panel with constant skin thickness

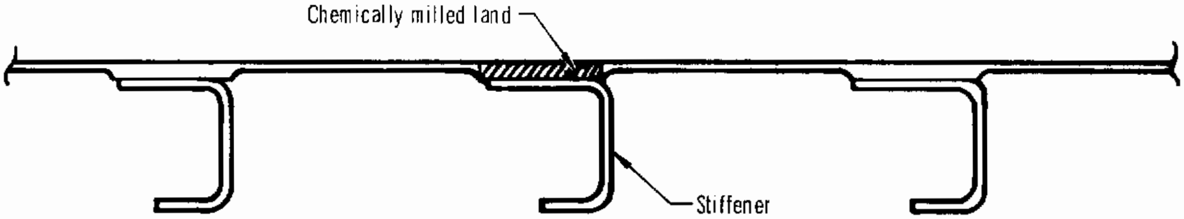
Chemically milled land
Stiffener

Configuration II
Stiffened panel with chemically milled lands

Figure 10 – Stiffened Panel Configurations

3.6.3 Crippling of Panels with Chemically Milled Lands - If countersunk fasteners are to be used to join thin beryllium skins to the substructure, it may be necessary to provide a chemically milled land (local increase in skin thickness) to avoid the knife-edge effect in the skin at the base of the countersink. This land does not necessarily result in a weight penalty. The increased skin area resulting from the land will carry its share of the load and, in effect, increase the "effective area" of the skin in compression. The method used to predict the crippling strength of stiffened panels with skin having chem-milled lands (Configuration II in Figure 10) is presented below:

(1) Calculate the stiffener crippling stress and the effective skin width as described previously for panels having constant skin thickness. For panel skins with chem-milled lands, the "effective width" is measured from the edge of the chem-milled land instead of from the skin-stiffener fastener line.

(2) Calculate the allowable load of the panel assuming the stiffener, the land, and the effective skin are acting at the stiffener crippling stress.

$$P = F_{cc_{st}} (A_{st} + 2w_e t + A_{land})$$

(3) The total load carried by a panel with a number of stringers is:

$$P_{total} = \Sigma P \text{ (from (2))}$$

3.7 Analysis of Beryllium Lugs - Nondimensional design curves for prediction of the static strength of symmetrically loaded lugs fabricated of beryllium sheet are presented in Figure 11. Given the lug geometry and the ultimate tensile stress (F_{tu}) of beryllium, the designer can predict the allowable lug load from the equation:

$$P_a = \frac{F_{br}}{F_{tu}} (F_{tu})\ Dt$$

$\frac{F_{br}}{F_{tu}}$ is the minimum value read from Figure 11 for $\frac{R}{D}$ or $\frac{W}{D}$.

F_{tu} is the ultimate tensile stress for beryllium sheet at temperature considered.

D is the hole diameter.

t is the lug thickness.

Note that the allowable load can be predicted for any temperature provided the ultimate tensile stress (F_{tu}) is known for the temperature considered. The element tests described in Section IV verify the adequacy of the lug design curves in the temperature range from -65°F (219°K) to 500°F (533°K). If design temperatures are significantly below -65°F (219°K) or above 500°F (533°K), the lug strength should be substantiated by test.

3.8 Joint Design Criteria - Mechanical fastening and adhesive bonding were used for joining the beryllium rudder structural members. These are, at present, the two most satisfactory means for joining beryllium. Adhesive bonding was used to join the trailing edge honeycomb core to the face skins, the rear spar, and the closure members. Mechanical fasteners were used to join all members forward of the rear spar and to attach the trailing edge assembly to the forward torque box structure.

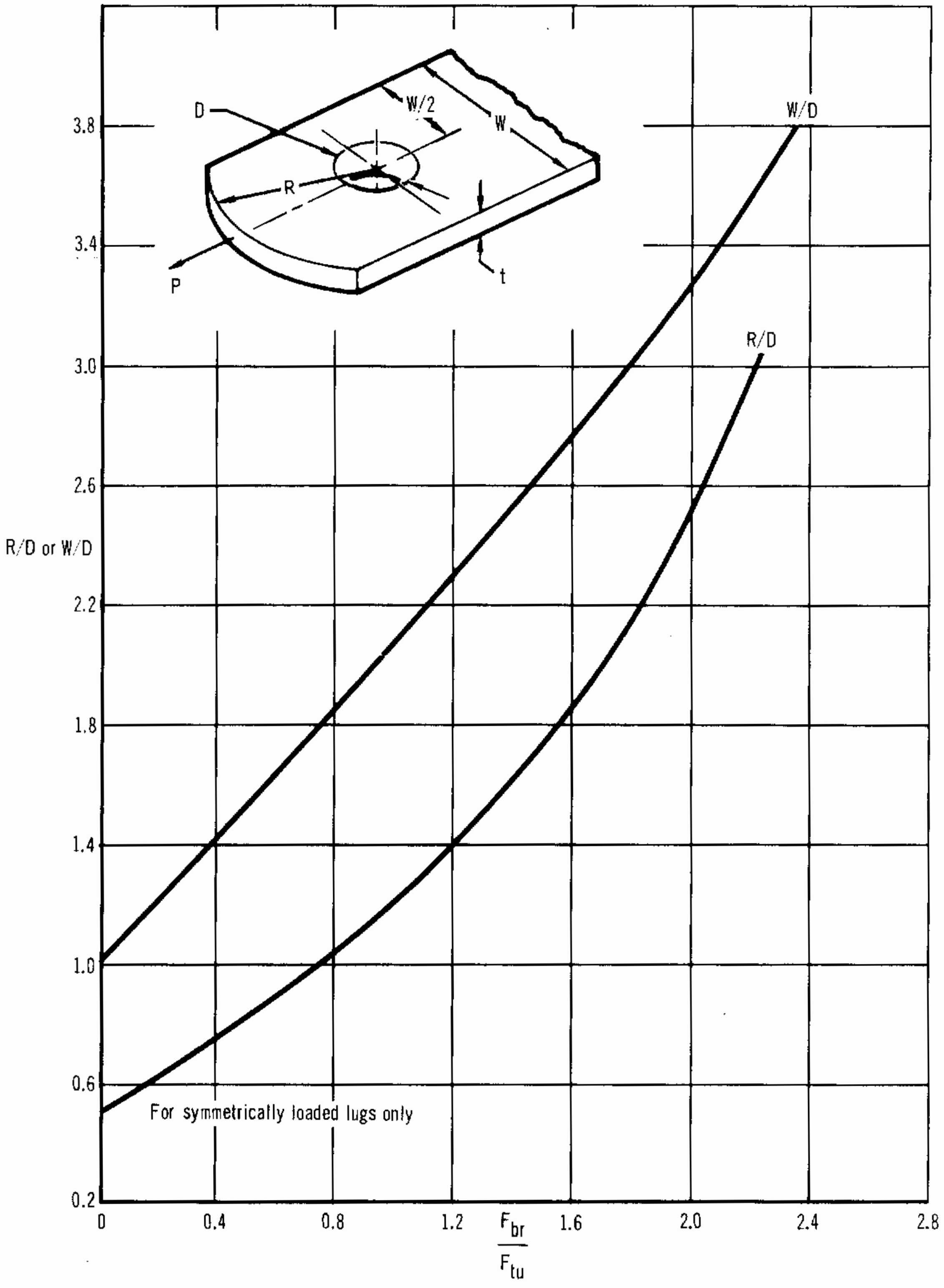

Figure 11 – Beryllium Lug Design Chart

Because the joints are relatively lightly loaded, except in a few areas, and the temperatures do not exceed 270°F (405°K), it was possible to use aluminum fasteners extensively. Aluminum cherry rivets were used in areas where blind fasteners were required or where space limitations precluded the installation of non-blind fasteners. Aluminum Hi-Shear rivets or solid aluminum rivets were used in all lightly loaded joints not requiring blind fasteners. Hi-Lok fasteners were used in highly loaded joints, and steel Jo-bolts were used where high strength blind fasteners were required.

Special consideration must be given to the geometry of the hole and/or countersink provided for mechanical fasteners. The edges of the hole should be chamfered so that no interference will exist at the fastener head-to-shank fillet radius, particularly when steel or titanium fasteners are used. Interference between the head-to-shank fillet radius and the edge of the hole can produce local damage in beryllium and can prevent the fastener from seating properly on installation. The depth of the countersink for flush fasteners must be at least .015 in. (.381mm) less than the thickness of the material to avoid a knife edge at the base of the countersink. If countersink depth exceeds material thickness, cracking or chipping of the knife edge will invariably occur. To avoid this condition, it is necessary to provide extra thickness in the beryllium at the countersunk fasteners.

Although some results have been published, there is not sufficient test data available to permit establishment of firm design allowables for any of the many possible mechanically fastened beryllium joint configurations. Until such data is generated, the designer and stress analyst will have to rely on conservative engineering estimates based on limited available information. The strength of critically loaded joints should be verified by element testing.

The following criteria for computing allowable loads for mechanically fastened beryllium joints have been found to yield conservative strength predictions when compared to available test results.

3.8.1 Fastener Shear Critical - Use fastener producers' minimum guaranteed shear strength.

3.8.2 Sheet Bearing Critical - The ultimate bearing stress of beryllium sheet is approximately equal to that of 7075-T6 aluminum sheet at room temperature; $F_{bru} \approx 145$ ksi (1000 MN/m^2). Therefore, when sheet bearing is critical, the beryllium joint strength is assumed equal to that of an identical 7178-T6 aluminum joint for both protruding head and flush fasteners. The joint allowables for many fastener types and aluminum sheet thickness combinations are readily available in MIL-HDBK 5 and company structures handbooks. To account for the effects of temperature, multiply the room temperature allowable by the ratio of ultimate bearing stress at temperature to ultimate bearing stress at room temperature.

3.8.3 Sheet Tension Critical - Since beryllium is notch sensitive at temperatures below approximately 400°F (478°K), joints subjected to tension loads in the plane of the sheet perpendicular to the fastener line may fail at loads less than those predicted by the fastener shear or sheet bearing criteria given above. This is particularly true when eccentric loading exists. To avoid a tension failure in the beryllium sheet between fasteners, the net tension stress should not exceed the notched tensile strength of the material. This requirement will sometimes result in a weight penalty since the material thickness will have to be increased locally at the fasteners to reduce net tension stresses to acceptable levels. The maximum net tension stress between fastener holes in the beryllium sheet should not be allowed to exceed:

- $f_{t_{net}} = 50$ ksi (345 MN/m^2) in joints having no eccentricity
- $f_{t_{net}} = 200$ ksi (1379 MN/m^2) in eccentrically loaded joint

where $f_{t_{net}} = \frac{P}{A} + \frac{Mc}{I}$

M = bending moment due to eccentric loading with no joint deflection

A = net material cross-sectional area between fasteners

These criteria have been found to be approximately 10% conservative when applied to element test specimens tested at McDonnell during this program.

3.8.4 Adhesive Bonded Joints - Beryllium is readily bonded with a number of commercially available adhesive systems. Tests of beryllium lap shear specimens bonded with the FM-61 epoxy adhesive system (see Section IV) and with the HT-424 epoxy-phenolic adhesive system (in Reference 2 program) resulted in bond shear stresses significantly higher than those obtained in tests of aluminum lap shear specimens bonded with the same adhesive systems. The design lap shear stresses for beryllium joints bonded with the FM-61 and HT-424 adhesive systems are given in Table 4. These design values are 80% of the minimum values obtained in the tests.

TABLE 4
DESIGN SHEAR STRESSES FOR BONDED BERYLLIUM LAP JOINTS

Adhesive	Temperature (°F)	Design Stress (psi)
FM-61	75 -65	3000 4300
HT-424	75 500	3200 1350

4. Beryllium Rudder Corrosion Protection Process

The finish requirements for corrosion protection of an F-4 beryllium rudder, subjected to flight service environment, were established from the results of the element test program discussed in Section IV of this report. It should be noted that the rudder fabricated and tested in this program was not provided with the corrosion protection finish described below, since no need for such protection existed. A flight test rudder, however, would have to undergo this process (or its equivalent) to protect it against the corrosive flight environment. This process is expected to adequately supply such protection. Following is a description of the corrosion protection process.

4.1 General Requirements

4.1.1 Finishing Sequence - Whenever possible, all forming, machining, drilling, welding, chemical milling, or other operations that could damage the finish system should be accomplished prior to the application of the finish system. The organic finish (Subsection 4.3) shall be applied as soon after chemical treatment (Subsection 4.2) as possible.

4.1.2 Treatment of Cut or Machined Surfaces - Where treated aluminum or beryllium is cut, machined or chemically milled through the protective coating, the affected surface shall be touched up with a brush applied alodine solution meeting the requirements of MIL-C-5541 and the same paint as is on the adjacent surface.

4.1.3 Protection During Fabrication and Storage - Aluminum parts and assemblies shall be protected during fabrication and temporary storage by treating with an alodine solution. Beryllium parts shall be treated with the alodine solution as soon as possible after final etch. The solution shall meet the requirements of MIL-C-5541 and may be a brush-on type or applied by immersion.

4.1.4 Metal Wool Precautions - Aluminum wool is permitted on beryllium, but steel and stainless steel wool are prohibited.

4.2 Inorganic Treatment of Beryllium

4.2.1 General - Beryllium shall be treated with an alodine solution meeting the requirements of MIL-C-5541. The method of applying this chemical film (chromate conversion coating) shall be by immersion. Whenever possible, parts shall be treated individually. Immersion of assemblies shall be avoided because dissimilar metals on the assembly may cause corrosion when in solution. Following is a description of the alodine solution to be used for immersion applications.

Chemical	Concentration	Temperature	pH
Turcoat 4178	9 lbs./100 gal. (11 kg/m^3) of tap water	60-95°F (289-308°K)	1.7-2.0
Nitric Acid(40°Bé)	2-4 pints/100 gal. (2.5-5 dm^3/m^3) of solution		

Surfaces to be coated shall be solvent or vapor degreased, alkaline cleaned and rinsed. An acid etch may also be used. The deoxidizing procedure in the alodine process is prohibited for beryllium.

4.2.2 Exceptions - Touch-up of inorganic treated beryllium which has been damaged shall be accomplished with a brush applied alodine solution meeting the requirements of MIL-C-5541. Following is a description of the brush applied alodine solution.

Material	Concentration	Temperature	pH
Alodine 1200 Anchem Products, Inc.	2-3 oz./gal. (15-22kg/m^3)	Room Temperature	1.50-1.75
Water	Remainder		

Surfaces to be coated shall be water scrubbed with a nylon abrasive pad to obtain a water break free surface. The solution shall be applied with a bristle brush or cheesecloth to the water wet surface.

Beryllium in the bonded honeycomb trailing edge assembly that is not treated in the bonding process shall be treated with the brush applied alodine solution. The treatment shall be accomplished after closure of the bonded honeycomb assembly.

Aluminum metals in the beryllium rudder assembly shall be treated with an alodine solution meeting the requirements of MIL-C-5541.

4.3 Organic Treatment of Beryllium

4.3.1 Internal Surfaces - Those areas not exposed to exterior environment shall be coated with two coats of MIL-P-8585 zinc chromate primer.

4.3.2 Exterior Surfaces - Those areas exposed to external environment shall be coated with one coat of MMS-405 epoxy primer, color yellow and two to three coats of MMS-405 epoxy enamel, color #17875.

4.3.3 Dissimilar Metal Protection - For dissimilar metal purposes, beryllium is considered as follows:

Similar to - aluminum, aluminum alloys, and cadmium

Dissimilar to - magnesium, titanium, steel, stainless steel,
copper alloys, chromium, nickel and tin.

Dissimilar metal contacts require a minimum of two coats of paint on each faying surface. The use of MIL-S-8802 sealant at the dissimilar metal faying surface is a substitute for the paint requirement.

Slip fits, press fits and threaded inserts that form dissimilar metal contacts shall be assembled using wet MIL-P-8585 primer or wet MMS-405 epoxy primer.

The interior surfaces of the beryllium skins on the bonded trailing edge assembly shall be cleaned, primed and bonded as specified in the bonding process and do not require any other treatments.

Similar metal contacts do not require any additional protection beyond the requirements established in Subsection 4.3.1 and 4.3.2.

4.3.4 Fasteners: Interior Surfaces - Fasteners that are dissimilar to beryllium per Subsection 4.3.3 shall be installed with wet MIL-P-8585 primer. Fasteners that are similar to beryllium do not require organic protection at the time of installation.

4.3.5 Fasteners: Exterior Surfaces - All permanent fasteners shall be installed with wet MIL-S-8802 sealant. All removable fasteners shall have an epoxy primer coating (a mixture of one volume of 515-006 Super Koropon Fluid Resistant Primer and one volume of 910-117 Activator - DeSoto Chemical Coatings, Inc.), and the countersinks shall be alodined per MIL-C-5541 prior to fastener installation.

4.3.6 Sealing - All mold line butt joints of the beryllium rudder assembly shall be sealed with MIL-S-8802 sealant.

SECTION III

RUDDER DESIGN AND ANALYSIS

1. Introduction

In the design phase of this program, complete interchangeability of the beryllium and aluminum rudders was postulated to provide for eventual flight testing. Accordingly, the layout of the beryllium rudder was controlled by the requirements of compatibility with the F-4 fin structure and with the rudder actuation system, resulting in the envelope and the support geometry of the beryllium rudder being virtually identical with the production configuration.

In defining the extent of beryllium utilization in the rudder structure, shown schematically in Figure 12, the primary objective was to save the maximum amount of weight within the limits prescribed by manufacturing state-of-the art, material availability, and reasonable costs. Since the F-4 rudder is a mass-balanced control surface, all weight saved aft of the hinge line results in additional weight savings due to a corresponding reduction in balance weights. Therefore, every effort was extended to convert the aluminum structure aft of the hinge line to beryllium. It may be seen from Figure 12 that this conversion was virtually 100%, the exception being the trailing edge honeycomb core, the mechanical fasteners, and some shear clips. The first two items are not currently available in beryllium, and the costs of beryllium shear clip fabrication would have been prohibitive for the weight to be saved. Forward of the hinge line, no redesign to beryllium was deemed desirable. Any structural weight saved in this area would be nullified by a corresponding increase in balance weights, and the manufacturing difficulties and costs associated with the fabrication of such items as the leading edge ribs were

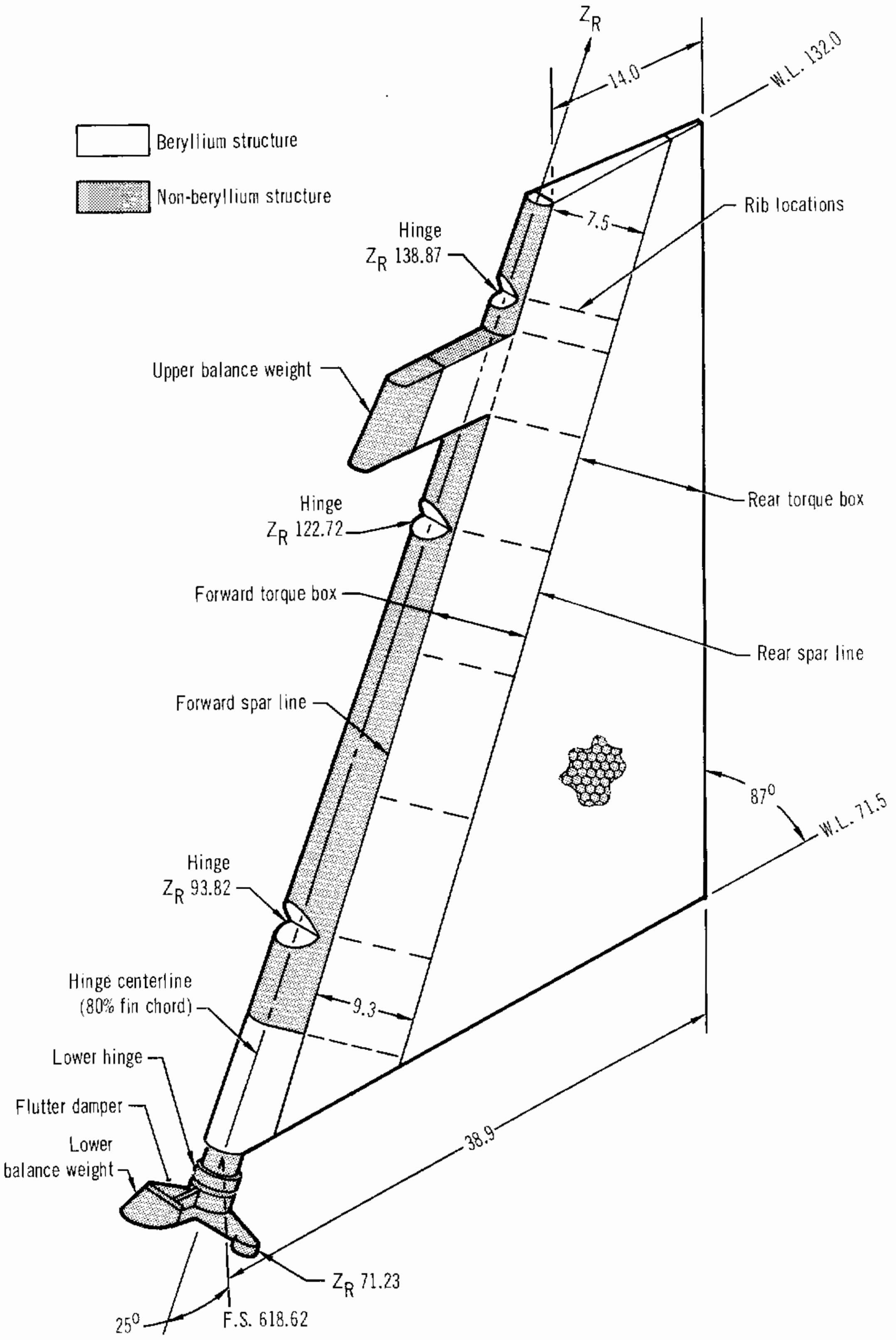

Z_R
14.0
W.L. 132.0
▭ Beryllium structure
▨ Non-beryllium structure
Hinge
Z_R 138.87
7.5
Rib locations
Upper balance weight
Rear torque box
Hinge
Z_R 122.72
Forward torque box
Rear spar line
Forward spar line
87°
W.L. 71.5
Hinge
Z_R 93.82
Hinge centerline (80% fin chord)
9.3
Lower hinge
Flutter damper
Lower balance weight
38.9
Z_R 71.23
25°
F.S. 618.62

Figure 12 – Beryllium Rudder Structure Schematic

considered excessive. An exception was made for the lower section of leading edge skin which transfers torque into the rudder, because it contributes significantly to overall torsional stiffness. The lower rudder fittings were left in aluminum due to difficulties in procurement of the material required (forgings and/or extrusions) and the associated high costs. The detail drawings of the beryllium rudder are shown in the Appendix.

The structural integrity of the beryllium rudder design was verified under loading conditions identical to those established for the production aircraft. The major design considerations and the design loading conditions are discussed in subsections 2 and 3, respectively, followed by the strength, structural dynamics and control dynamics analyses, subsections 4, 5, and 6, respectively. Mass balancing of the rudder, the rudder moment of inertia, and the weight are discussed in subsections 7, 8, and 9, respectively. It is shown that the beryllium rudder is 40.4% lighter than its aluminum counterpart.

2. Design Considerations

The beryllium rudder, like its production aluminum counterpart, is a two-cell torque box supported along its leading edge by four hinges. The structural arrangement of the beryllium rudder is similar to that of the production rudder; the forward torque box is of conventional multirib-skin-spar construction, whereas the aft torque box structure consists of skin-faced honeycomb core with edging members. The forward torque box was designed to carry the primary rudder loads, with the front spar at the hinge line as the main bending member. The aft torque box was designed to distribute local airloads into the forward torque box. Figures 13 and 14 show the beryllium and aluminum rudder structures, respectively, and illustrate their major differences.

Both the aluminum and beryllium rudders were designed to be actuated by a hydraulic power cylinder attached to the rudder torque tube at the lower hinge point. Two balance weights (locations shown in Figures 13 and 14) are provided for rudder static and dynamic balance.

The production aluminum rudder requires two dampers to prevent flutter. These are located in the area of the lower hinge and just below the upper balance weight (see Figure 14). Because of its increased stiffness and reduced weight, the beryllium rudder requires a damper at the lower hinge only. Furthermore, as a direct result of beryllium utilization and the corresponding increase in stiffness, the number of stiffening ribs was reduced from 17 in the production rudder to 10 in the beryllium rudder (Figures 13 and 14).

In fabricating the beryllium rudder, extensive use was made of chem-milling to provide effective skin-cap areas where needed, to save weight in shear panels where thinner gauges could be utilized, and to preclude the occurrence of knife-edges and corresponding fatigue problems at countersunk fasteners. Aluminum Hi-Shear and Cherry rivets were used for joining most structural

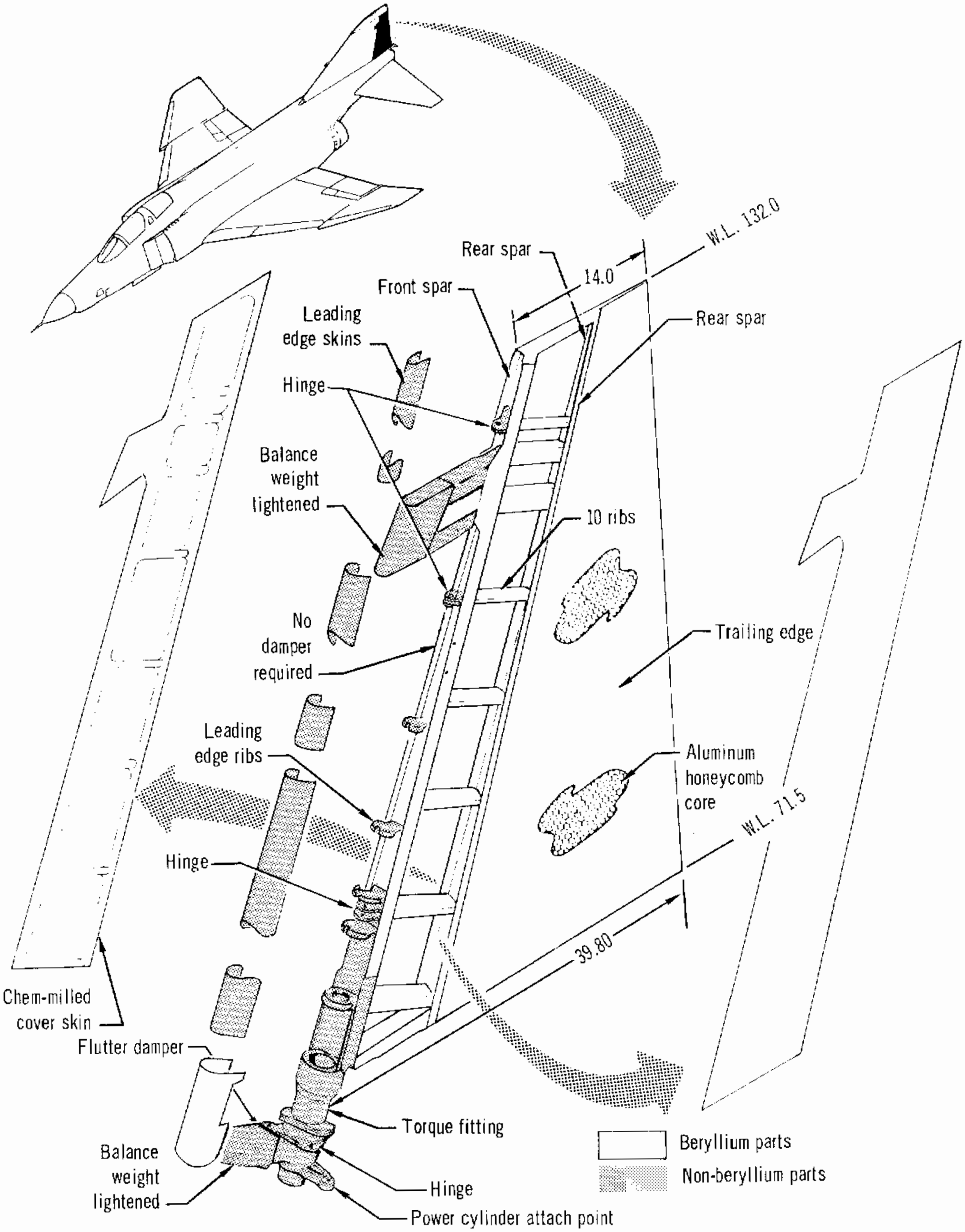
Rear spar
Front spar
14.0
W.L. 132.0
Leading edge skins
Rear spar
Hinge
Balance weight lightened
10 ribs
No damper required
Trailing edge
Leading edge ribs
Aluminum honeycomb core
W.L. 71.5
Hinge
39.80
Chem-milled cover skin
Flutter damper
Torque fitting
Balance weight lightened
Hinge
Power cylinder attach point
☐ Beryllium parts
▨ Non-beryllium parts

Figure 13 – F-4 Beryllium Rudder Structural Configuration

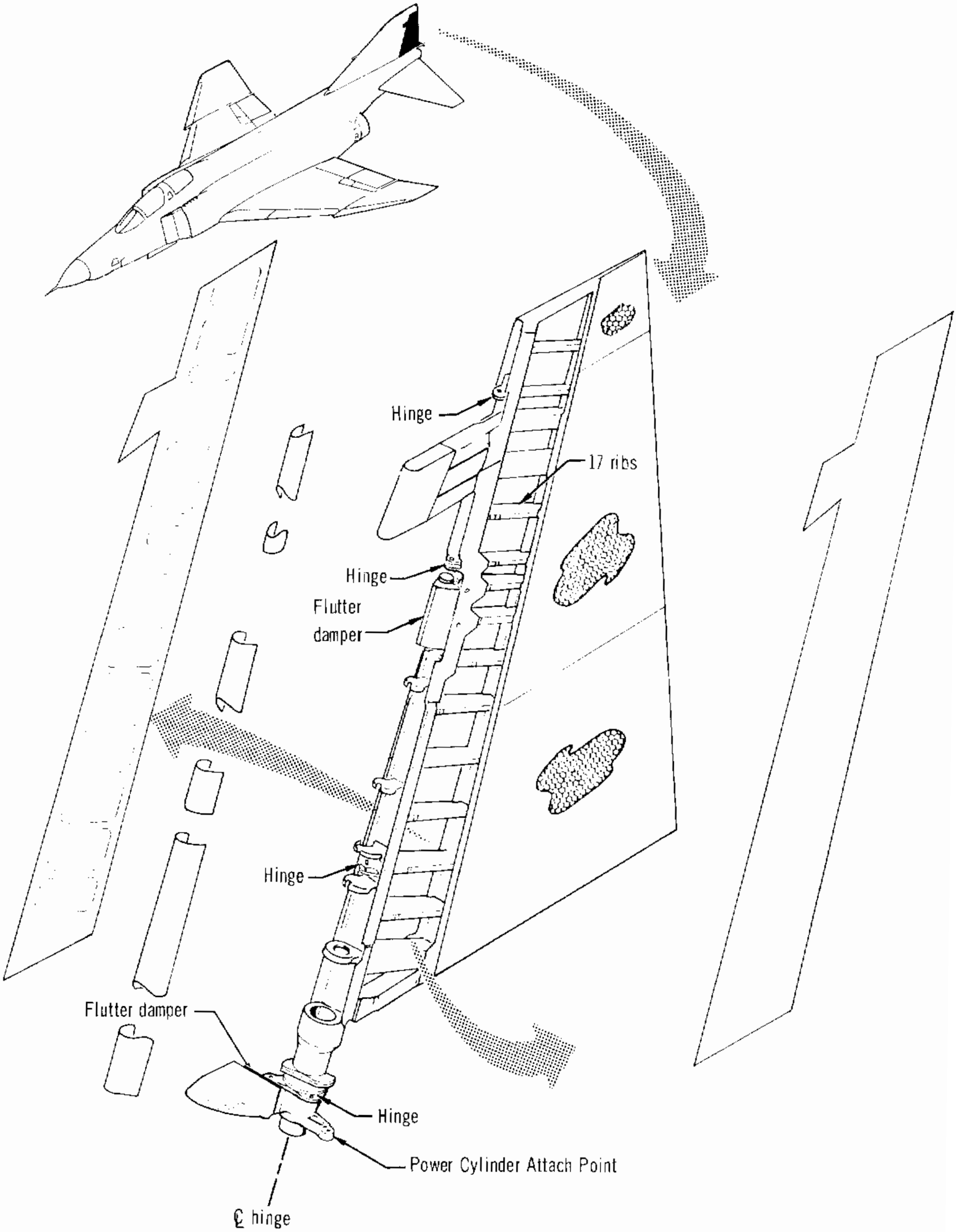
Hinge
17 ribs
Hinge
Flutter damper
Hinge
Flutter damper
Hinge
Power Cylinder Attach Point
℄ hinge

Figure 14 – F-4 Aluminum Rudder Structural Configuration

elements. High strength steel fasteners were used as required at the torque tube and hinge fitting attachments. No vibration-driven rivets were allowed due to the poor impact strength of beryllium.

3. Design Conditions

Design loading conditions, thermal environment, and requirements for vibration and flutter established for the F-4 aircraft were used in the structural analysis of the beryllium rudder, and are described below.

Design limit (maximum obtainable in service) loading conditions for the F-4 rudder are:

Condition I - Full available actuator hinge moment, with airload center of pressure at 30% chord.

Condition II - Full available actuator hinge moment, with airload center of pressure at 45% chord.

Condition III - Rolling pullout flight condition, with loads on the entire vertical tail assembly, i.e. rudder and fin.

Conditions I and II airloads are the maximum loads that can be attained, at the extreme limits of airload center of pressure travel, without exceeding the actuator output. Fin deflections are assumed to be zero for these conditions. Loading Conditions I and II result in maximum air pressures, chordwise bending, torque, and actuator load, and are critical for all of the rudder structure aft of the front spar, except the forward torque box cover skins and the backup ribs for the hinge fittings.

Condition III is critical for the rudder hinges, hinge backup ribs, front spar and forward torque box cover skins. Condition III airloads, developed on the aircraft vertical tail during the rolling pullout maneuvers, produce maximum vertical tail bending deflections. The magnitude of these deflections depends on the combined stiffness of the vertical fin and the rudder. Since the beryllium rudder is from four to six times as stiff as the production aluminum rudder (see Subsection 4), vertical tail bending deflections were calculated to be slightly less with the beryllium rudder than with the production rudder. A redundant analysis, using conventional elastic energy methods, was performed to establish the rudder hinge loads and bending moments for the Condition III rolling pullout maneuver, considering compatibility of deflections between the vertical fin and the rudder. The results of this analysis, presented in Figure 18, showed that the bending moments are larger for the beryllium rudder than for the aluminum rudder due to the greater stiffness of the former.

Running airloads on the rudder for the three design conditions are shown in Figure 15. Rudder shear and bending moment diagrams for Conditions I, II, and III are shown in Figures 16, 17, and 18, respectively. Rudder torque about the elastic axis is presented in Figure 19.

The rudder balance weights and their local support structure were designed in compliance with the production aircraft requirements: (1) static side load of ± 100 g's on the balance weight, perpendicular to the aircraft symmetry plane, and (2) 50,000 cycles of fully reversed inertial load of ± 40 g's on the balance weights, perpendicular to the aircraft symmetry plane .

The panel flutter criteria used in the design and analysis of the beryllium rudder are presented in Figure 20. These criteria, as indicated, are based on analytical as well as flight test data. A critical M/q (Mach number/dynamic pressure) ratio of .0985 was determined from the production aircraft speed-altitude diagram. Furthermore, the beryllium rudder was designed to function in a thermal environment identical to that established for the F-4 aircraft production rudder. Normal operating temperatures on the rudder range from -65°F (219°K) to 230°F (383°K) with a transient overspeed condition which could produce short time temperatures up to 270°F (405°K).

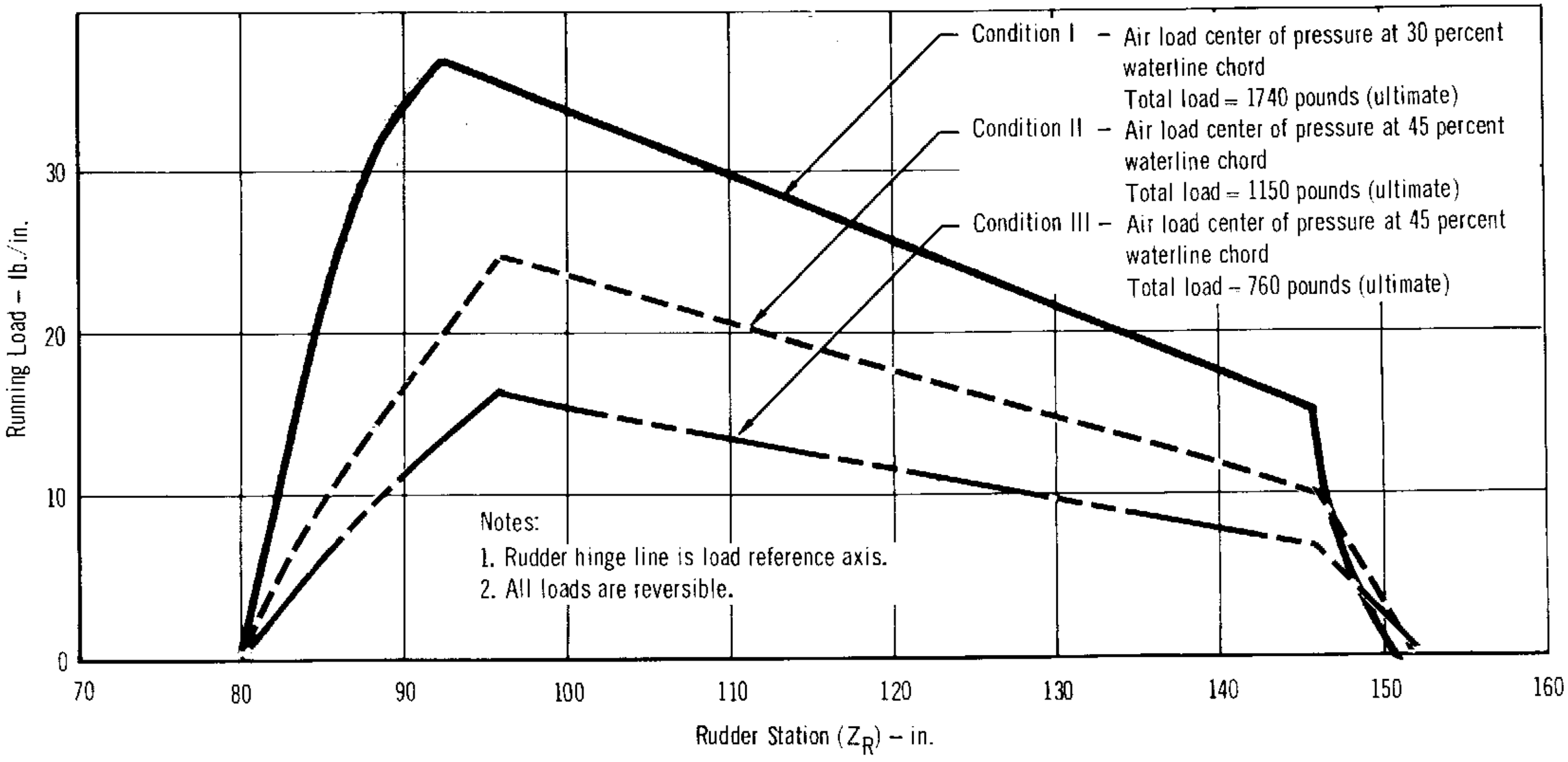

Figure 15 – Ultimate Running Load

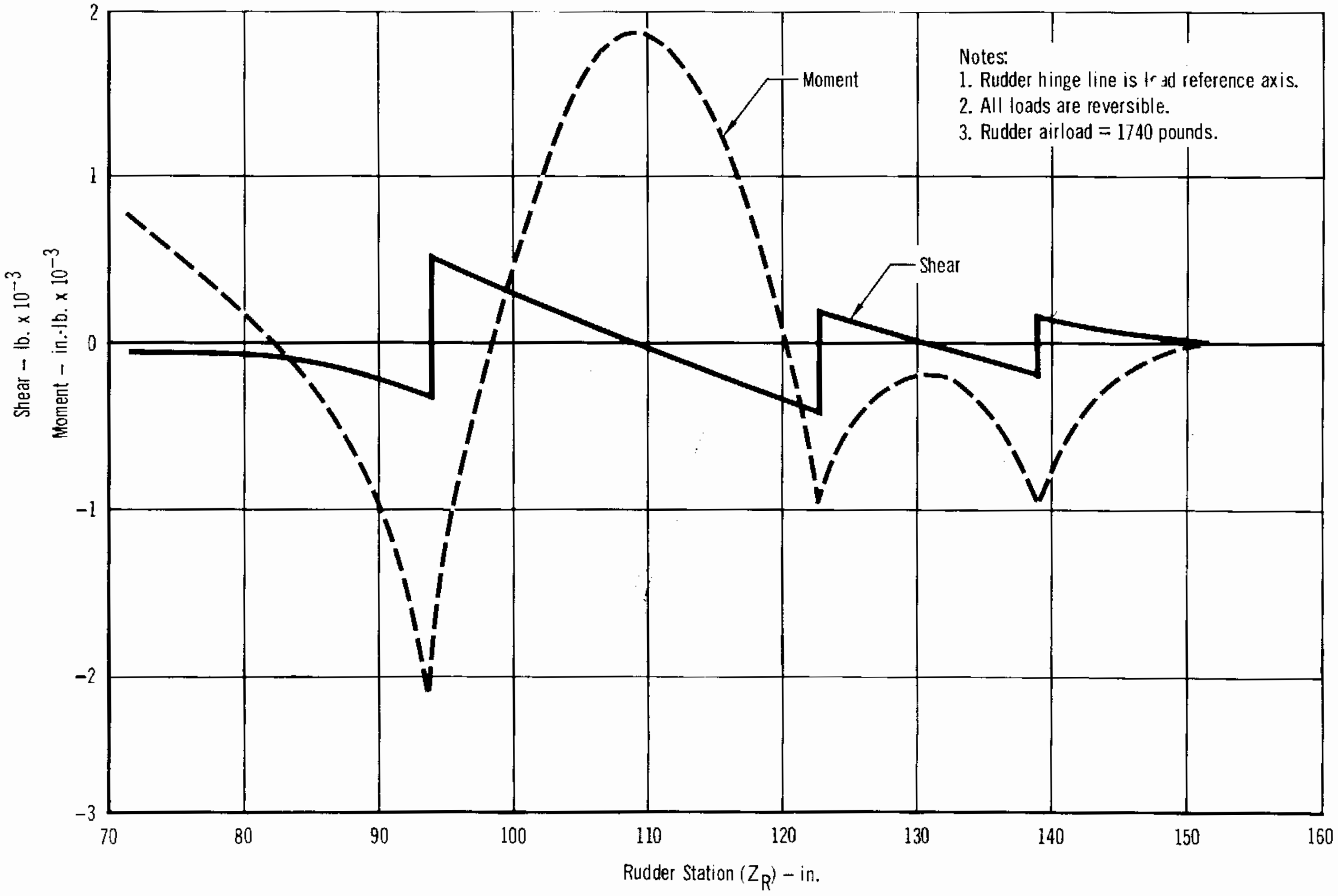

Figure 16 – Condition I Ultimate Shear and Moment

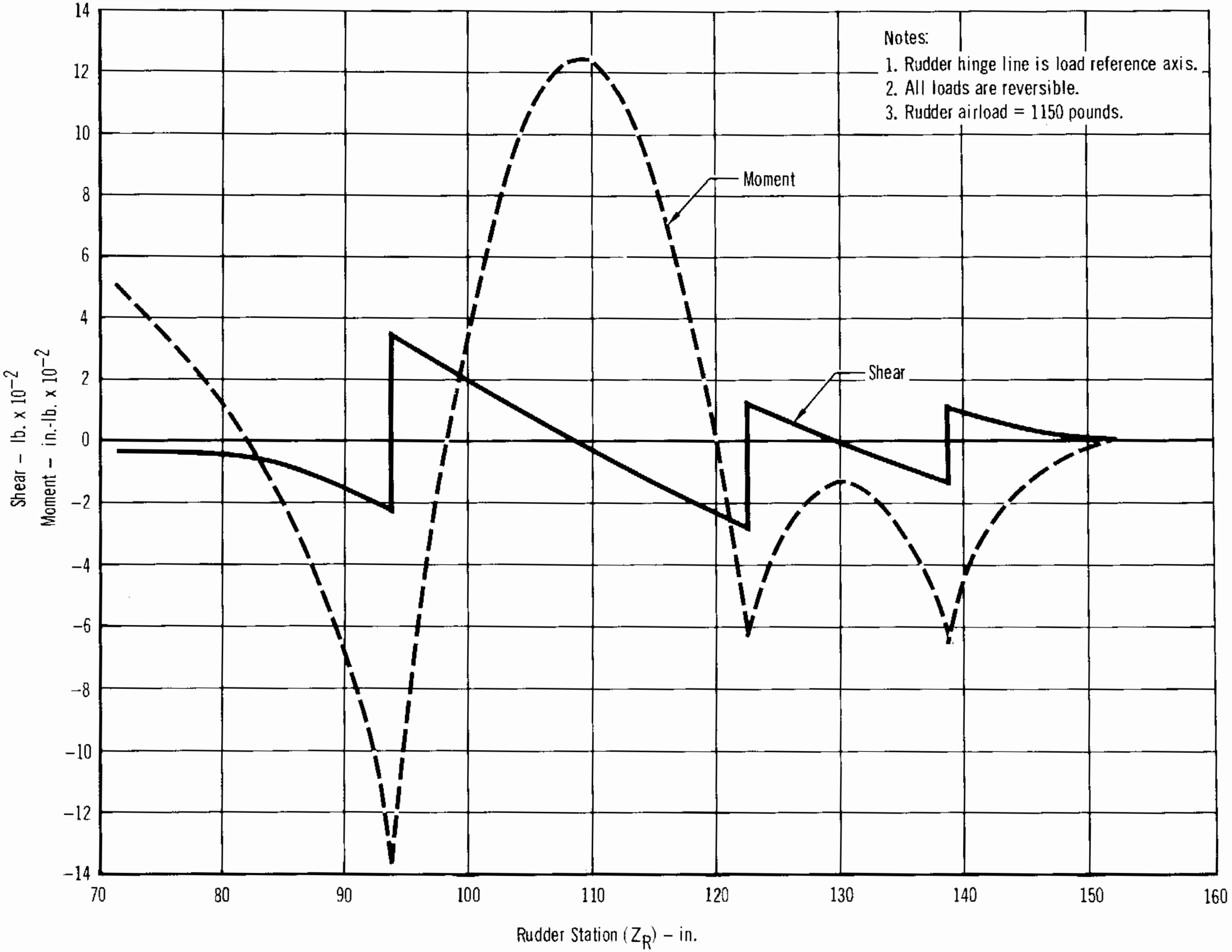

Figure 17 - Condition II Ultimate Shear and Moment

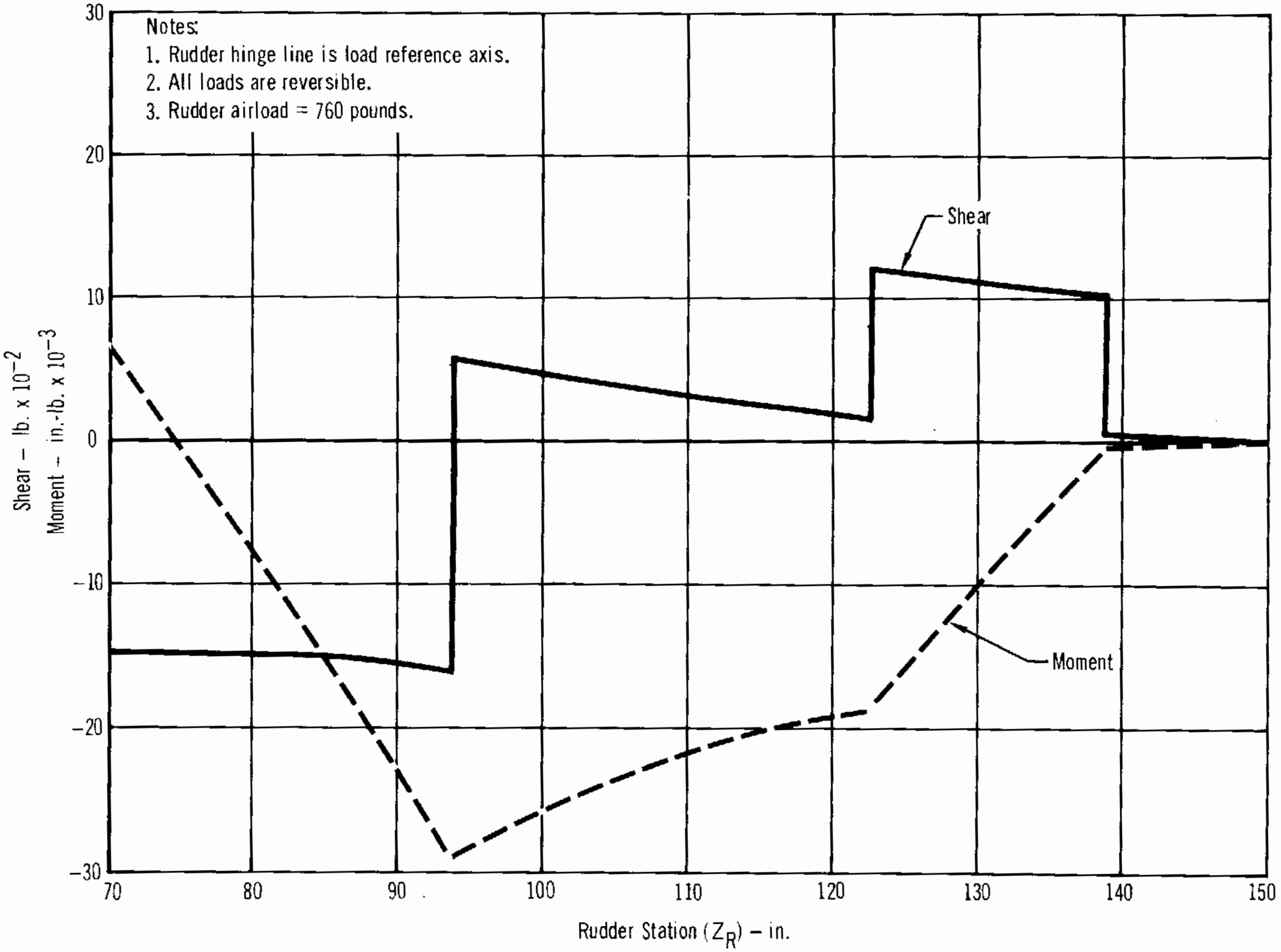

Figure 18 – Condition III Ultimate Shear and Moment

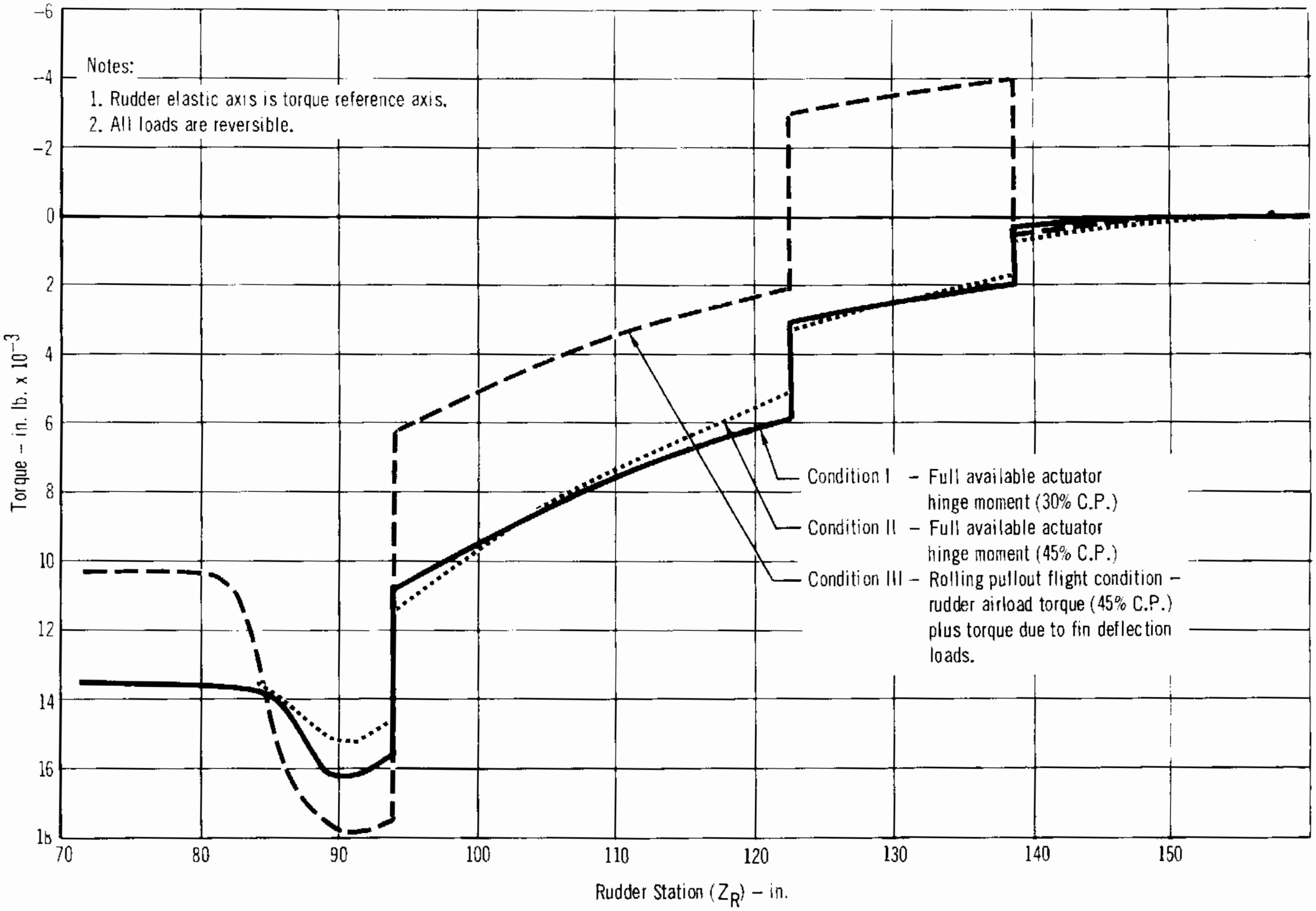

Figure 19 – Ultimate Torque

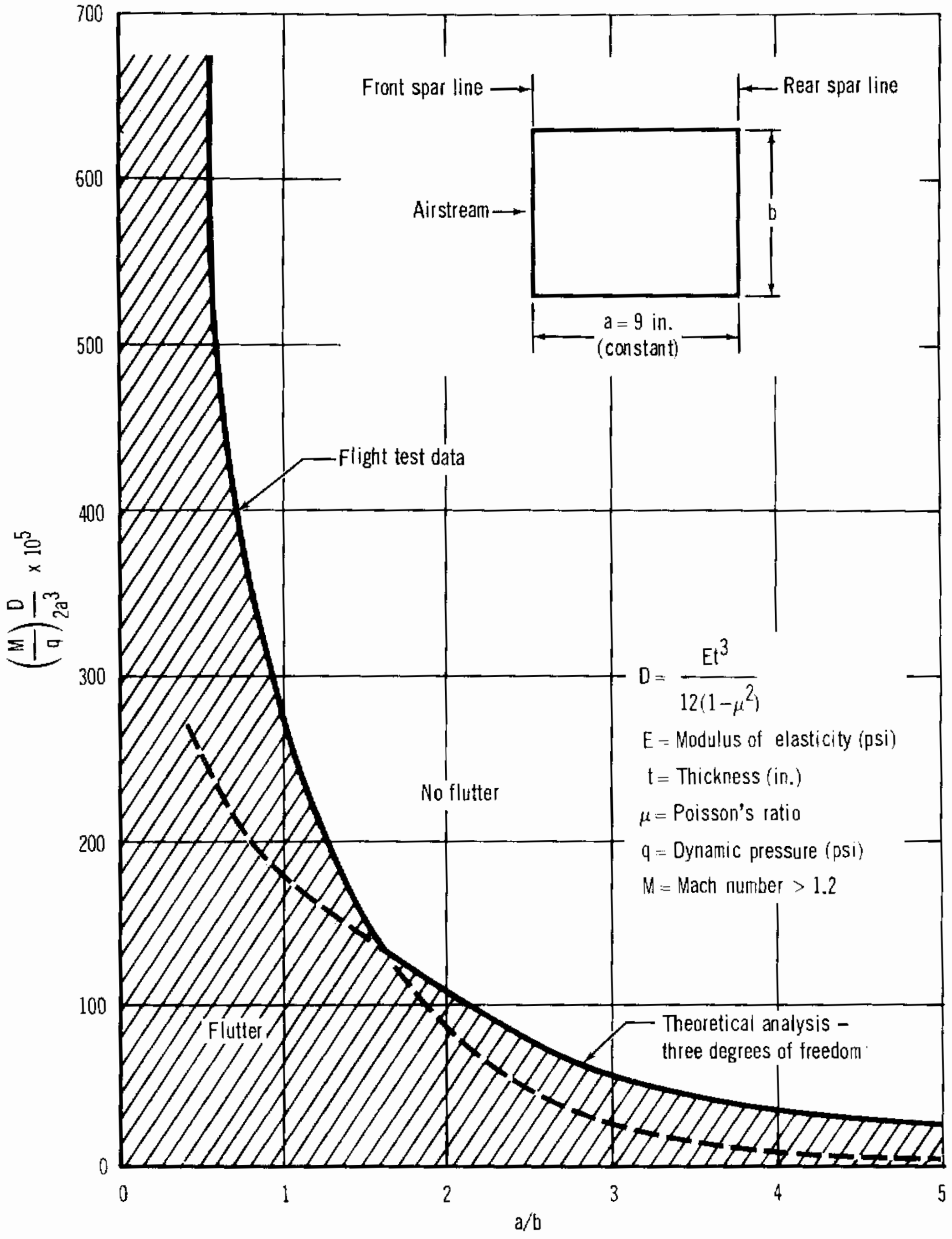

Figure 20 – Panel Flutter Criteria

4. Strength Analysis

The approach to the rudder strength analysis and some pertinent results are discussed below. The discussion is limited to the major structural elements of the rudder.

The forward torque box panel cover skins were chemically milled to a thickness of .023 inch (.584mm) established by the panel flutter requirements of Figure 20. Rib spacing was made a variable for determining an optimum panel configuration. A plot of skin thickness versus rib spacing is shown in Figure 21. In all cases, a constant panel length "a" of 9 in. (23cm) was assumed reflecting the approximate chordwise distance between the forward and aft spars (see Figure 12). As indicated in Figure 21, 9.6 in. (24.4cm) was selected as the maximum rib spacing. For the aft torque box, fabrication and handling requirements dictated the bonded honeycomb cover skin thickness of .012 in. (.305mm).

Figure 22 shows the maximum shear flow in the rudder skins resulting from the rudder torque presented in Figure 19. The relative stiffnesses of the two torque boxes defines the percent of total torque in each. The design curve for determining the shear post buckling strength of the beryllium skins was developed from test data obtained during the element test program (see discussion of panel shear tests in Section IV). The panel thickness required to preclude flutter provided more than adequate post buckling strength.

Typical cross-sections of the rudder spars are shown in Figure 23. The forward spar was analyzed conservatively as resisting all spanwise bending imparted to the rudder structure. The bending moments of Loading Condition III, previously described and shown in Figure 18, are the most severe. Material gauges were established by crippling strength requirements of the spar caps. Allowable crippling stresses were determined using the non-dimensional crippling curves for beryllium presented in Figure 8 of Section II. Rear spar

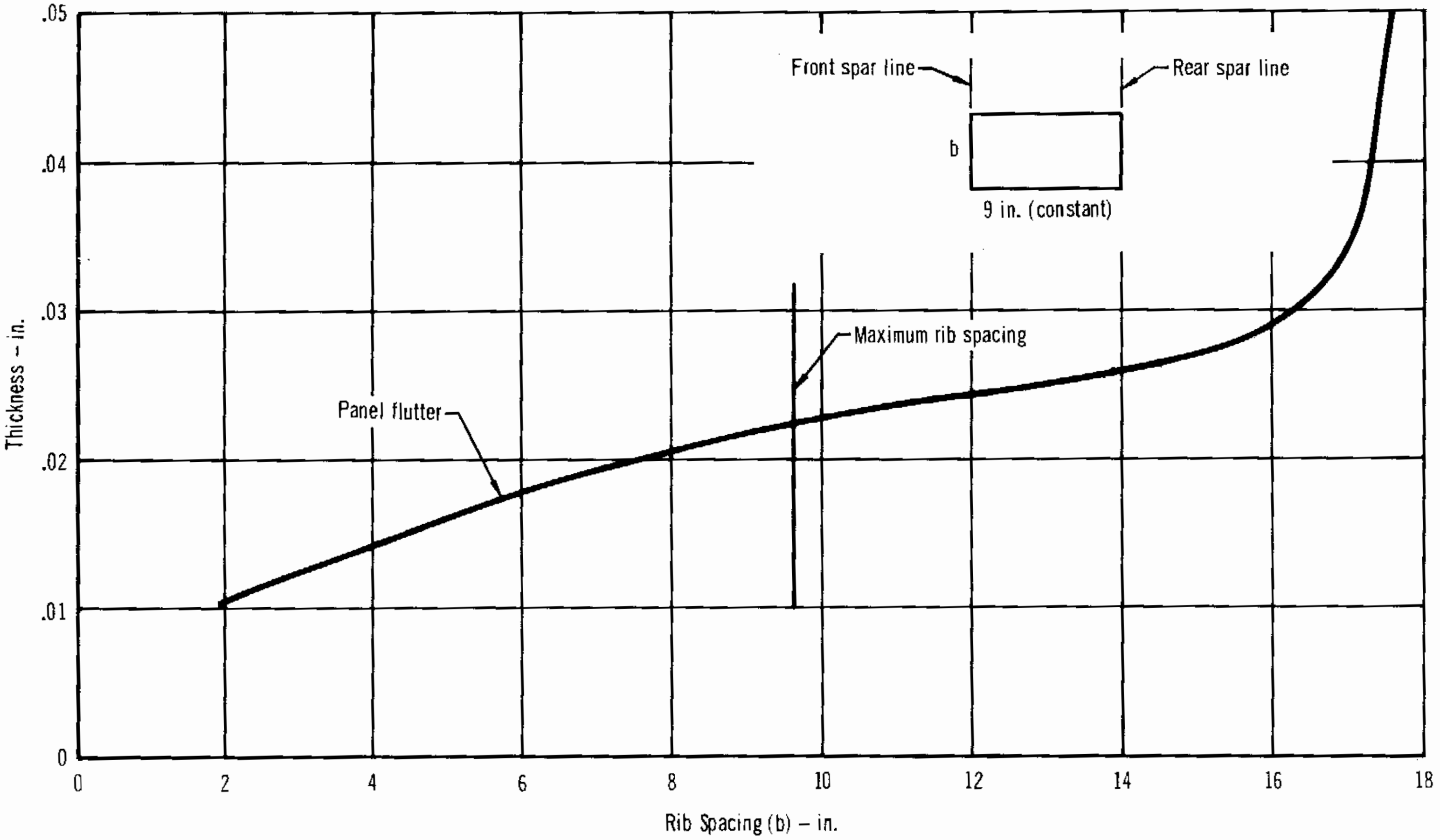

Figure 21 – Cover Skin Thickness Requirements

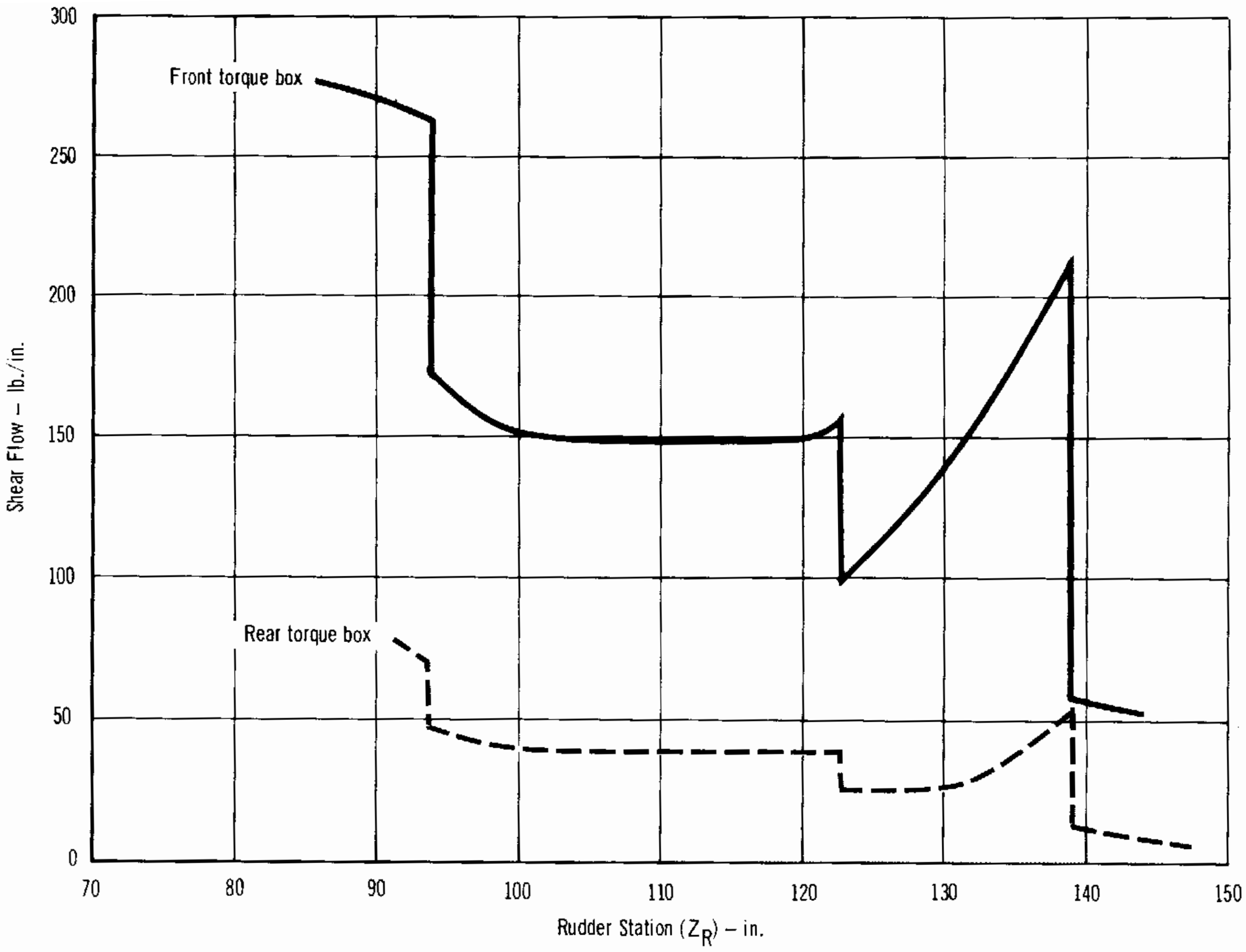

Figure 22 – Ultimate Shear Flows

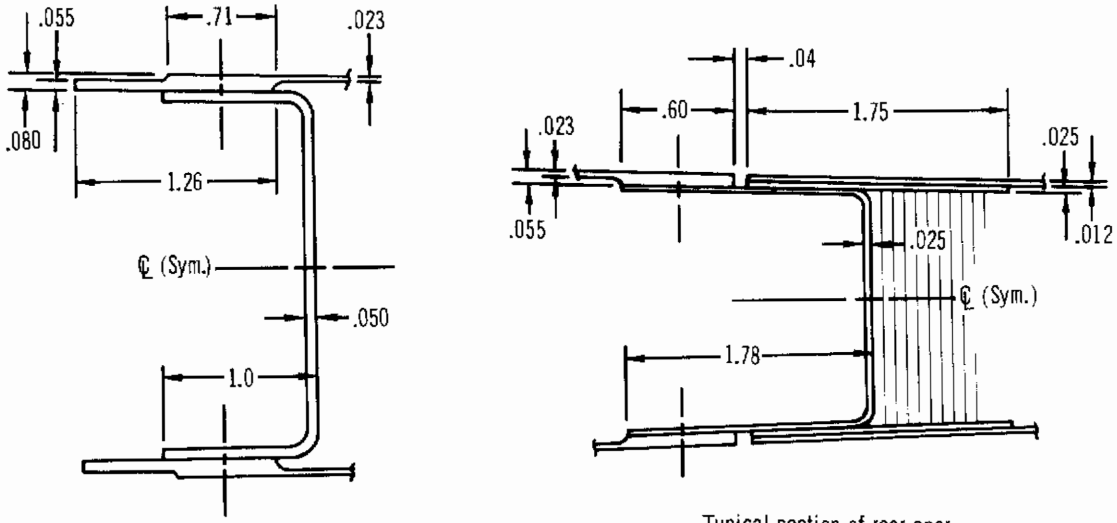
.055
.71
.023
.080
1.26
℄ (Sym.)
.050
1.0
.04
.60
1.75
.023
.025
.055
.025
.012
℄ (Sym.)
1.78

Typical section of forward spar

Typical section of rear spar

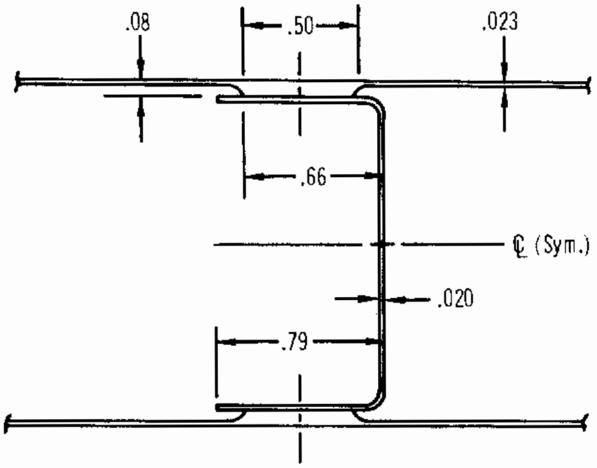
.08
.50
.023
.66
℄ (Sym.)
.020
.79

Typical section of rib

All material shown is beryllium

Figure 23 – Beryllium Rudder Rib and Spar Cross-Sections

thickness was dictated by strength requirements for transferring trailing edge loads into the forward torque box.

The spar webs were analyzed for maximum shears and shown to be shear resistant. Bearing stresses were checked at the fastener locations of the hinge support fittings.

Ribs in the forward torque box are located at the upper balance weight attachment, hinge support points, torque tube attachment, and at intermediate positions, as required to preclude panel flutter. A cross-section at a rib is shown in Figure 23. The two upper balance weight ribs were analyzed for redistributing the balance weight inertia loads into the forward torque box. To account for balance weight sweepback relative to the front spar, 60 percent of the total load was applied to the lower rib and 40 percent to the upper rib. The ribs at the upper three hinges were analyzed for the hinge loads of Condition III. This condition was found to be the most severe as a result of combining the fin deflection loads with rudder airloads. The two drive ribs at the lower portion of the rudder were analyzed for transmitting torque between the rudder and torque tube.

In addition to the above, all ribs were analyzed for reacting cover skin airloads. In particular, the honeycomb trailing edge structure was assumed to act as a cantilever "built in" at the aft spar. Thus, airload induced moment and shear forces along the spar length are reacted at the forward torque box ribs and skins. Furthermore, an analysis was made to establish thermal stresses in the rudder and to determine the extent of superposition of thermal and mechanical stresses. The maximum calculated thermal stresses were found not to occur at the same time as the maximum flight loads.

Bending and torsional stiffnesses of the beryllium rudder are presented in Figure 24. For comparison, the stiffnesses of the production aluminum rudder are included.

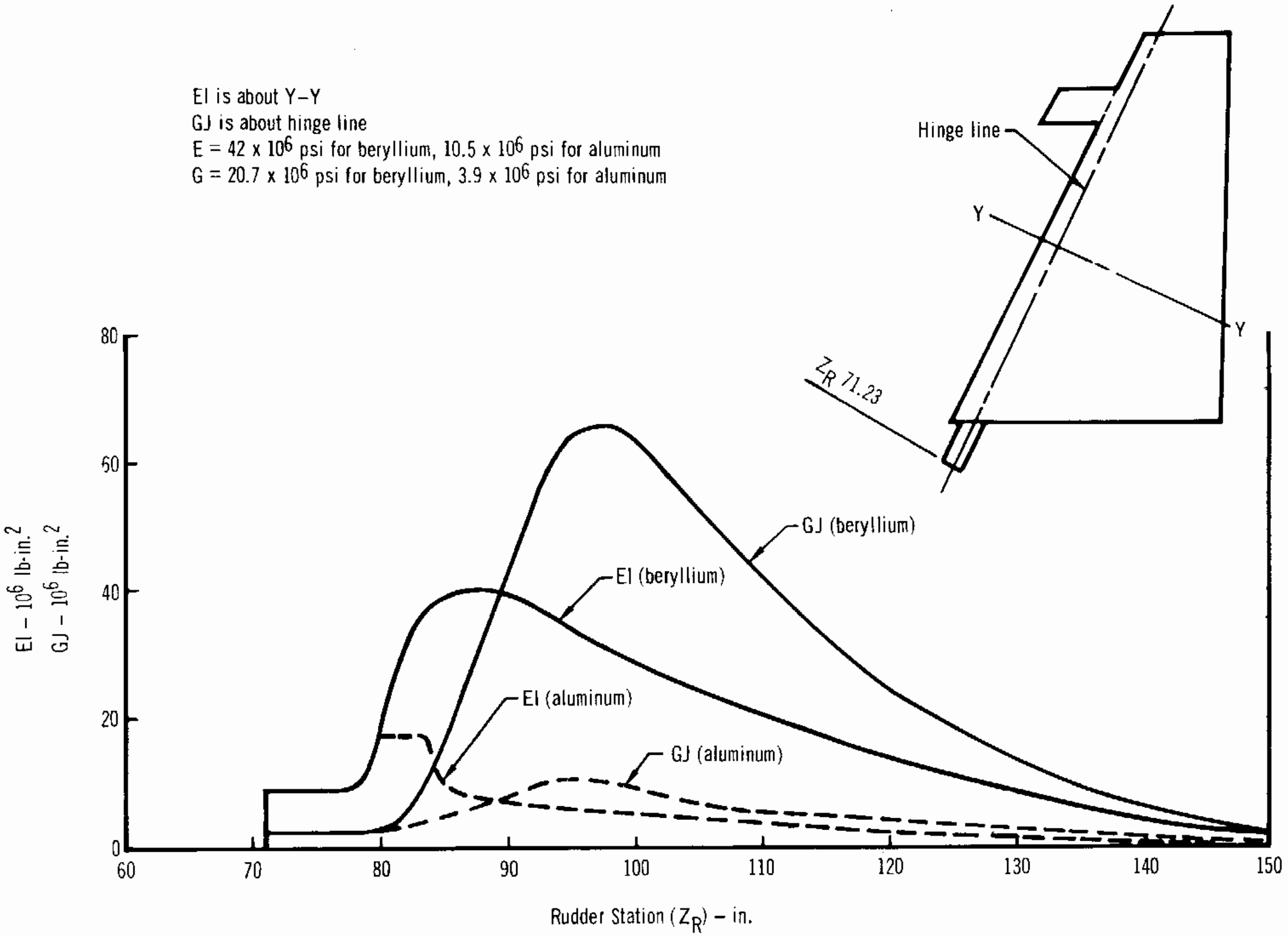

EI is about Y–Y
GJ is about hinge line
E = 42 x 10^6 psi for beryllium, 10.5 x 10^6 psi for aluminum
G = 20.7 x 10^6 psi for beryllium, 3.9 x 10^6 psi for aluminum

Figure 24 – Rudder Bending and Torsional Stiffnesses

5. Structural Dynamics Analysis

An analysis of the structural dynamic characteristics of the beryllium rudder and of the fin with the beryllium rudder installed was conducted to establish: (1) the influence of the beryllium rudder on fin stability, and (2) the need for rudder dampers to prevent transonic rudder buzz. The analysis showed that (1) fin stability is slightly improved, and (2) the upper rudder damper on the production aluminum rudder is not required on the beryllium rudder; the frequency separation is more favorable for the beryllium rudder design than for the aluminum rudder design, as shown below.

Mode	Aluminum Design	Beryllium Design
Fin Bending	19 cps (Hz)	19 cps (Hz)
Rudder Rotation	27 cps (Hz)	42 cps (Hz)
Fin Torsion	39 cps (Hz)	40 cps (Hz)
Rudder Torsion	40 cps (Hz)	110 cps (Hz)

There are several types of instabilities caused by modal coupling. The modes which could couple to reduce the speed at which flutter occurs or to increase the response amplitude are:

(1) Fin Bending and Fin Torsion

(2) Fin Bending and Rudder Rotation

(3) Fin Torsion and Rudder Torsion

(4) Fin Torsion and Rudder Rotation

The frequency separation in the first three of these was found to be more favorable for the beryllium rudder than for the production aluminum rudder. Condition (4) type flutter is prevented by the lower rudder damper.

Figure 25 shows that the lower damper is adequate to prevent transonic buss problems in the beryllium rudder. This curve shows that the beryllium rudder is stable for all values of effective stiffness. Stability over a wide range of effective stiffness is required since the aerodynamic forces acting on the rudder greatly influence its effective stiffness.

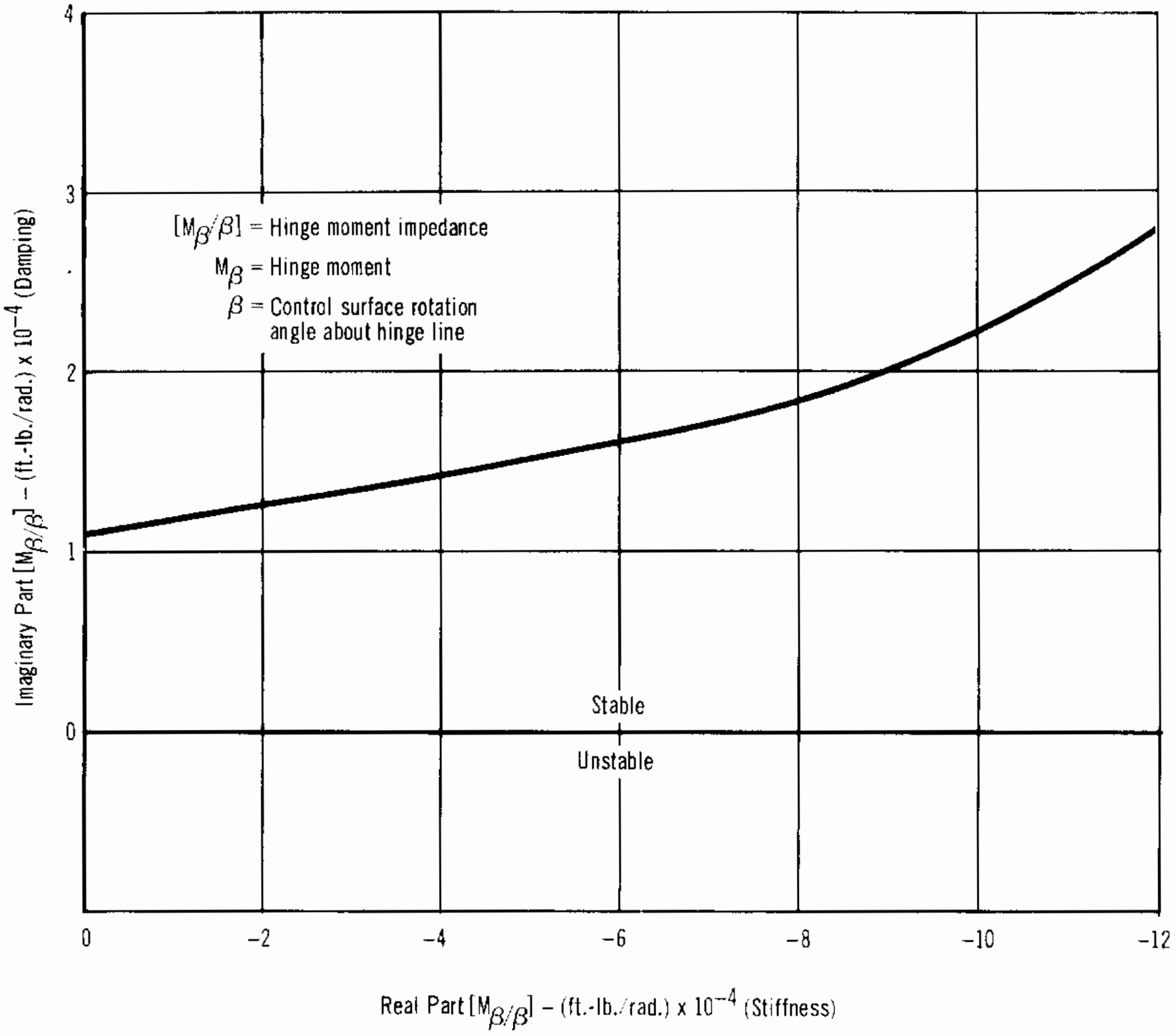

Figure 25 – Stability of Rudder With Upper Damper Removed

6. Control Dynamics Analysis

An analysis of the stability of the F-4 rudder power cylinder with the beryllium rudder installed was conducted. With no airloads present, the stability of the power cylinder is dependent on valve gain, installation stiffness, surface coupling stiffness, and surface inertia. Past experience shows that most aircraft installations have nonlinearities which result in an externally supplied damping of about 2.5% critical. Thus, the power cylinder, to be stable under no load conditions, must require less than this amount of damping or external dampers are necessary. Figure 26 shows the relative stability of the beryllium rudder as compared to the present aluminum rudder. The aluminum rudder requires 1.12% external damping whereas the beryllium rudder requires only .88%. This is due mainly to the decrease in inertia about the hinge line of the beryllium rudder, which increases the rotational natural frequency (ω_Σ) of the rudder from 17.4 cps (Hz) to 21.1 cps (Hz).

The increased stiffness of the beryllium surface has a direct effect on yaw damper operation, since there is less lost motion due to surface distortion at high speed. The effect of the lost motion is a gain attenuation for the servo used for the yaw damper. Increased stiffness results in an increase in gain at higher speeds. The attendant 40% increase in aircraft damping may possibly require a reduction in gain, since the pilots feel that the present system is "on the tight side." Because this is a matter of pilot opinion, the final answer would necessarily come from flight tests.

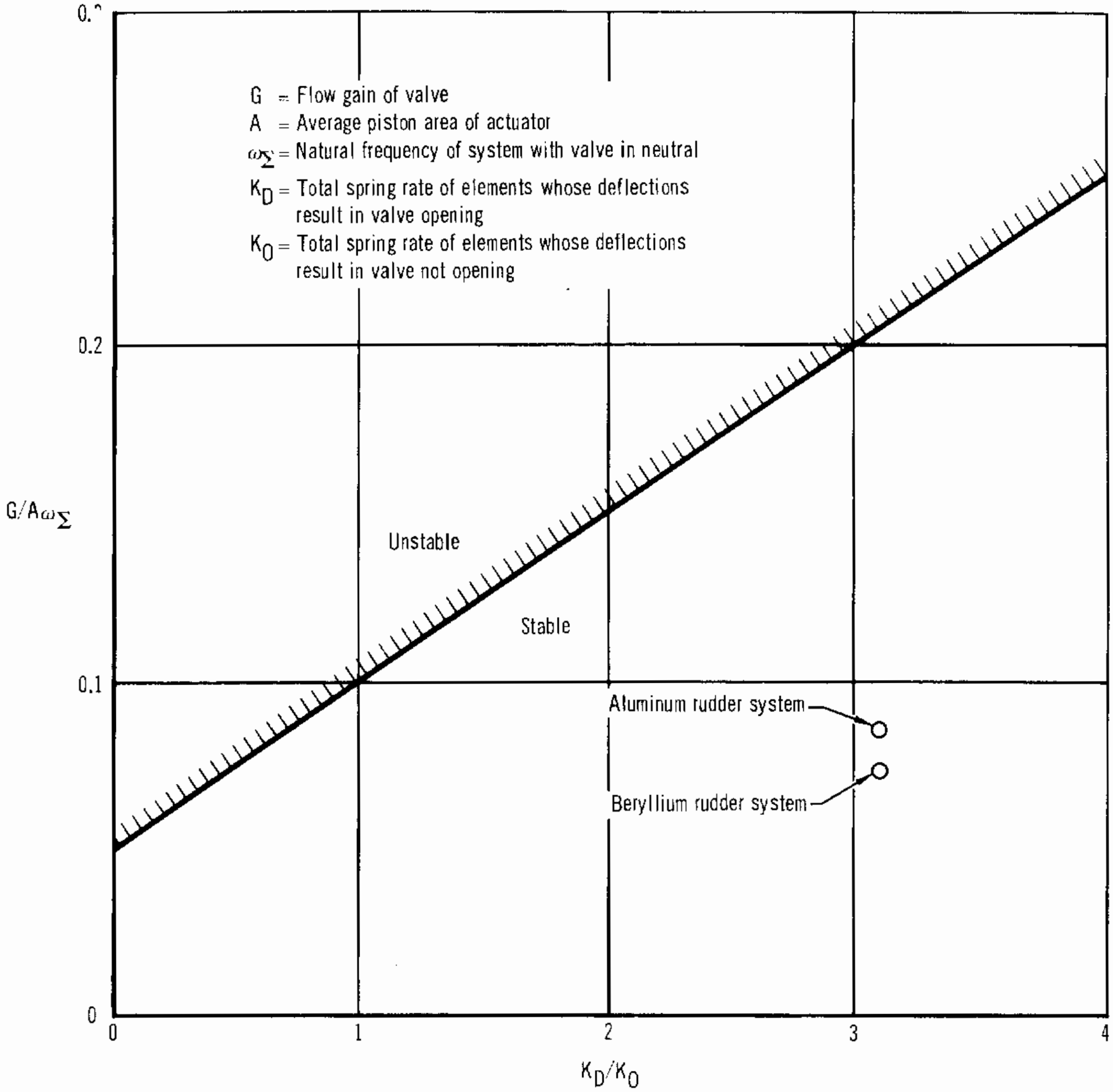

Figure 26 – Beryllium Rudder Power Cylinder Stability

7. Rudder Mass Balance

The required balance conditions for the beryllium rudder were established to decouple dynamically the rudder motion from that of the fin. The procedure and equipment used in mass balancing the beryllium rudder were analogous to those used for the production aluminum rudder. A description of this procedure is given below.

(1) The lower balance weight and the upper balance weight were removed from the rudder assembly. The balance weight attaching bolts were reinstalled.

(2) The rudder assembly was supported in the balance fixture as shown in Figure 27.

(3) The upper balance weight was installed and adjusted to give the rudder an under-balance (tail heavy) condition of 45.3 to 47.3 in.-lbs. (5.1 to 5.3 m-N) about the rudder hinge line.

(4) With the rudder balanced as specified in (3), the lower balance weight was installed and adjusted to give an over-balance (nose heavy) condition of 9.7 to 13.5 in.-lbs. (1.1 to 1.5 m-N) about rudder hinge line.

(5) Final adjustments of the balance weights were then made to give the desired balance condition.

Figure 27 shows the rudder supported in the balance fixture. The final balance condition of the beryllium rudder was established as 10.63 in.-lbs. (1.2m-N) over-balance (nose heavy) about the hinge line. The final weights of the upper and lower balance weights are 8.87 lbs. (4.02 kg) and 6.92 lbs. (3.14 kg), respectively.

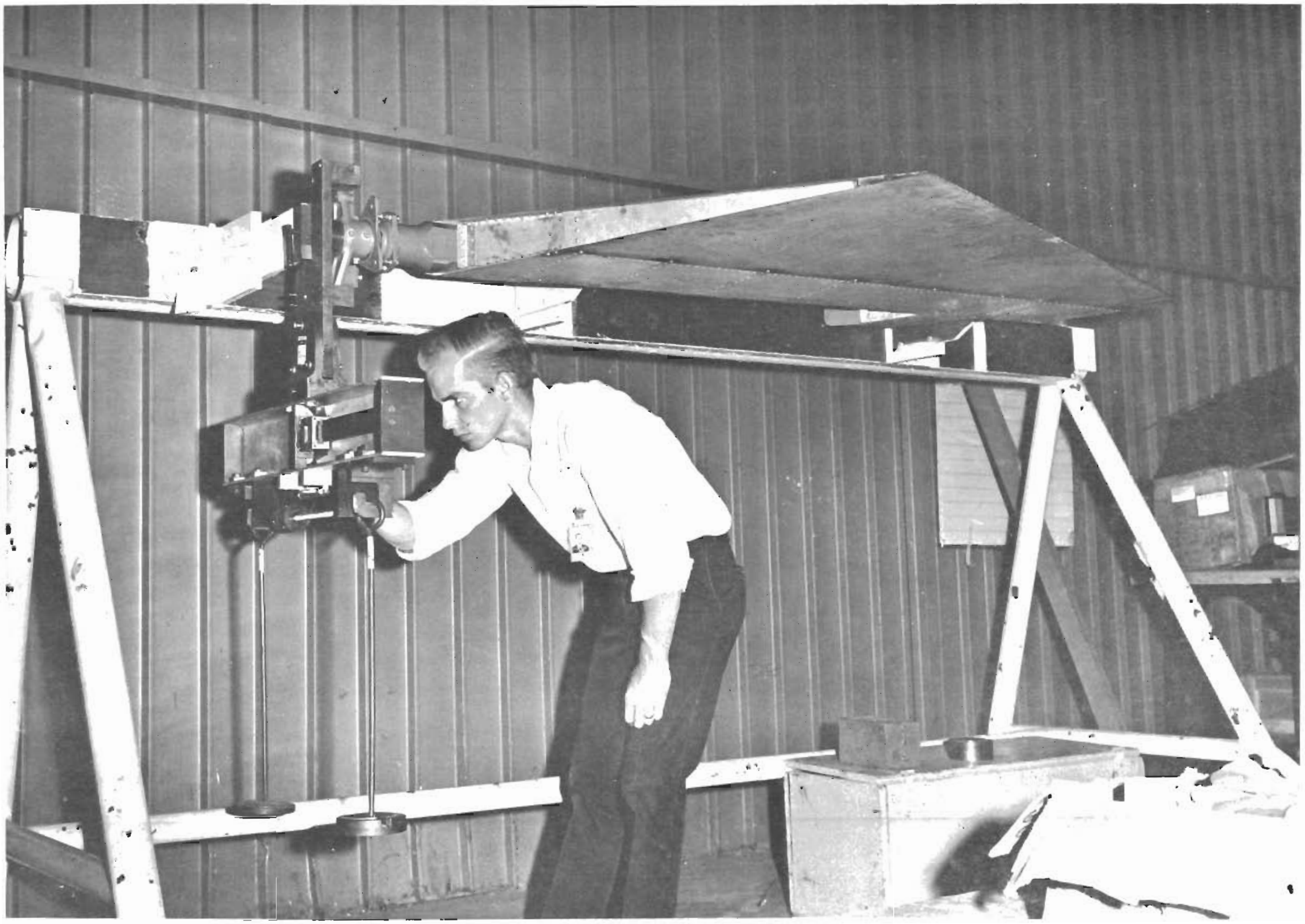

Figure 27 – Mass Balancing of Beryllium Rudder

8. Rudder Moment of Inertia

A calibrated spring oscillation system was used to determine the beryllium rudder moment of inertia about the hinge line. This system incorporated eight calibrated springs, two hinge fittings for adapting the rudder to the system, and an oscillation timing device.

The two special fittings were bar shaped with provisions at their centers for attaching to the rudder hinges. A conical point was located at one end of each bar to provide an accurately located and virtually friction free axis of rotation for the rudder. A spherical bearing was located at the other end to accept the positioned springs which, when attached, were adjusted to balance the rudder on the conical points of the fittings. The rudder was balanced in a vertical position with the hinge line horizontal. Figure 28 shows the rudder and oscillation system. The rudder was then oscillated, and the period of the oscillations determined with a stop watch. With the locations of the rudder center-of-gravity, springs, and rotation axis known relative to one another, and the weight of the various components predetermined, the rudder moment of inertia about the hinge line was determined using the following equations.

$$I_R = P^2[K_s l^2 - Wd]/4\pi^2$$

$$I_{C.G.} = I_R - W[(l/2)^2 + d^2]$$

$$I_{H.L.} = I_{C.G.} + W(x^2 + y^2)$$

where: I_R = Moment of inertia about the axis of rotation

P = Period of oscillation

K_s = Spring constant of springs

l = Linear distance from axis of rotation to spring attach point

ω = Rudder weight

d = Vertical distance from axis of rotation to center of mass

$I_{C.G.}$ = Moment of inertia about the rudder center of mass

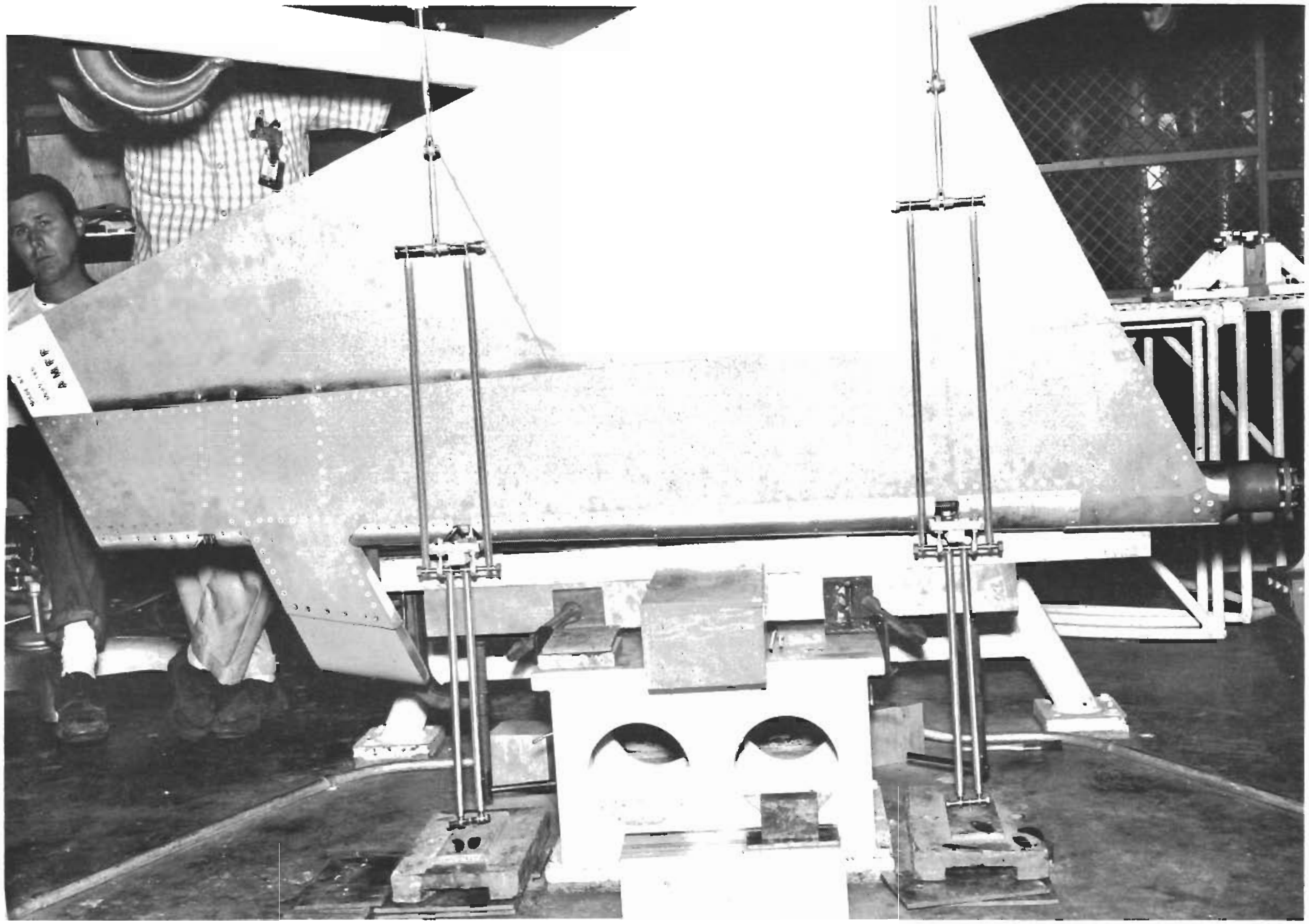

Figure 28 – Spring Oscillation System for Determining Beryllium Rudder Moment of Inertia

$I_{H.L.}$ = Moment of inertia about the hinge line

x = Vertical distance from rudder C.G. to rudder hinge line

y = Horizontal distance from rudder C.G. to rudder hinge line

The beryllium rudder moment of inertia about the hinge line was determined to be 3491 lb.-in.^{2} (1021g-m^2). The moment of inertia of the production aluminum rudder is 5185 lb.-in.^{2} (1517g-m^2).

9. Rudder Weight

Following is a breakdown of the rudder weight and a comparison of the weights of the beryllium and production aluminum rudders.

Item	Production Rudder	Beryllium Rudder	Weight Reduction
Primary Rudder Structure	31.23 lbs. (14.17 kg)	21.80 lbs. (9.89 kg)	9.43 lbs. (4.28 kg)
Balance Weights	23.90 lbs. (10.84 kg)	15.79 lbs. (7.16 kg)	8.11 lbs. (3.68 kg)
Upper Damper Installation	7.90 lbs. (3.58 kg)	0	7.90 lbs. (3.58 kg)
Total	63.03 lbs. (28.59 kg)	37.59 lbs. (17.05 kg)	25.44 lbs. (11.54 kg)

The 25.44 lbs. (11.54kg) is a 40.4% weight reduction achieved through the use of beryllium. It includes, as indicated above, weight saved in the primary structure, the balance weights, and the elimination of the upper flutter damper. The balance weight reduction is a direct result of the weight reduction obtained in the primary structure. The weight saved by elimination of the upper flutter damper is due to the increased torsional stiffness and the primary structure weight reduction. This comparison illustrates the "snowballing" effect on weight reduction that can result from the use of beryllium on a mass balanced control surface. The weights of the beryllium and non-beryllium materials in the beryllium and production rudders are summarized in Table 5.

TABLE 5

WEIGHT SUMMARY FOR BERYLLIUM AND ALUMINUM RUDDERS

Material	Rudder Weight (lb.)	
	Production	Beryllium
Beryllium	0	7.61
Aluminum	35.83	10.06
Steel	3.31	3.31
Lead	20.67	13.10
Glass reinforced plastic	0	.25
Bonding adhesive	1.42	1.42
Rivets, nuts, and bolts	1.80	1.84
Total	63.03	37.59

SECTION IV

ELEMENT TEST PROGRAM

1. Introduction

The objectives of the element test program were to verify material properties, to obtain design data, and to evaluate certain structural details which were subsequently incorporated into the rudder assembly. Table 6 presents a summary of the element test program and is followed by a detailed description of each test with a discussion of the test results.

TABLE 6
ELEMENT TEST PROGRAM

Test	Sub-section	Test Loading	No. of Tests at Temperature			Data Required
			−65°F	R.T.	500°F	
Material Acceptance Tests	2	Tension (Note 1)	–	14	–	F_{tu}, F_{ty}, and e.
Metal-to-Metal Bond Tests	3	Shear	1	3	–	Bond Shear Stress
		Flatwise Tension	1	3	–	Tension Stress in Bond at Failure
Bonded Honeycomb Panel Tests	4	Flatwise Tension	1	3	–	Tension Stress in Bond at Failure
		Core Shear	1	3	–	Shear Stress in Core at Failure
		Compression	1	3	–	Compression Stress in Face Skin at Failure
		Bond Shear	1	3	–	Shear Stress in Bond at Failure
Effect of Stress Concentrations and Interference Fit Fasteners	5	Tension	–	12	–	Failing Stress
		Fatigue	–	23	–	Cycles to Failure
Joint Tests	6	Tension	6	6	–	Joint Failing Load
Panel Shear Tests	7	Shear	–	7	–	Initial Buckling Stress and Failing Stress
Spliced Panel Shear Tests	8	Shear	3	9	–	Joint Shear Strength
Lug Tests	9	Tension	6	6	6	Lug Strength
Tests of Specimens with Corrosion Protection Finishes	10	None (Note 3)	–	16	–	Corrosion Rates
		Tension	–	8	–	Effect on Mechanical Properties
Stress-Strain Tests	11	Tension	6	6	6	Stress-Strain Curves
		Compression	3	6	3	
Rudder Composite Section	12	(Note 2)	–	1	–	(Note 2)
Crack Repair Evaluation Tests	13	Tension	–	6	–	Failure Mode

Notes:
1. Seven each tested in tension in longitudinal and transverse grain directions.
2. Four tests performed: 1) Chordwise bending to limit load, 2) Torsion to limit load, 3) Spanwise bending to 120% limit load, and 4) Combined chordwise bending, spanwise bending and torsion to failure.
3. Specimens were subjected to 5% salt spray for 500 hours.

2. Material Acceptance Tests

Material acceptance tests were conducted on a portion of the beryllium sheet material purchased for this program. Specimens were selected from each different sheet thickness of several material lots. The test set-up, test procedures, and test results are discussed below.

A total of fourteen room temperature tension tests were conducted in a 30,000 lbs. capacity Wiedemann-Baldwin Universal Testing machine. A Wiedemann-Baldwin Strip Chart Recorder was used in conjunction with an extensometer to plot load versus strain for each test specimen until material yield. The extensometer was then removed to prevent it from being damaged when the specimen ruptured. A strain rate of .005 in./in./minute was maintained until the extensometer was removed; thereafter the head travel rate was held constant at .030 in./minute until specimen failure. Figure 29 shows the test set-up.

Table 7 gives the test results and, for comparison, the producer's certified mechanical properties for the sheet material from which the specimens were fabricated. All recorded test values are in acceptable agreement with the producer's certified properties and above the minimum acceptance values (F_{tu} = 70 ksi, F_{ty} = 50 ksi, e = 5%) of the material specification to which the beryllium was purchased.

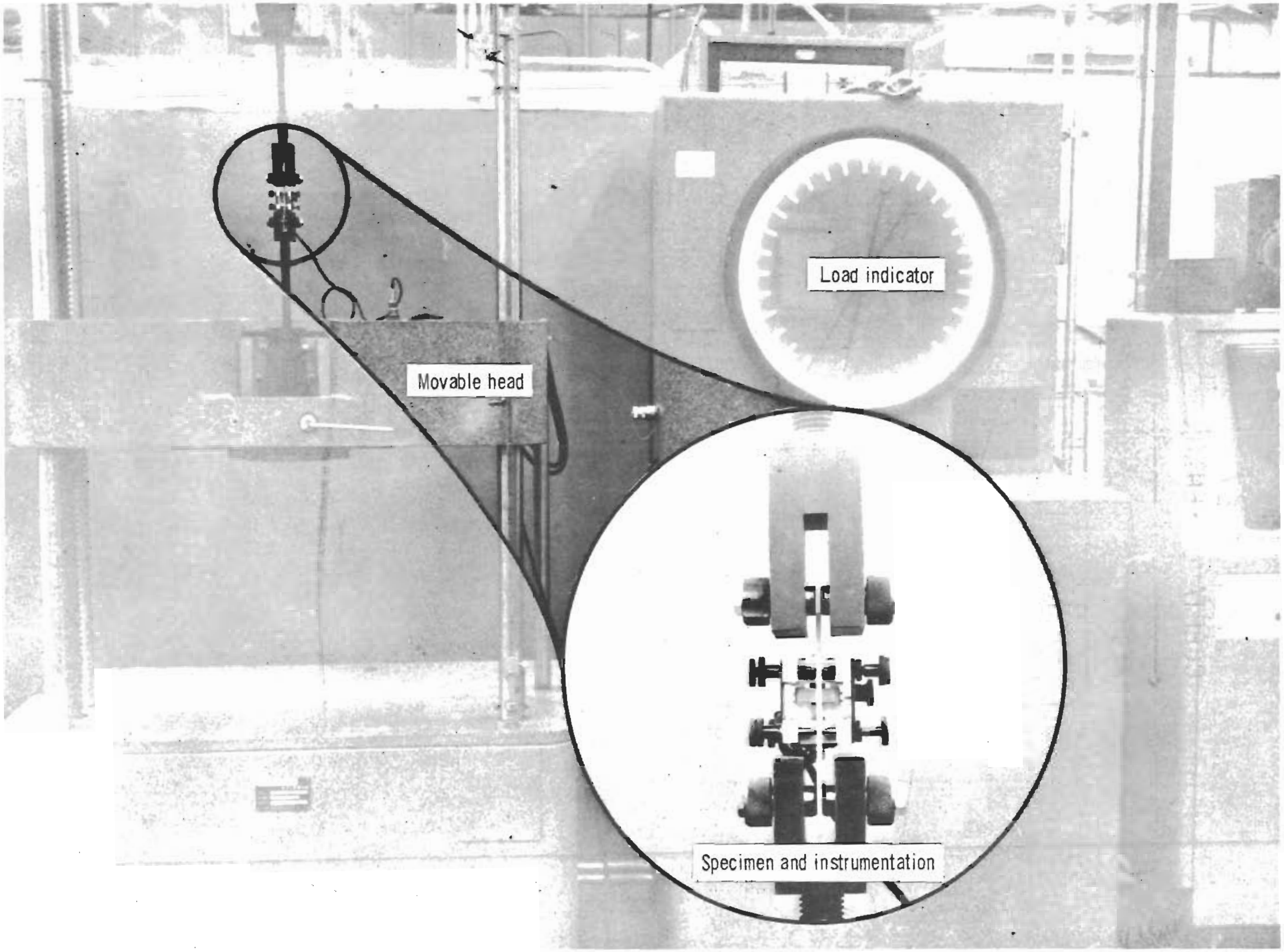
Load indicator
Movable head
Specimen and instrumentation

Figure 29 – Material Acceptance Test Set-Up

TABLE 7
MATERIAL ACCEPTANCE TENSION TEST RESULTS

Test Results								Producer's Certified Mechanical Properties		
Specimen Designation	Sheet Number	Lot Number	Specimen Thickness (in.)	Specimen Width (in.)	Yield Stress (ksi)	Failure Stress (ksi)	Percent Elongation	Yield Stress (ksi)	Failure Stress (ksi)	Percent Elongation
404-001-2	1026B	2938	.0103	.2298	53.8	74.5	12	54.6	79.2	14.0
404-001-3	1040A	3379	.0443	.2207	57.6	83.4	20	58.9	83.2	27.5
404-001-4	1040A	3379	.0448	.2437	58.1	83.8	23	56.5	81.9	21.0
404-001-6	996B	2452	.0286	.2429	50.4	74.4	16	51.2	77.2	27.0
404-001-7	1072B	3516	.0282	.2427	58.2	80.1	19	60.2	84.2	15.0
404-001-8	1072B	3516	.0291	.2432	57.2	74.6	18	60.1	82.2	18.0
404-001-11	1062B	3422	.0535	.2496	60.7	75.7	9	59.7	79.4	15.0
404-001-13	1187C	3890	.0533	.2348	60.2	81.1	11	60.5	83.0	20.0
404-001-14	1187C	3890	.0519	.2236	59.2	79.3	24	61.2	80.8	17.0
404-001-15	1053A	3422	.0631	.2504	55.7	70.4	(5)	55.1	79.2	28.0
404-001-16	1053A	3422	.0621	.2475	56.0	75.5	10	56.5	78.6	21.0
404-001-17	1034B	3318	.0852	.2248	50.9	78.6	18	52.5	78.5	19.0
404-001-19	1048B1	3379	.0810	.2352	59.1	87.1	15	57.0	81.6	22.5
404-001-20	1048B1	3379	.0805	.2323	55.3	82.1	11	55.6	77.7	29.0

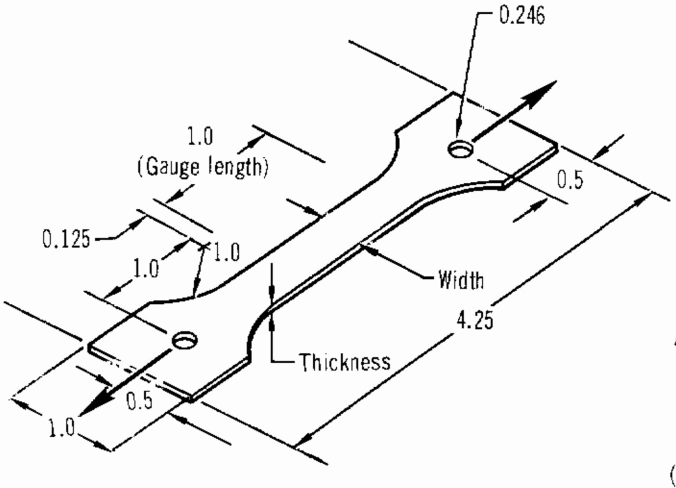

Notes:

1. Hot rolled, stress relieved, ground and etched beryllium sheet.
2. After machining and deburring, specimens were chem-milled to remove 0.003 to 0.004 inch total width and thickness.
3. Tested at room temperature with a strain rate of .005 ± .002 in./in./min. up to yield, thereafter head travel rate of .030 in./minute held constant until failure.
4. Specimens with odd dash numbers had longitudinal grain direction parallel to load axis. Specimens with even dash numbers had transverse grain direction parallel to load axis.

(5) Broke outside of gage.

3. Metal-To-Metal Bond Tests

Lap shear and flatwise tension tests were conducted to determine the joint strength of bonded beryllium sheet. These test results, in conjunction with those for the bonded honeycomb panels, subsequently discussed, were useful in determining the structural adequacy of the bonded honeycomb trailing edge section of the beryllium rudder. The test specimens, test set-up and procedures, and test results are discussed below.

A total of four tests were conducted on each type specimen (lap shear and flatwise tension) with three at room temperature and one at -65°F ± 5°F. The bonding agent used was FM-61 adhesive, a nitrile phenolic/epoxy composite film. All tests were conducted in a 30,000 lbs. capacity Wiedemann-Baldwin Universal Testing Machine. The test specimens in the loading grips are shown in Figure 30. For the tests at -65°F, the specimens were enclosed in an insulated box into which cold gas was directed from a bottle containing liquid nitrogen. A Honeywell Strip Chart Recorder was used to plot test temperatures and control the gas flow through the operation of a solenoid valve activated by a copper-constantan thermocouple. A typical cold temperature test set-up is shown in Figure 31.

The lap shear test and metal-to-metal flatwise tension test results are presented in Tables 8 and 9, respectively. Included in Table 8, for comparison, is the minimum allowable lap shear strength of aluminum alloy sheet bonded with FM-61 adhesive. As shown, the bond shear strength achieved in the tests is higher than the minimum value in all cases. All the flatwise tension specimens failed at the bond line between the specimen and loading block. This type of failure probably resulted from bonding the loading blocks to an improperly cleaned beryllium surface. Nevertheless, the strength demonstrated in the test is considered adequate.

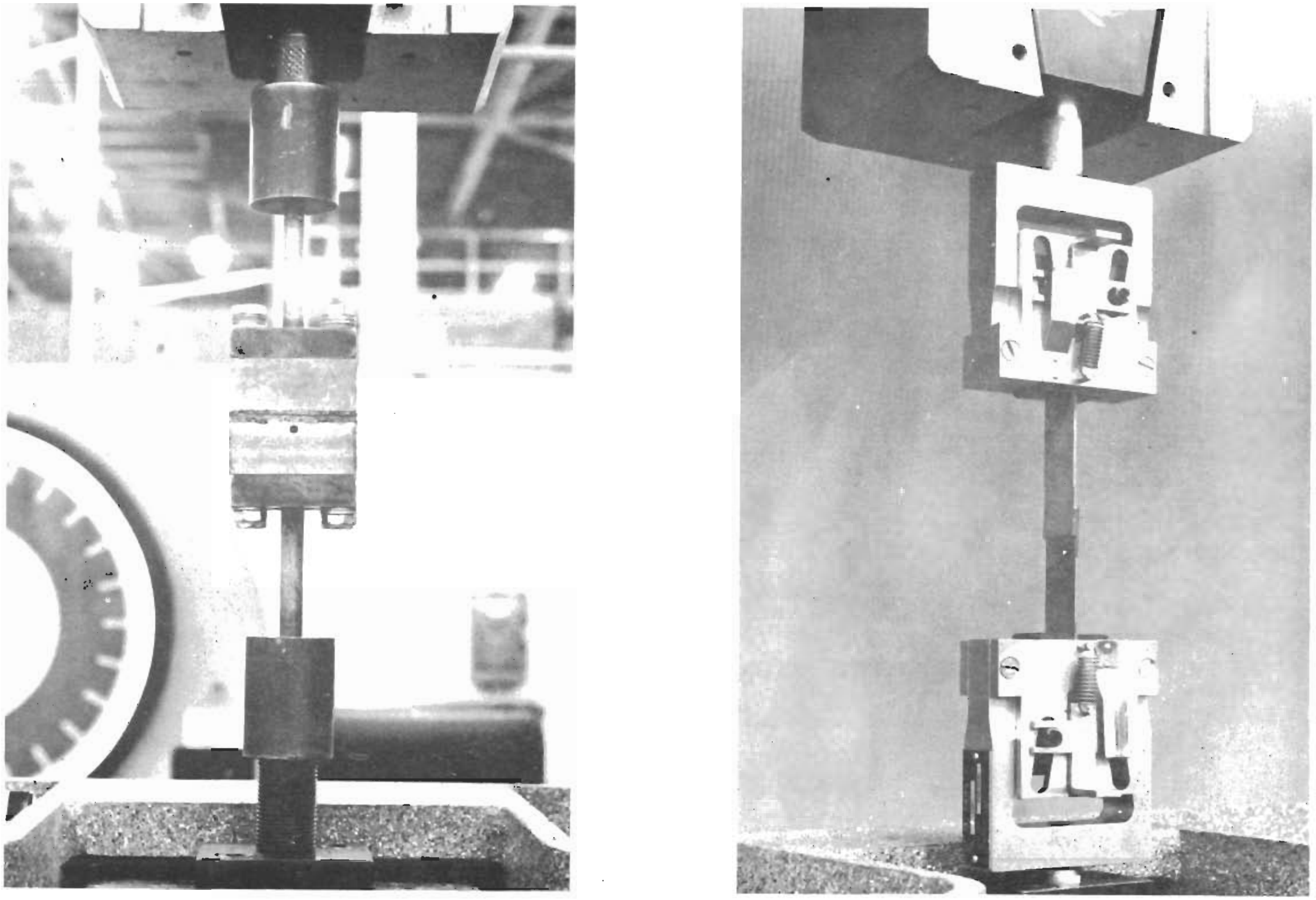

Flatwise tension

Lap shear

Figure 30 – Bonded Lap Shear and Flatwise Tension Tests

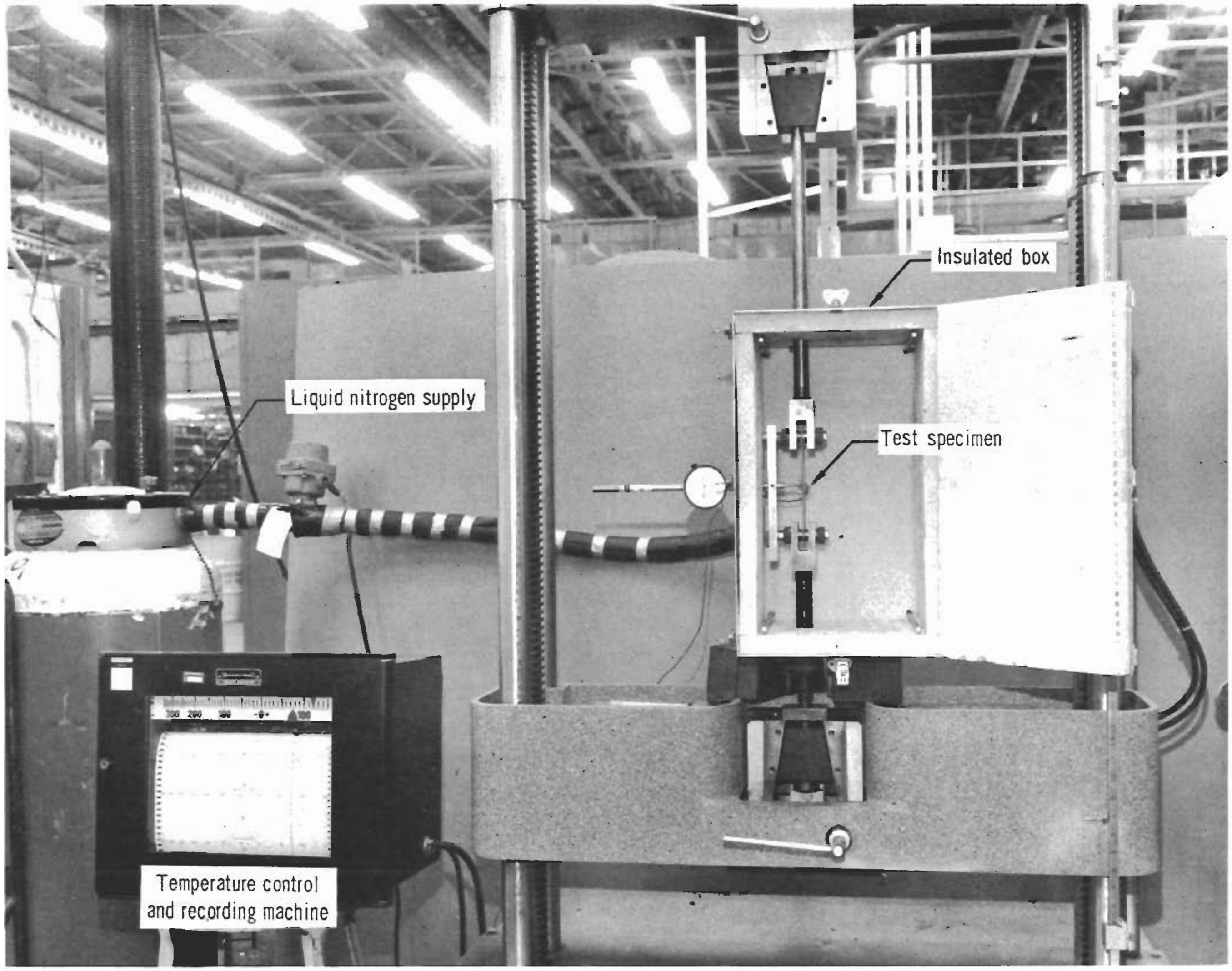
Insulated box
Liquid nitrogen supply
Test specimen
Temperature control
and recording machine

Figure 31 – Cold Temperature (-65^0F) Test Set-Up

TABLE 8
BONDED LAP SHEAR TEST RESULTS

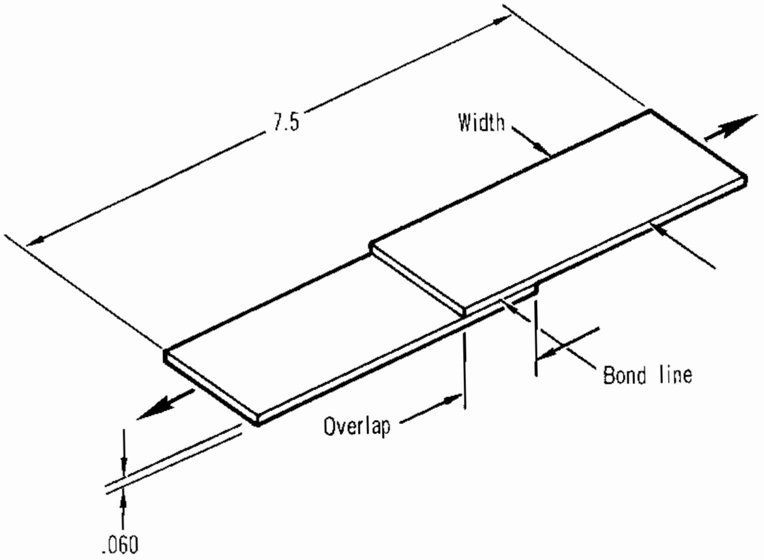

Specimen Designation	Test Temperature (ºF)	Specimen Width (in.)	Bond Line Thickness (in.)	Over-lap (in.)	Failure Load (lb.)	Failure Stress (psi)	Minimum Allowable Strength (psi)
404–004–9–1	R.T.	9936	.0086	.51	2000	3945	2250
404–004–9–2	R.T.	.9916	.0082	.52	1925	3731	2250
404–004–9–3	R.T.	.9923	.0082	.51	1895	3745	2250
404–004–9–4	–65	.9943	.0086	.51	2735	5394	2250

Notes:

1. Hot rolled, stress relieved, ground and etched beryllium sheet, bonded with FM–61 adhesive.
2. After machining and deburring, specimens were chem-milled to remove 0.003 to 0.004 inch total thickness.
3. Total exposure time to test temperature was approximately 15 minutes.
4. Load rate was 600–1200 pounds/minute.

TABLE 9
BONDED METAL-TO-METAL FLATWISE TENSION TEST RESULTS

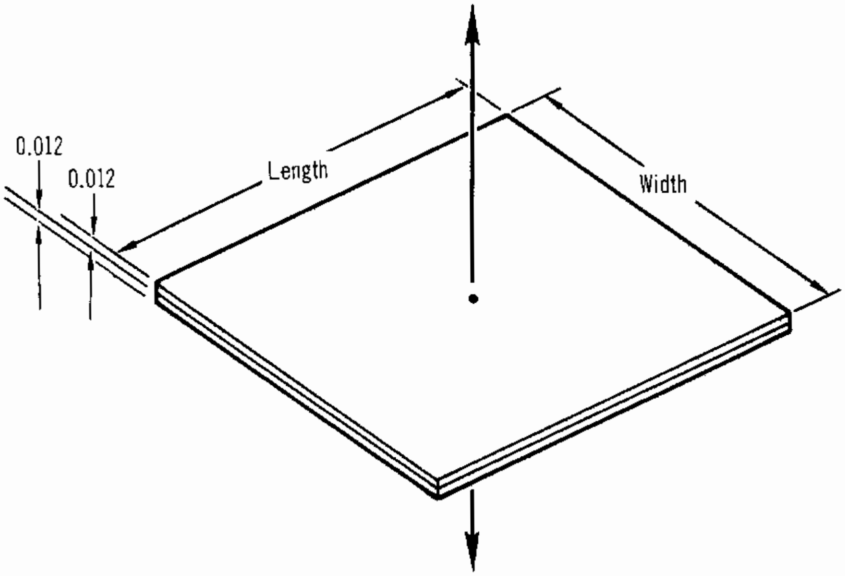

Specimen Designation	Test Temperature (^{0}F)	Specimen Length (in.)	Specimen Width (in.)	Failure Load (lb.)	Failure Stress (psi)
404–004–3–1	R.T.	2.00	2.00	7000	1750
404–004–3–2	R.T.	2.00	2.00	7175	1794
404–004–3–3	R.T.	2.00	2.00	5150	1288
404–004–3–4	–65	2.00	2.00	4450	1112

Notes:

1. Hot rolled, stress relieved, ground and etched beryllium sheet bonded with FM–61 adhesive.
2. After machining and deburring, specimens were chem-milled to remove 0.003 to 0.004 inch total thickness.
3. Total exposure time to test temperature was approximately 15 minutes.
4. Specimens failed at the bond line between the specimen and loading block.
5. Adhesive used for connecting specimen to load block was HT–424.
6. Load rate was 600–1200 pounds/minute.

4. Bonded Honeycomb Panel Tests

Core shear, flatwise tension, edgewise compression, and core-to-edge-member shear tests were conducted to determine the strength of bonded honeycomb panels with aluminum core and beryllium face skins. The structural details of the test specimens are virtually identical with those used in the rudder trailing edge section. The test specimens, test set-up and procedures, and test results are discussed below.

A total of 16 tests were conducted with three at room temperature and one at -65°F ± 5°F for each of the four types of loading mentioned above. The panel core material was 5052-H39 aluminum alloy with a 1/4 inch cell size and .001 inch foil thickness. The bonding agent was FM-61 adhesive. All testing was conducted in a 30,000 lbs. capacity Wiedemann-Baldwin Universal Testing Machine. The core shear and edgewise compression room temperature test set-ups, with the failed specimens, are shown in Figures 32 and 33, respectively. The bonded honeycomb flatwise tension specimens were loaded in the same fashion as the metal-to-metal flatwise tension specimens shown in Figure 30. Figure 34 shows the core-to-edge-member shear test specimen in the loading jig. The set-up for the cold temperature tests was virtually identical with that previously described and is shown in Figure 31.

The flatwise tension test results are presented in Table 10. Also shown is the flatwise tension minimum allowable strength of panels similar to the test specimens but with aluminum rather than beryllium facings. In all cases the flatwise tension strength achieved in the tests exceeds the minimum allowable stress. All the flatwise tension test specimens failed in the core material as expected for that type of lightweight core panel.

The core shear test results are shown in Table 11. Included for comparison is the minimum allowable core shear strength of comparable all-aluminum

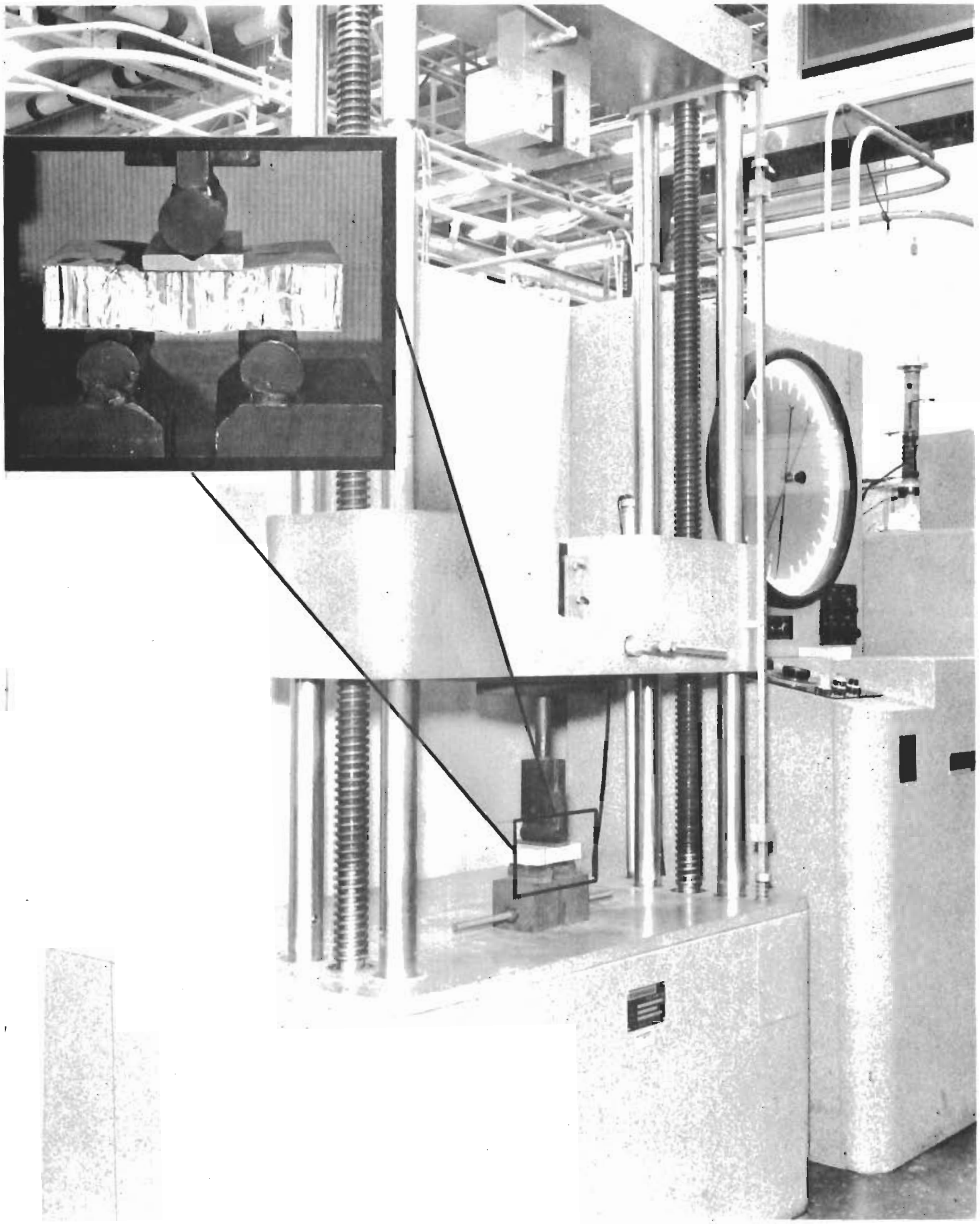

Figure 32 – Bonded Honeycomb Panel Core Shear Test

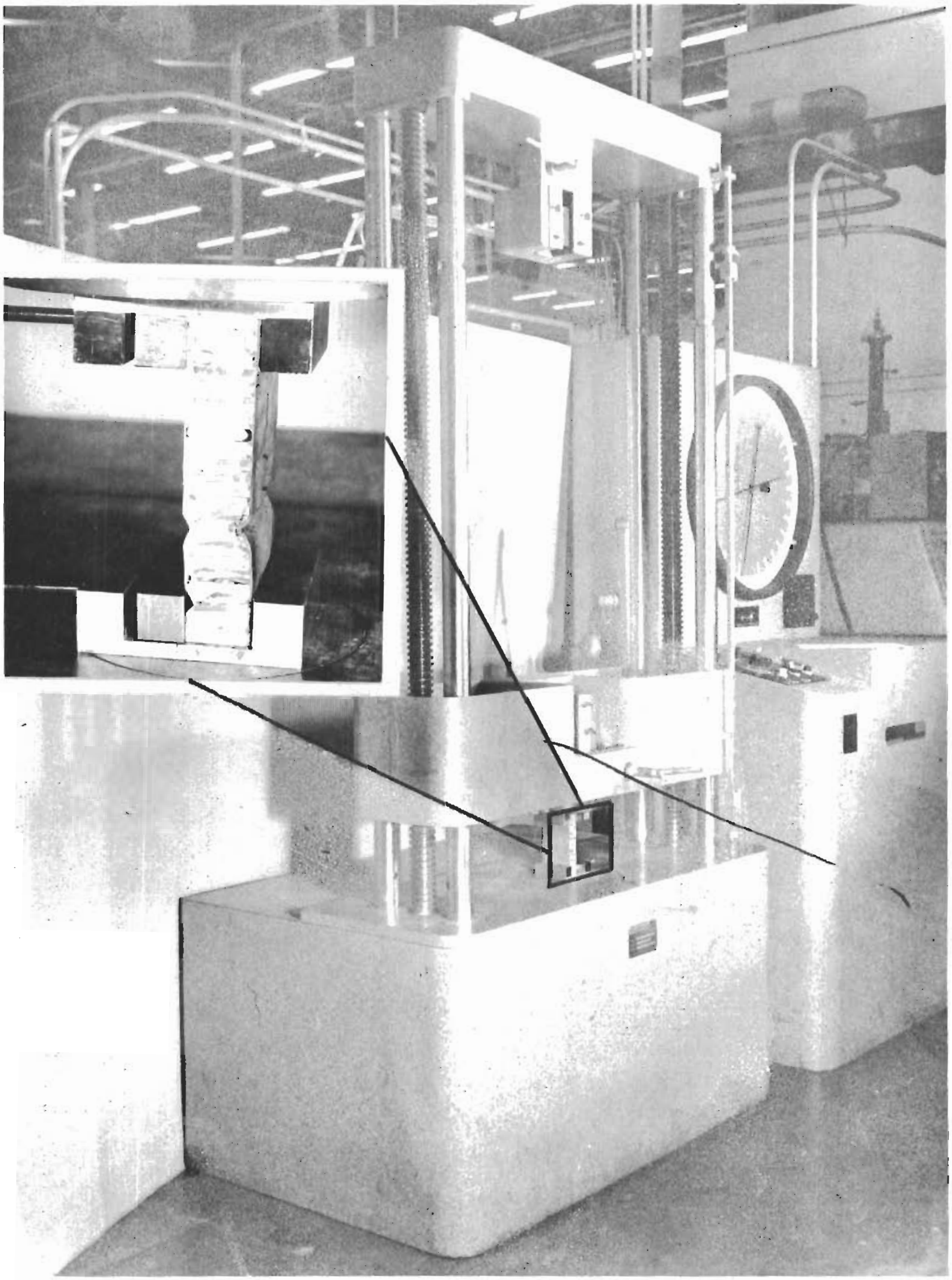

Figure 33 – Bonded Honeycomb Panel Edgewise Compression Test

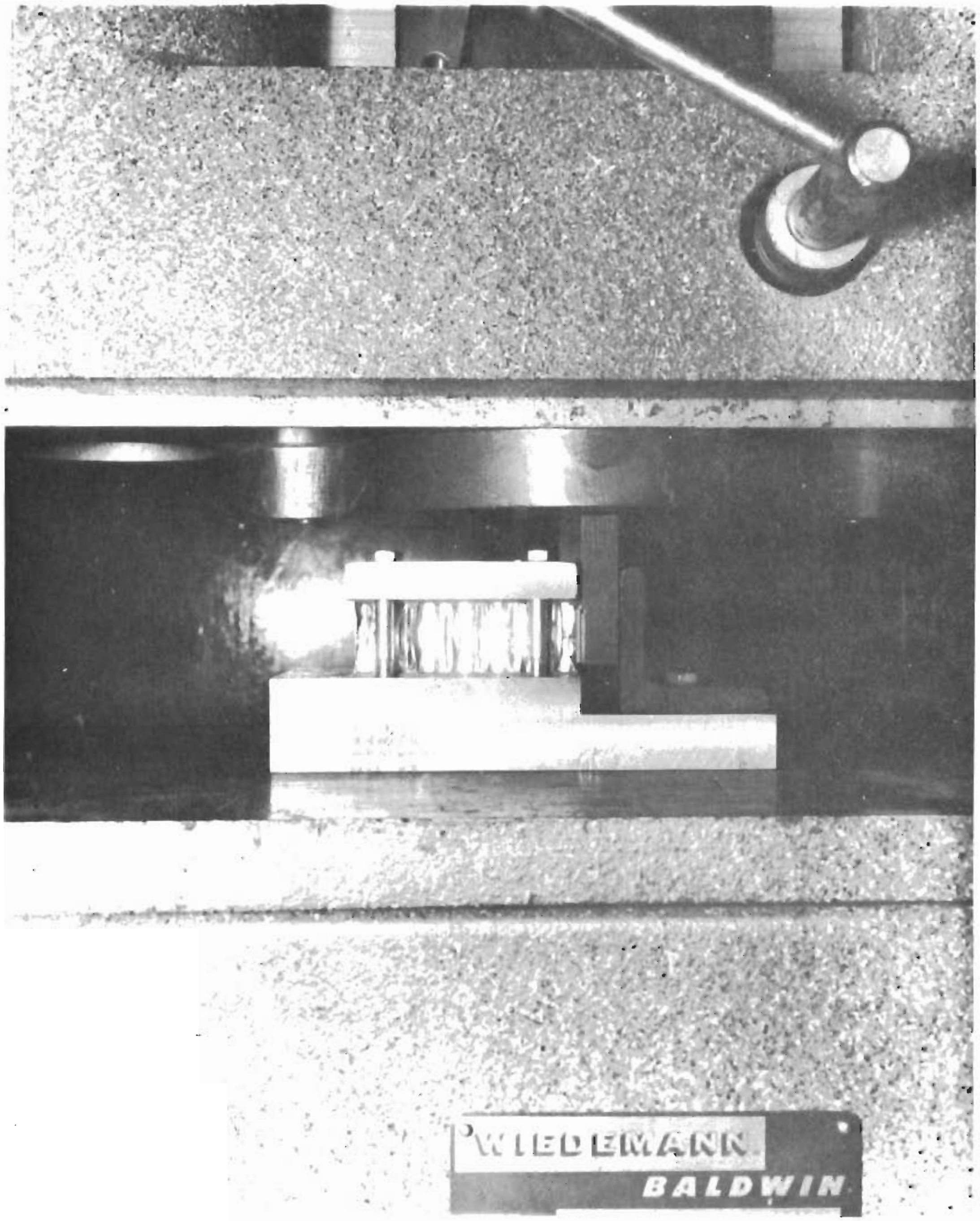
WIEDEMANN
BALDWIN

Figure 34 – Core to Edge Member Shear Test

TABLE 10
BONDED HONEYCOMB PANEL FLATWISE TENSION TEST RESULTS

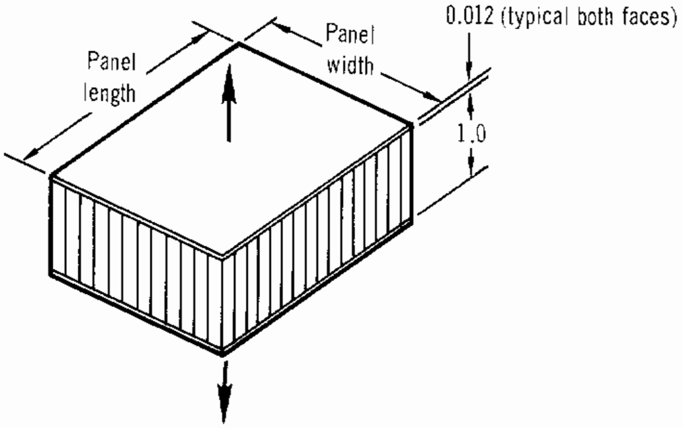

Specimen Designation	Test Temperature (°F)	Panel Width (in.)	Panel Length (in.)	Failure Load (lb.)	Failure Stress (psi)	Minimum Allowable Strength (psi)
404-004-1-1	R.T.	2.00	2.00	2205	551	400
404-004-1-2	R.T.	2.00	2.00	2100	525	400
404-004-1-3	R.T.	2.00	2.00	2175	544	400
404-004-1-4	-65	2.00	2.00	2115	529	400

Notes:

1. Hot rolled, stress relieved, ground and etched beryllium sheet bonded with FM-61 adhesive to aluminum alloy core with ¼-inch cell size and 0.001-inch foil thickness.
2. After machining and deburring, skins were chem-milled to remove 0.003 to 0.004 inch total thickness.
3. Total exposure time to test temperature was approximately 15 minutes.
4. Load rate was 600-1200 pounds/minute.

TABLE 11

BONDED HONEYCOMB PANEL CORE SHEAR TEST RESULTS

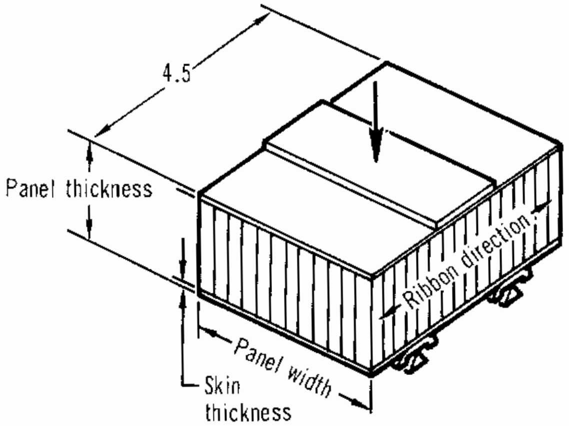

Specimen Designation	Test Temperature (^{0}F)	Panel Thickness (in.)	Skin Thickness (in.)	Panel Width (in.)	Failure Load (lb.)	Failure Stress (psi)	Minimum Allowable Strength (psi)
404-004-7-1	R.T.	1.0299	.0155 .0162	3.00	914	140	76
404-004-7-2	R.T.	1.0277	.0152 .0158	3.01	975	161	76
404-004-7-3	R.T.	1.0269	.0140 .0148	3.01	916	151	76
404-004-7-4	-65	1.0282	.0140 .0145	3.01	932	153	76

Notes:

1. Hot rolled, stress relieved, ground and etched beryllium sheet bonded with FM-61 adhesive to aluminum alloy core with ¼-inch cell size and 0.001-inch foil thickness.
2. After machining and deburring, skins were chem-milled to remove 0.003 to 0.004 inch total thickness.
3. Total exposure time to test temperature was approximately 15 minutes.
4. Load rate was 600-1200 pounds/minute.

panels. As shown, the strength achieved in the tests is significantly greater than the minimum allowable. This, in part, may be a result of the greater bending stiffness of the test panels associated with the high Young's Modulus of beryllium.

Table 12 presents the edgewise compression test results. The edgewise compression strength of the test panels exceeds the beryllium face skin compression yield stress (F_{cy} = 55 - 60 ksi).

The core-to-edge-member shear test results are presented in Table 13. The minimum allowable strength of comparable all-aluminum panels is also shown. While conducting the first room temperature core-to-edge-member shear test, it was noted that the beryllium edge member plate was rotating slightly (bottom edge inward) relative to the loading plate and crushing the honeycomb core to which it was bonded. To prevent this,the remaining tests were conducted with the edge member plate bonded to the loading plate. As shown in Table 13, the subsequent test failing loads are higher and, it is felt, more indicative of the core shear strength. In all the core-to-edge-member shear tests, the adhesive bond strength was adequate to preclude failure at the bonded surface.

TABLE 12

BONDED HONEYCOMB PANEL EDGEWISE COMPRESSION TEST RESULTS

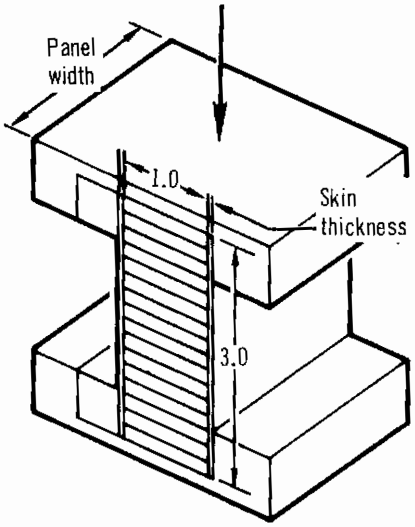

Specimen Designation	Test Tempera-ture (°F)	Skin Thickness (in.)	Panel Width (in.)	Failure Load (lb.)	Failure Stress (ksi)
404-004-11-1	R.T.	.0153 .0159	3.05	5775	60.7
404-004-11-2	R.T.	.0148 .0158	3.03	5625	60.7
404-004-11-3	R.T.	.0156 .0151	3.05	5800	62.0
404-004-11-4	-65	.0148 .0133	2.81	5460	69.2

Notes:

1. Hot rolled, stress relieved, ground and etched beryllium sheet bonded with FM-61 adhesive to aluminum alloy core with ¼-inch cell size and 0.001-inch foil thickness.
2. After machining and deburring, skins were chem-milled to remove 0.003 to 0.004 inch total thickness.
3. Total exposure time to test temperature was approximately 15 minutes.
4. Load rate was 600–1200 pounds/minute.

TABLE 13
CORE TO EDGE MEMBER SHEAR TEST RESULTS

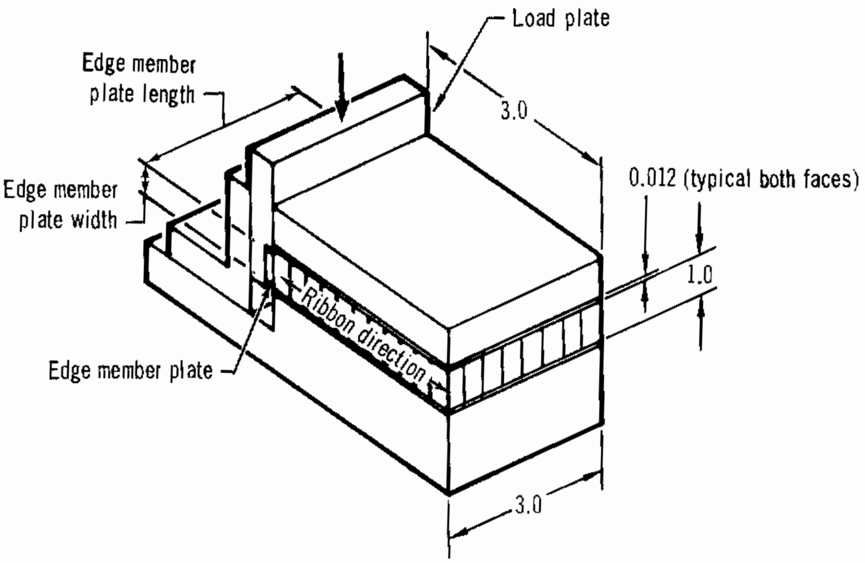
Load plate
Edge member plate length
3.0
0.012 (typical both faces)
Edge member plate width
1.0
Ribbon direction
Edge member plate
3.0

Specimen Designation	Test Temperature (°F)	Plate Width (in.)	Plate Length (in.)	Failure Load (lb.)	Failure Stress (psi)	Minimum Allowable Strength (psi)
404-004-5-1	R.T.	.74	2.72	171	85(4)	76
404-004-5-2	R.T.	.74	2.87	312	147	76
404-004-5-3	R.T.	.74	2.72	235	117	76
404-004-5-4	-65	.74	2.89	188	88	76

Notes:

1. Hot rolled, stress relieved, ground and etched beryllium sheet bonded with FM-61 adhesive to aluminum alloy core with ¼-inch cell size and 0.001-inch foil thickness.
2. After machining and deburring, skins were chem-milled to remove 0.003 to 0.004 inch total thickness.
3. Load rate was 600-1200 pounds/minute.

(4) Edge member plate rotated and therefore was bonded to load plate for subsequent tests.

5. Total exposure time to test temperature was approximately 15 minutes.

5. Effect of Stress Concentrations and Interference Fit Fasteners

Tests were conducted to evaluate the effects of stress concentrations and interference fit (or hole filling) fasteners on the static and fatigue strength of beryllium sheet. Fastener types in these tests were identical with those used in the beryllium rudder. The test specimens, test set-up and procedures, and test results are discussed below.

All testing was conducted at room temperature. A total of 35 specimens, of four different configurations, were fabricated and tested: (1) three static and five fatigue tests of specimens with unfilled holes drilled but not countersunk for NAS1094AD4 solid one-piece aluminum rivets (404-006-41), (2) three static and six fatigue tests of specimens with holes drilled and countersunk with CR2248-4 aluminum cherry rivets installed (404-006-7), (3) three static and six fatigue tests of specimens with unfilled holes drilled and countersunk for NAS1097AD4 rivets (404-006-37), and (4) three static and six fatigue tests of specimens the same as (3) with NAS1097AD4 rivets installed (404-006-9). The test specimen configurations are shown in Figure 35. The fatigue tests were conducted in a Sonntag Fatigue Test Machine at a rate of 1800 cycles per minute. The machine automatically maintains a constant maximum and minimum load on the test specimen which allows fatigue testing with stress in excess of the material yield stress. All fatigue testing was conducted using a stress ratio R = 0.2 (R = minimum stress/maximum stress). The fatigue test set-up is shown in Figure 36. The static tests were conducted in a 30,000 lbs.capacity Wiedemann-Baldwin Universal Testing Machine. A strain rate of .005 in./in./minute was maintained during the static tests.

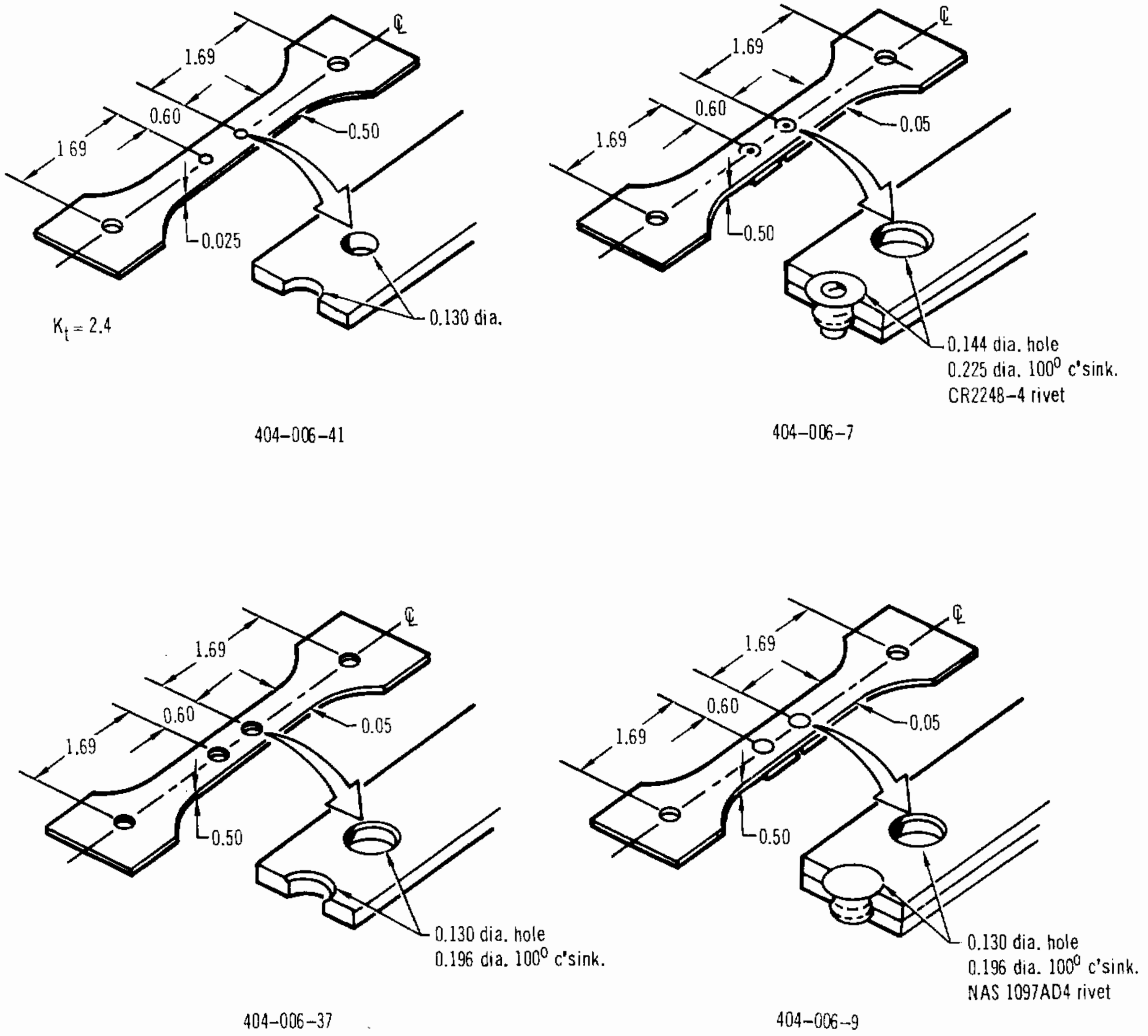
1.69
0.60
1 69
0.50
0.025
℄
0.130 dia.
$K_t = 2.4$
1.69
0.60
1.69
0.05
0.50
℄
0.144 dia. hole
0.225 dia. 100° c'sink.
CR2248-4 rivet
1.69
0.60
1.69
0.05
0.50
℄
0.130 dia. hole
0.196 dia. 100° c'sink.
1.69
0.60
1.69
0.05
0.50
℄
0.130 dia. hole
0.196 dia. 100° c'sink.
NAS 1097AD4 rivet

404-006-41

404-006-7

404-006-37

404-006-9

Figure 35 – Stress Concentration and Interference Fit Fastener Test Specimen Configurations

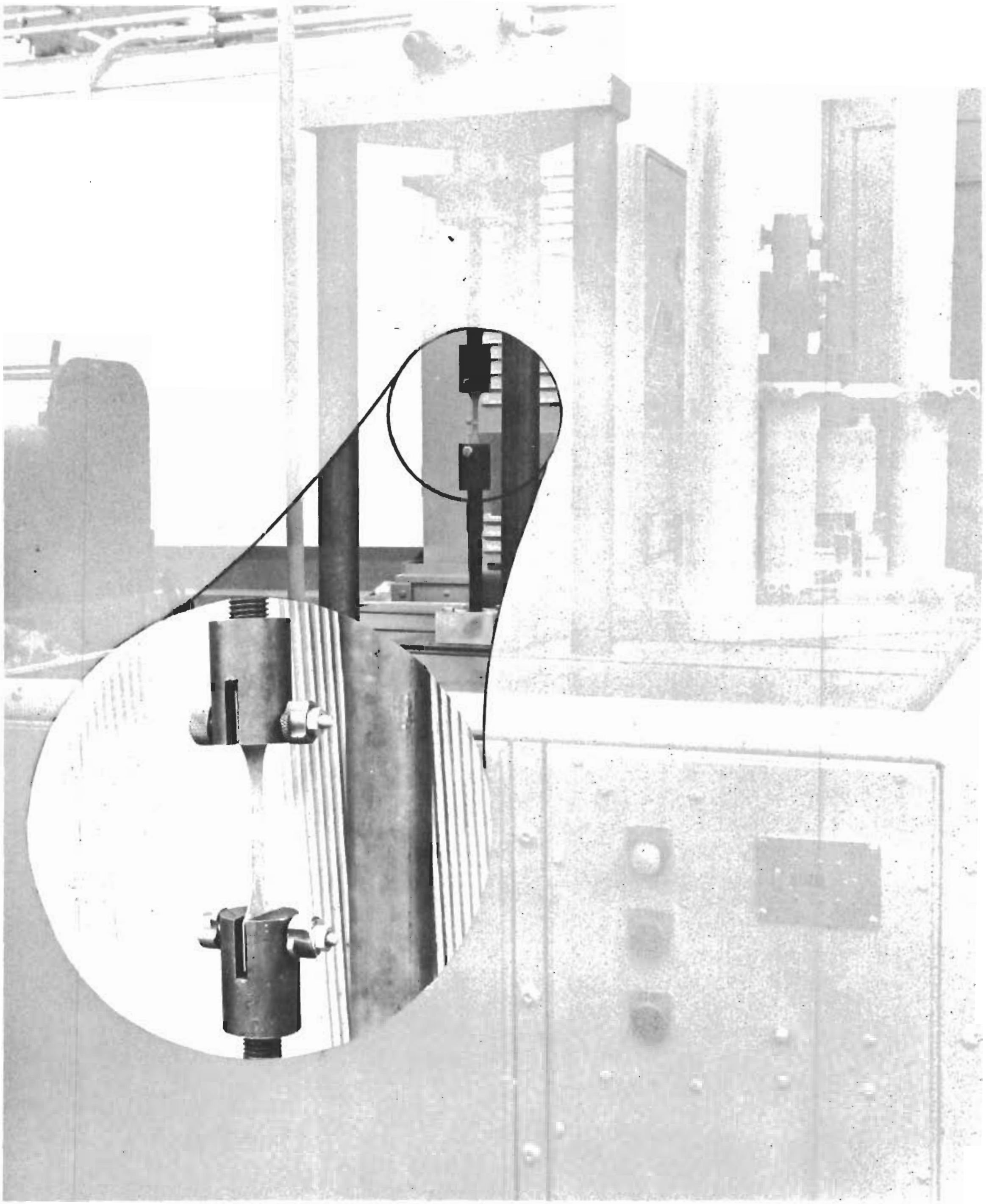

Figure 36 – Tension-Tension Fatigue Test Set-Up

Fatigue test results are presented in Table 14. The f-N curves developed from the test data are presented in Figures 37 through 40. A significant loss in fatigue strength resulted from stress concentrations in the form of filled or unfilled fastener holes. However, the fatigue strength is still unusually high; the minimum endurance limit of the four configurations tested is equal to approximately 75 percent of the minimum guaranteed tensile yield stress of 50 ksi. The test specimens with interference fit fasteners appear to have a greater endurance limit than the same specimens with the holes unfilled (compare the endurance limits shown in Figures 38 and 40 with those shown in Figures 37 and 39). This is probably due to a reduction in the alternating stress caused by tension stresses induced around the holes by the interference fit fasteners. The failed fatigue specimens are shown in Figure 41. The fatigue strengths of beryllium, aluminum, and titanium are compared in Figure 42, and the fatigue strength-to-weight efficiency curves for these materials are presented in Figure 43. f-N curves established from the fatigue data obtained in this program and in Reference 2 program are presented in Section II of this report.

Static test results are shown in Table 15. For comparison, the unnotched tensile strengths of the sheet material from which the specimens were fabricated, as certified by the producer, are also shown. The notched strength of the test specimens averages approximately 91 percent of the certified unnotched strength. This is in general agreement with the strength predicted with the data presented in Figure 4 of Section II using a stress concentration factor of 2.4. This concentration factor is applicable to specimens with unfilled holes and no countersinks, and the test results indicate there is no significant variation of this factor for the other specimens tested. The failed static test specimens are shown in Figure 44.

TABLE 14
TENSION-TENSION FATIGUE TEST RESULTS

Specimen Designation	Thick-ness (in.)	Width (in.)	Hole Dia. (in.)	C'sink Dia. (in.)	Max. Load (lb.)	Min. Load (lb.)	Max. Stress (ksi)	Min. Stress (ksi)	Cycles to Failure x 10^{-3}
404–006–41–31	.0281	.5106	.1305	—	535	107	50.0	10.0	350
404–006–41–32	.0288	.5107	.1312	—	600	120	55.0	11.0	101
404–006–41–33	.0280	.5107	.1311	—	615	123	58.0	11.6	44
404–006–41–34	.0291	.5158	.1302	—	672	134	60.0	12.0	24
404–006–41–35	.0282	.5103	.1323	—	424	85	40.0	8.0	4307 (5)
404–006–41–35	.0282	.5103	.1323	—	477	95	45.0	9.0	273
404–006–7–22	.0553	.5112	.144 (4)	.225 (4)	1056	211	55.8	11.2	68
404–006–7–23	.0568	.5175	.144 (4)	.225 (4)	1212	242	61.2	12.2	19
404–006–7–24	.0560	.5166	.144 (4)	.225 (4)	990	198	50.8	10.2	859
404–006–7–25	.0561	.5182	.144 (4)	.225 (4)	896	179	45.8	9.1	5157 (5)
404–006–7–25	.0561	.5182	.144 (4)	.225 (4)	1094	219	55.8	11.2	101
404–006–7–26	.0555	.5132	.144 (4)	.225 (4)	970	194	50.8	10.2	3836
404–006–7–27	.0563	.5133	.144 (4)	.225 (4)	1261	252	65.1	13.0	19
404–006–37–4	.0557	.4998	.130 (4)	.196 (4)	1084	217	55.1	11.0	38
404–006–37–5	.0551	.5134	.130 (4)	.196 (4)	1212	242	60.0	12.0	32
404–006–37–6	.0570	.5130	.130 (4)	.196 (4)	1045	209	50.0	10.0	117
404–006–37–7	.0566	.5002	.130 (4)	.196 (4)	900	180	45.0	9.0	234
404–006–37–8	.0560	.5020	.130	.200	1346	269	68.0	13.6	10
404–006–37–9	.0560	.5150	.130	.205	771	154	38.0	7.6	4582 (5)
404–006–37–9	.0560	.5150	.130	.205	1116	223	55.0	11.0	107
404–006–9–13	.0568	.5003	.130 (4)	.196 (4)	1106	221	55.0	11.0	22
404–006–9–14	.0558	.5017	.130 (4)	.196 (4)	990	198	49.9	10.0	5000 (5)
404–006–9–14	.0558	.5017	.130 (4)	.196 (4)	1089	218	54.9	11.0	130
404–006–9–15	.0560	.4986	.130 (4)	.196 (4)	1182	236	60.0	12.0	33
404–006–9–16	.0573	.4998	.130 (4)	.196 (4)	1299	260	64.1	12.8	16
404–006–9–17	.0547	.4995	.130 (4)	.196 (4)	1312	262	68.0	13.6	2
404–006–9–18	.0546	.4994	.130 (4)	.196 (4)	998	200	52.0	10.4	141

Notes:

1. Hot rolled, stress relieved, ground and etched beryllium sheet tested at room temperature.
2. After machining and deburring, specimens were chem-milled to remove 0.003 to 0.004 inch total thickness.
3. Longitudinal grain direction was parallel to applied loads.

(4) Nominal dimensions – all others as measured.

(5) No failure at this stress – retested to failure at higher stress level as indicated.

6. R = .2 (R = minimum stress/maximum stress).

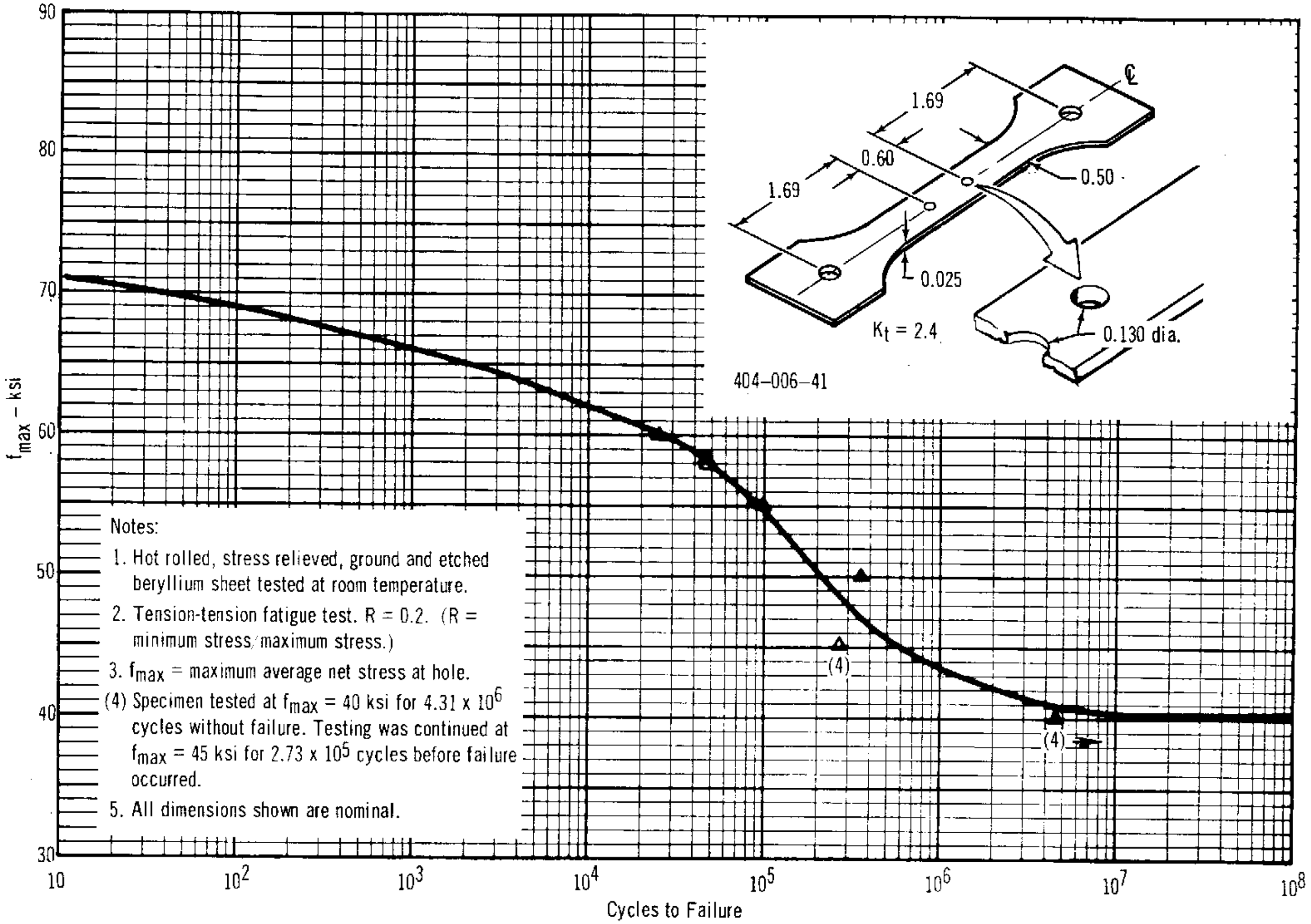

Notes:

1. Hot rolled, stress relieved, ground and etched beryllium sheet tested at room temperature.
2. Tension-tension fatigue test. R = 0.2. (R = minimum stress/maximum stress.)
3. f_{max} = maximum average net stress at hole.

(4) Specimen tested at $f_{max} = 40$ ksi for 4.31×10^6 cycles without failure. Testing was continued at $f_{max} = 45$ ksi for 2.73×10^5 cycles before failure occurred.

5. All dimensions shown are nominal.

Figure 37 – Fatigue Test Results: Specimens with Drilled Holes

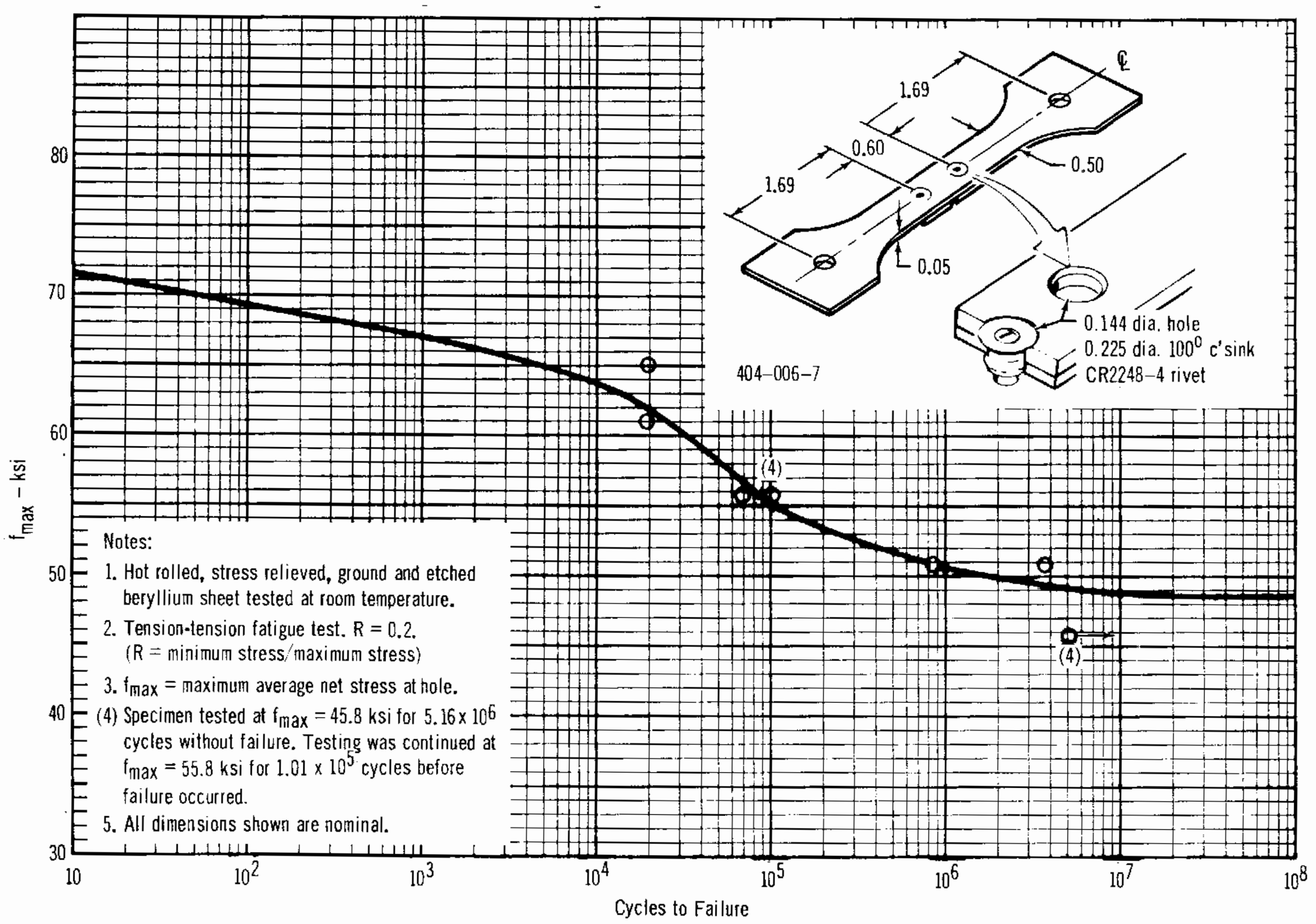

Notes:

1. Hot rolled, stress relieved, ground and etched beryllium sheet tested at room temperature.
2. Tension-tension fatigue test. R = 0.2. (R = minimum stress/maximum stress)
3. f_{max} = maximum average net stress at hole.

(4) Specimen tested at $f_{max} = 45.8$ ksi for 5.16×10^6 cycles without failure. Testing was continued at $f_{max} = 55.8$ ksi for 1.01×10^5 cycles before failure occurred.

5. All dimensions shown are nominal.

Figure 38 – Fatigue Test Results: Specimens with Countersunk Cherry Rivets

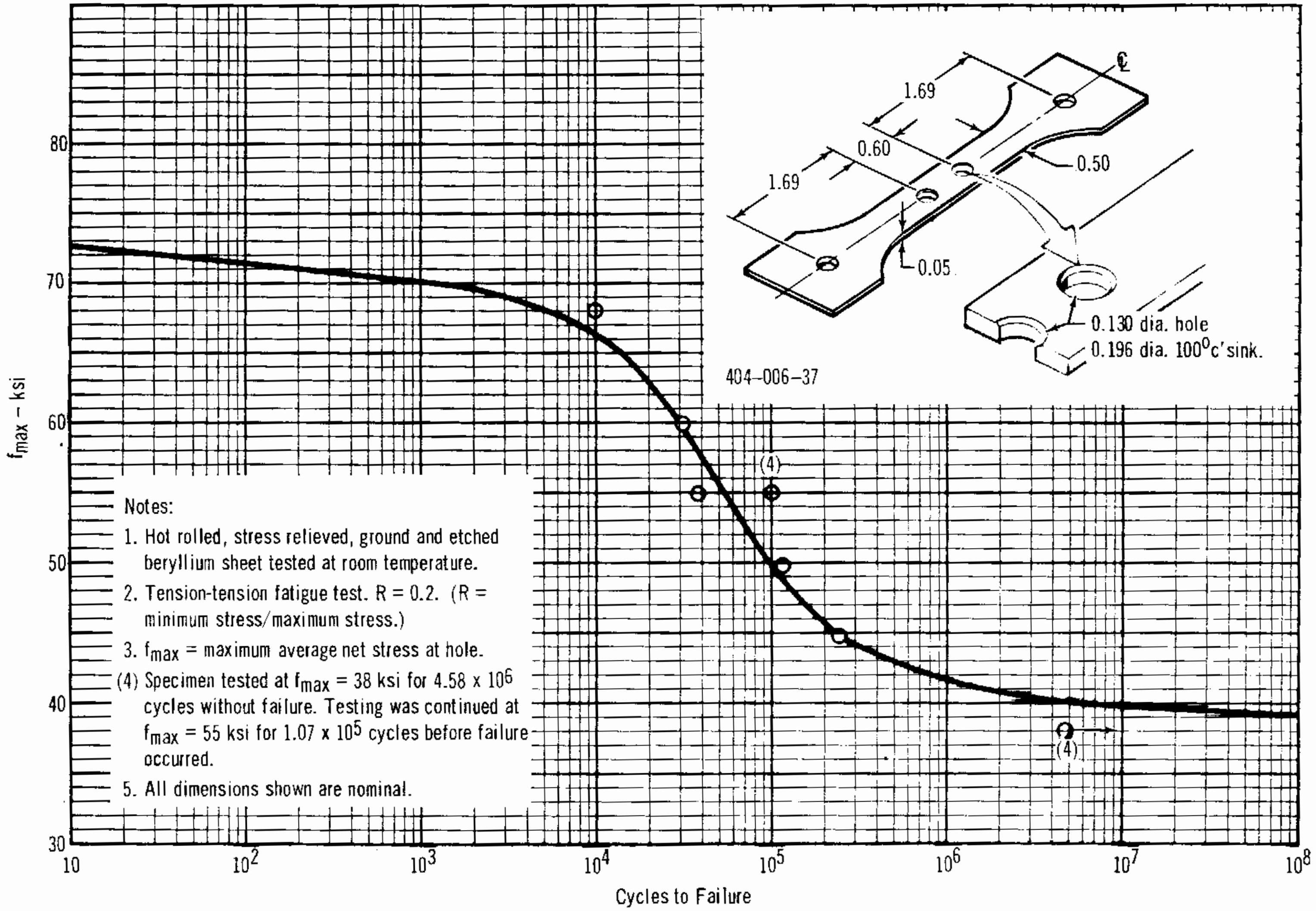

Notes:

1. Hot rolled, stress relieved, ground and etched beryllium sheet tested at room temperature.
2. Tension-tension fatigue test. R = 0.2. (R = minimum stress/maximum stress.)
3. f_{max} = maximum average net stress at hole.

(4) Specimen tested at f_{max} = 38 ksi for 4.58 x 10^6 cycles without failure. Testing was continued at f_{max} = 55 ksi for 1.07 x 10^5 cycles before failure occurred.

5. All dimensions shown are nominal.

Figure 39 – Fatigue Test Results: Specimens with Drilled and Countersunk Holes

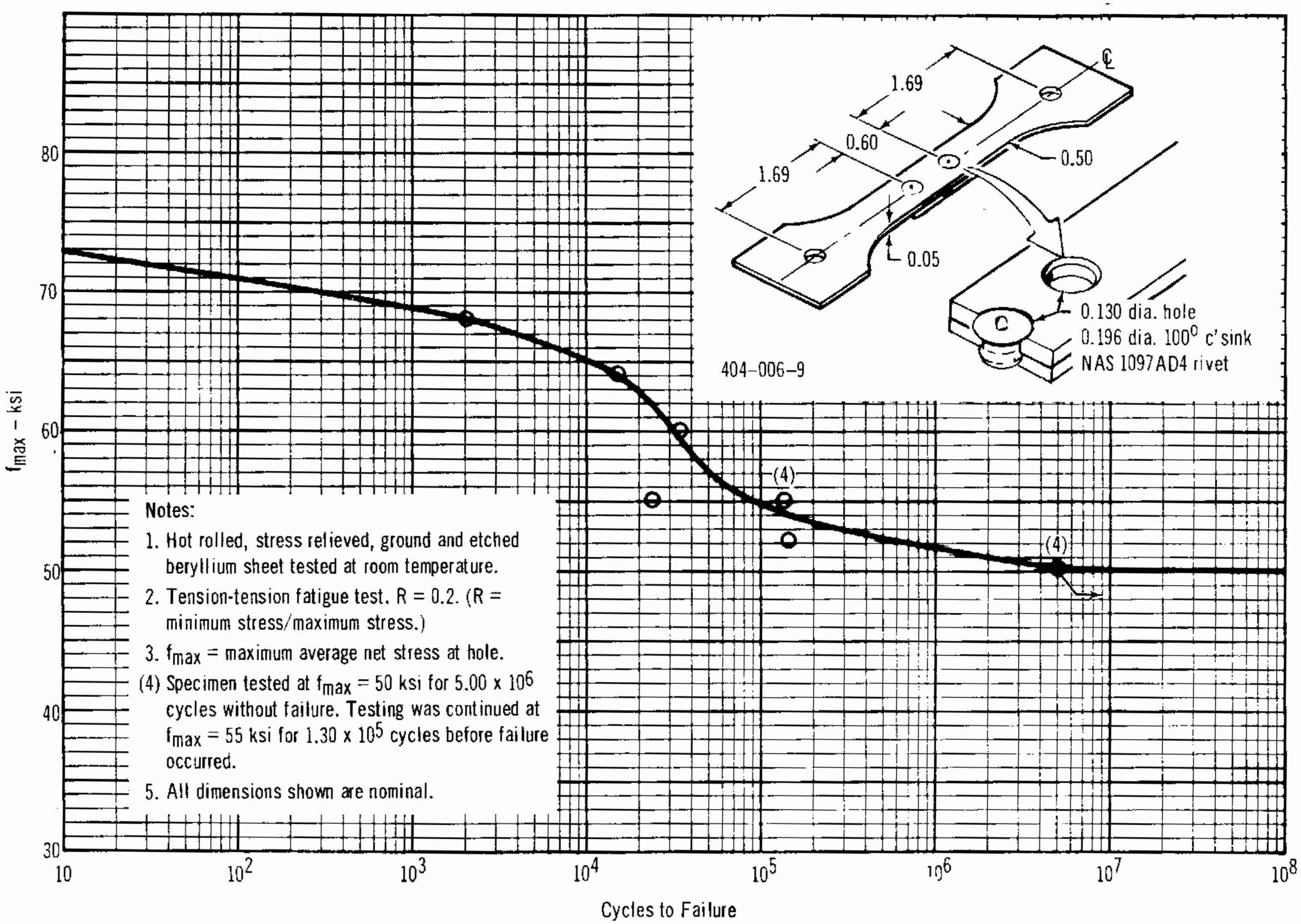

Notes:

1. Hot rolled, stress relieved, ground and etched beryllium sheet tested at room temperature.
2. Tension-tension fatigue test. R = 0.2. (R = minimum stress/maximum stress.)
3. f_{max} = maximum average net stress at hole.

(4) Specimen tested at $f_{max} = 50$ ksi for 5.00×10^6 cycles without failure. Testing was continued at $f_{max} = 55$ ksi for 1.30×10^5 cycles before failure occurred.

5. All dimensions shown are nominal.

Figure 40 – Fatigue Test Results: Specimens with Countersunk Solid Rivets

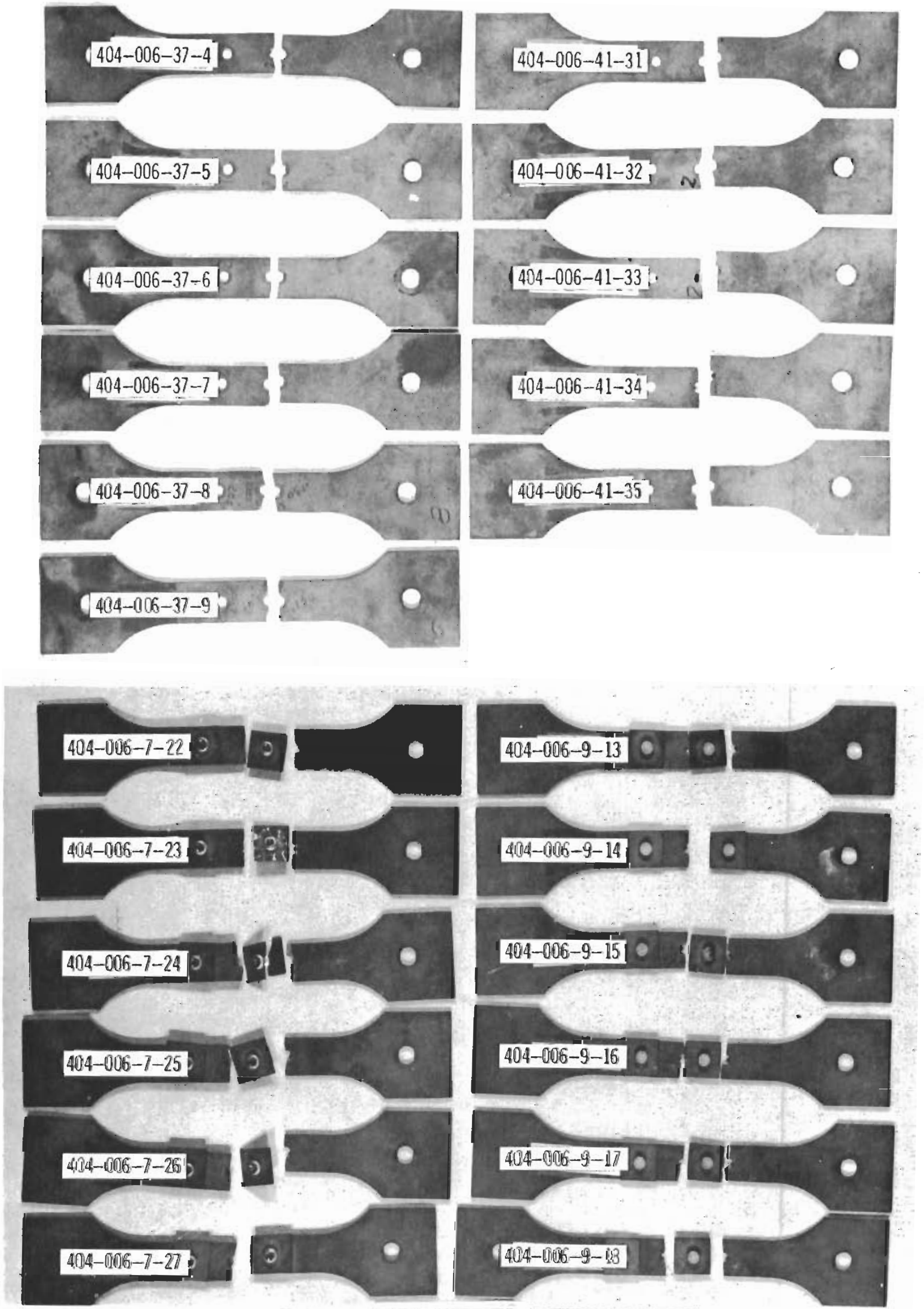
404-006-37-4
404-006-41-31
404-006-37-5
404-006-41-32
404-006-37-6
404-006-41-33
404-006-37-7
404-006-41-34
404-006-37-8
404-006-41-35
404-006-37-9
404-006-7-22
404-006-9-13
404-006-7-23
404-006-9-14
404-006-7-24
404-006-9-15
404-006-7-25
404-006-9-16
404-006-7-26
404-006-9-17
404-006-7-27
404-006-9-18

Stress Concentration and Interference Fit Fastener Specimens

Figure 41 – Tension-Tension Fatigue Test Failed Specimens

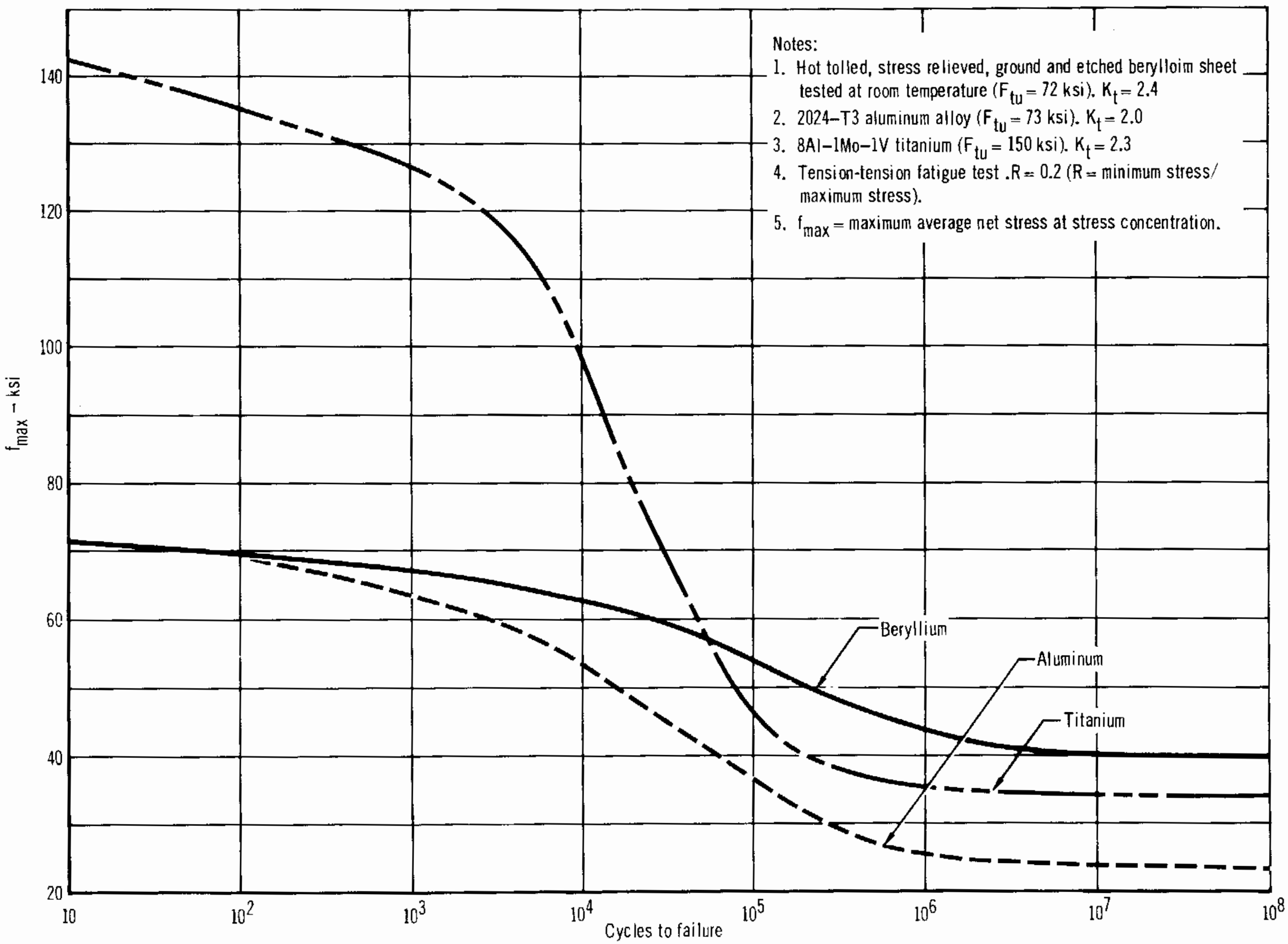

Notes:

1. Hot tolled, stress relieved, ground and etched berylloim sheet tested at room temperature (F_{tu} = 72 ksi). K_t = 2.4
2. 2024–T3 aluminum alloy (F_{tu} = 73 ksi). K_t = 2.0
3. 8Al–1Mo–1V titanium (F_{tu} = 150 ksi). K_t = 2.3
4. Tension-tension fatigue test .R = 0.2 (R = minimum stress/ maximum stress).
5. f_{max} = maximum average net stress at stress concentration.

Figure 42 – Fatigue Strength of Notched Sheet: Beryllium, Aluminum and Titanium

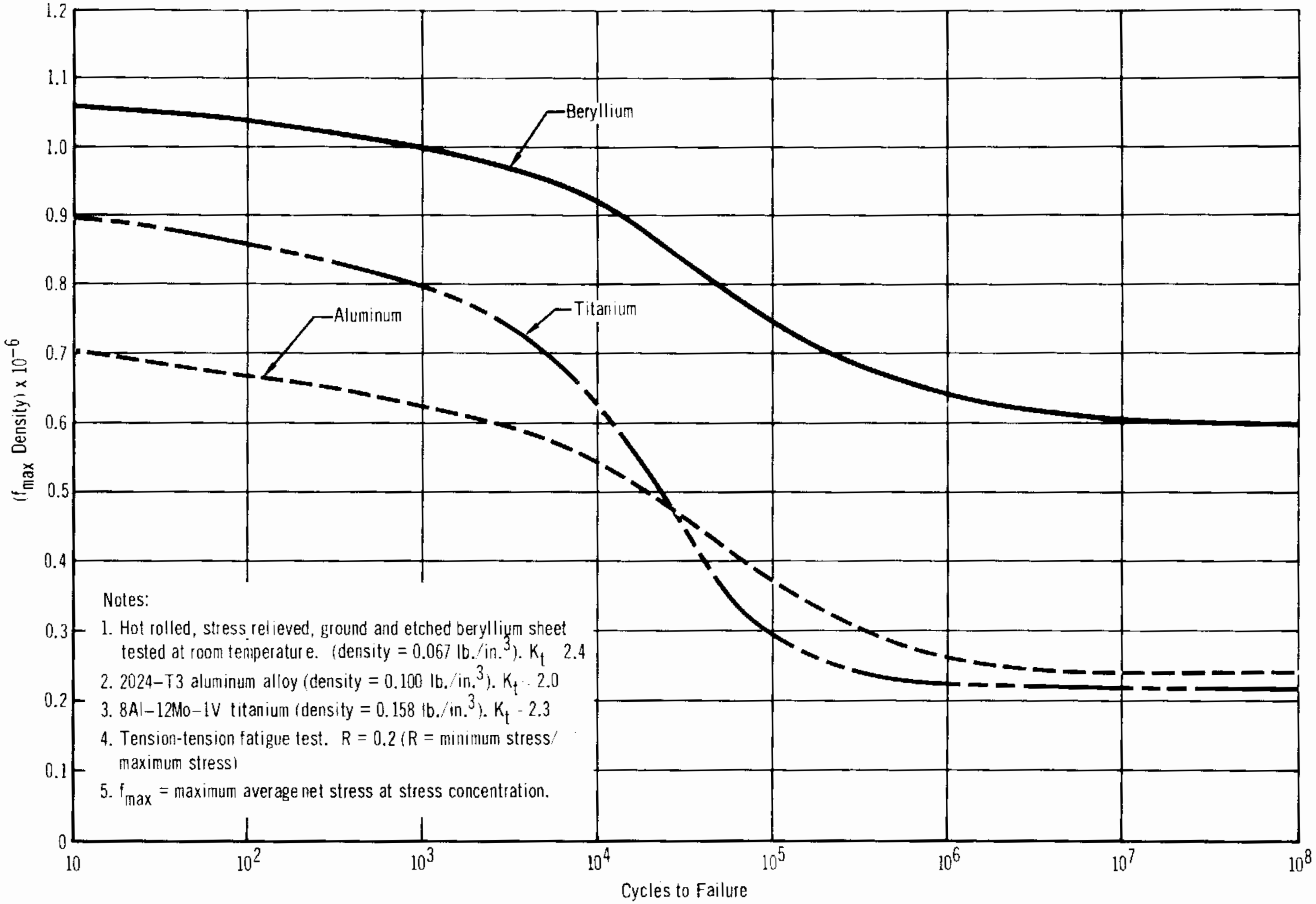

Notes:

1. Hot rolled, stress relieved, ground and etched beryllium sheet tested at room temperature. (density = 0.067 lb./in.^{3}). K_t = 2.4
2. 2024–T3 aluminum alloy (density = 0.100 lb./in.^{3}). K_t = 2.0
3. 8Al–12Mo–1V titanium (density = 0.158 lb./in.^{3}). K_t = 2.3
4. Tension-tension fatigue test. R = 0.2 (R = minimum stress/maximum stress)
5. f_{max} = maximum average net stress at stress concentration.

Figure 43 – Fatigue Strength-to-Weight Efficiency of Notched Material: Beryllium, Aluminum and Titanium

TABLE 15
STATIC TENSION TEST RESULTS

Specimen Designation	Specimen Thickness (in.)	Specimen Width (in.)	Hole Diameter (in.)	Countersink Diameter (in.)	Failure Load (lb.)	Failure Stress (ksi)	Certified Tensile Strength (ksi)
404-006-41-29	.0291	.5152	.1300	——	628	56.0	84.2
404-006-41-30	.0285	.5152	.1311	——	830	75.8	84.2
404-006-41-36	.0289	.5143	.1330	——	820	74.5	84.2
404-006-7-19	.0558	.5181	.144(4)	.225(4)	1410	72.5	79.4
404-006-7-20	.0548	.5121	.144(4)	.225(4)	1350	71.9	79.4
404-006-7-21	.0551	.5179	.144(4)	.225(4)	1435	74.6	79.4
404-006-37-1	.0561	.4985	.1324	.196(4)	1370	69.6	79.4
404-006-37-2	.0555	.5145	.1322	.196(4)	1710	84.0	79.4
404-006-37-3	.0562	.5005	.1314	.196(4)	1460	72.2	79.4
404-006-9-10	.0559	.5207	.130(4)	.196(4)	1425	71.5	79.4
404-006-9-11	.0560	.5149	.130(4)	.196(4)	1615	78.0	79.4
404-006-9-12	.0566	.4997	.130(4)	.196(4)	1530	76.0	79.4

Notes:

1. Hot rolled, stress relieved, ground and etched beryllium sheet tested at room temperature.
2. After machining and deburring, specimens were chem-milled to remove 0.003 to 0.004 inch total thickness
3. Longitudinal grain direction parallel to load axis.

(4) Nominal dimension – all others as measured.

5. Strain rate was .005/in./in./min.

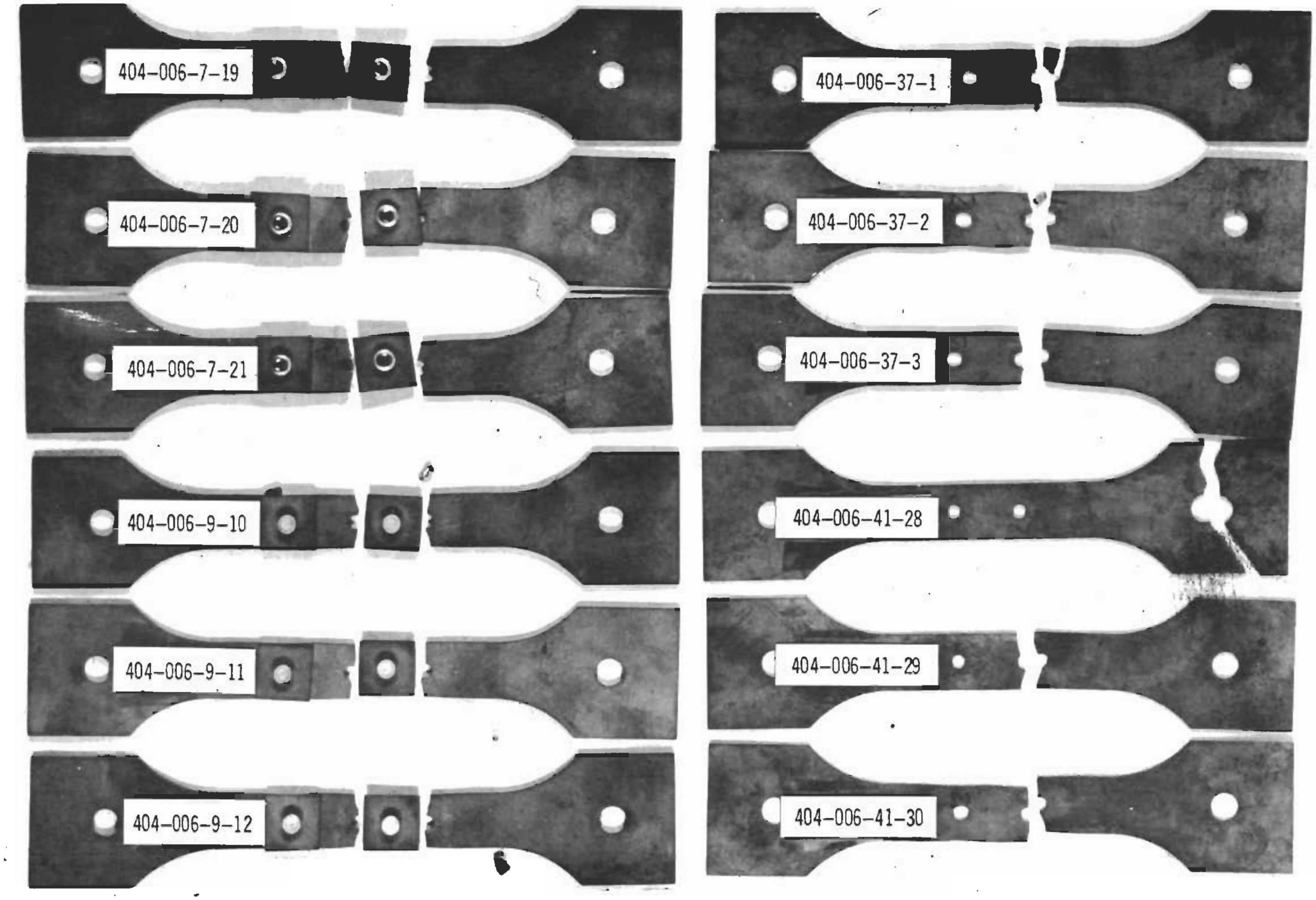
404-006-7-19
404-006-7-20
404-006-7-21
404-006-9-10
404-006-9-11
404-006-9-12
404-006-37-1
404-006-37-2
404-006-37-3
404-006-41-28
404-006-41-29
404-006-41-30

Stress Concentration and Interference Fit Fastener Specimens

Figure 44 – Static Tension Test Failed Specimens

6. Joint Tests

Tension tests were conducted to determine the splice strength of beryllium sheet and obtain data useful in establishing beryllium joint design criteria. The joints tested had structural details similar to those in the beryllium rudder. The test specimens, test set-up and procedures, and test results are discussed below.

A total of twelve tests were conducted with two at room temperature and two at -65°F ± 5°F on each of three different splice joint configurations: (1) splice attached with CR 2248-4 aluminum cherry rivets on one side and bonded with FM-61 adhesive on the other (404-006-1), (2) splice attached with NAS 1670 alloy steel Jo-bolts (404-006-3), and (3) splice attached with NAS 1097 AD4 solid one-piece aluminum rivets on one side and bonded with FM-61 adhesive on the other (404-006-5). The three types of test specimens are shown in Figure 45. The tests were conducted in a 30,000 lbs.capacity Wiedemann-Baldwin Universal Testing Machine. Loading rates of 2000 lbs./minute for the -1 and -5 specimens and 3500 lbs./minute for the -3 specimens were maintained during the tests. A dial-indicator measured lateral deflection at each specimen center during load application. These data were subsequently used to determine bending stresses caused by load path eccentricities at the splice. A test specimen in the loading grips, with instrumentation, is shown in Figure 46.

The test results shown in Table 16 indicate that beryllium sheet can be spliced using conventional methods to provide adequate and predictable joint strength. As indicated in Table 16, the general mode of failure is fastener shear for the -1 and -5 specimens and skin rupture for the -3 specimens. Failure stresses in the skins of the -3 specimens, resulting from both

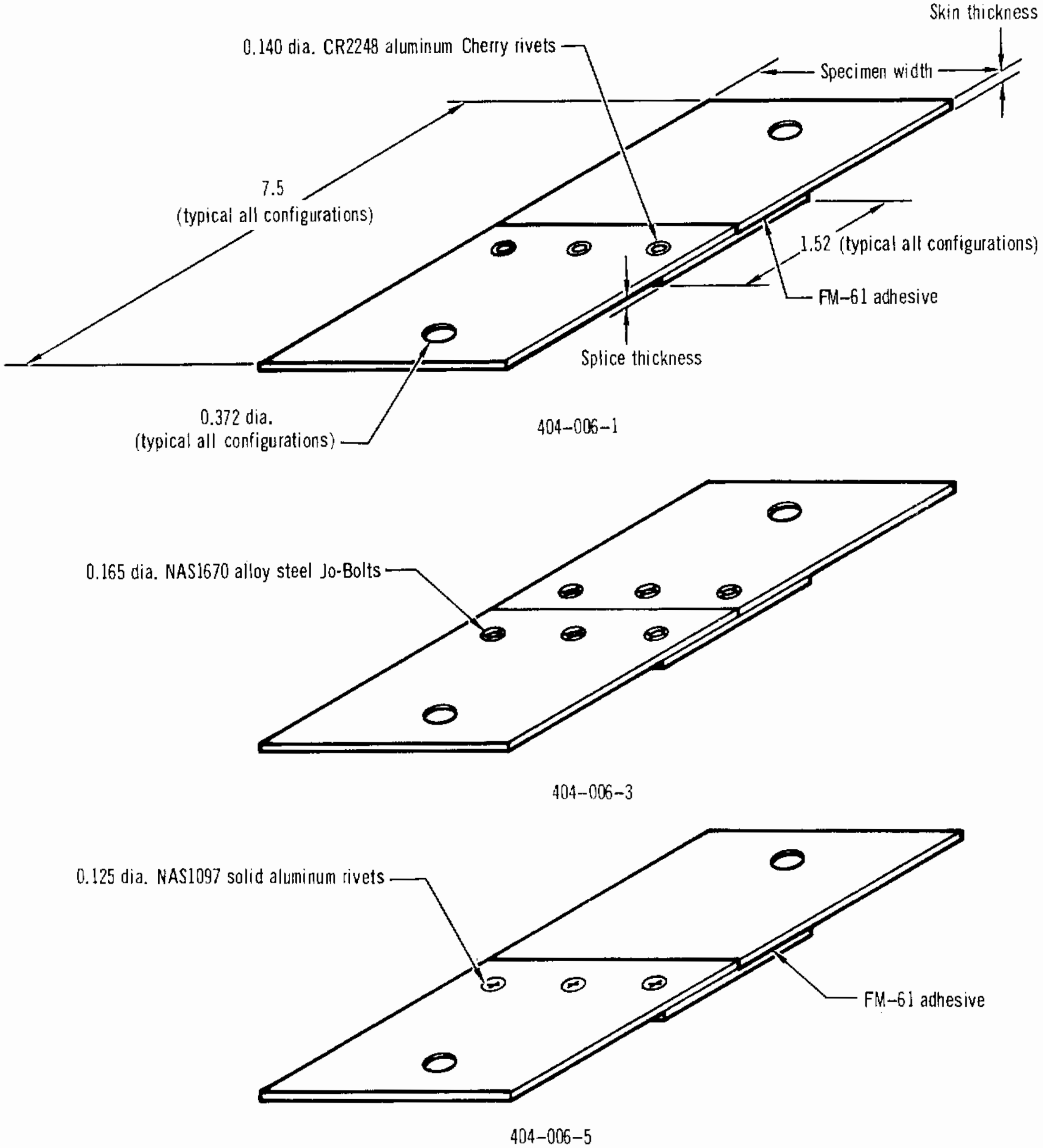
Skin thickness
0.140 dia. CR2248 aluminum Cherry rivets
Specimen width
7.5
(typical all configurations)
1.52 (typical all configurations)
FM-61 adhesive
Splice thickness
0.372 dia.
(typical all configurations)
404-006-1
0.165 dia. NAS1670 alloy steel Jo-Bolts
404-006-3
0.125 dia. NAS1097 solid aluminum rivets
FM-61 adhesive
404-006-5

Figure 45 – Spliced Joint Test Specimen Configurations

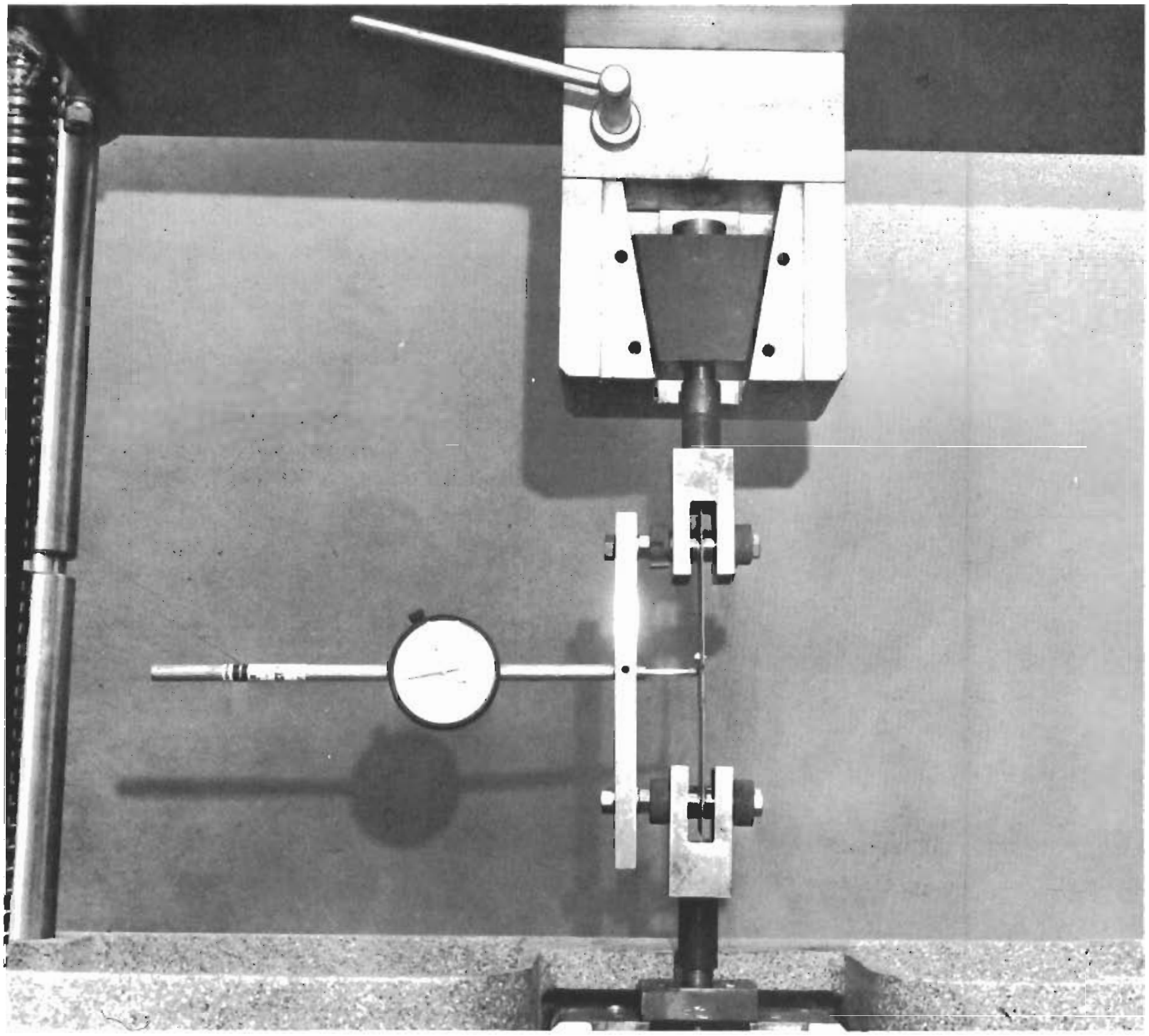

Figure 46 – Spliced Joint Tension Test Set-Up

TABLE 16

SPLICED JOINT TENSION TEST RESULTS

Specimen Designation	Test Temp. (°F)	Skin Thickness / Splice Thickness (in.)	Specimen Width (in.)	Lateral Deflection (in.)	Failure Mode	Failure Load (lb.)	Maximum Elastic Stress at Splice Center (psi)		
							Bending	Tension	Total
404-006-1-1	R.T.	.0533 / .0284	2.250	.0258	Fastener Shear	1280	63,700	20,000	83,700
404-006-1-2	R.T.	.0547 / .0279	2.225	.0220	Fastener Shear	1055	70,500	17,000	87,500
404-006-1-3	-65	.0570 / .0281	2.240	.0157	Fastener Shear	1180	107,300	18,800	126,100
404-006-1-4	-65	.0532 / .0285	2.230	.0214	Splice Rupture	1270	81,900	20,000	101,900
404-006-3-1	R.T.	.0865 / .0560	2.240	.0425	Splice Rupture	3325	81,500	26,500	108,000
404-006-3-2	R.T.	.0874 / .0551	2.240	.0281	Splice Rupture	3120	118,800	25,300	144,100
404-006-3-3	-65	.0866 / .0546	2.240	.0203	Grip Hole Rupture	3025	136,700	24,700	161,400
404-006-3-4	-65	.0865 / .0559	2.240	.0465	Splice Rupture	3070	65,000	24,600	89,600
404-006-5-5	R.T.	.0530 / .0266	2.245	.0249	Fastener Shear	1290	72,600	21,600	94,200
404-006-5-6	R.T.	.0525 / .0278	2.245	.0278	Fastener Shear	1385	59,300	22,200	81,500
404-006-5-7	-65	.0531 / .0281	2.230	.0212	Splice Rupture	1400	92,500	22,300	114,800
404-006-5-8	-65	.0535 / .0274	2.240	.0260	Fastener Shear	1395	72,000	22,700	94,700

Notes: 1. Hot rolled, stress relieved, ground and etched beryllium sheet.
2. After machining and deburring, skins were chem-milled to remove 0.003 to 0.004 inch total thickness.
3. Total exposure time to test temperature was approximately 15 minutes.
4. Load rate was 2000 pounds per minute for the –1 and –5 specimens and 3500 pounds per minute for the –3 specimens.

bending and tension loads, are significantly greater than the material tensile strength (F_{tu} = 70-80 ksi), being in excess of 100 ksi for all specimens except one. This implies that beryllium has a bending modulus of rupture considerably larger than the tensile strength of the material. No bonding failures occurred in those specimens with one side of the splice joined to the skin with FM-61 adhesive. Figure 47 shows the failed specimens.

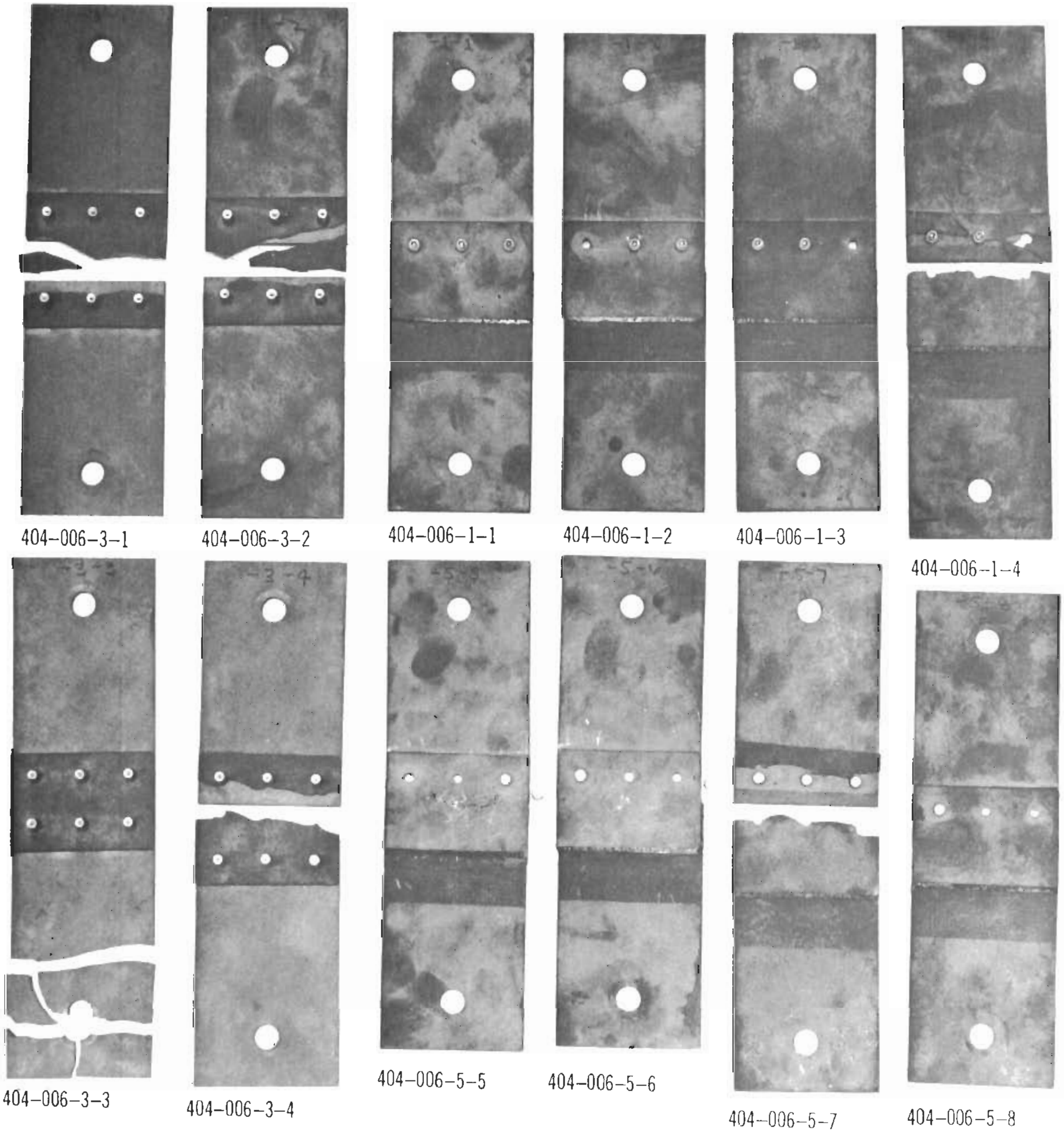

404-006-3-1
404-006-3-2
404-006-1-1
404-006-1-2
404-006-1-3
404-006-1-4
404-006-3-3
404-006-3-4
404-006-5-5
404-006-5-6
404-006-5-7
404-006-5-8

Figure 47 – Spliced Beryllium Joint Test Failed Specimens

7. Panel Shear Tests

Shear tests were conducted to obtain design data on the post buckling strength of flat beryllium panels. The test specimens, test set-up and procedures, and test results are discussed below.

Five specimens were tested in two basic panel sizes, 10x10.5 inches and 10x20 inches, with thicknesses ranging from .014 inch to .053 inch. In addition, two 7178-T6 aluminum alloy panels were tested with the beryllium panels for purposes of comparison. The panels were tested at room temperature in a cantilevered jig assembly. Loading straps, fastened to the jig at the free end, were attached to a calibrated resistance strain link which was connected to a hydraulic load cylinder. The hydraulic cylinder and strain link were used in conjunction with a servo-mechanism system to provide control of the loading rate which was maintained at 2000 pounds/minute until failure for the beryllium panels and 1000 pounds/minute for the aluminum panels. Figure 48 shows the test set-up. Strains were measured during the testing of each panel by two strain rosettes mounted back to back at the geometric center of the specimen. In addition, the diagonal deflection of the panel was measured by a calibrated bending beam transducer mounted between the two diagonally opposite jig corner pins. All data recording was accomplished with a calibrated Honeywell Strip Chart Recorder.

The initial buckling strength of the beryllium panels was predicted with the classical buckling equation,

$$\frac{F_{s_{cr}}}{\eta} = \frac{\pi^2 K_s E}{12(1 - \mu^2)} \left(\frac{t}{b}\right)^2$$

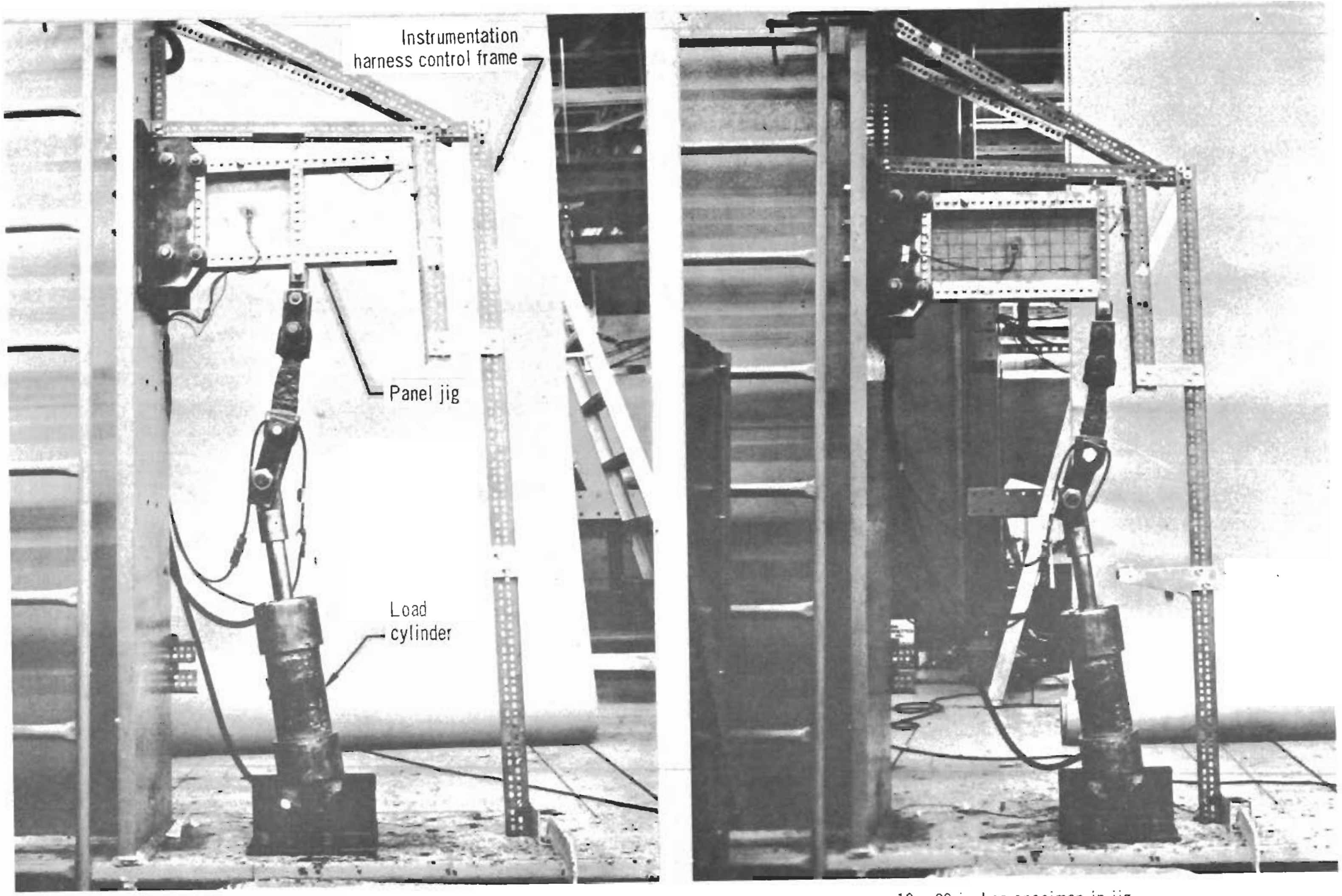
Instrumentation
harness control frame
Panel jig
Load
cylinder

10 x 10.5 inches specimen in jig

10 x 20 inches specimen in jig

Figure 48 – Panel Shear Test Set-Up

The basic information on the post buckling shear strength of the seven panels tested is presented in Table 17. All panels developed normal two-buckle patterns which were visible prior to failure, although the buckles in the beryllium panels were less pronounced than those in the aluminum panels. Figure 49 shows a failed beryllium panel in the loading jig with a relatively prominent buckle pattern. The beryllium test specimens shattered at maximum load and appeared to fail by cracking in the buckle pattern due to excessive bending stresses. One of the aluminum panels apparently failed in diagonal tension while the other failed by shearout of the fasteners. Figure 50 shows the panel specimens after failure. The diagonal tension angle of the failed specimens is approximately 45° for the square panels, and between 35° and 40° for the rectangular panels. It is evident from the information presented in Table 17 that aluminum panels have greater strength in shear than beryllium panels having the same dimensions, for the specified test conditions. A post buckling shear strength design curve for beryllium cross-rolled sheet developed from the test data is presented in Section II.

TABLE 17
FLAT PANEL SHEAR TEST RESULTS

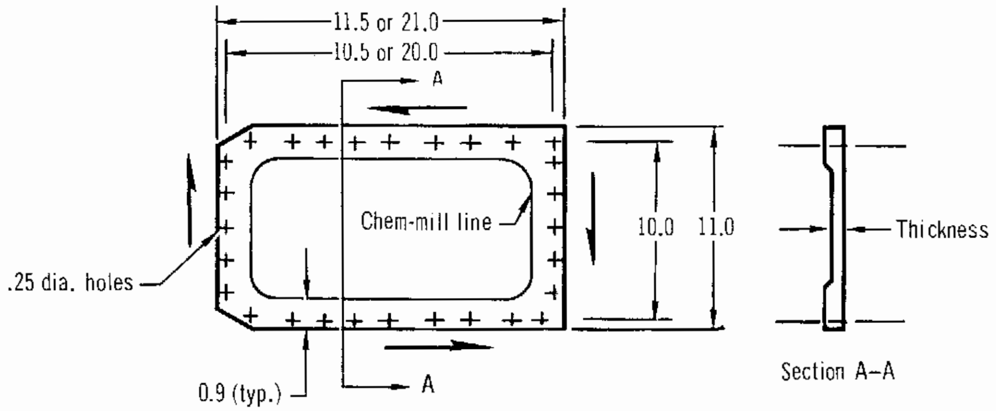

Test Data	Panel Designation						
	404–002–15	404–002–17	404–002–19	404–002–23	404–002–25	404–002–27	404–002–29
Specimen Material	Beryllium	Beryllium	Beryllium	Beryllium	Beryllium	Aluminum	Aluminum
Specimen Size (in.)	10 x 20	10 x 20	10 x 20	10 x 10.5	10 x 10.5	10 x 10.5	10 x 20
Thickness (in.) (4)	0.014	0.030	0.052	0.032	0.053	0.032	0.032
Test Temperature (°F)	R.T.	R.T.	R.T.	R.T.	R.T.	R.T.	R.T.
Maximum Shear (lb./in.)	307	535	1,061	735	1,257	1,289	1,301
Maximum Stress (psi)	21,929	17,833	20,404	22,969	23,717	40,281	40,656

Notes:

1. Material was 7178–T6 aluminum alloy and hot rolled, stress relieved, ground and etched beryllium sheet.
2. After machining and deburring, beryllium specimens were chem-milled to remove 0.003 to 0.004 inch total thickness.
3. Load rate of 2000 pounds/minute for beryllium panels and 1000 pounds/minute for aluminum panels.

(4) Average thickness from nine readings taken over panel surface.

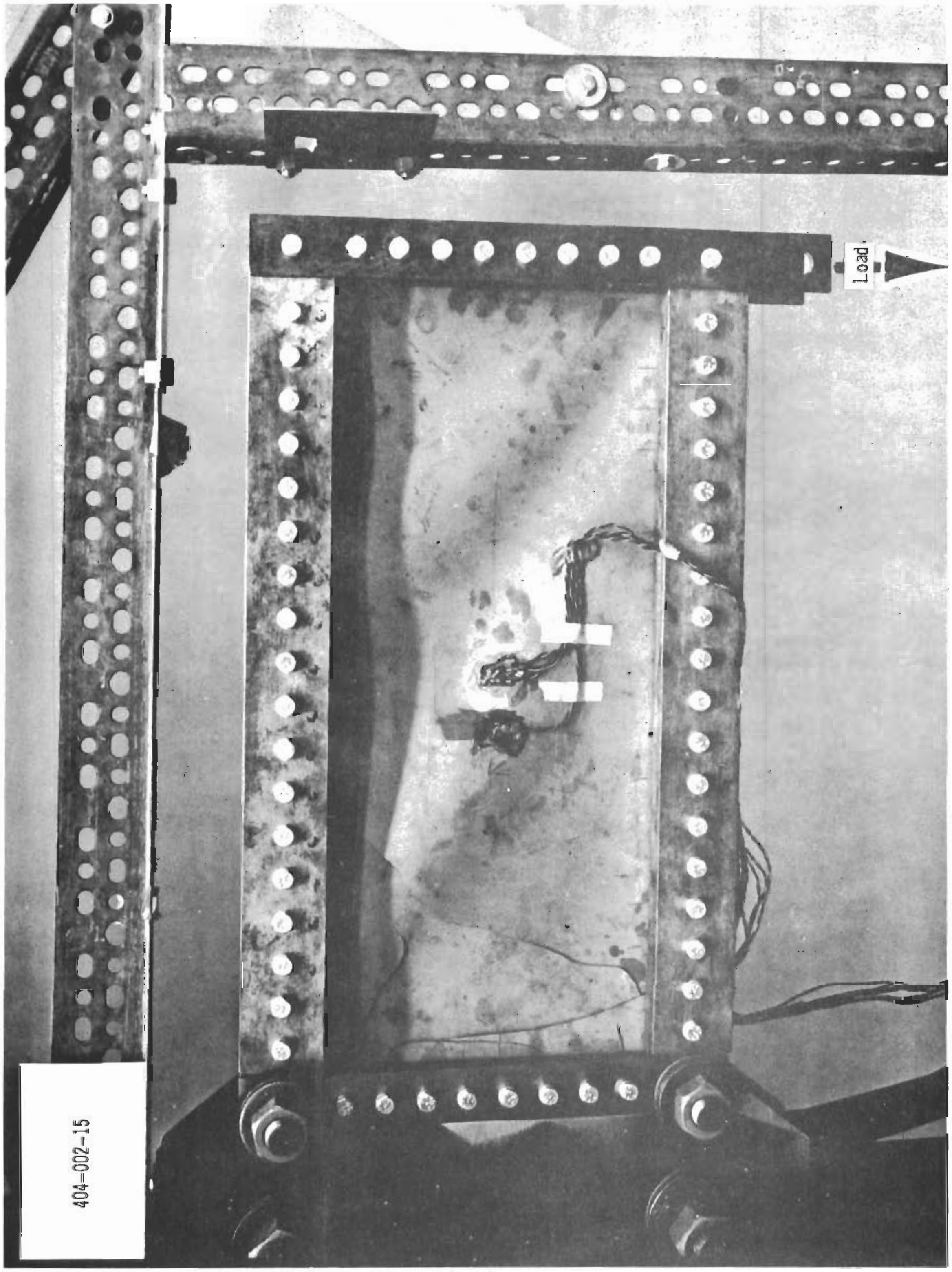
Load
404-002-15

Figure 49 – Loading Jig and Failed Shear Panel

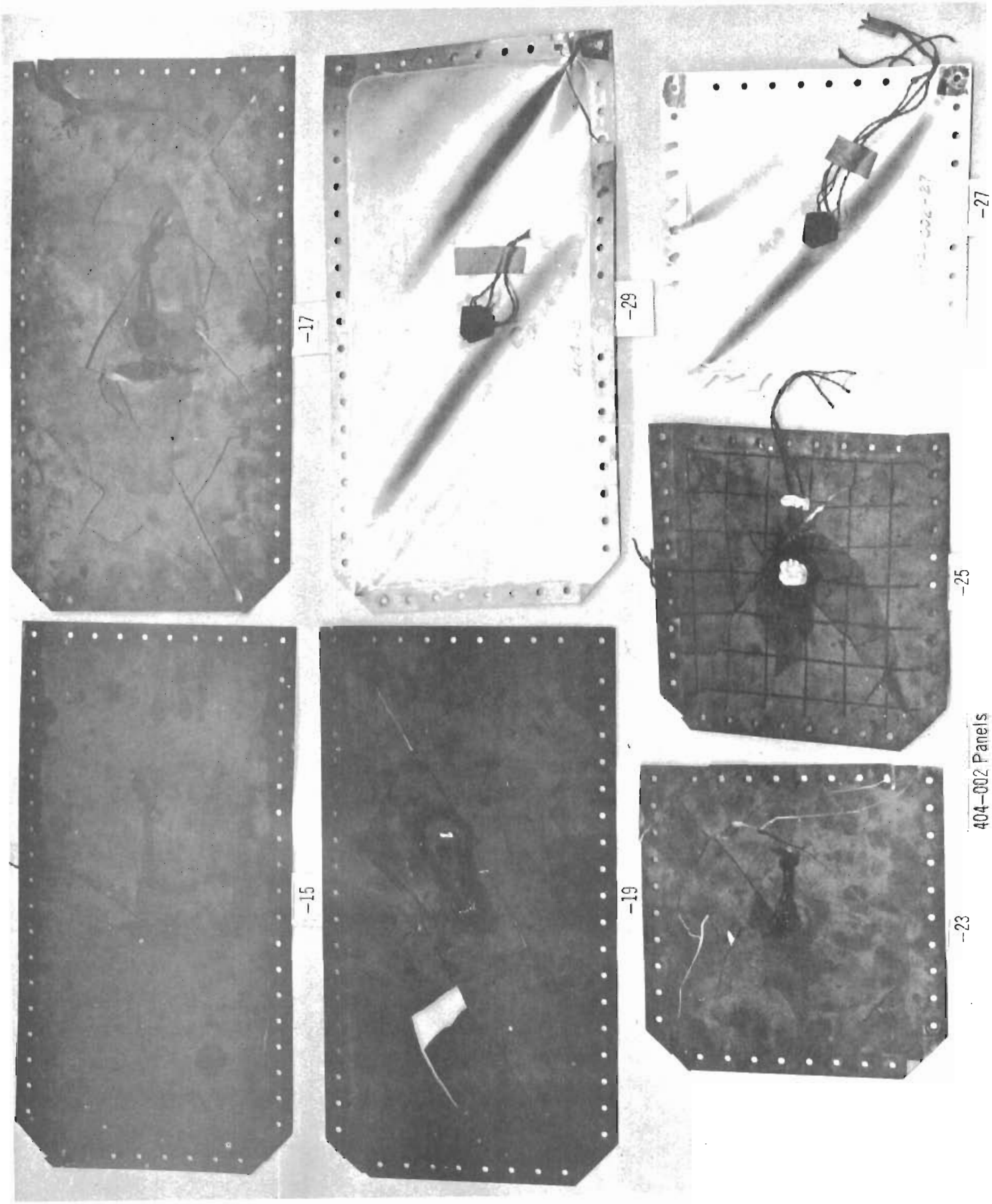
-17
-29
-27
-25
-15
-19
-23
404-002 Panels

Figure 50 - Panel Shear Test Failed Specimens

8. Spliced Panel Shear Tests

Shear tests of spliced, flat beryllium panels were performed. The data from these tests supplement those obtained from the joint tests, previously discussed, in establishing beryllium joint design criteria. The test specimens, test set-up and procedures, and test results are discussed below.

Twelve tests were conducted on panels 10x10.5 inches in size, with three at room temperature and one at -65° ± 5°F on each of three different splice configurations: (1) splice attached with HT-424 epoxy-phenolic adhesive (404-003-1), (2) splice attached with CR2248 aluminum cherry rivets (404-003-3), and (3) splice attached with NAS 1670 alloy steel Jo-bolts (404-003-5). Figure 51 shows the test specimens. The cantilevered loading jig previously described, shown in Figure 48 , was used for all tests. A load rate of 2000 pounds/minute was maintained until specimen failure. For the sub-zero (-65°F) tests, the specimens were enclosed in an insulated box. Dry air, cooled by passing through a heat exchanger, was introduced into the insulated box until the test temperature was attained. Two chromel-alumel thermocouples were installed on the specimen for the purpose of monitoring test temperatures.

Table 18 shows the test results. The beryllium panels shattered at maximum load and appeared to crack in the buckle pattern which was not very prominent. This type of failure was similar to that experienced by the plain beryllium panels previously discussed. However, the true mode of failure could not be determined with any degree of certainty since initial failure of any panel could have occurred at the splice joint causing the panel to shatter in the buckle pattern as a secondary result. It can be concluded from the test results that beryllium shear panels can be spliced by

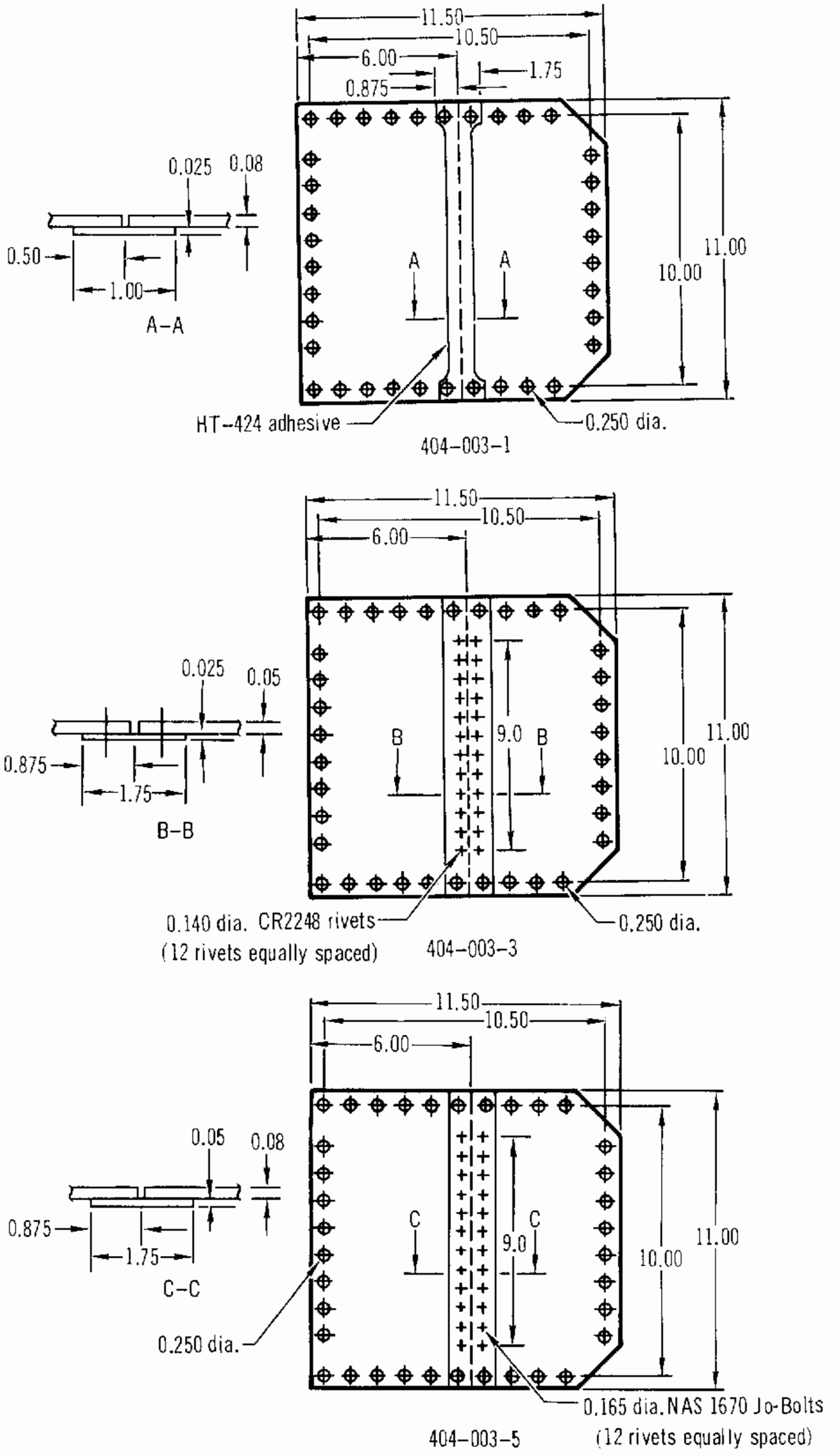
11.50
10.50
6.00
1.75
0.875
0.025
0.08
0.50
1.00
A–A
A
A
10.00
11.00
HT-424 adhesive
0.250 dia.
404–003–1
11.50
10.50
6.00
0.025
0.05
0.875
1.75
B–B
B
9.0
B
10.00
11.00
0.140 dia. CR2248 rivets
(12 rivets equally spaced)
404–003–3
0.250 dia.
11.50
10.50
6.00
0.05
0.08
0.875
1.75
C–C
C
9.0
C
10.00
11.00
0.250 dia.
0.165 dia. NAS 1670 Jo-Bolts
(12 rivets equally spaced)
404–003–5

Figure 51 – Spliced Panel Shear Test Specimen Configurations

conventional means, and the panel strengths are comparable to structurally similar unspliced panels. Figure 52 shows a failed specimen of each configuration tested.

TABLE 18
SPLICED PANEL SHEAR TEST RESULTS

Specimen Designation	Skin Thickness (in.)	Splice Thickness (in.)	Test Temperature (°F)	Splice Attachment	Failure Load (lb.)
404-003-1-1	0.080	0.025	R.T.	Adhesive	17,530
404-003-1-2	0.080	0.025	R.T.	Adhesive	18,310
404-003-1-3	0.080	0.025	R.T.	Adhesive	16,800
404-003-1-4	0.080	0.025	-65	Adhesive	16,030
404-003-3-1	0.050	0.025	R.T.	Rivets	10,090
404-003-3-2	0.050	0.025	R.T.	Rivets	11,230
404-003-3-3	0.050	0.025	R.T.	Rivets	9,580
404-003-3-4	0.050	0.025	-65	Rivets	10,430
404-003-5-1	0.080	0.050	R.T.	Jo-Bolts	17,510
404-003-5-2	0.080	0.050	R.T.	Jo-Bolts	19,600
404-003-5-3	0.080	0.050	R.T.	Jo-Bolts	19,460
404-003-5-4	0.080	0.050	-65	Jo-Bolts	17,300

Notes:

1. Hot rolled, stress relieved, ground and etched beryllium sheet spliced with HT-424 adhesive, CR2248-4 rivets and NAS1670-08 Jo-bolts.
2. After machining and deburring, specimens were chem-milled to remove 0.003 to 0.004 inch total thickness.
3. Loading rate was 2000 pounds/minute.
4. Total exposure time to test temperature was approximately 15 minutes.
5. All dimensions shown are nominal.

404-003 Panels

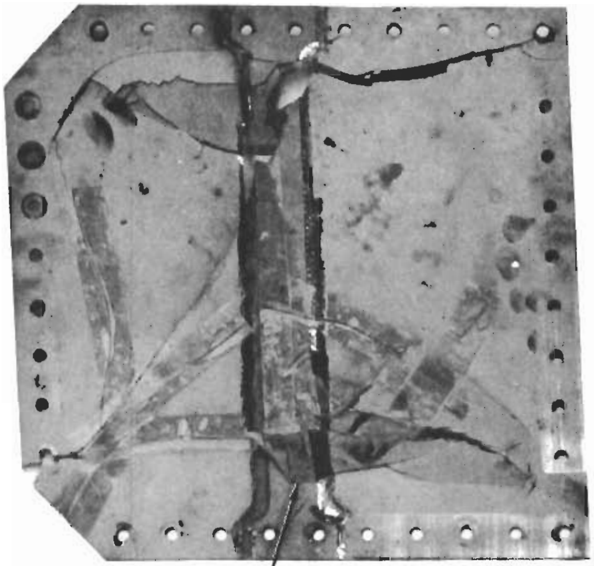

Splice bonded to skins with HT-424 adhesive

-1

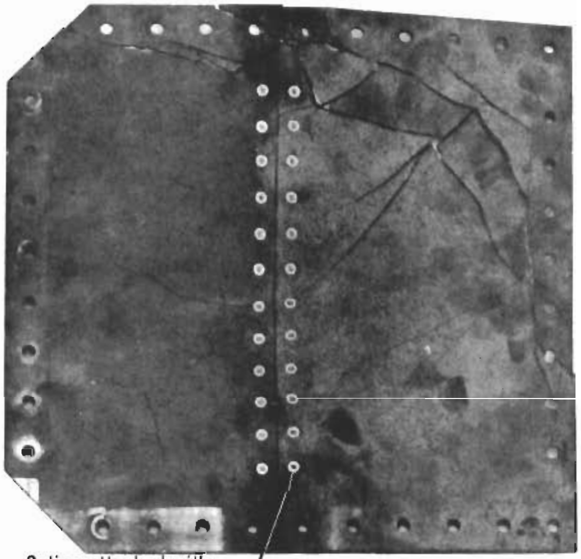

Splice attached with 0.140 dia. CR2248 countersunk aluminum Cherry rivets

-3

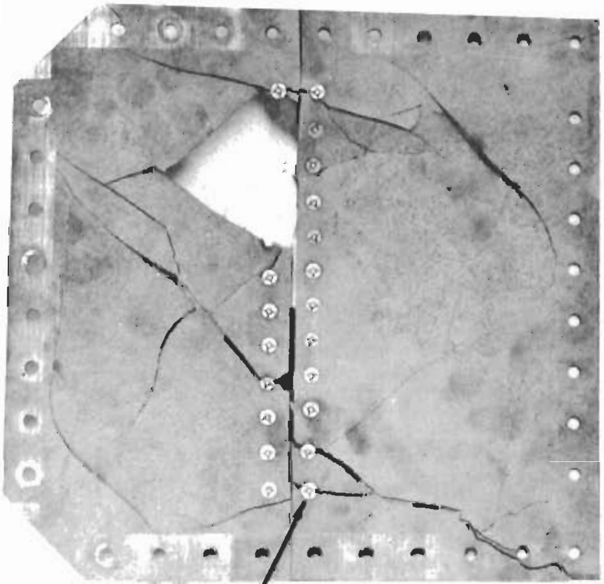

Splice attached with 0.165 dia. NAS1670 countersunk alloy steel Jo-Bolts

-5

Figure 52 – Spliced Panel Shear Test Failed Specimens

9. Lug Tests

Tests were conducted to obtain design data on the strength of symmetrical, axially loaded lugs fabricated from beryllium sheet. The test specimens, test set-up, and test results are discussed below.

Three specimens of each of the six lug configurations were tested (one each at -65°F, ± 5°F, room temperature, and 500°F ± 10°F). Tests were conducted in a 30,000 lbs. capacity Wiedemann-Baldwin Universal Testing Machine. The procedures and equipment used to establish and maintain the -65°F test temperature condition have been described previously in this section. For the 500°F tests, the specimen was enclosed in a resistance wire-wound furnace. The temperature was regulated by a Barber-Colman Controller in conjunction with a chromel-alumel thermcouple attached to the test specimen. A Leed's and Northrop Model "H" Temperature Indicator was used to monitor test temperatures. A Wiedemann-Baldwin Strip Chart Recorder, in conjunction with an extensometer, was used to plot total elongation (between the two lug loading pins) vs. load. The elongation measured approximates the total elongation of the two loading holes and was obtained so that the lug yield load (load at .012 inch permanent elongation of the .25 inch diameter hole) could be determined. These criteria for determining yield loads conform to those used in MIL-HDBK-5 for establishing joint bearing yield loads. For design, the ultimate load may not exceed 150% of the yield load. Therefore, the yield load was established to determine if the design ultimate strength should be limited by these yield-ultimate criteria. However, the ultimate load was less than 150% of the yield load for all of the lugs tested. Therefore, lugs fabricated from beryllium sheet should be designed by ultimate strength.

The failed test specimens are shown on Figure 53. The mode of failure of the specimens tested at 500°F is well defined. The material, in the area of the loading hole, yielded and underwent a significant amount of elongation; thereafter the specimens with relatively high W/D (specimen width/hole diameter) ratios failed by shear-out of the loading hole, and those with lower W/D ratios failed in tension at a section through the loading hole.

The failure mode for some of the room temperature and -65°F test specimens is not obvious. There are several lines of fracture emanating from the loading hole, and since failure occurred very rapidly, the location of the initial fracture could not be determined with any degree of certainty at the time of testing. However, it appears that most of the specimens failed primarily due to tension at a section through the loading hole, probably as a result of the stress concentration at the hole and the notch sensitivity of the material at the lower temperatures. The actual geometry of the test specimens, the test conditions, and the lug failing loads are presented in Table 19. A beryllium lug design chart developed from the test data is shown in Section II.

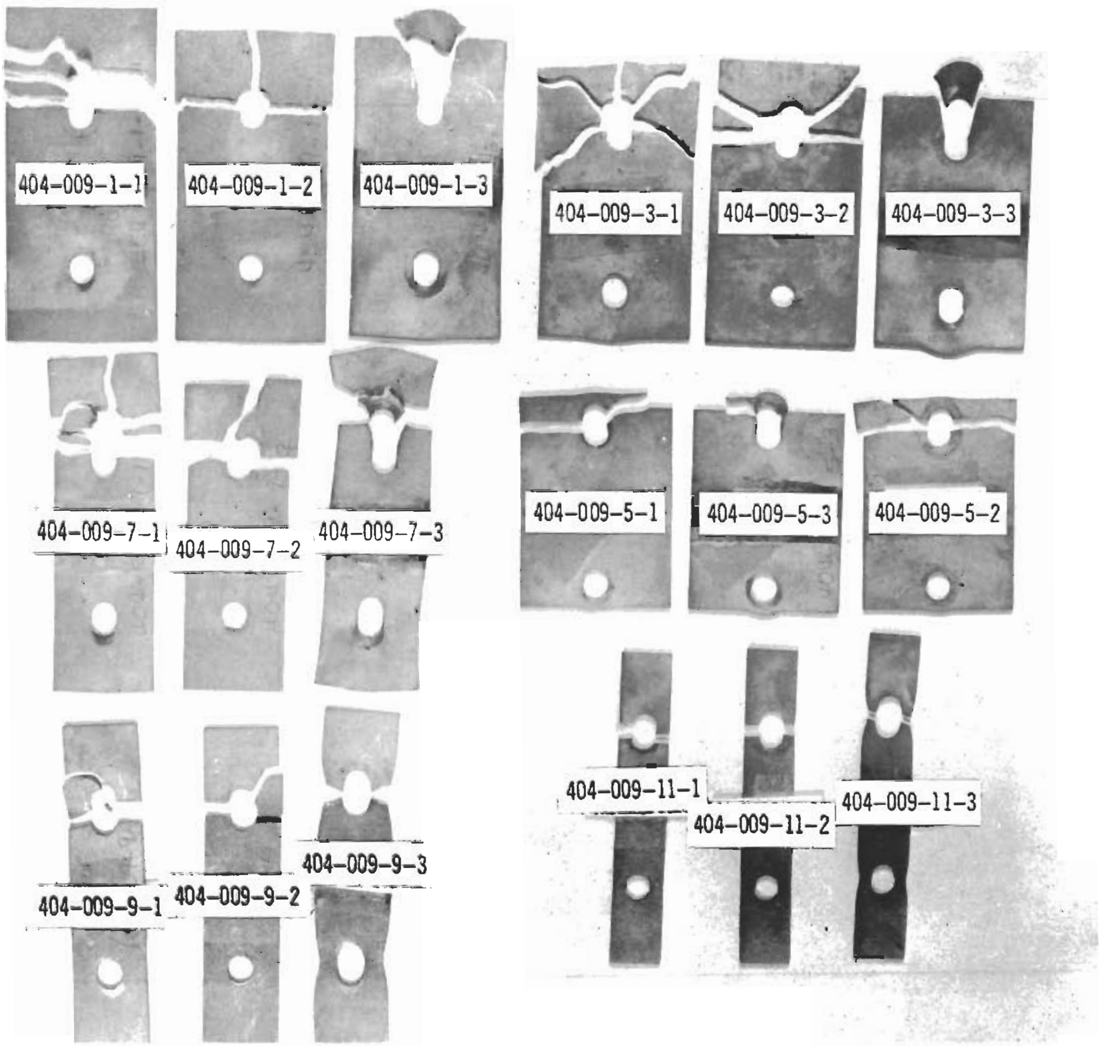
404-009-1-1
404-009-1-2
404-009-1-3
404-009-3-1
404-009-3-2
404-009-3-3
404-009-7-1
404-009-7-2
404-009-7-3
404-009-5-1
404-009-5-3
404-009-5-2
404-009-9-1
404-009-9-2
404-009-9-3
404-009-11-1
404-009-11-2
404-009-11-3

Figure 53 – Failed Beryllium Lug Specimens

TABLE 19

BERYLLIUM LUG TEST RESULTS

Specimen Designation	Test Temp.	R (in.)	W (in.)	D (in.)	t (In.)	R/D	W/D	(1) P (lb.)	(2) F_{br} (psi)	$\left(\frac{F_{br}}{F_{tu}}\right)$
404-009-1-1	R.T.	.75	1.48	.251	.0860	2.99	5.90	4250	197,000	2.51
-2	-65°F	.75	1.48	.251	.0852	2.99	5.90	4075	191,000	2.90
-3	500°F	.75	1.48	.251	.0858	2.99	5.90	3400	158,000	2.99
404-009-3-1	R.T.	.52	1.50	.251	.0860	2.07	5.97	3575	165,500	2.11
-2	-65°F	.53	1.50	.251	.0860	2.11	5.97	2225	103,000	1.56
-3	500°F	.53	1.50	.251	.0858	2.11	5.97	2415	112,000	2.12
404-009-5-1	R.T.	.27	1.50	.250	.0866	1.08	6.00	1655	76,500	0.975
-2	-65°F	.27	1.50	.251	.0865	1.075	5.97	1720	79,300	1.20
-3	500°F	.27	1.50	.251	.0870	1.075	5.97	1299	59,500	1.125
404-009-7-1	R.T.	.75	0.99	.251	.0866	2.99	3.94	4370	201,000	2.56
-2	-65°F	.76	0.99	.251	.0865	3.02	3.94	3515	163,000	2.47
-3	500°F	.76	0.99	.251	.0866	3.02	3.94	3050	140,200	2.66
404-009-9-1	R.T.	.76	0.75	.251	.0861	3.02	2.99	3120	61,800	1.84
-2	-65°F	.76	0.75	.251	.0863	3.02	2.99	2820	130,000	1.97
-3	500°F	.76	0.75	.251	.0862	3.02	2.99	2525	117,000	2.22
404-009-11-1	R.T.	.76	0.50	.250	.0856	3.04	2.00	1500	70,000	0.892
-2	-65°F	.75	0.50	.250	.0857	3.00	2.00	1655	77,200	1.17
-3	500°F	.76	0.50	.250	.0862	3.04	2.00	1265	58,700	1.11

Notes:

(1) P = Lug load at failure

(2) Bearing stress at failure = P/Dt

3. Hot rolled, stress relieved, ground and etched beryllium sheet.
4. All specimens were fabricated from the same sheet stock. For this material F_{tu} = 78,500 psi at room temperature

   F_{tu} = 66,000 psi at -65°F

   F_{tu} = 52,800 psi at 500°F
5. After machining and deburring, specimens were chem-milled to remove 0.003 to 0.004 inch total thickness.

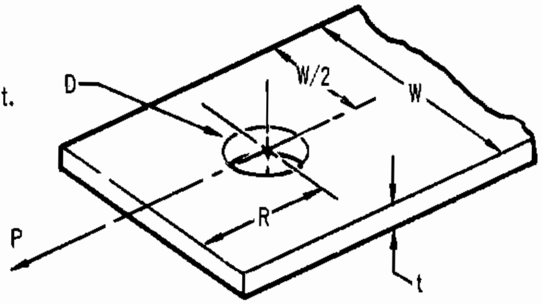

10. Corrosion Tests

Corrosion tests were performed in a 5% salt solution spray to establish the effectiveness of the surface finishes considered for corrosion protection of a beryllium rudder. The test specimens, corrosion protection systems used, test conditions and test results are discussed below.

Sixteen specimens were tested in two groups. The configuration of the nine specimens in the first group was designed to duplicate material and fastener combinations in the beryllium rudder. The second group of specimens was tested when it was found that the surface treatments tested in the first group, while providing adequate corrosion protection, adversely affected the mechanical properties of beryllium or would not adhere adequately to the beryllium surface. Simple beryllium panels were used for the second group of seven specimens. The corrosion test specimen configurations and the surface treatment and finishes are detailed in Figure 54. A chromic acid electrolyte was used to anodize (chemically oxidize) the beryllium. The SermeTel (Type W) coating, an inorganically (ceramically) bonded aluminum coating was developed specifically for corrosion protection by Teleflex, Incorporated, SermeTel Division of North Wales, Pennsylvania. The alodine treatment, a chromate conversion coating, was evaluated in the test of the second group of specimens. The epoxy enamel paint system, tested in both groups of specimens, is used for corrosion protection of the external surface of the F-4 aircraft. As indicated in the table in Figure 54, more than one surface treatment or finish was applied (one on top of the other) to some of the specimens. This was done to determine whether increased resistance to corrosion would result, and whether the coatings might adhere to a previously treated, or coated, beryllium surface better than to a bare beryllium surface.

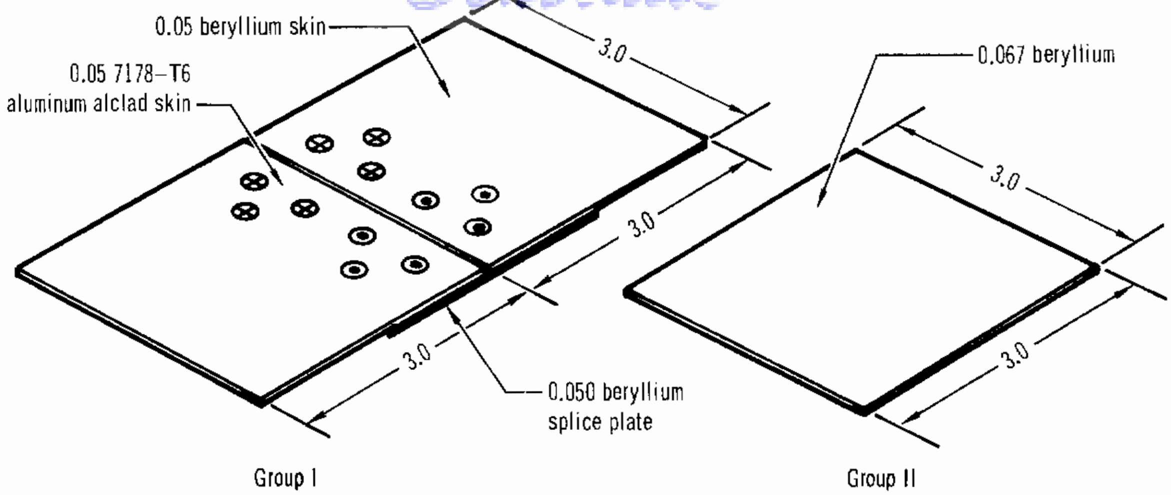

Notes:

1. ⊗ Aluminum Hi-Shear flush head rivet and collar.
2. ⊙ Steel Hi-Lok flush head fastener and collar.
3. Hot rolled, stress relieved, ground and etched beryllium sheet.
4. After machining and deburring, skins were chem-milled to remove 0.003 and 0.004 inch total thickness.
5. Specimens finished as indicated in the table below. Where a specimen received more than one finish, or coating, they were applied in the order indicated in the table. Finishes are applied after the detail parts were machined, drilled, and chemically etched.

I. Anodize.

II. Two coats Serme Tel (Type W) – total thickness 0.0015–0.0030 per surface.

III. Two coats zinc chromate primer on backs of aluminum and beryllium skins and on all surfaces of the beryllium splice plates before assembly of the specimens.

IV. Alodined and dried at ambient.

V. Alodined and dried at 275°F.

VI. Epoxy paint system. For Group I, system applied only to upper surface (countersunk fastener head side) and all edges after installing fasteners.

VII. Faying surfaces taped with silicone glass cloth tape.

VIII. Epoxy paint system applied after specimen baked for 30 minutes at 275°F.

	Specimen Designation		Finish						
		I	II	III	IV	V	VI	VII	VIII
Group I	404–007–1–1								
	404–007–1–2								
	404–007–1–3			√			√		
	404–007–1–4	√		√					
	404–007–1–5		√	√					
	404–007–1–6	√		√			√		
	404–007–1–7		√	√			√		
	404–007–1–8	√	√						
	404–007–1–9	√	√	√			√		
Group II	10								√
	11				√				
	12				√				
	13				√		√		
	14				√		√		
	15					√	√		
	16					√	√		

Figure 54 – Corrosion Test Specimens

All specimens of each group were simultaneously subjected to a 5% salt (NaCl) spray solution for 500 hours. Test conditions conformed to Federal Test Method Standard 151A, Method 811.1, except that the test temperature of the first group of specimens varied from 90-104°F, instead of the specified 92-97°F during the early stages of the test. Total exposure time at temperature outside the specified limits was approximately 12 hours. All specimens were held in a plexiglass rack at an angle of 15 degrees from vertical. Specimens of Group I were held with skin surfaces up. Before the tests commenced, each specimen was given a careful visual examination to detect flaws in the protective finishes. These areas were carefully monitored throughout the tests to see whether corrosion would initiate at the flaw. All specimens were examined periodically throughout the tests. The condition of each specimen was recorded at each inspection. The following paragraphs summarize the significant observations made as the tests progressed.

10.1 Group 1 - The specimens are shown before and after the 500 hours salt spray test in Figures 55, 56 and 57. The bare beryllium skin and splice plate on specimens 1 and 2 had corrosion pits after only 12 hours exposure to the salt spray and continued to corrode throughout the test. The beryllium on specimen 1 was much more severely attacked than the beryllium on specimen 2. This was due to the fact that specimen 1 was tested with the beryllium skin on top, and specimen 2 was tested with the beryllium skin on the bottom where it collected additional moisture in the form of runoff from the aluminum skin.

There was no evidence of corrosion on the anodized beryllium surface (specimen 4) at completion of the tests except at the fastener holes (galvanic corrosion) and adjacent to the fasteners where the anodic film had been

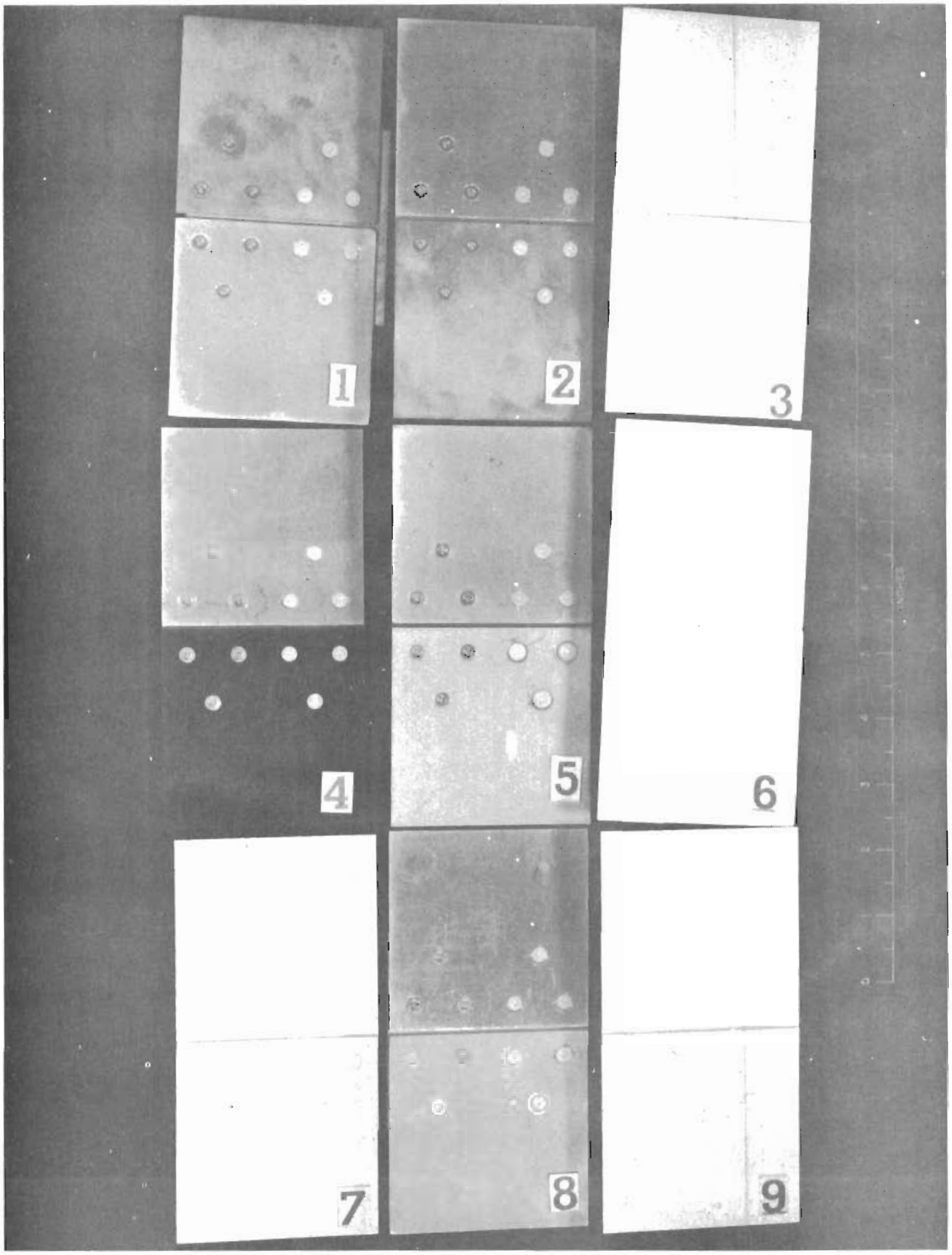

Figure 55 – Group 1 Corrosion Test Specimens Before 500 Hours Exposure

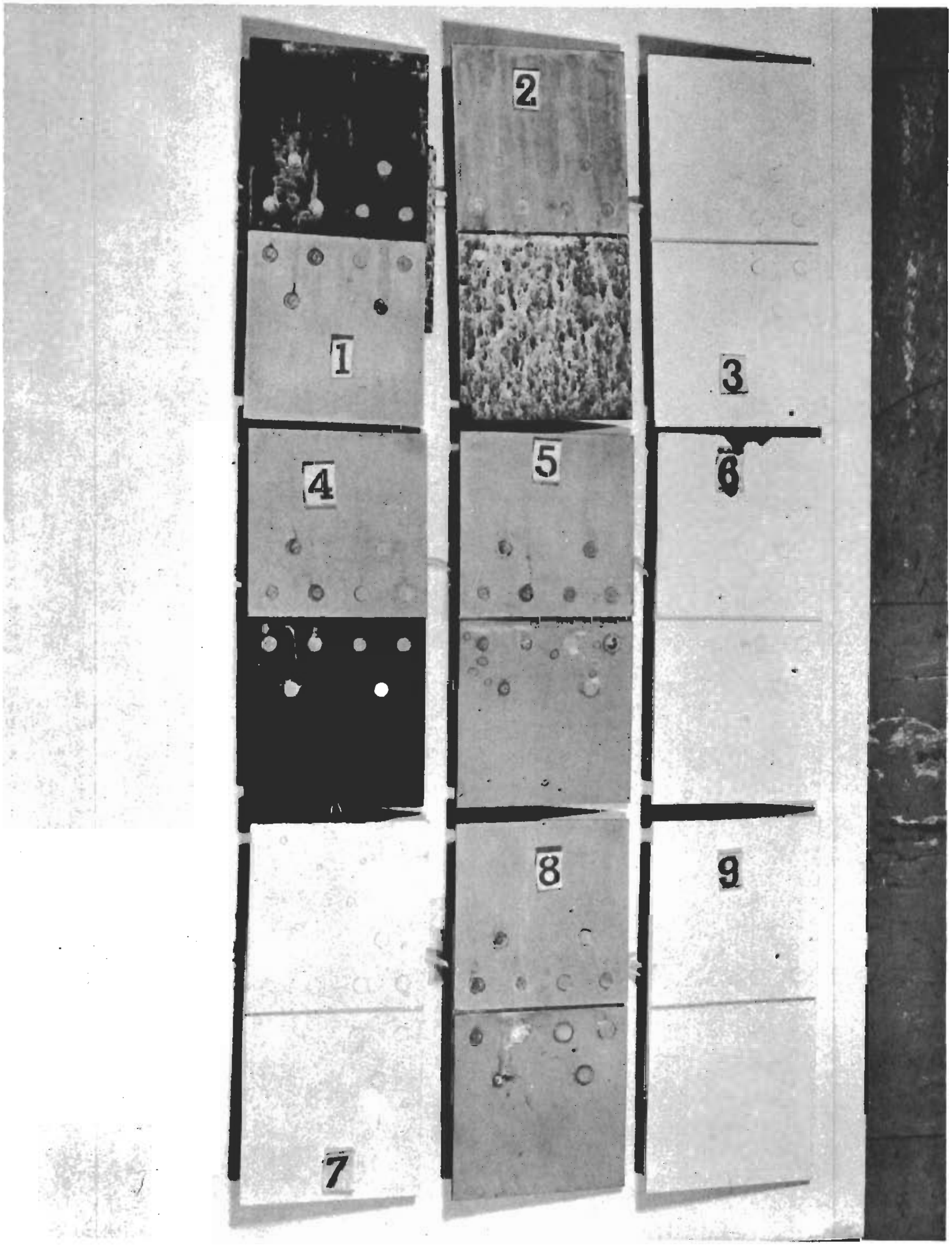

Figure 56 – Group I Corrosion Test Specimens After 500 Hours Exposure

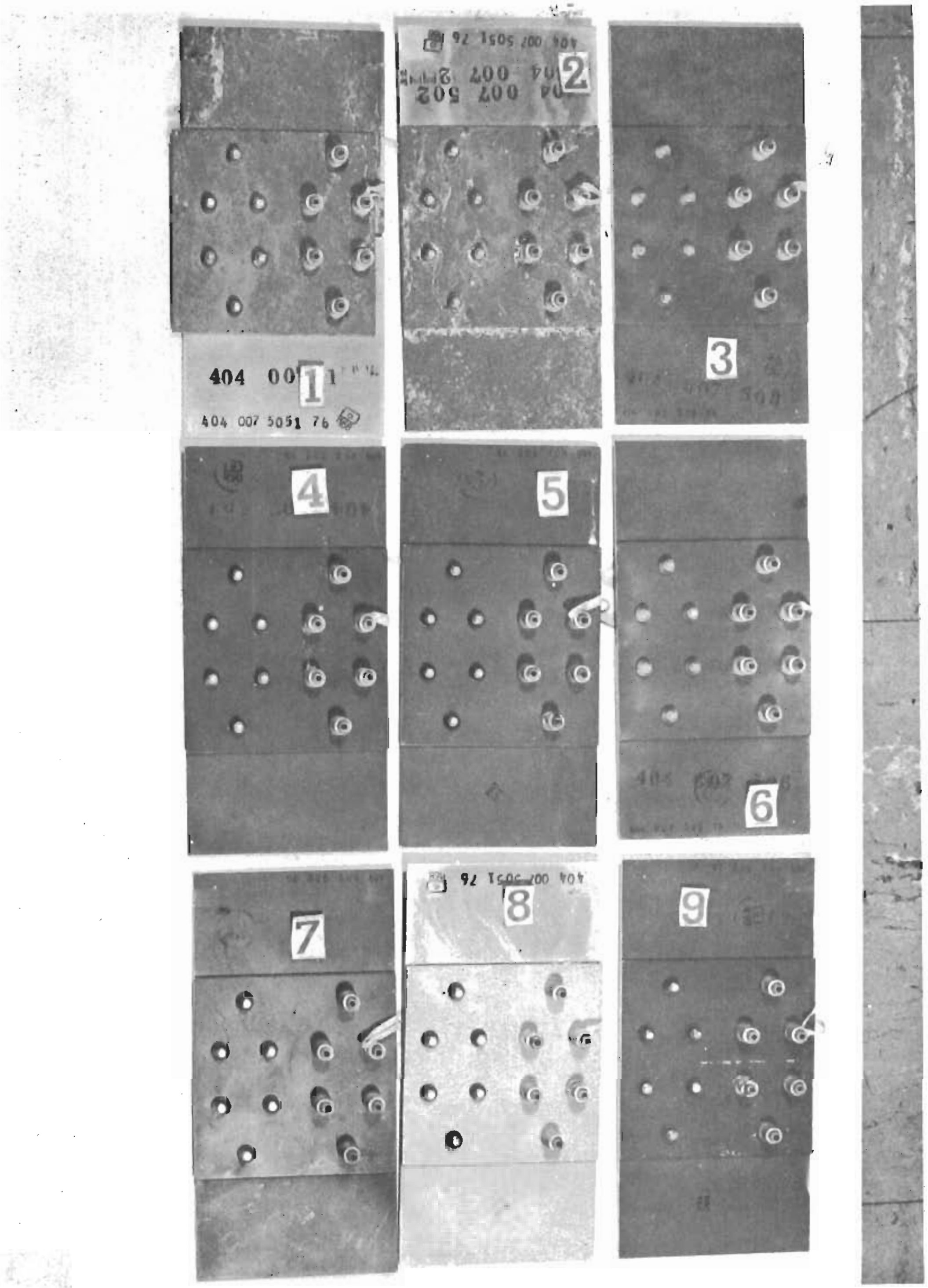

Figure 57 – Backs of Group I Corrosion Specimens After 500 Hours Exposure

marred during installation of the fasteners. The anodic film provided much better corrosion protection than had been expected.

The SermeTel coating (specimens 5 and 8) provided excellent corrosion protection. There was no evidence of corrosion except at the fasteners (galvanic corrosion). Since beryllium must be chemically etched after machining, the SermeTel coating was applied after drilling and countersinking the fastener holes. The coating thickness was .0015-.0030 inch thick, and had to be removed from the fastener holes so that the fasteners could be installed. As a result, there was no protection against galvanic corrosion between the beryllium and the fasteners.

The epoxy enamel paint system provided excellent corrosion protection. Even though the paint blistered on specimens 3 and 6 before the test was completed, there was no evidence of corrosion at the blisters. There was evidence of galvanic corrosion at the fasteners on these specimens also. The blistering of the epoxy paint was thought to be associated with the type surface to which it was applied. The paint blistered on specimen 3 (paint applied to etched beryllium surface) after 12 hours exposure. On specimen 6 (paint over anodized surface) blistering occurred after 120 hours. The paint did not blister on specimen 7 (paint over SermeTel W coating). When the blistering was first noticed, an investigation was begun to see if the blistering could be eliminated. It was found that liquid honing of the surface, after the final etch and before painting, eliminated the blistering. Two samples were prepared in this way, and after 500 hours in the salt spray there was no evidence of paint blistering or corrosion. To establish any possible adverse effect of liquid honing on the mechanical properties of beryllium, five tensile specimens were fabricated, etched, liquid honed, painted, and static tested. The results of these tests showed that the specimen ultimate tensile strength was reduced approximately 15% and elongation was reduced to less than 6% and to as low as 1%. Therefore, further investigations were required to develop a satisfactory method of applying the epoxy enamel paint system. A paint system would be the most desirable for corrosion protection of the rudder since it could be applied after fabrication and assembly were completed and could be easily repaired in service if it was scratched or chipped accidentally.

There was no evidence of corrosion on the zinc chromate primed surfaces of the specimens. Zinc chromate primer was applied to the back of specimens 3, 6, 7, and 9 (representing the rudder substructure and interior surfaces). In the test, as it would be on the rudder, the zinc chromate primed surfaces were not subjected to as severe an environment as the front (exterior surface) of the specimens. Two coats of zinc chromate primer would be selected for use on the substructure, the interior surfaces of the external skins, and all faying surfaces of a beryllium flight test rudder.

After the test was completed and the specimens were disassembled, it was found that galvanic corrosion existed on the beryllium at the fastener holes. There was evidence of galvanic corrosion, especially at the cadmium plated steel fasteners, on all specimens including those where the fastener holes were anodized or coated with SermeTel (Type W). It was probable that the anodic film and the SermeTel coating were damaged during fastener installation and galvanic corrosion resulted. The fasteners themselves were not corroded. To avoid this galvanic corrosion, the fastener holes could be sealed with Polysulfide (MIL-S8802) sealant and the fasteners installed wet. This should eliminate galvanic corrosion at the fasteners.

Because of the appearance of specimens 6, 7, 8, and 9 at the conclusion of the test, there does not appear to be any merit in using multiple finishes for corrosion protection. There was no noticeable difference between these specimens and those to which only one protective finish was applied.

Based on the test results discussed above, any one of the surface finishes, anodize, SermeTel W, or epoxy enamel (if blistering was prevented) would provide adequate corrosion protection for a flight test beryllium rudder. To establish any possible adverse effect of the anodize or SermeTel treatment on the mechanical properties of beryllium, six room temperature tension tests were conducted on three black anodized and three SermeTel (Type W) coated specimens. The loading procedure and instrumentation in these tests were identical with those used in the material acceptance tests previously discussed.

Table 20 gives the tension test results and, for comparison, the producer's certified mechanical properties of the beryllium sheet from which the specimens were fabricated. There is a significant and unexpected reduction in elongation of the anodized specimens. Microscopic examination of the fractured surface of the test specimens, and metallographic examination of sections away from the fracture, showed the anodized surfaces to be pitted. In all cases, the fracture appeared to originate at a pit. Figure 58 shows a test specimen anodized surface and, for comparison, the untreated surface of a section taken from the same beryllium sheet. Such surface defects can reduce ductility without affecting yield or ultimate strength significantly.

The SermeTel (Type W) coating apparently had no adverse effect on the mechanical properties of beryllium. However, the coating was inadequately bonded to the beryllium material. In all tests, the coating began to crack and separate prior to material yield and was completely removed from the test specimen prior to failure. Figure 59 shows the failed specimens.

TABLE 20
TENSION TEST RESULTS OF SURFACE TREATED SPECIMENS

Test Results									Producer's Certified Mechanical Properties		
Specimen Designation	Surface Treatment	Specimen Thickness (in.)	Specimen Width (in.)	Yield Load (lb.)	Yield Stress (ksi)	Failure Load (lb.)	Failure Stress (ksi)	Percent Elongation	Yield Stress (ksi)	Failure Stress (ksi)	Percent Elongation
404-001-300	Anodize	.0788	.2350	1017	54.9	1310	70.7	4	52.5	78.5	19.0
404-001-301	Anodize	.0797	.2343	1046	56.0	1330	71.2	4	52.5	78.5	19.0
404-001-302	Anodize	.0794	.2368	1022	54.4	1405	74.7	8	52.5	78.5	19.0
404-001-303	SermeTel	.0926	.2498	1195	51.7	1705	73.8	14	52.5	78.5	19.0
404-001-304	SermeTel	.0947	.2508	1190	50.0	1710	71.8	- (4)	52.5	78.5	19.0
404-001-305	SermeTel	.0922	.2478	1215	53.3	1750	76.8	28	52.5	78.5	19.0
404-001-306	Alodine	.0661	.2401	9570	60.3	1311	82.6	28.5	57.8	82.2	32.5
404-001-307	Alodine	.0661	.2430	9750	60.7	1322	82.3	26.0	57.8	82.2	32.5

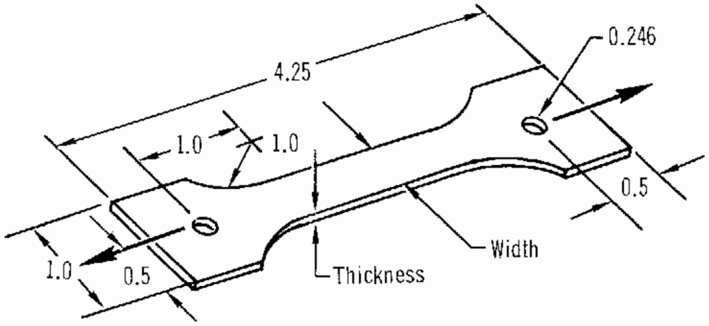

Notes:

1. Hot rolled, stress relieved, ground and etched beryllium sheet.
2. After machining and deburring, specimens were chem-milled to remove 0.003 to 0.004 inch total thickness.
3. Tested at room temperature with a strain rate of .005 in./in./minute up to yield, thereafter head travel rate of .030 in./minute held constant until failure.

(4) Broke outside of gage length.

5. Longitudinal grain direction parallel to load axis.

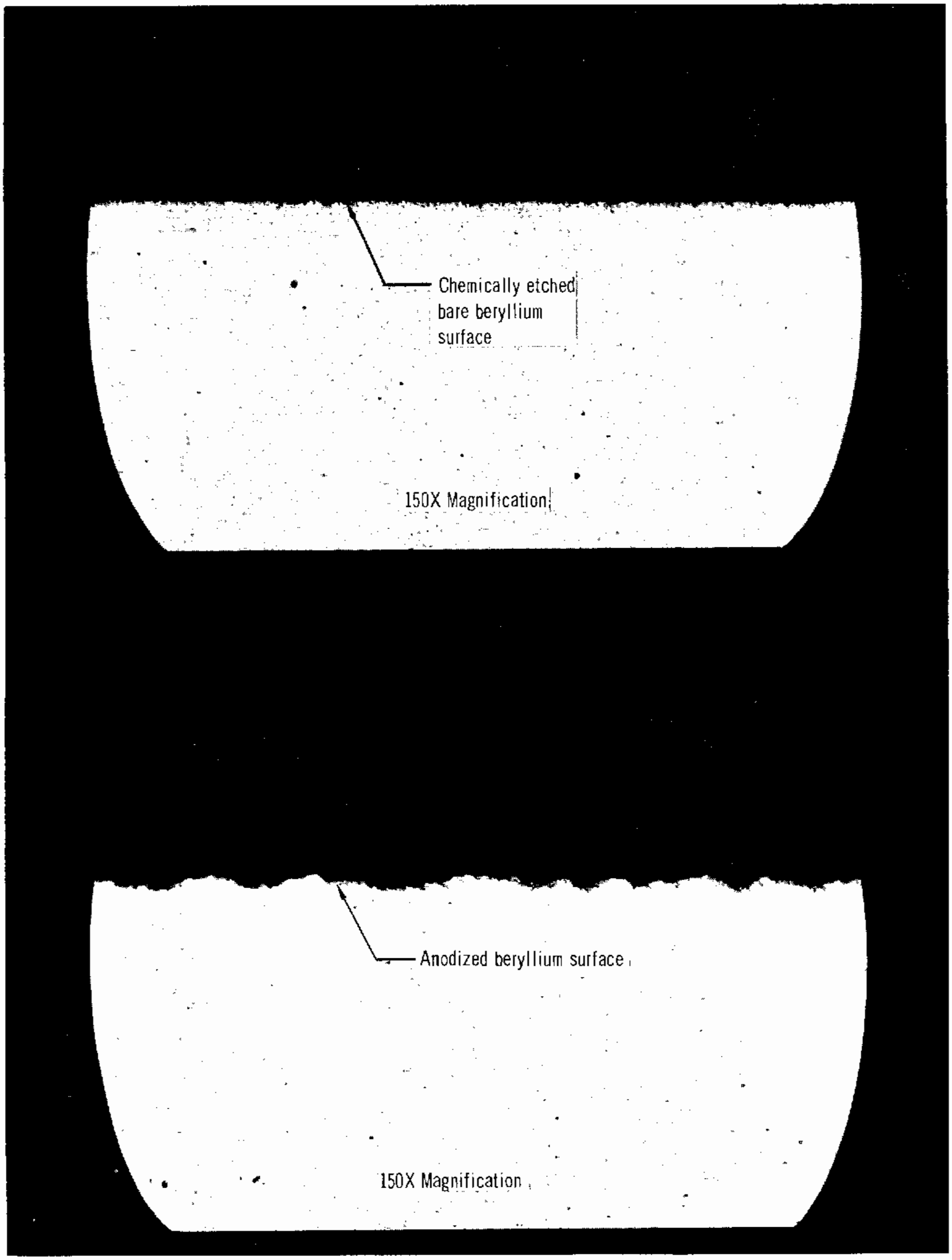
Chemically etched bare beryllium surface
150X Magnification
Anodized beryllium surface
150X Magnification

Figure 58 - Effect of Anodize on Beryllium Surface Finish

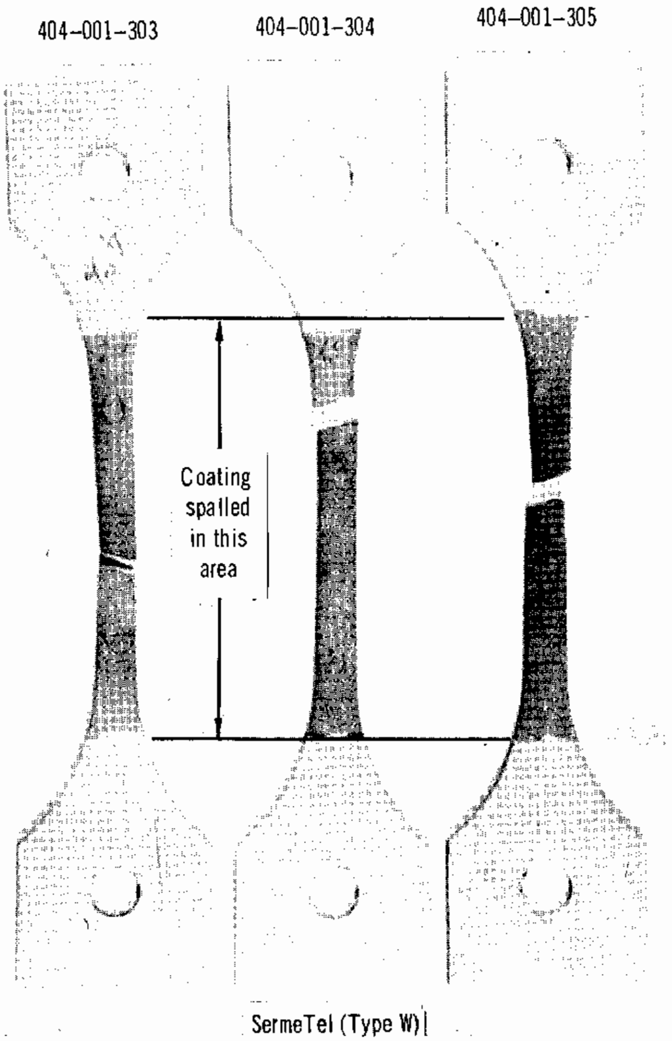
404-001-303
404-001-304
404-001-305
Coating spalled in this area
SermeTel (Type W)

Figure 59 – Surface Coated Tension Test Failed Specimens

Since both the anodized and SermeTel treated specimens proved unsatisfactory, two alodined specimens were fabricated and tensile tested to determine if this treatment would affect the mechanical properties of beryllium. The results of these tests are also shown in Table 20. The alodine treatment apparently had no adverse effect on the mechanical properties of beryllium. As shown, the test results are in good agreement with the certified properties of the untreated material. The pitting associated with the anodized treatment evidently is not characteristic of the alodine process. As a result of these tension tests, the second group of beryllium specimens, incorporating the alodine process, were fabricated and corrosion tested.

10.2 Group 2 - The corrosion specimens are shown before and after the 500 hours salt spray test in Figures 60 and 61. The epoxy enamel paint system (specimen 10) provided excellent corrosion protection. The paint blistering, which was experienced during the test of the first group of specimens, was prevented by baking the beryllium specimens for 30 minutes at 275°F prior to applying the paint. However, adhesion tests showed that the bond between the paint and beryllium surface still was inadequate. The same adhesion tests were performed on specimens which had been alodined prior to being painted, and excellent results were achieved. Therefore, it can be concluded that a surface treatment, such as alodining, is required if the epoxy enamel paint system is used for corrosion protection.

The alodined panels (specimens 11 and 12) showed initiation of pitting, with traces of white oxide at the pits, after 22 hours exposure to the 5% salt spray. At the conclusion of the 500 hours salt spray test, pitting in the panels had increased to about 30 active corrosion sites with approximately half of these giving off white oxide.

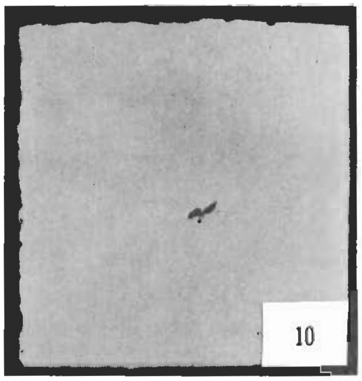

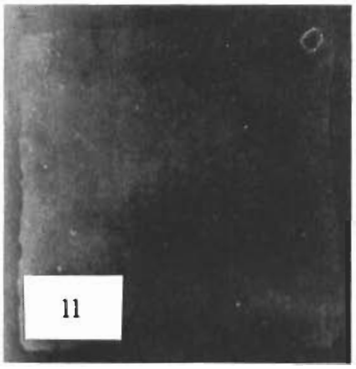

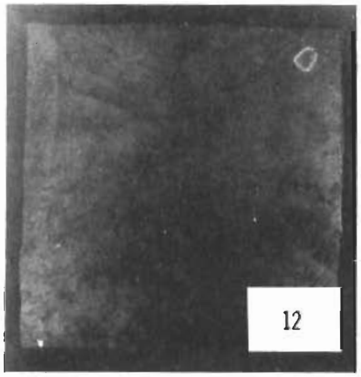

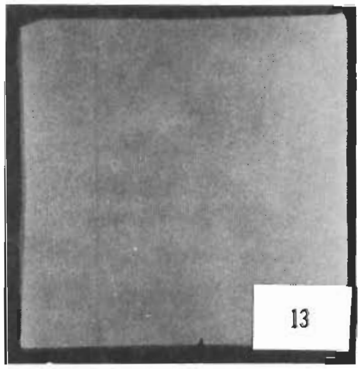

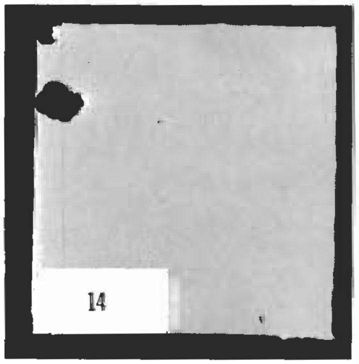

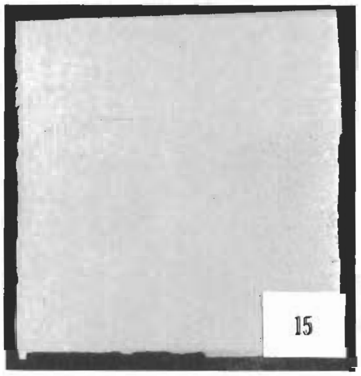

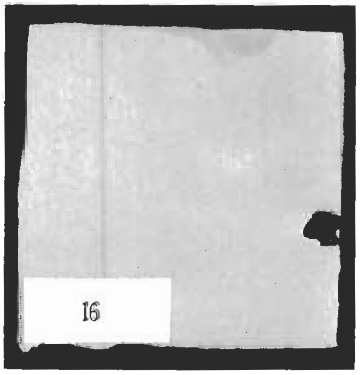

Figure 60 – Group 2 Corrosion Test Specimens Before 500 Hours Exposure

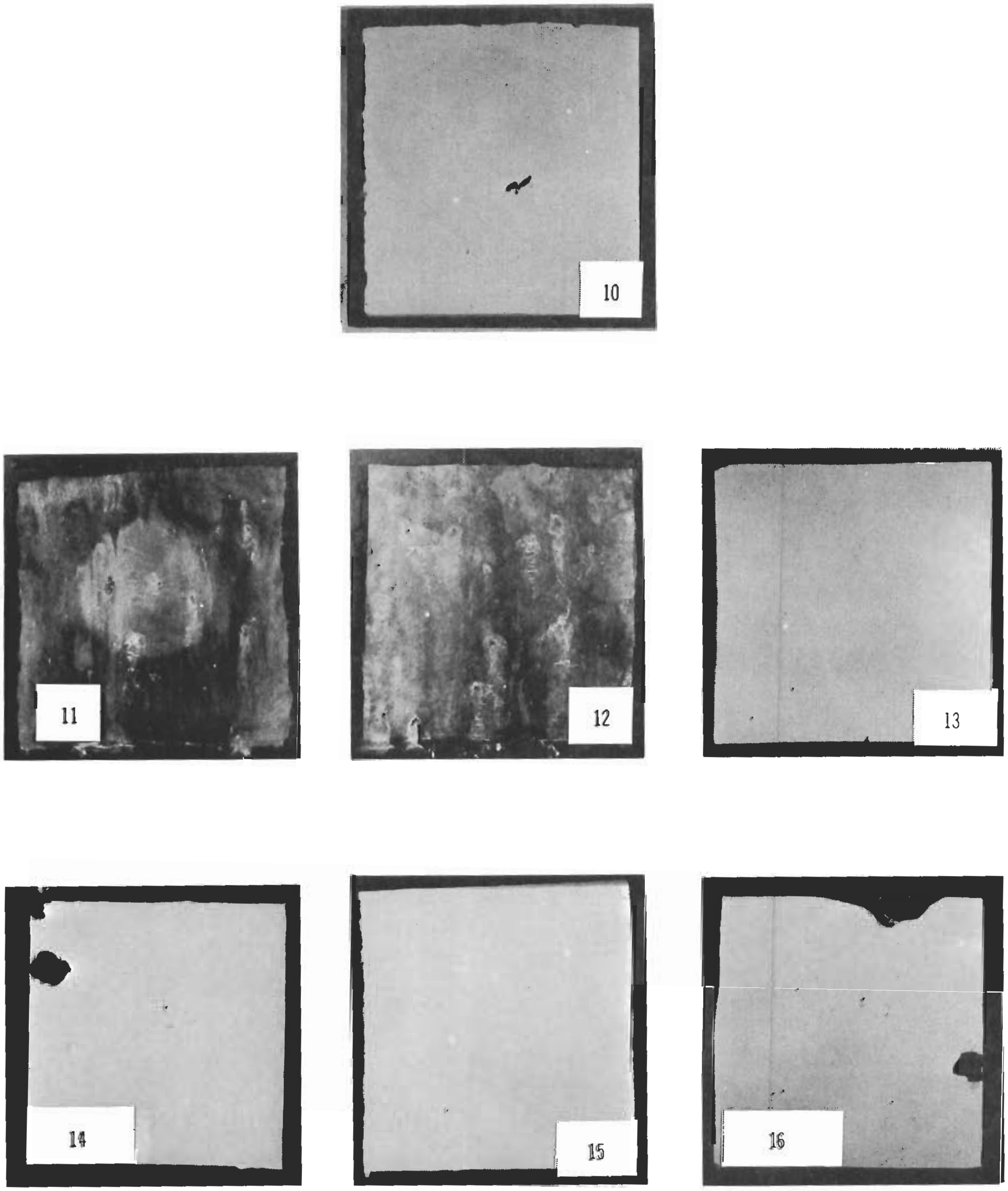
10
11
12
13
14
15
16

Figure 61 – Group 2 Corrosion Test Specimens After 500 Hours Exposure

At the conclusion of the test, metallographic examination showed no evidence of corrosion on the specimens which had been alodined and then painted with the epoxy enamel. As discussed above, this system also exhibited excellent adhesion to the beryllium surface. No difference in paint adhesion or corrosion protection was apparent between specimens which had been dried at ambient (specimens 13 and 14) and those dried at 275°F (specimens 15 and 16). The specimens were dried after the inorganic coatings were applied and before the paint was applied. Since the tension tests of beryllium specimens with the alodine treatment showed that the mechanical properties were not adversely affected, the alodine treatment followed by the application of epoxy enamel paint would likely be selected for use on all external surfaces of a beryllium rudder subjected to flight environment.

11. Stress-Strain Tests

Tests were conducted to determine the stress-strain relationships of beryllium sheet at various temperatures. The data provided by these tests both supplement and confirm basic information on the mechanical properties of the beryllium material from which the rudder was fabricated. The test specimens, test set-ups and procedures, and test results are discussed in the following paragraphs.

The tension and compression test specimens are shown in Figure 62. A total of thirty tests (twelve compression and eighteen tension) were completed with satisfactory results. The specimens were fabricated from three different sheet thicknesses (.084 inch, .064 inch, and .044 inch) and tested at -65°F ± 5°F, 500°F ± 5°F, and room temperature. Compression tests were conducted in a 60,000 lbs. capacity Wiedemann-Baldwin Universal Testing Machine; a 30,000 lbs.capacity Universal Testing Machine was used for the tension tests. The equipment and procedures for establishing and maintaining the -65°F and 500°F test temperature conditions have been described previously in this section. A Tuckerman Optical Strain Gage was employed for all tests. The load was applied in increments of approximately ten percent of F_{tu}. A strain reading was taken after each increment of load. The test set-up for a 500°F tension test and a room temperature compression test are shown in Figures 63 and 64, respectively. Note the two-block jig assembly which encloses the compression test specimen and restrains it from buckling during loading.

The ranges of elastic modulus and yield stress as determined from the test data are presented in Table 21. The stress-strain curves developed from the test data are presented in Figures 65 through 70.

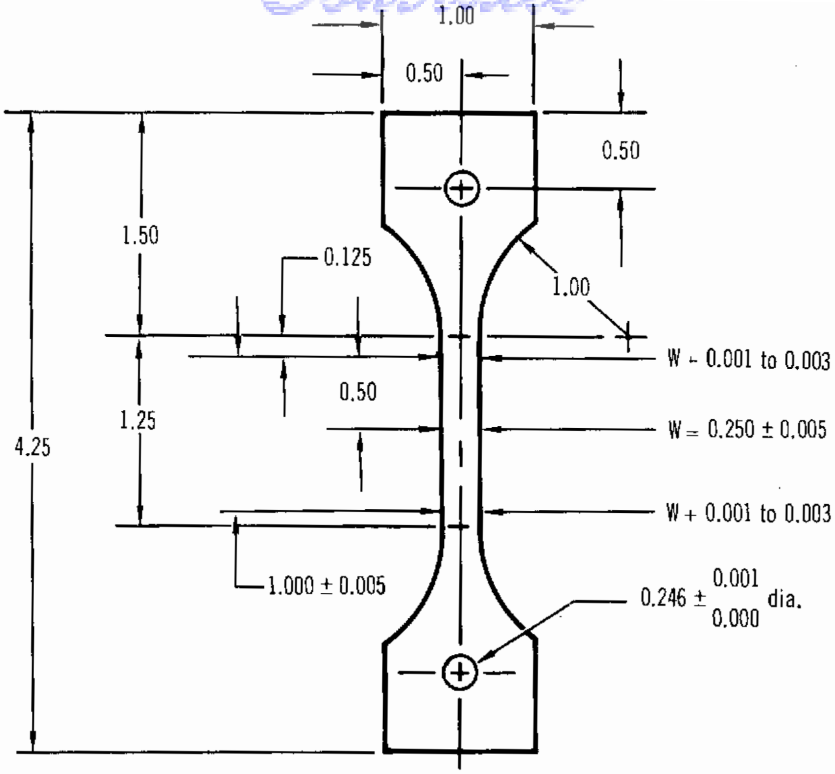
1.00
0.50
0.50
1.50
0.125
1.00
W - 0.001 to 0.003
0.50
1.25
4.25
W = 0.250 ± 0.005
W + 0.001 to 0.003
1.000 ± 0.005
0.246 ± 0.001 0.000 dia.

Tension specimen

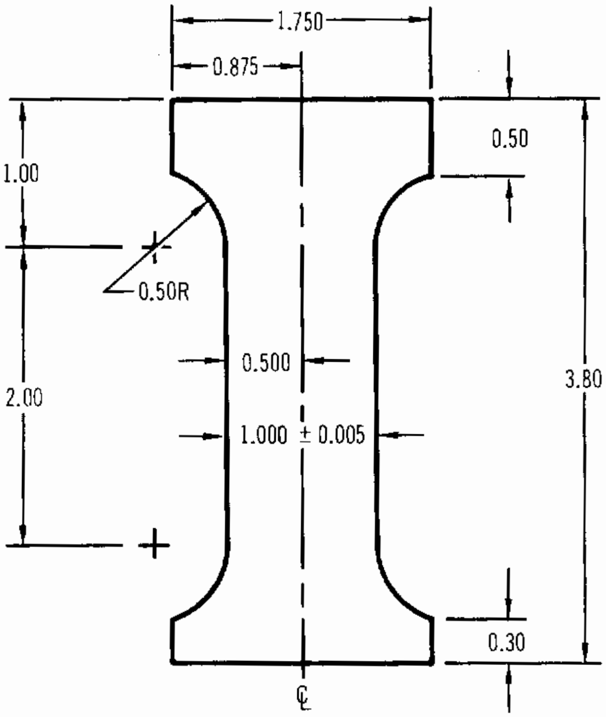
1.750
0.875
1.00
0.50
0.50R
0.500
2.00
3.80
1.000 ± 0.005
0.30
℄

Compression specimen

Figure 62 – Stress-Strain Test Specimen Configurations

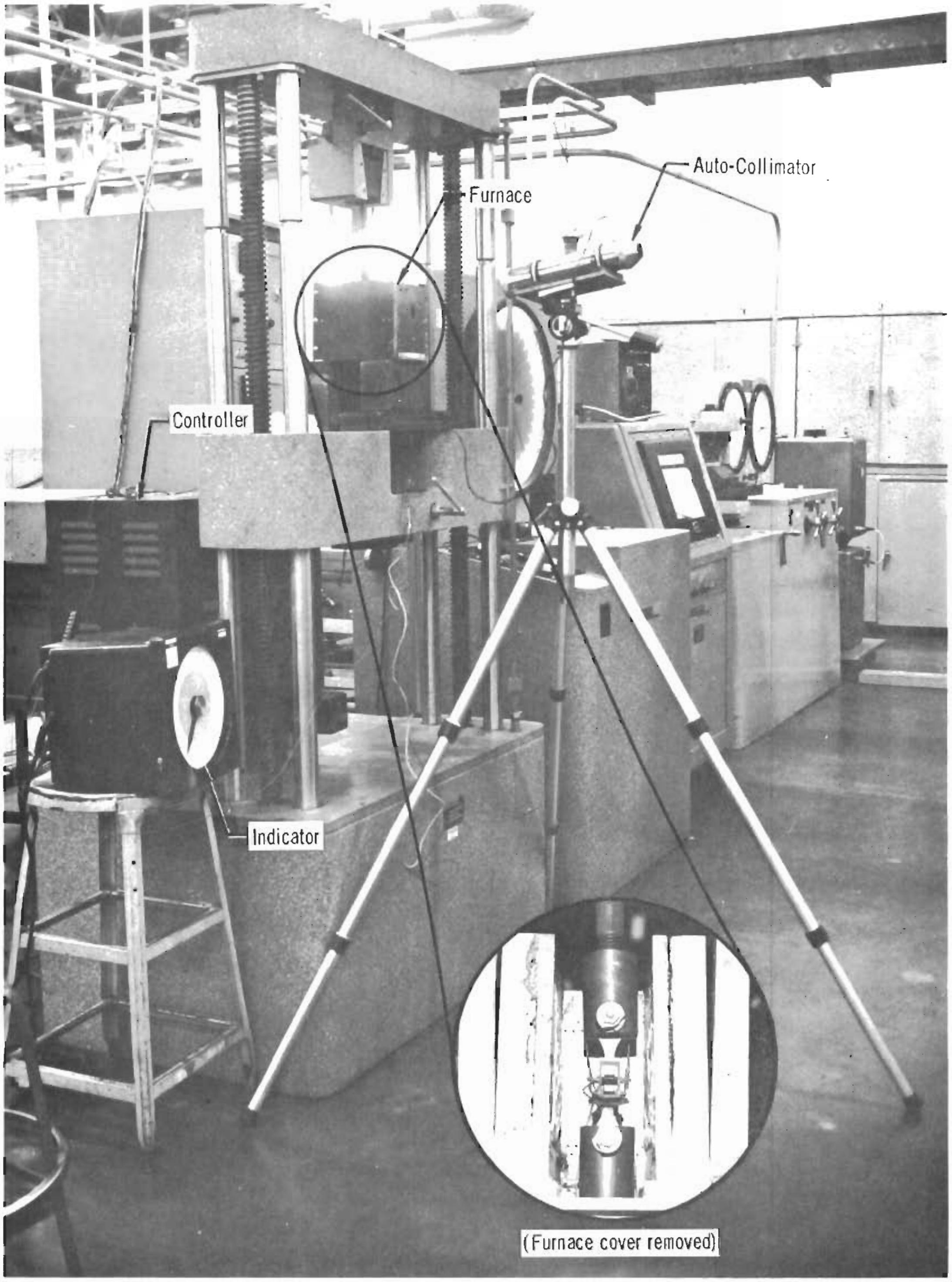
Auto-Collimator
Furnace
Controller
Indicator
(Furnace cover removed)

Figure 63 – Tension Stress-Strain Test Set-Up (500°F)

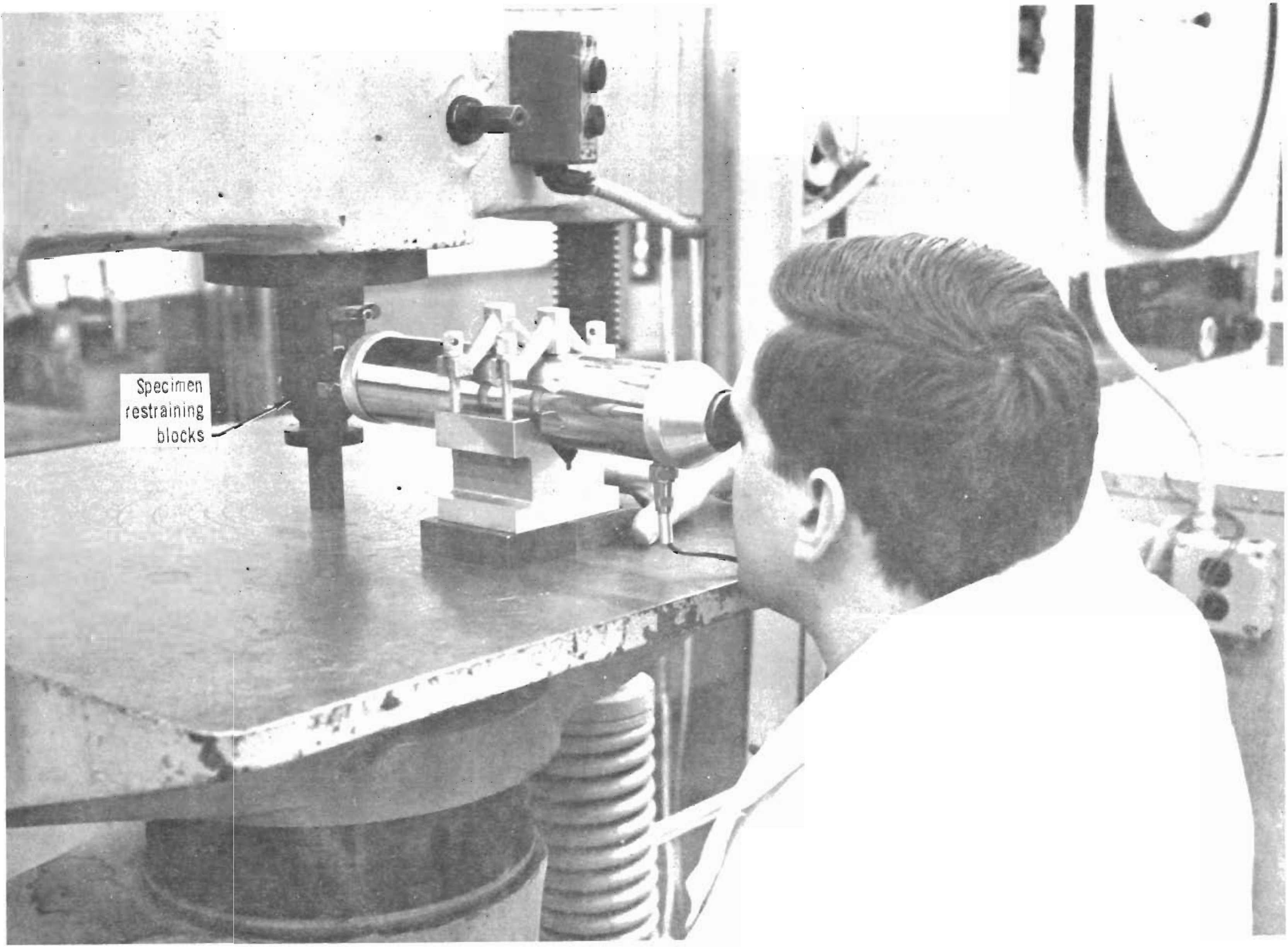
Specimen restraining blocks

Figure 64 – Compression Stress-Strain Test Set-Up

TABLE 21

TENSION AND COMPRESSION STRESS-STRAIN TEST RESULTS

Test	Temperature	Elastic Modulus (10^6 psi)	Yield Stress (10^3 psi)
Tension	R.T.	41.7–47.7	55.0–60.0
	–65°F	39.0–45.0	55.0–61.5
	500°F	37.0–40.0	36.5–49.0
Compression	R.T.	38.0–42.8	57.0–60.0
	–65°F	43.0–46.0	57.7–60.0
	500°F	38.5–39.0	45.0–50.0

Notes:

1. Hot rolled, stress relieved, ground and etched beryllium sheet.
2. After machining and deburring, material was chem-milled to remove 0.003 to 0.004 inch total thickness.
3. Total exposure time to test temperature was approximately 15 minutes.
4. Load was applied in increments of approximately ten percent of F_{tu}.

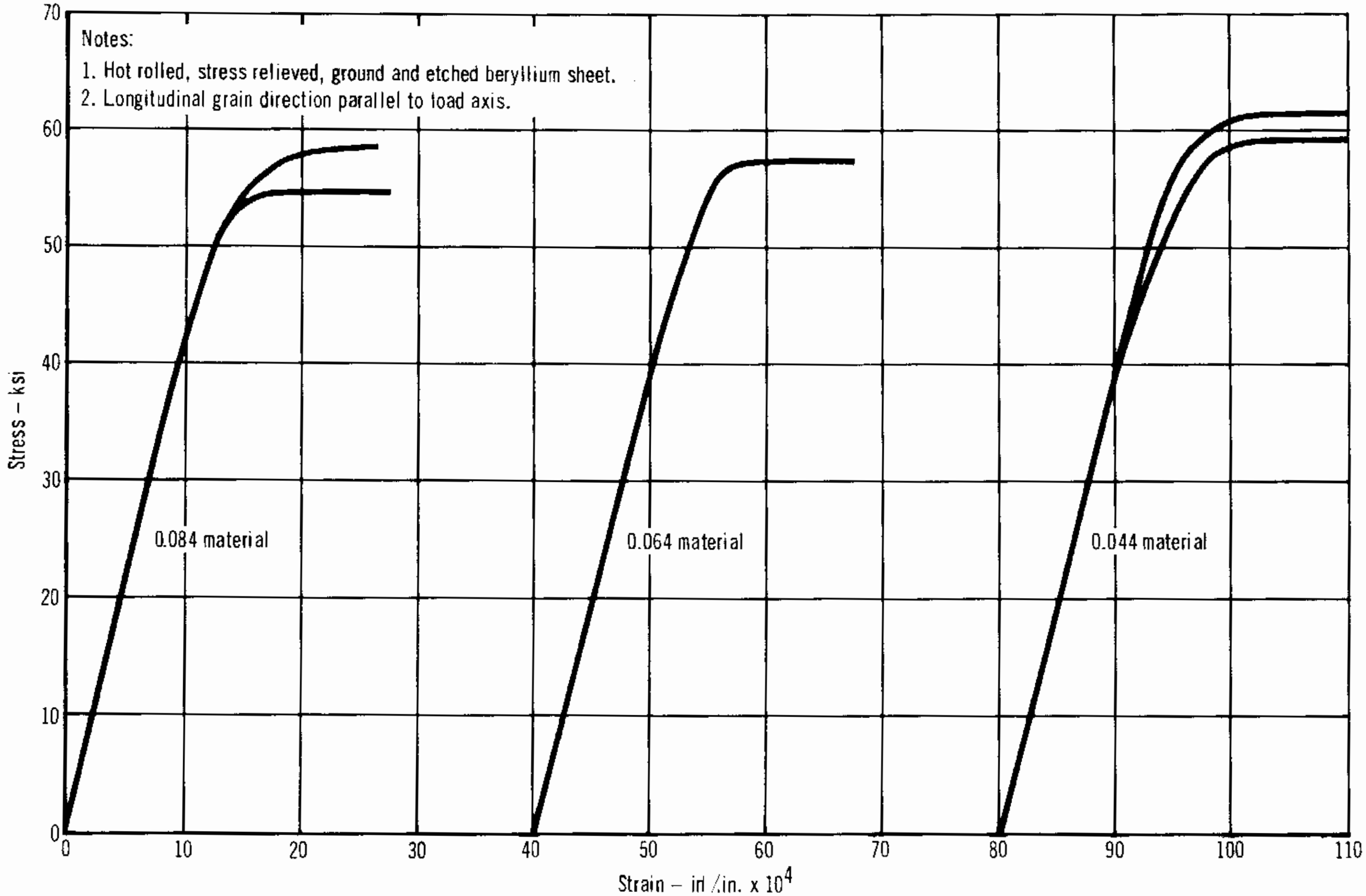

Notes:
1. Hot rolled, stress relieved, ground and etched beryllium sheet.
2. Longitudinal grain direction parallel to load axis.

Figure 65 – Tension Stress-Strain Curves: –65°F

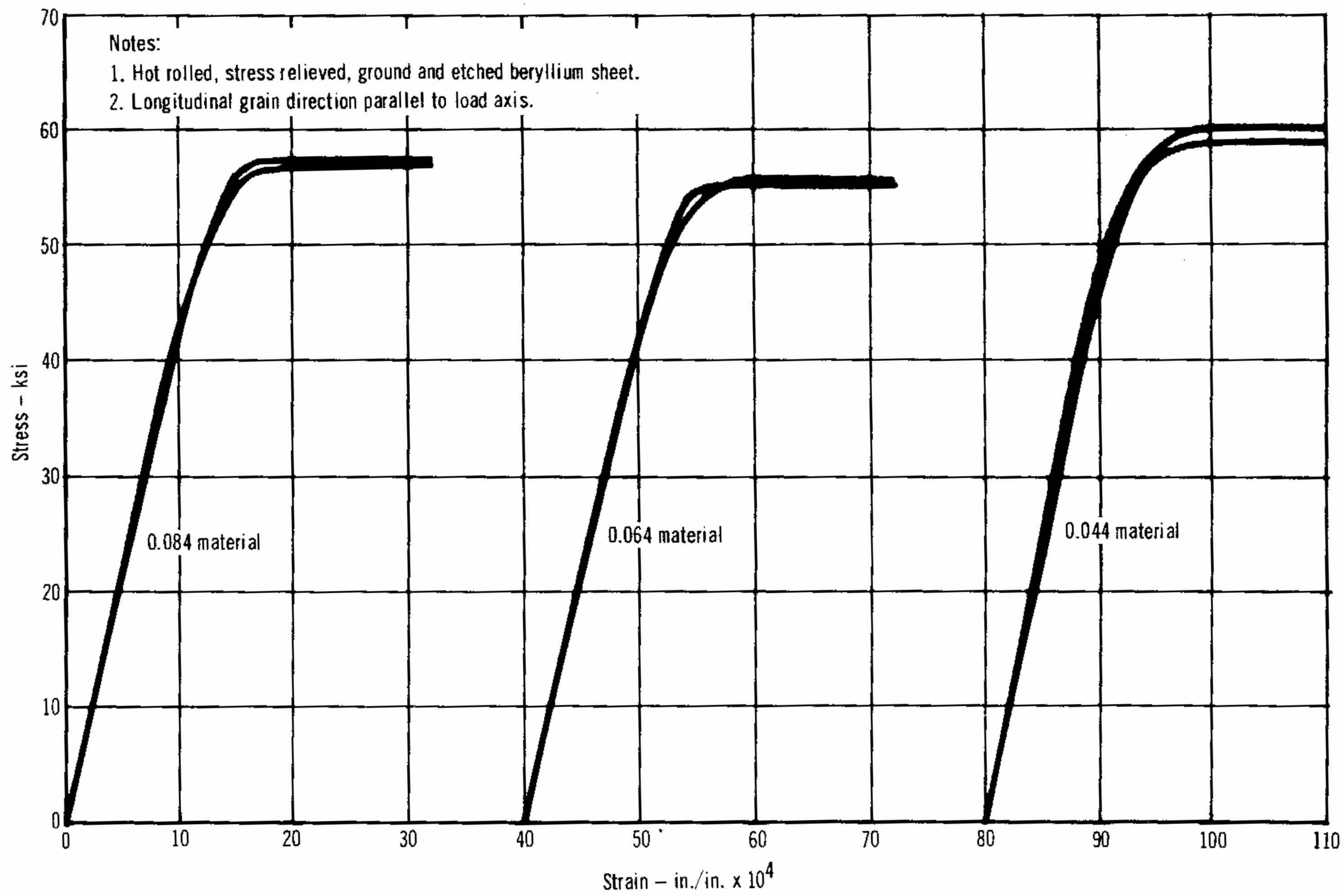

Figure 66 – Tension Stress-Strain Curves: Room Temperature

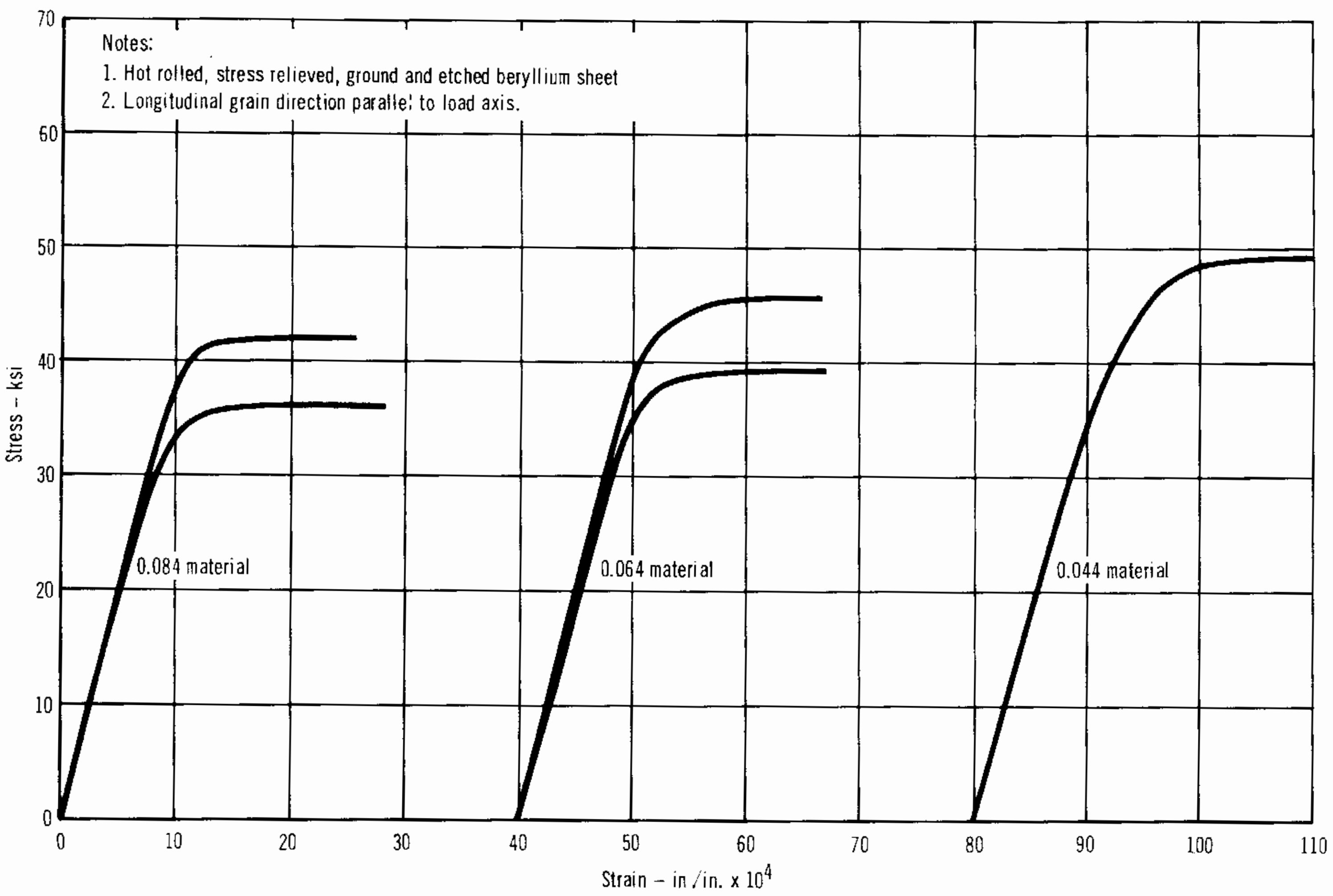

Figure 67 – Tension Stress-Strain Curves: 500°F

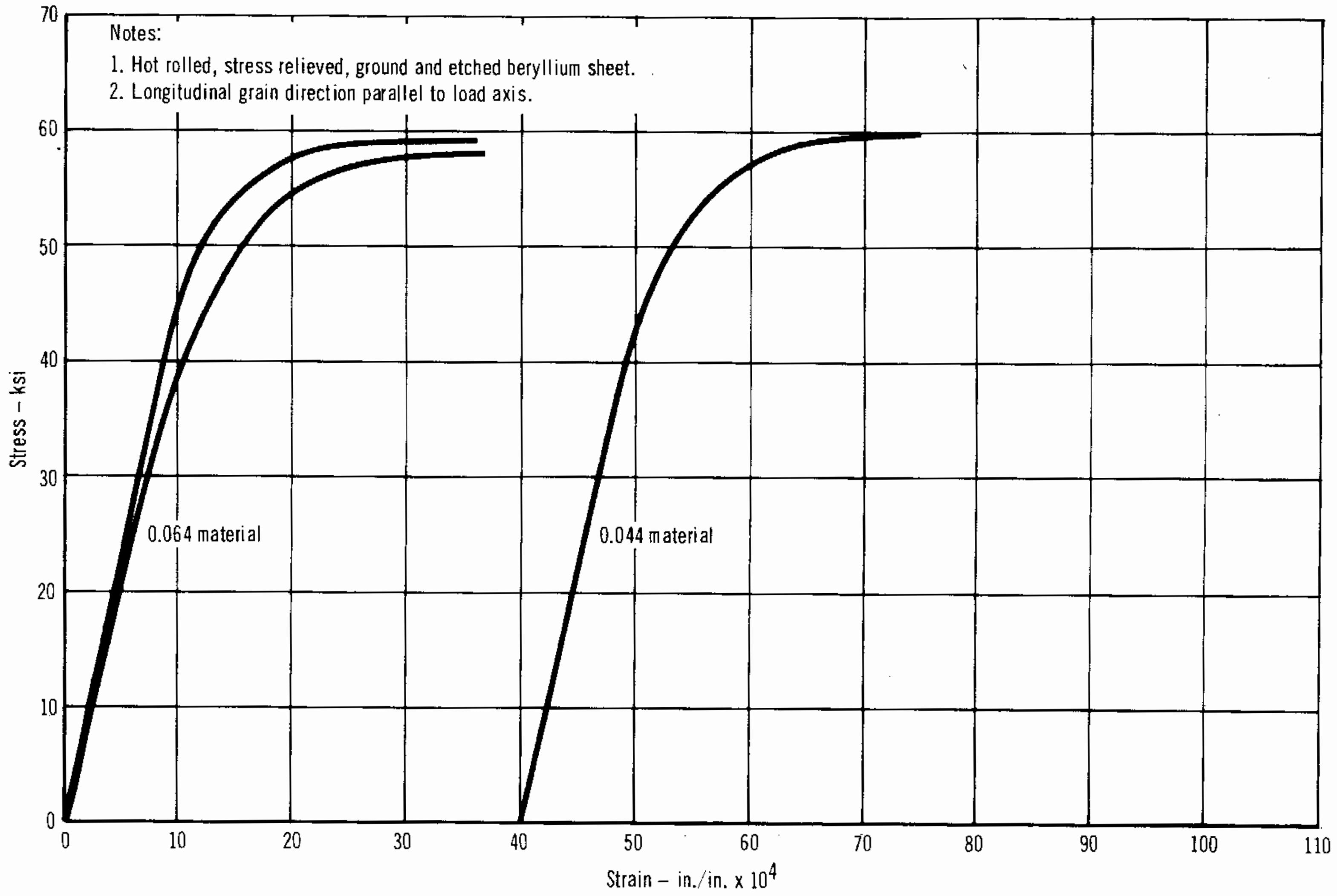

Notes:

1. Hot rolled, stress relieved, ground and etched beryllium sheet.
2. Longitudinal grain direction parallel to load axis.

Figure 68 – Compression Stress-Strain Curves: -65^{0}F

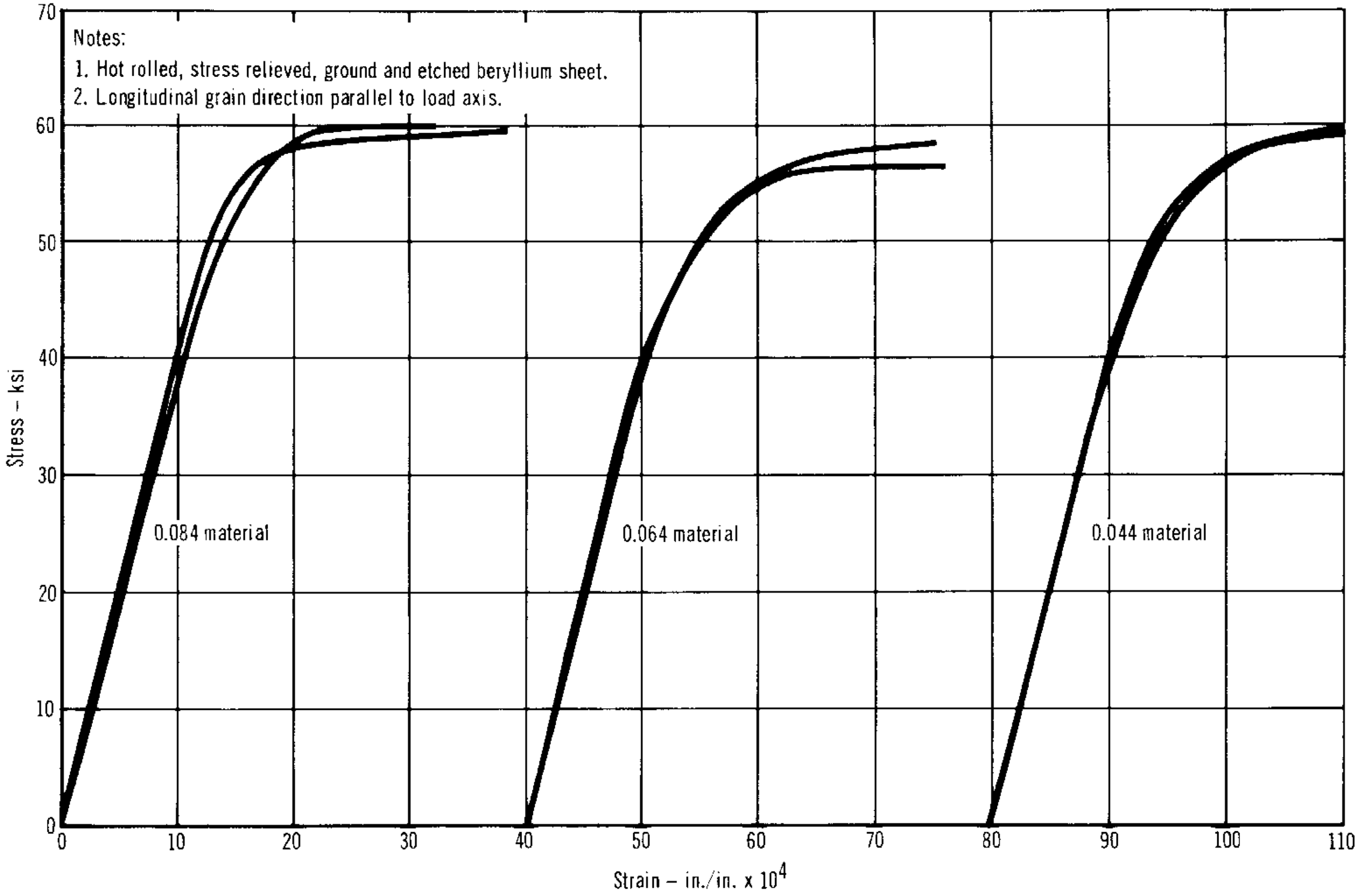

Notes:
1. Hot rolled, stress relieved, ground and etched beryllium sheet.
2. Longitudinal grain direction parallel to load axis.

Figure 69 – Compression Stress-Strain Curves: Room Temperature

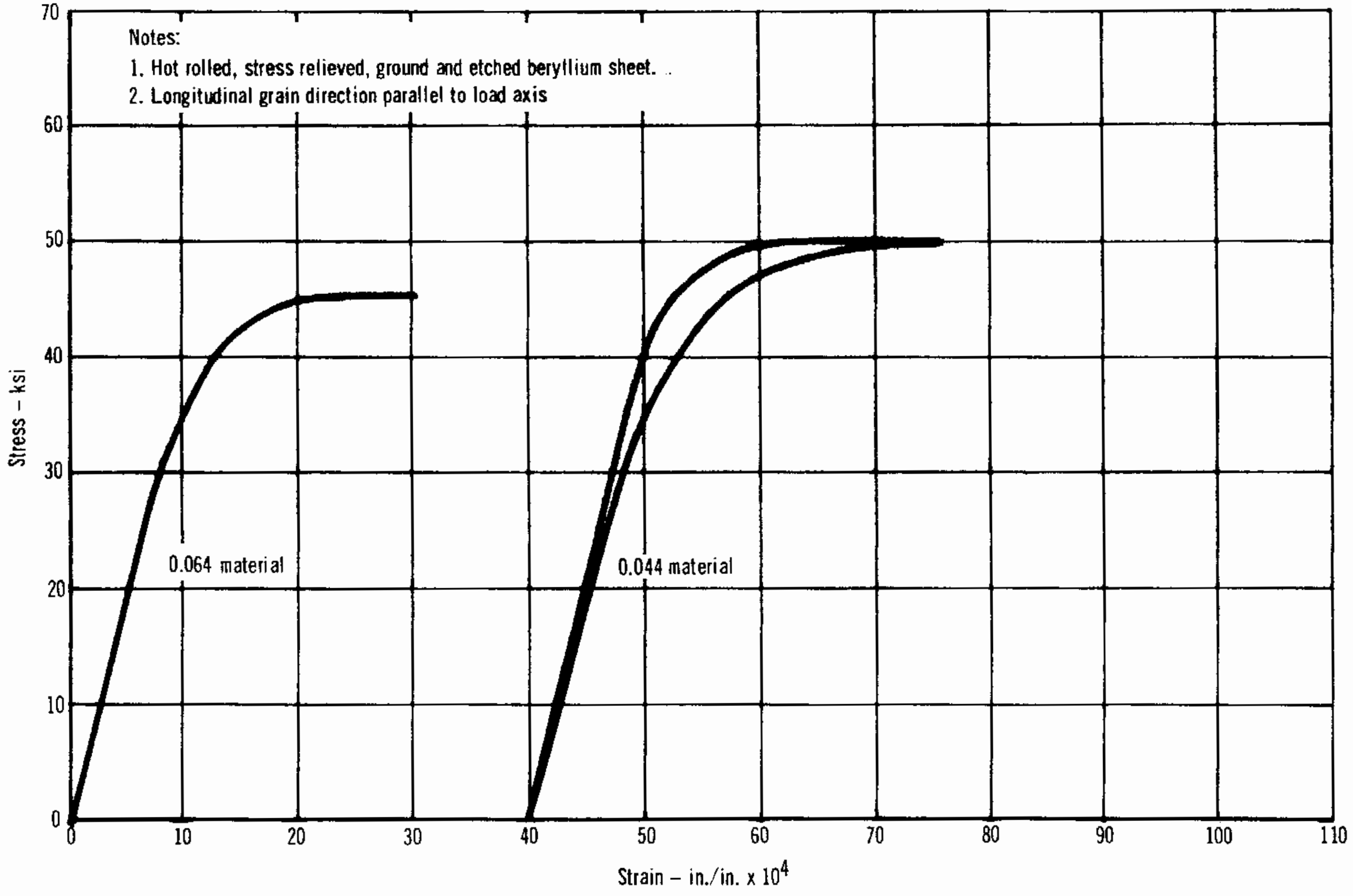

Figure 70 – Compression Stress-Strain Curves: 500°F

12. Rudder Composite Section Tests

Tests of the rudder composite section, a virtual replica of a major portion of the beryllium rudder, were conducted to verify the adequacy of the design data and criteria used in the design and analysis of the rudder, and of the manufacturing procedures and techniques subsequently used in its fabrication and assembly. It was anticipated that a successful completion of the composite section tests would provide a good probability of similar success in the ground test program of the complete assembly. Accordingly, the test specimen was subjected to loading conditions closely approximating the design loads existing in the corresponding portion of the rudder assembly. The materials, material thicknesses, detail shapes and sizes, mechanical fasteners, and bonding agent used in the specimen were the same as those in the beryllium rudder. Minor modifications to the mold line tapers in the span and chord directions were incorporated to reduce costs. Fabrication and assembly procedures were identical to those used for the actual rudder, and are described in Section V. Figure 71 shows the relative size of the composite section and the complete rudder. The rudder composite section detail drawings are shown in the Appendix. The set-up, procedure, and results for the testing performed are discussed in the following paragraphs.

A total of 26 strain gages and 8 strain rosettes were used to continuously record specimen strains during each test from 10 seconds before the start of loading until the loading returned to zero at the conclusion of the test. The exact location and identification number of each strain gage and strain rosette are given on the test specimen detail drawings in the Appendix. All strain gages and strain rosettes were bonded to the beryllium with GA-2 bonding agent (Budd Gage Company) and sealed, to prevent accumulation of contaminants or moisture, with DC-140 sealant (Dow-Corning).

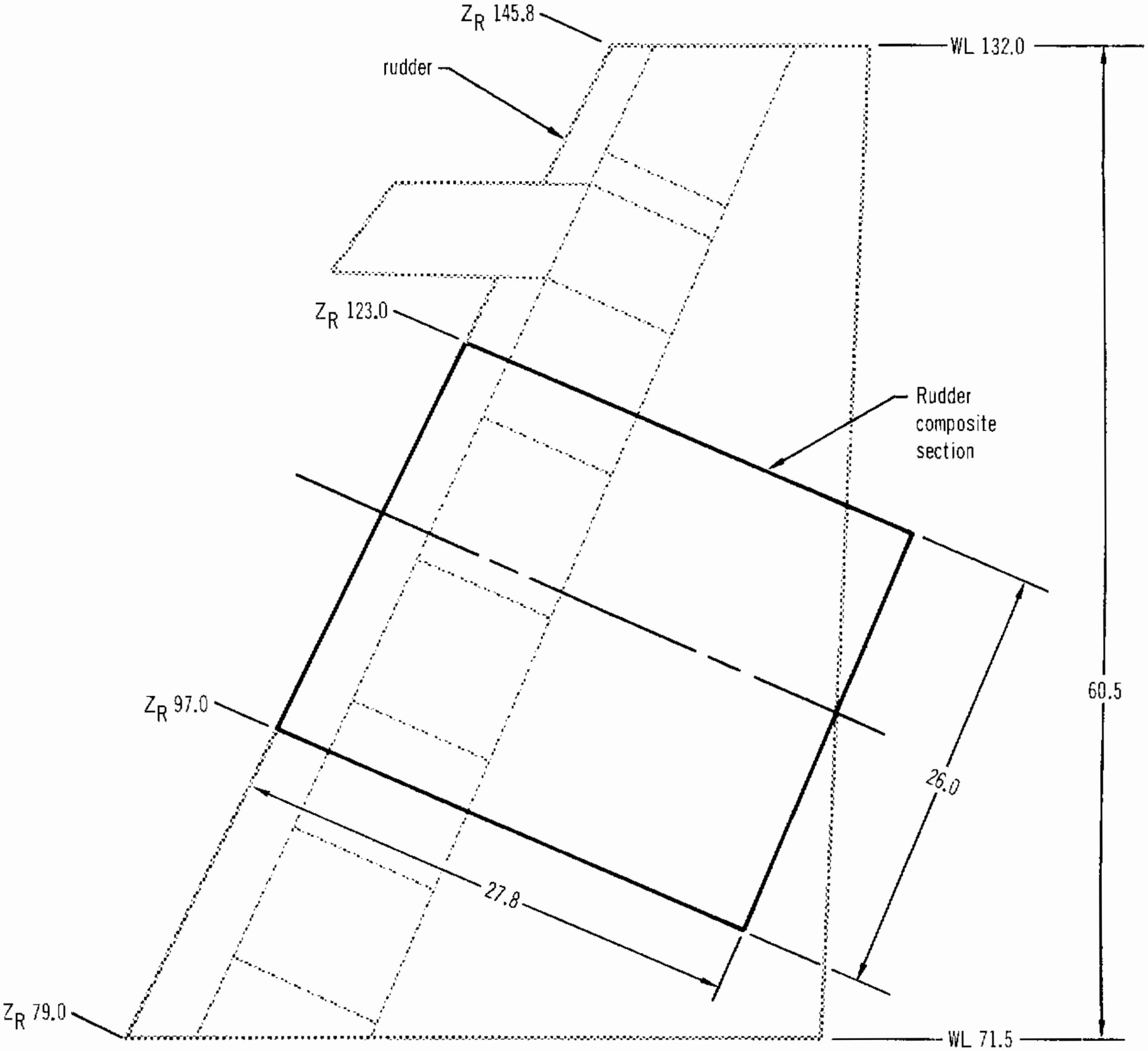
Z_R 145.8
rudder
WL 132.0
Z_R 123.0
Rudder composite section
Z_R 97.0
60.5
26.0
27.8
Z_R 79.0
WL 71.5

Figure 71– Relative Sizes of Rudder Composite Section and F–4 Rudder

The rudder of the F-4 aircraft is subjected to airloads, shear, chordwise bending, spanwise bending, and torque. Rudder design loading conditions are presented in Figures 15 through 19 in Section III of this report. In the analysis of the rudder, it was found that the bending moment and torque resulting from Condition III loading, fin bending plus rudder airloads, would be critical for most of the rudder primary structural members. Therefore, the rudder composite section was tested to these Condition III loads.

Four static tests were performed on the rudder composite section. The first three tests were non-destructive with the objective of establishing the behavior of the structure under individual loading conditions. In Test 4, which was carried to destruction, the purpose was to verify the analytically predicted ultimate strength of the structure. Loading conditions for all four tests are summarized below.

Test 1 - Chordwise Bending - Condition III, 100% of limit load.

Test 2 - Torsion - Condition III, 100% of limit load.

Test 3 - Spanwise Bending - Condition II, 120% of limit load.

Test 4 - Spanwise Bending, Torque, Chordwise Bending and Rudder Airloads - Condition III, to destruction.

The rudder composite section test set-up is shown in Figure 72. Loads applied to the rudder composite section for each test are given in Figure 73. The four tests performed on the rudder composite section are discussed below.

12.1 Test No. 1: Chordwise Bending - The loads applied to the rudder composite section during this test represented 100% of the Condition III design limit airload. The applied loads were reacted (see Figure 73) so as to produce a chordwise bending moment equal to that existing in the rudder at design limit load. The maximum loads attained in the test are given in Figure 73.

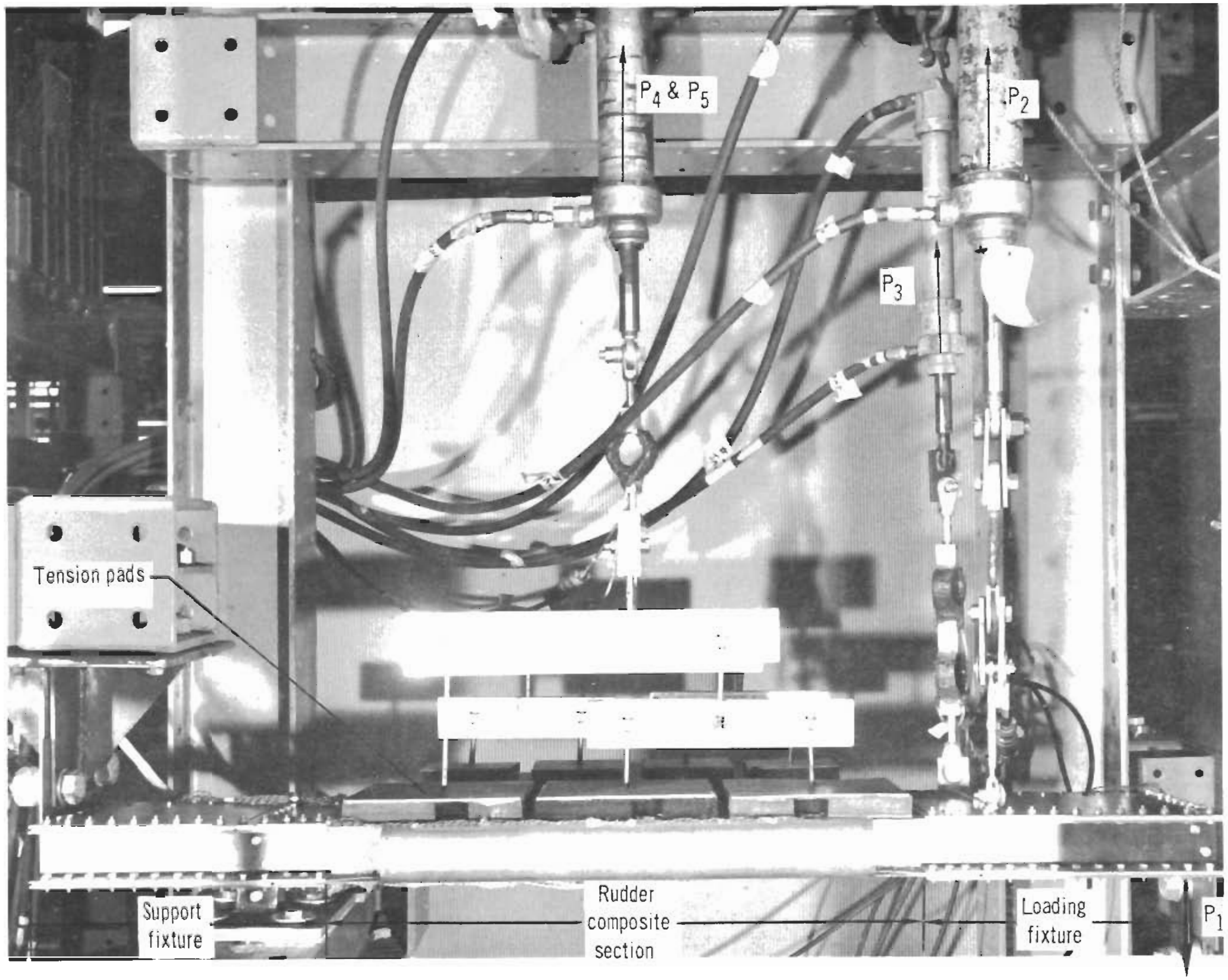
P_4 & P_5
P_2
P_3
Tension pads
Support fixture
Rudder composite section
Loading fixture
P_1

Figure 72 – Rudder Composite Section Test Set-Up

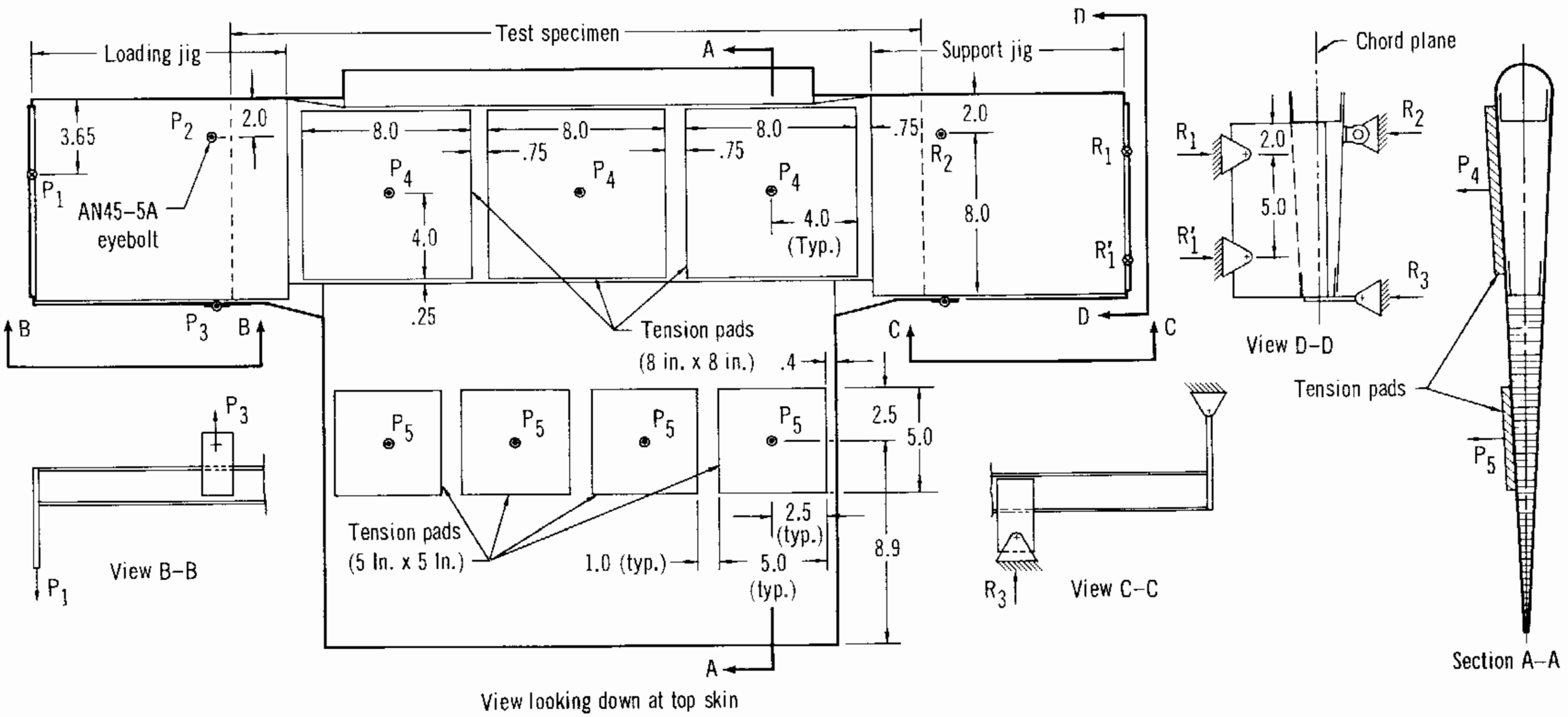
Loading jig
Test specimen
Support jig
A
D
3.65
P_2
2.0
P_1
AN45–5A eyebolt
8.0
.75
P_4
4.0
4.0 (Typ.)
.25
.75
2.0
R_2
8.0
R_1
R'_1
B
P_3
B
Tension pads (8 in. x 8 in.)
.4
C
D
C
P_5
2.5
5.0
8.9
2.5 (typ.)
5.0 (typ.)
1.0 (typ.)
Tension pads (5 In. x 5 In.)
A
View looking down at top skin
P_3
P_1
View B–B
Chord plane
R_1
R'_1
R_2
R_3
2.0
5.0
View D–D
Tension pads
R_3
View C–C
P_4
P_5
Section A–A

Maximum Applied Test Loads

Test No.	Condition	Applied Load (lb.)					Reaction (lb.)			
		P_1	P_2	P_3	P_4	P_5	R_1	R'_1	R_2	R_3
1	Chordwise Bending	0	44	-233	55	53	0	0	44	-233
2	Torque	0	-270	-270	55	53	-310	-310	49	-1045
3	Spanwise Bending	1820	1510	120	55	53	920	920	955	698
4	Combined Loading	2175	1150	792	67	63	1103	1103	1790	190

Figure 73 – Rudder Composite Section Test Loads

There was no evidence of failure or permanent deformation resulting from this test.

12.2 Test No. 2: Torque - During this test the rudder composite section was subjected to a torque equal to 100% of the Condition III design limit torque. Simulated rudder airloads were also applied to obtain the proper variation in torque in the test specimen. The maximum loads attained in the test are given in Figure 73. There was no evidence of failure or permanent deformation from this test.

12.3 Test No. 3: Spanwise Bending - During this test, the rudder composite section was loaded to 120% of the Condition III design limit spanwise bending moment. The maximum loads applied to the composite section during this test are given in Figure 73. There was no evidence of failure or permanent deformation at the conclusion of the test.

12.4 Test No. 4: Combined Loading - The rudder composite section was loaded to failure during this test under combined airloads, chordwise bending, torque and spanwise bending. These loads closely approximated the actual design loads existing in that portion of the beryllium rudder which the test specimen represents. The maximum loads attained in the test (at failure) are shown in Figure 73. In Figure 74, the loads existing in the rudder composite section at failure are compared to Condition III design ultimate loads (150% of design limit loads existing in the corresponding portion of the flight rudder). Figure 75 shows the failed rudder composite section and indicates the areas where the failure occurred.

The rudder composite section failed in two different areas. Both failures occurred at the maximum loading attained during the test (160% of the design limit loads existing in the rudder). Initially, the front spar cap failed in tension adjacent to the loading fixture (see Figure 75). However, after the

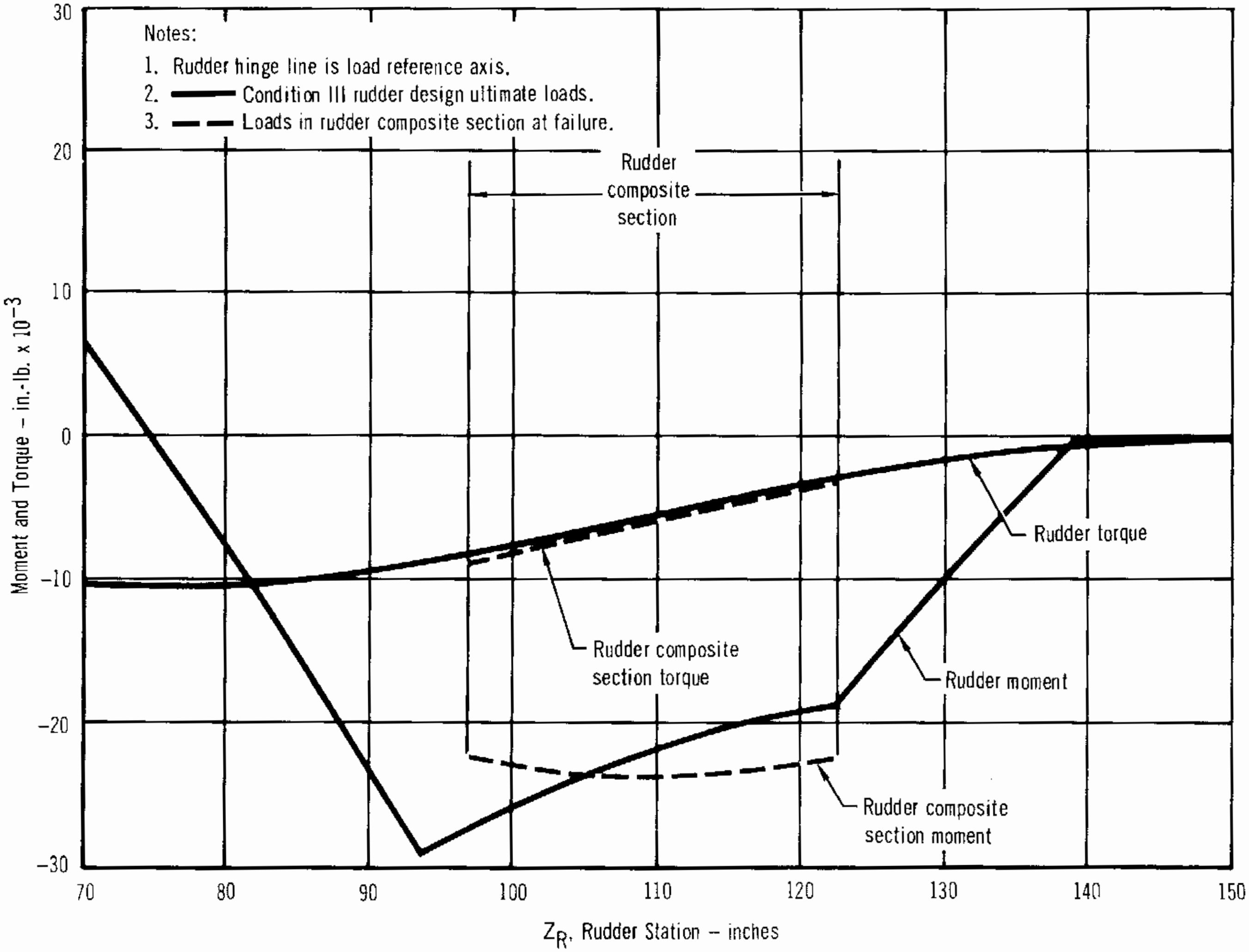

Figure 74 – Loads in Rudder Composite Section at Failure

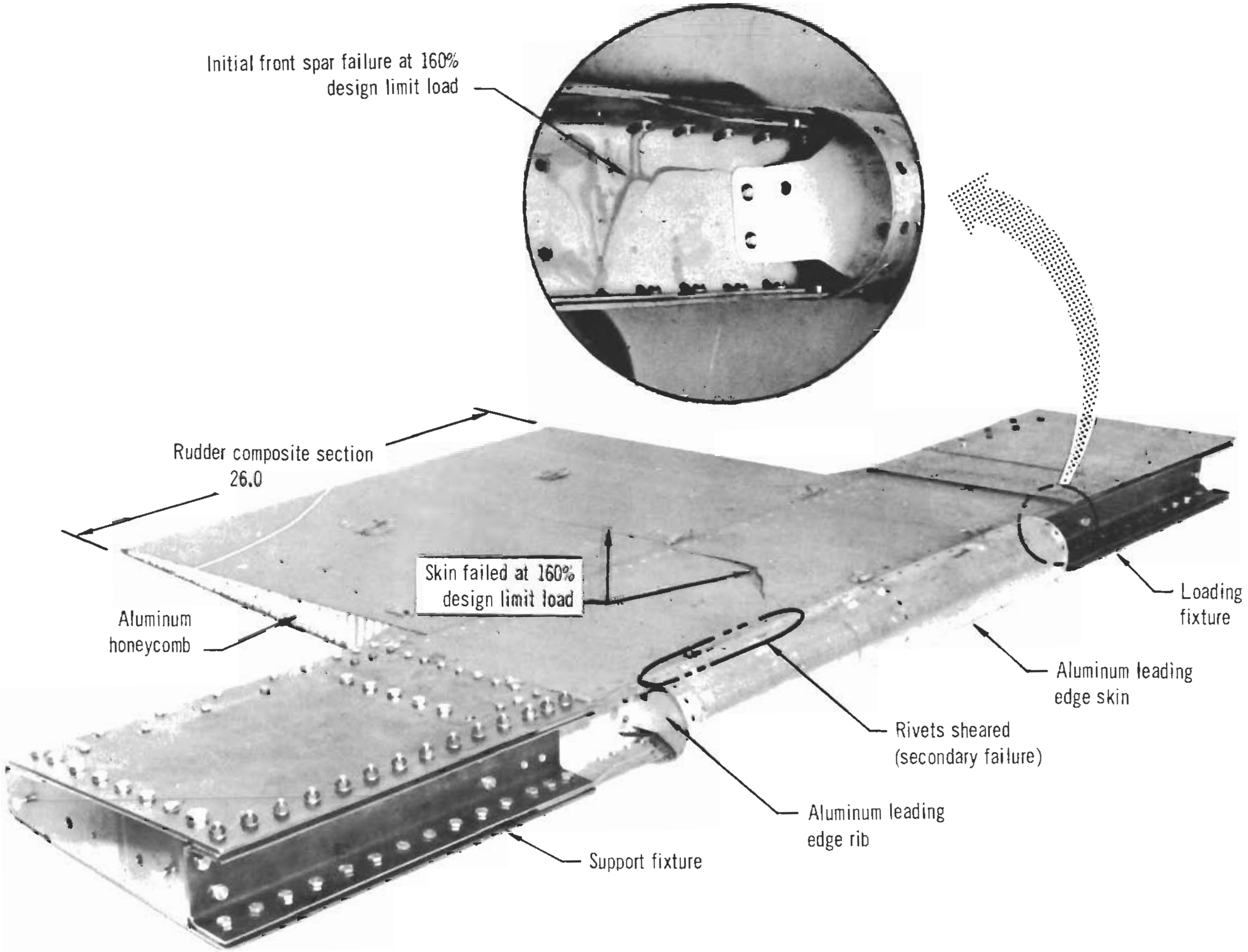
Initial front spar failure at 160%
design limit load
Rudder composite section
26.0
Skin failed at 160%
design limit load
Aluminum
honeycomb
Loading
fixture
Aluminum leading
edge skin
Rivets sheared
(secondary failure)
Aluminum leading
edge rib
Support fixture

Figure 75– Rudder Composite Section Static Test Failure

spar cap failed, it was still possible to maintain the same loading that existed at failure while the specimen was being examined and photographed. After the loads had been held constant for approximately four minutes, complete and catastrophic failure occurred near the center of the specimen (see Figure 75). The front and rear spar caps, and all cover skins on one side of the rudder failed. Examination of the area where initial failure occurred (front spar cap) showed that the crack did not originate or pass through an obvious stress concentration (such as a fastener hole) and the beryllium cover skin had not failed. Because the cover skin did not fail, it was still possible to maintain the loads. At the center of the specimen where catastrophic failure occurred, it was not possible to determine with any degree of certainty where the fracture originated or how it propagated. However, since the maximum tensile stress existed at the front spar, it was surmised that the front spar cap, or the cover skin at the front spar cap, failed first. The fracture propagated through the cover skin to the rear spar and then throughout the rear spar and trailing edge honeycomb skin.

The fact that the rudder composite section withstood loads in excess of the rudder ultimate design loads indicated that the design data and design criteria used for the beryllium rudder were adequate. This conclusions was subsequently substantiated by the successful completion of the ground test program of the complete rudder assembly, as described in Section VI.

13. Crack Repair Evaluation Tests

Element tests were conducted to substantiate the structural adequacy of using bonded beryllium doublers for the repair of beryllium structural elements containing cracks or other material defects. Such a repair was used in the fabrication of the beryllium rudder when a crack was discovered in one of the trailing edge assembly cover skins upon completion of the bonding process (see discussion in Section V). Following is a description of the tests and discussion of the test results.

Since the results of these tests were required before rudder fabrication could be satisfactorily completed, test specimen configuration and test procedures were selected which minimized the time required for fabrication and testing. Test specimen configurations are shown with Table 22. Six flat sheet specimens, 2.5 x 6.0 inches, were fabricated from beryllium sheet varying in thickness from .012 to .016 inch. The specimens had cracks, 0.8 inch long and 0.003 inch wide, formed by electrical discharge machining. The cracks were machined in the middle area of the specimen transversely to the specimen longitudinal center-line. Three of the specimens had .016 x 2.5 x 3.0 inch beryllium doublers bonded with FM-61 over the area containing the crack. To minimize the fabrication effort, grip holes were not provided in the specimens nor was the specimen chemically etched after being machined to size (normally all beryllium parts are chemically etched to remove any microscopic surface cracks or mechanical twins resulting from machining operations). The six specimens were tested in tension at room temperature using a 30,000 lbs. capacity Wiedemann-Baldwin Universal Testing Machine. Non-aligning friction grips were incorporated, and the specimens loaded to failure at a load rate of 300 pounds per minute.

TABLE 22
TENSION TEST RESULTS OF SLOTTED BERYLLIUM COUPONS WITH AND WITHOUT BONDED DOUBLERS

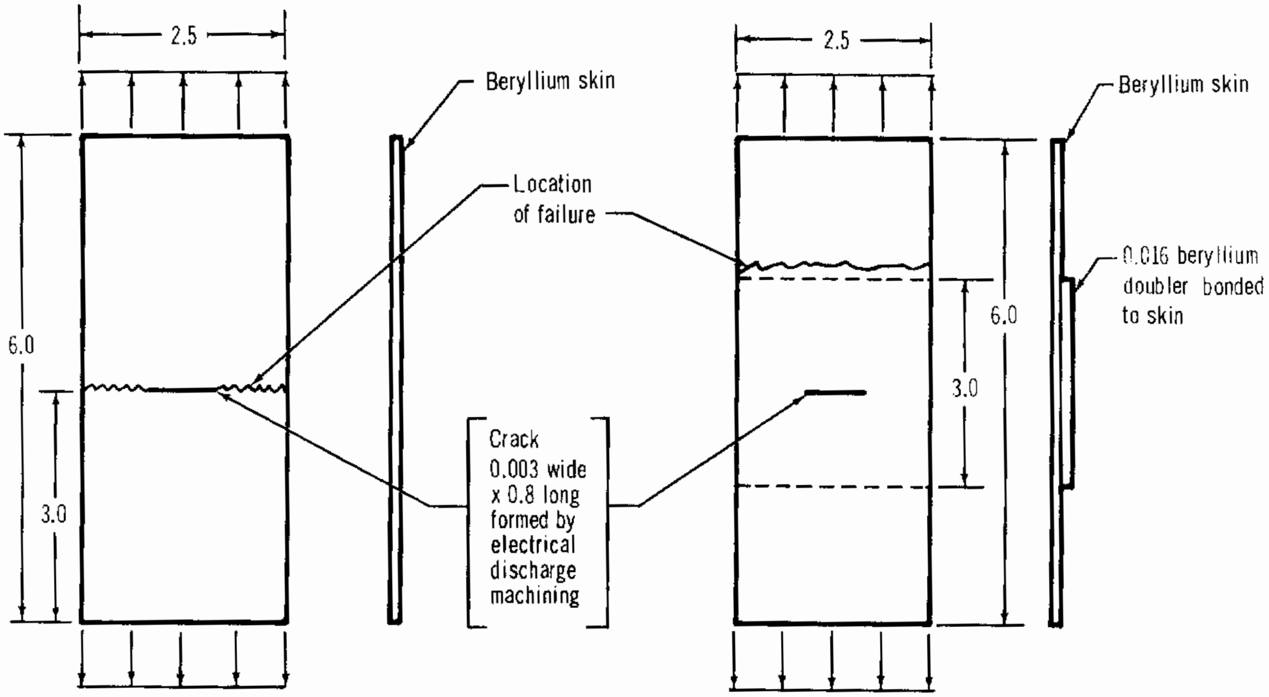
2.5
Beryllium skin
Location of failure
6.0
3.0
Crack 0.003 wide x 0.8 long formed by electrical discharge machining
2.5
Beryllium skin
0.016 beryllium doubler bonded to skin
6.0
3.0

Specimen without doubler

Specimen with doubler

Specimen Configuration	No.	Width at Failed Section (in.)	Average Skin Thickness at Failed Section (in.)	Failure Load (lb.)	Net Tension Stress at Failed Section (psi)	Location of Failure
Specimens Without Doublers	1	2.49	0.0150	1040	41,000	All specimens failed at machined crack
	2	2.49	0.0155	1090	41,600	
	3	2.49	0.0145	970	39,600	
Specimens With Doublers	4	2.49	0.0130	1525	47,100 (3)	All specimens failed in basic skin at edge of doubler
	5	2.49	0.0150	1915	51,300 (3)	
	6	2.49	0.0125	1620	52,000 (3)	

Notes:

1. Beryllium skins not chem-etched after machining .
2. Tested at room temperature at load rate of 300 lb/minute.
3. Bending stress not included.

Test results are presented in Table 22. Because the beryllium material was not chemically etched, and the specimen shape and manner of loading would not preclude load path eccentricities, high failure loads were not anticipated. Of greater interest and importance was the type and location of failure. As expected, the specimens with the machined crack and no doubler failed in tension at the crack. The specimens with the machined crack and bonded doubler failed in tension at higher loads, and in all cases failure occurred away from the crack, near the doubler bond line. This demonstrates the ability of the doubler and adhesive to transfer load and to inhibit crack propagation. The tension stresses presented in Table 1 for the bonded doubler specimens do not include bending stresses which result from load path eccentricities at the bonded doubler. The test results clearly demonstrate the structural adequacy of a bonded beryllium doubler for the repair of cracks in the rudder area under consideration.

SECTION V

BERYLLIUM RUDDER FABRICATION AND ASSEMBLY

1. Introduction

Manufacturing techniques and procedures developed in Reference 2 program, supplemented and improved as needed, were used in fabrication and assembly of the beryllium rudder. Fabrication and assembly operations were greatly facilitated by the experience gained in Reference 2 program. Beryllium is brittle, notch sensitive, and potentially toxic. The limitations these material characteristics impose on fabrication and handling, and some general recommended shop practices, are discussed in Subsection 2. Equipment and techniques used in sawing, machining, drilling, countersinking, forming, chemical milling, adhesive bonding, inspection and assembly of the beryllium rudder are described in Subsections 3 through 11.

2. General Shop Practices

Beryllium is potentially toxic; therefore, precautions should be taken to prevent dispersion of beryllium particles in work areas. An air exhaust system should be provided for collection of beryllium dust wherever sawing, grinding, sanding, or machining operations are performed. This requirement dictates the establishment of a special facility for certain manufacturing operations. The McDonnell beryllium facility used in the performance of this program is shown in Figure 76. This facility is well equipped with all necessary vacuum dust collecting equipment for machining and assembly work.

The need for extreme care in the handling and fabrication of beryllium parts, particularly those made of material less than .030 inch thick, cannot be overemphasized. In the course of the manufacturing effort for this program, several parts were broken or cracked. In every case, the broken or cracked part was of sheet material less than .030 inch thick. Parts of thicker material are much less susceptible to damage from mishandling and are more tolerant to slight variations from optimum manufacturing techniques.

The application of high local bearing stresses to the material surface during fabrication should be avoided. A foreign object between the part and the die during forming, or on the faying surfaces of mechanically fastened joints, can cause part breakage, as can excessive pressure from a C-clamp being used to hold the part during fabrication.

The use of scribe lines to mark hole locations or trim lines on detail beryllium parts cannot be tolerated. Work areas should be kept clean of metal chips or other sharp objects which could cause surface scratches. Surface defects, such as scratches, are known to seriously reduce strength and ductility, and time consuming rework is required to remove them.

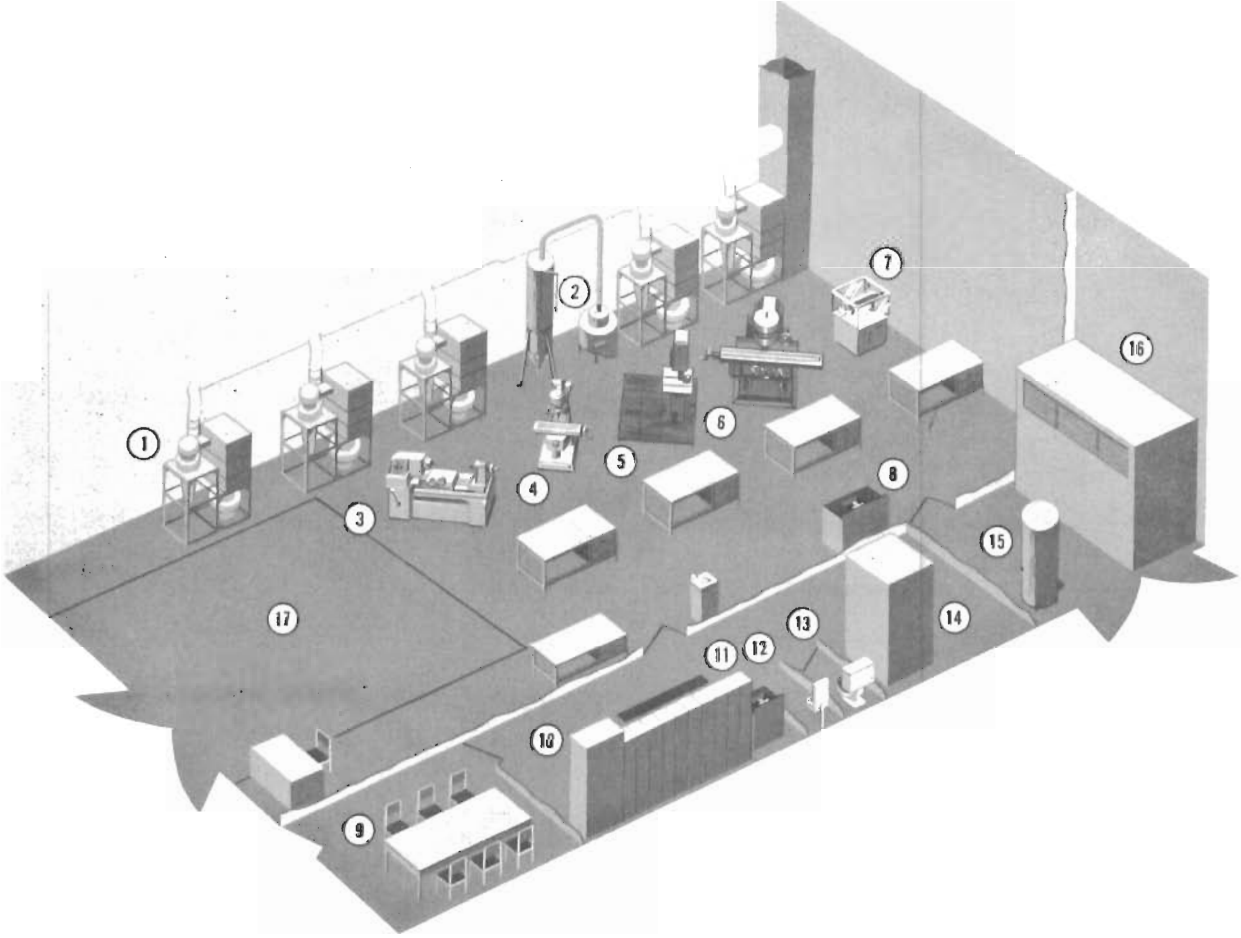

1. Dust collectors (5)
2. Vacuum cleaner
3. Rivett lathe
4. Tornetic drill
5. Band saw
6. K & T vertical mill
7. Cut-off saw
8. Rinsing sink
9. Conference room
10. Clean clothes cabinet
11. Lockers
12. Sink
13. Rest room
14. Shower
15. Hot water heater
16. Air conditioner
17. Assembly area

Figure 76 – Beryllium Facility

3. Sawing Beryllium

Sawing beryllium sheet was accomplished with a bandsaw. Equipment and procedures used are listed below.

Machine	- DoAll band saw
Blade	- 1/4 inch wide Heller Nucut (T-SBCS #12) with 32 wave set hardened teeth per inch
Blade Speed	- 552 feet per minute
Feed	- Hand feed
Coolant	- 30 parts water to 1 part Macco coolant

It should be carefully ensured that the material being sawed is in direct contact with the saw table at the blade throughout the operation, to reduce vibration and chatter. For sawing large beryllium sheets, which were often quite wavy, a foot-like support was added to the saw table at the blade, as shown in Figure 77. During sawing, the beryllium sheet always rested solidly upon this support, and thus vibration and chatter were minimized. There may be some chipping and microcracking along the sawed edge. Therefore, approximately 1/8 inch excess material was allowed on the sawed edge for clean-up by finish machining. Of the more than three hundred beryllium rudder and element test specimen detail parts which were rough sawed in the rudder program, only four parts cracked during sawing.

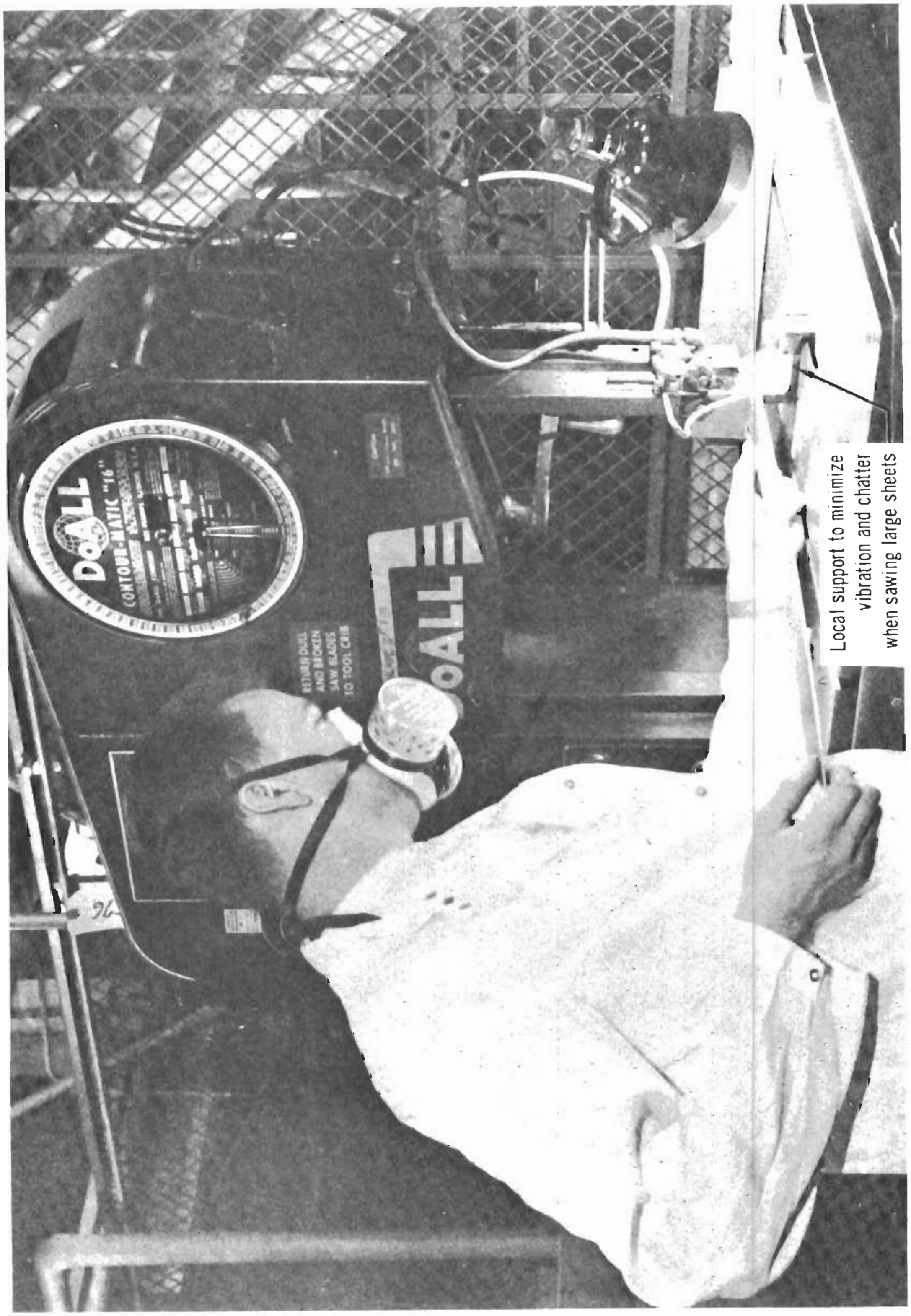

Local support to minimize vibration and chatter when sawing large sheets

DoALL
CONTOUR-MATIC "16"
RETURN DULL AND BROKEN SAW BLADES TO TOOL CRIB
DoALL

Figure 77 – Set-Up for Sawing Beryllium Sheet

4. Machining Beryllium

All beryllium part blanks were reduced to finished dimensions by machining. The use of adequate part support, special tools, proper feed and speed, and small depths of cut results in successful machining of beryllium. Equipment and procedures used for machining beryllium parts are listed below.

Equipment - Vertical Milling Machine

Cutter - Square end master mill from Metal Removal Company in 3/8, 1/2, 1 and 2 inch diameter sizes

Speed - 1115 rpm for the 3/8 and 1/2 inch diameter cutters - considerably slower for the larger cutters.

Feed - 5-6 inches per minute for thickness up to .08 inch, 3-4 inches per minute for thicknesses from .08 to .25 inch

Depth of cut - .050 inch maximum depth of cut
.010 inch intermediate cuts
.005 inch next to last cut
.001 inch last cut

Coolant - None

Stack milling of 3 to 6 parts results in a considerable reduction in machining time. Figure 78 shows a set-up for machining beryllium and Figure 79 shows tools used to machine, drill, and countersink beryllium. Conventional tungsten carbide milling cutters may be used for machining beryllium. However, the square end master mill cutters designed specifically for beryllium are preferred. The number of defects is greatly reduced when the special cutters are used. Two .020 doublers for the rudder were cracked in machining and had to be replaced. No other significant problems were encountered in machining.

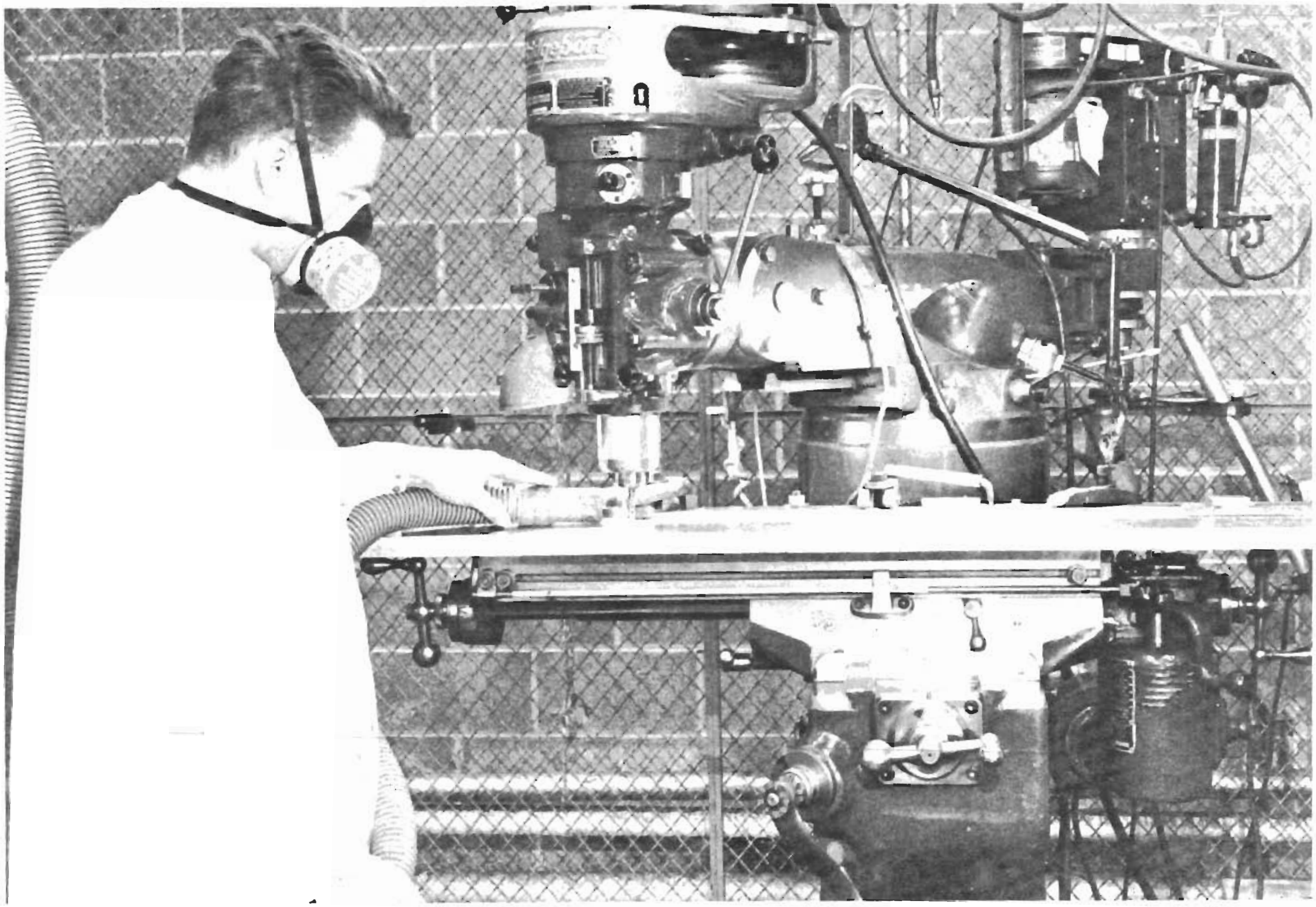

Figure 78 – Machining Beryllium

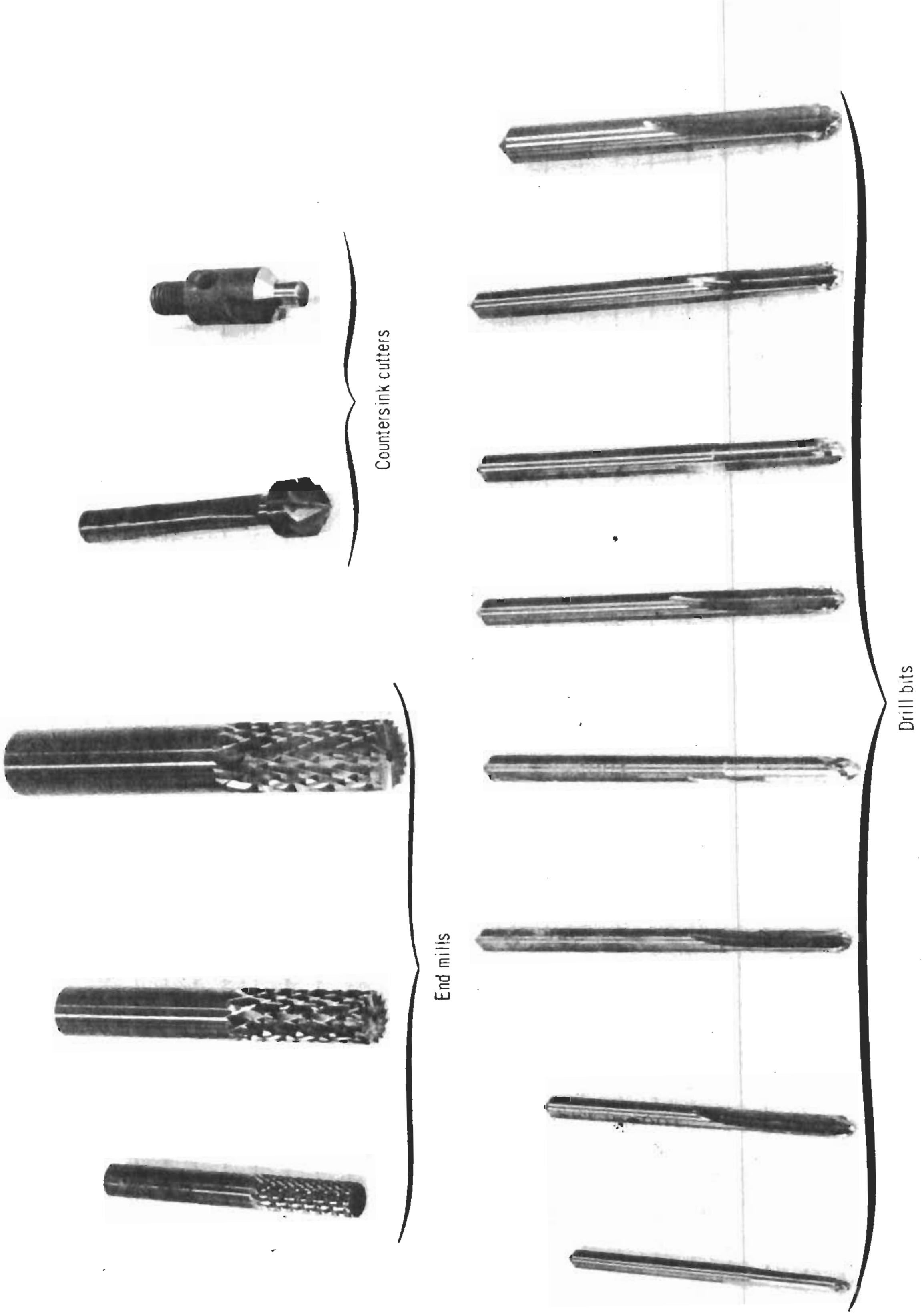
Countersink cutters
End mills
Drill bits

Figure 79 – Tools Used to Machine, Drill and Countersink Beryllium

5. Drilling Beryllium

Three types of defects, all of which are cause for part rejection, can occur when drilling beryllium. They are: (1) delaminations, (2) spalling, and (3) cracking. In order to consistently drill good holes in beryllium, special equipment, tools, and procedures are required. The Tornetic driller, shown in Figure 80, and special drill bits designed for beryllium, shown in Figure 79, were used in this program. The Tornetic driller provides positive control of torque and speed to remove material at the most efficient rate. The torque control system senses changes in torque at the cutting tool and compensates for spindle speed and feed. Care was exercised to prevent the work piece from moving during drilling. When the drill bit has a rounded tip, there is a natural tendency for it to "walk." The drill bits were discarded before they became dull. Following is a description of the equipment and procedures used for drilling beryllium.

Equipment - Tornetic Model CM-100-D-100 Driller (Duna-Systems, Inc.)
Tools - Special carbide drill for beryllium (Metal Removal Co.)
Coolant - None
Back-up - A solid back-up is preferable, especially when drilling through thin flexible members.
Speed & Feed - Table 23 gives Tornetic driller control settings.

TABLE 23
CONTROL SETTINGS FOR DRILLING BERYLLIUM

Drill Dia.	Drive Pulley Numbers		Pressure Gauge Setting (psig)	Torque Dial Setting	Speed Dial Setting	Torque Meter Reading
	Motor	Spindle				
0.1250	29	24	30	20	100	10
0.1890	24	29	30	20	100	20
0.2500	24	29	30	20	100	20
0.3750	16	36	30	40	100	20
0.4375	16	36	30	40	100	20

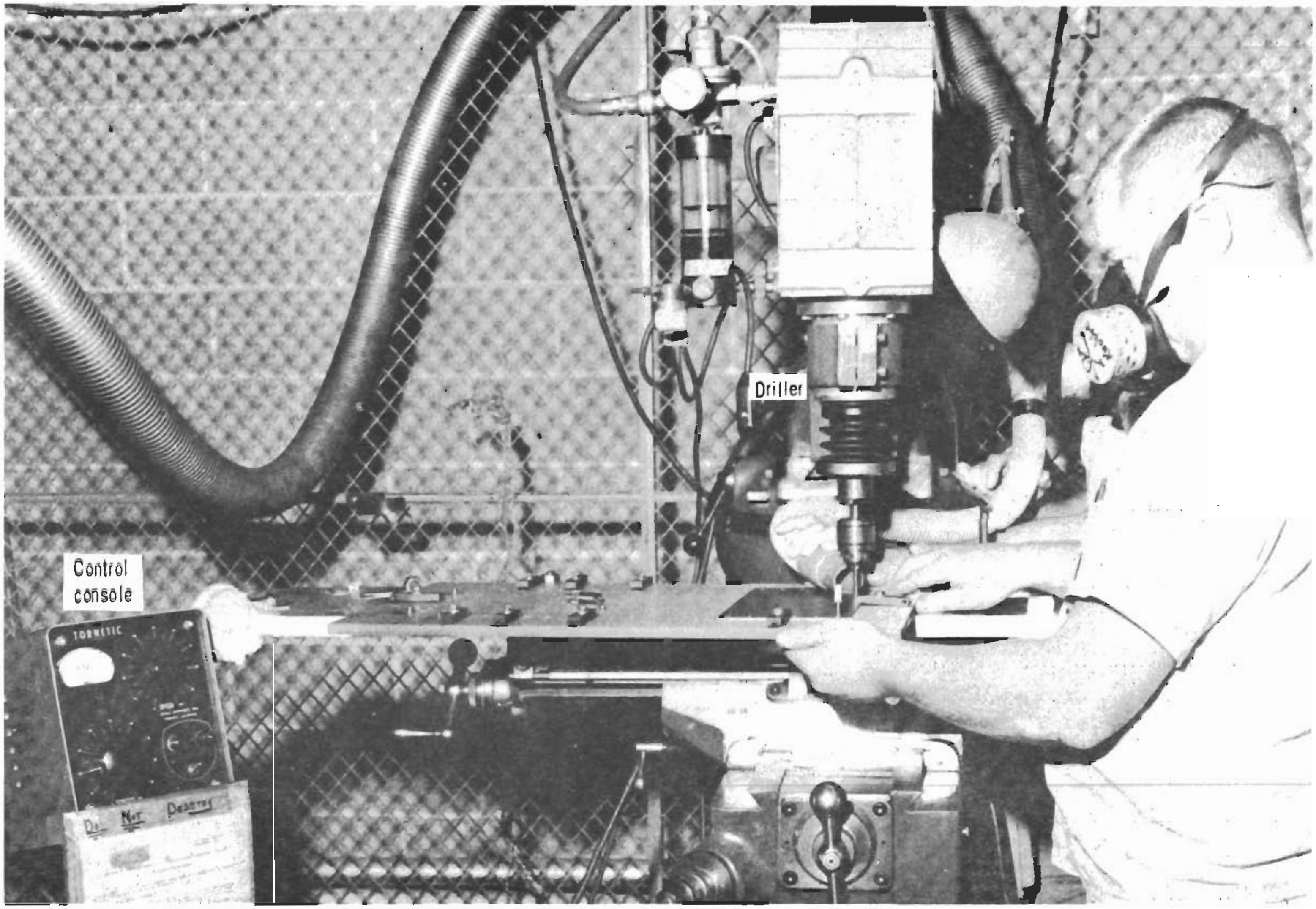
Driller
Control console
TORNETIC
Do Not Destroy

Figure 80 – Tornetic Driller Used for Drilling Beryllium

As in Reference 2 program, some difficulty was encountered during fabrication of the test specimens in the drilling operation, particularly drilling mating holes through beryllium and other materials. The difficulty stems from the fact that special equipment is required to drill consistently good holes in beryllium, and that beryllium has to be chemically etched after drilling to eliminate surface defects on the machined edges. The special drill bits used for beryllium do not perform satisfactorily in steel or aluminum (the size and shape of the flutes do not allow the free passage of the removed material and, consequently, the bits load up badly). Conversely, the high speed drill bits normally used to drill steel or aluminum do not perform consistently well in beryllium. The requirement for chemical etching of beryllium after machining dictates that all holes be drilled undersize to allow for chemical etching and that all machining be completed before assembly begins. Furthermore, since the Tornetic drill used in this program is not portable, additional time was required for set-up of all drilling operations. The procedure for drilling the holes for the fasteners joining the beryllium rudder to its mating aluminum torque tube is as follows:

> The mating aluminum and beryllium parts were located in an assembly fixture and all hole locations marked with a pencil. A small pilot hole was drilled through all parts using a conventional carbide twist drill in a portable air motor or the Tornetic driller. The pilot hole was drilled small enough (1/2 the final hole size) so that any defect introduced in the beryllium would be removed in final drilling and etching. After all fastener holes were pilot drilled, the parts were disassembled and the holes in the aluminum parts were conventionally drilled to final size. The holes in the beryllium were then drilled to full size (less allowance for chemical etching) using the special equipment and procedures described previously.

This procedure for drilling mating holes in beryllium and aluminum did not yield 100% good holes. Spalling occurred at 12 of the holes in the beryllium. In all cases except one, the spalling was not severe and the rough edges were removed by hand sanding with 180-400 grit emery paper prior to the final etching operation. The more severely spalled hole was redrilled oversize to remove the spalled area, and an oversized repair fastener was installed. No parts were rejected because of defective holes.

Less difficulty was experienced in drilling holes in mating beryllium parts. Fewer than 2% of such holes were found to be defective, and in most cases it was possible to salvage the part. Two of the .020 ribs were found to have cracks resulting from drilling and were replaced. These cracks are believed to have resulted from the lack of an adequate backup during drilling.

When spalling occurred it was always immediately evident. Delaminations were usually not evident until after the part had been chemically etched. If the defective hole was found, and redrilled for a repair fastener after the other holes were chemically etched, it was necessary to locally etch the redrilled hole using a felt rod or 'Q'-Tip. This procedure for salvaging beryllium parts is quite satisfactory for removing the damaged area and eliminating its deleterious effects on material strength. However, when a hole is locally etched by hand, it is often oversized and out of round due to the difficulty of etching all surfaces uniformly. Therefore, this salvage procedure is not suitable for highly loaded joints where all fasteners must be fully effective to develop the required joint strength.

6. Countersinking Beryllium

Excellent results were obtained machining the countersink recesses in beryllium for flush fasteners. After the fastener hole was drilled to size (less the allowance for chemical etching), the countersink recess was machined by means of a conventional stop countersink with a carbide cutter in a drill press. Cutter speed was 1115 rpm and hand feed was used. A piloted backup was used to avoid dimpling. It was found that approximately 50 countersink recesses for 5/32 or 3/16 flush fasteners could be machined before the cutter had to be resharpened.

The use of flush fasteners does impose one design limitation. The countersink depth should be approximately .015 inch less than the skin thickness to avoid a knife edge which will invariably chip at the base of the countersink. This limitation does not necessarily result in a weight penalty. The beryllium rudder cover skins were attached with flush fasteners. To accommodate the flush fasteners, the cover skin thickness was varied by chemical milling so that the skin was of greater thickness along the fastener line than between fastener lines. Thus, for axial loading, all of the material was effective and no weight penalty resulted.

7. Forming Beryllium

Equipment and procedures used in forming beryllium structural elements are described below.

7.1 Equipment - Forming was performed in a 500 ton hydraulic press. Two electrically heated platens, installed in the hydraulic press, were used to heat the forming dies to the desired forming temperature (1325° ± 25°F). Temperature was controlled automatically and recorded continuously. The platens incorporated retainers for holding the forming dies in position during forming.

7.2 Form Dies - Mated dies, machined from H-13 steel, were used for all beryllium forming. This is temporary tooling suitable for limited production only, since H-13 steel oxidizes readily at beryllium forming temperature and must be cleaned after use. For volume production, ceramic or super-alloy, e.g., Hastelloy X, dies are more efficient. Some of the forming dies for beryllium channel sections are shown in Figure 81. Figure 82 shows the mated forming die for the rudder balance weight rib at station $Z_R = 130.87$. This particular rib is a channel section with closed flanges. To form the closed flanges, the sides of the male and female die halves were slightly tapered in a closed angle shape. In addition, the sides of the female half of the die were made to be moved together slightly with manually operated cams affixed to the base of the die. With the movable sides in the wide open position, the die halves were mated in the press. The closed angle of the rib flanges was then attained by closing the sides on the female half of the die thus forcing the flanges of the formed part to close upon the male die.

Two of the rudder ribs were formed with joggled flanges. This was accomplished satisfactorily, with no modifications to the forming procedure, using dies with joggled faces as shown in Figure 81. Joggle length was ten times joggle depth.

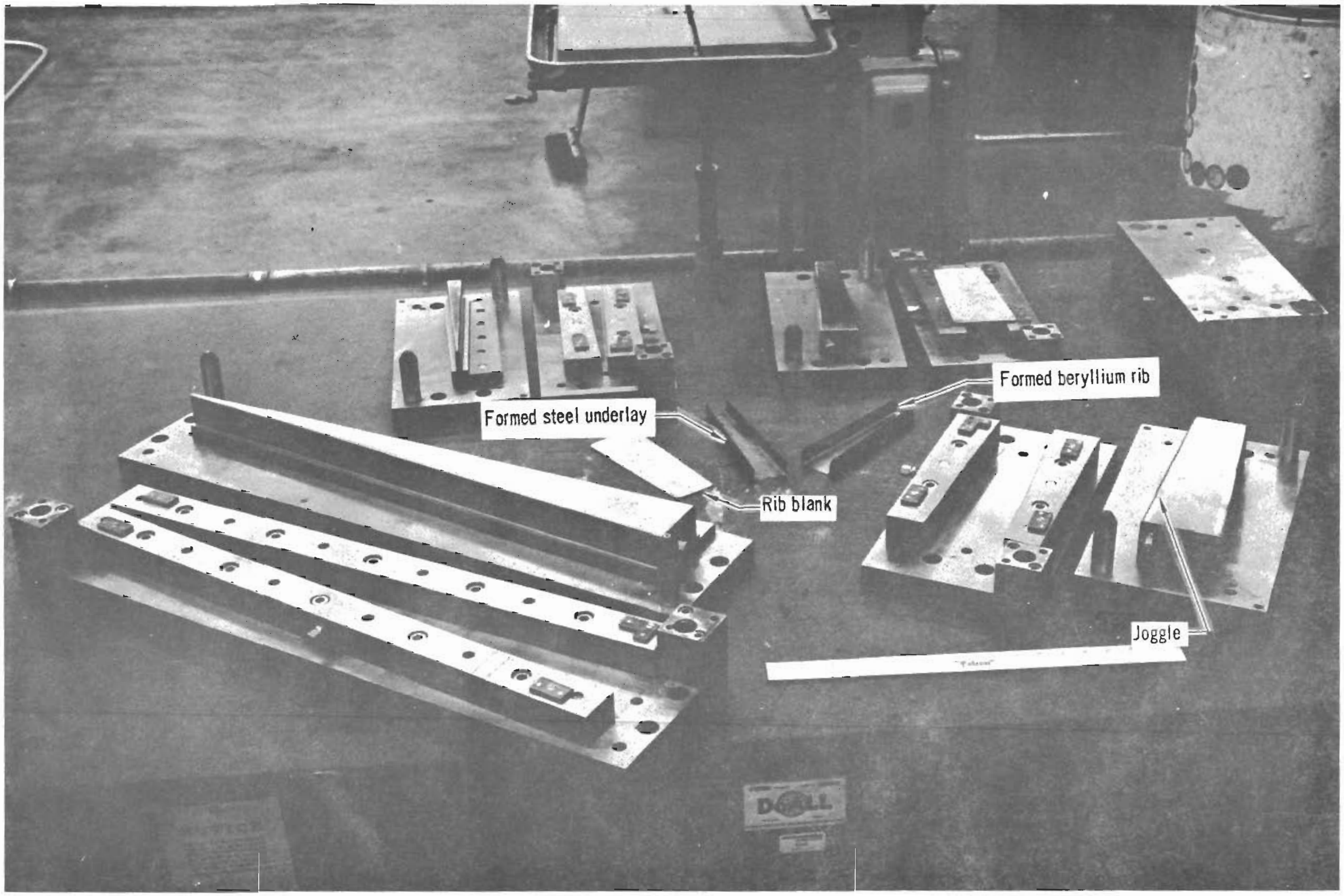
Formed beryllium rib
Formed steel underlay
Rib blank
Joggle

Figure 81 – Mated Hot Forming Dies for Beryllium Rudder Ribs

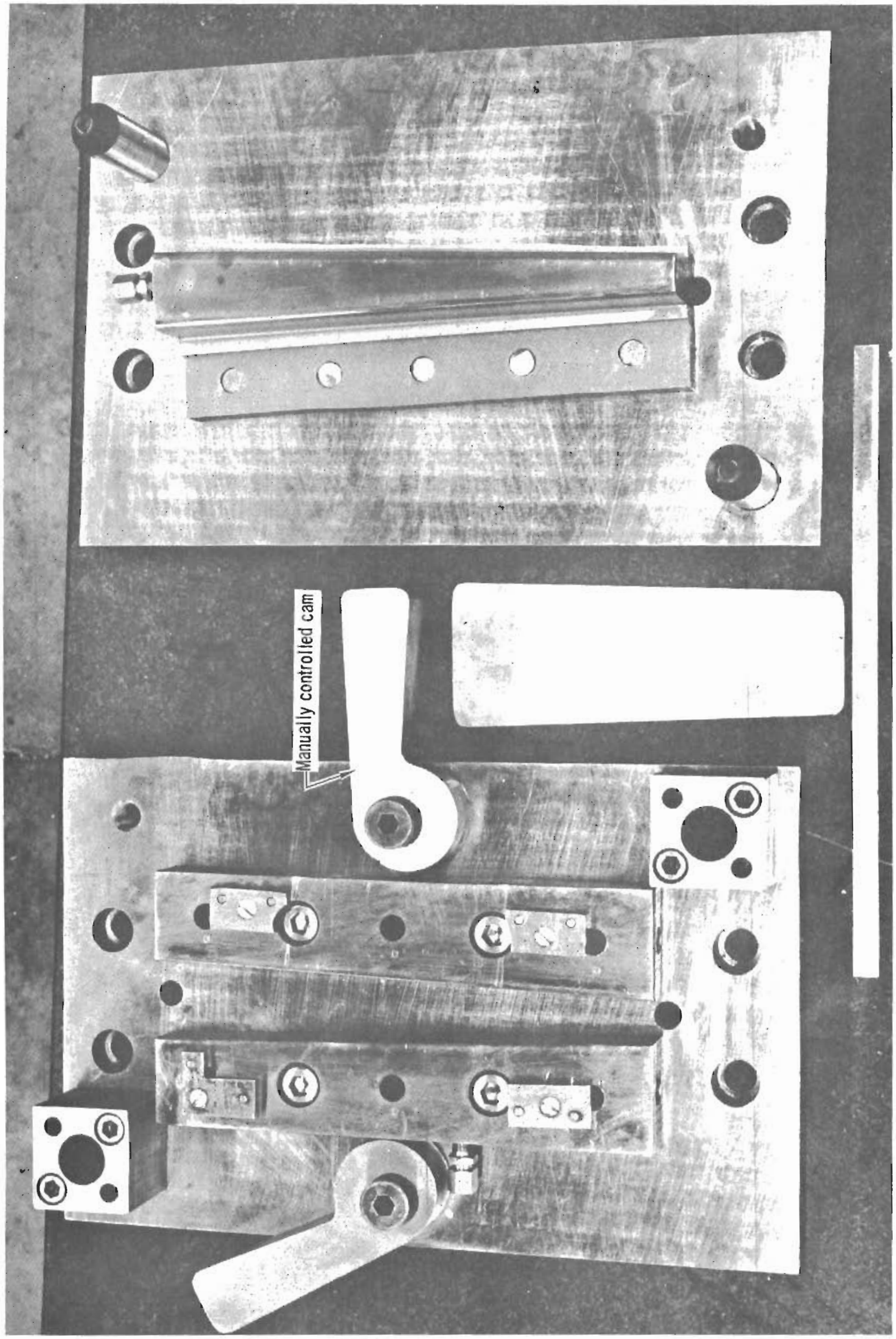
Manually controlled cam

Figure 82 – Mated Hot Forming Die for Rib with Closed Angle Flanges

The dies were heated by conduction and radiation from the heated platens. Thermocouples were installed on each die half to insure that proper forming temperatures were maintained. No spring back allowance was provided. The dies used in forming the details of the element test specimens had clearances between the mating halves of .004 inch plus the thickness of the material to be formed. A die lubricant (Everlube T-50) was used. The dies used in forming the rudder parts had oversized clearances to allow for the thickness (.012) of an alloy steel underlay (rub strip). This steel underlay was used to prevent abrasive action between the forming die and the beryllium material. With the underlay in place, it was considered unnecessary to use the die lubricant, especially as the lubricant had the tendency to dry into a hard crust at the high forming temperature, and this crust was difficult to remove. Stops were provided on all female die halves to position the beryllium blanks for forming. It is mandatory that sufficient stops be provided to prevent beryllium from slipping on the die during the initial stages of forming.

7.3 Forming Procedure - After the temperature had stabilized at 1325°F ± 25°F, the beryllium part blank was placed on the die. Approximately three minutes were required to bring the part up to temperature, as determined by a hand-held probe thermocouple. The hydraulic press head was then closed at a rate of .10 to .15 inch per minute until forming was completed. A dwell time of 15 minutes, with the die closed, was allowed to accomplish stress relief. After stress relief, the heating elements were turned off; thereafter, the larger parts were allowed to cool in the die to minimize distortion and warpage. Parts less than 12 inches long were removed from the die immediately after stress relief and air cooled without excessive deformation. The channel ribs and spars were formed with a bend radius of 5t (5 x material thickness).

The 1325°F forming temperature, the slow forming rate of .10 to .15 inch per minute, and the minimum bend radius of 5t are extremely important factors in forming beryllium. If forming temperature is less than 1300°F, cracks may develop in the bend radii regardless of forming rate or bend radius size. If forming temperature exceeds 1350°F, mechanical properties may be affected depending on the exposure time. Experience has shown that forming bend radii smaller than 5t and/or increasing the forming rate may cause cracking in the bend radii resulting in excessive reject rates. The slow forming rate does not significantly affect the total time required to form a part. Most of the time is spent in setup, stress relief, and cool-down after forming. For volume production, several parts could be formed simultaneously by attaching more than one forming die to the platens. This procedure was used in this program to form two ribs simultaneously. Data is not available on the forming temperatures and rates required for forming bend radii less than 5t. Until this data becomes available, 1300°F - 1350°F should be used for the forming temperature of beryllium, with a bend radii of 5t or greater.

All formed beryllium parts were of excellent quality. Bend angle variations were approximately ± 1/4° and the parts were straight within .01 inch total indicator reading over their length. The channel web widths were within .005 inch of those specified on the drawings.

7.4 Post Forming Cleaning - Liquid honing with a slurry containing Burr-Al-220 aluminum oxide abrasive was most satisfactory for cleaning beryllium after forming. An air pressure of 60 - 80 psi was used.

8. Chemical Milling of Beryllium

A sulfuric acid solution was used for chemical milling and etching of all beryllium parts for this program. The solution is described below, with the surface finish and metal removal rates obtained.

10% sulfuric acid by volume

Balance - tap water

Temperature - 90°F

Surface finish - 100-125 rms

Metal removal rate - .008 inch per minute

Chemical milling was used to vary the material thickness of the detail parts in order to achieve minimum weight consistent with design requirements. Figure 83 shows the extent of chemical milling on the front torque box cover skins. The maximum amount of metal removed from a surface by chemical milling was .080 inch. The tolerance specified (± .001 inch) was achieved in all cases. Chemical etching (.0015 - .0025 inch per surface) was required on every beryllium detail part to remove any microscopic surface cracks or mechanical twins that may have been introduced during machining. No difficulty was experienced in chemical milling or etching.

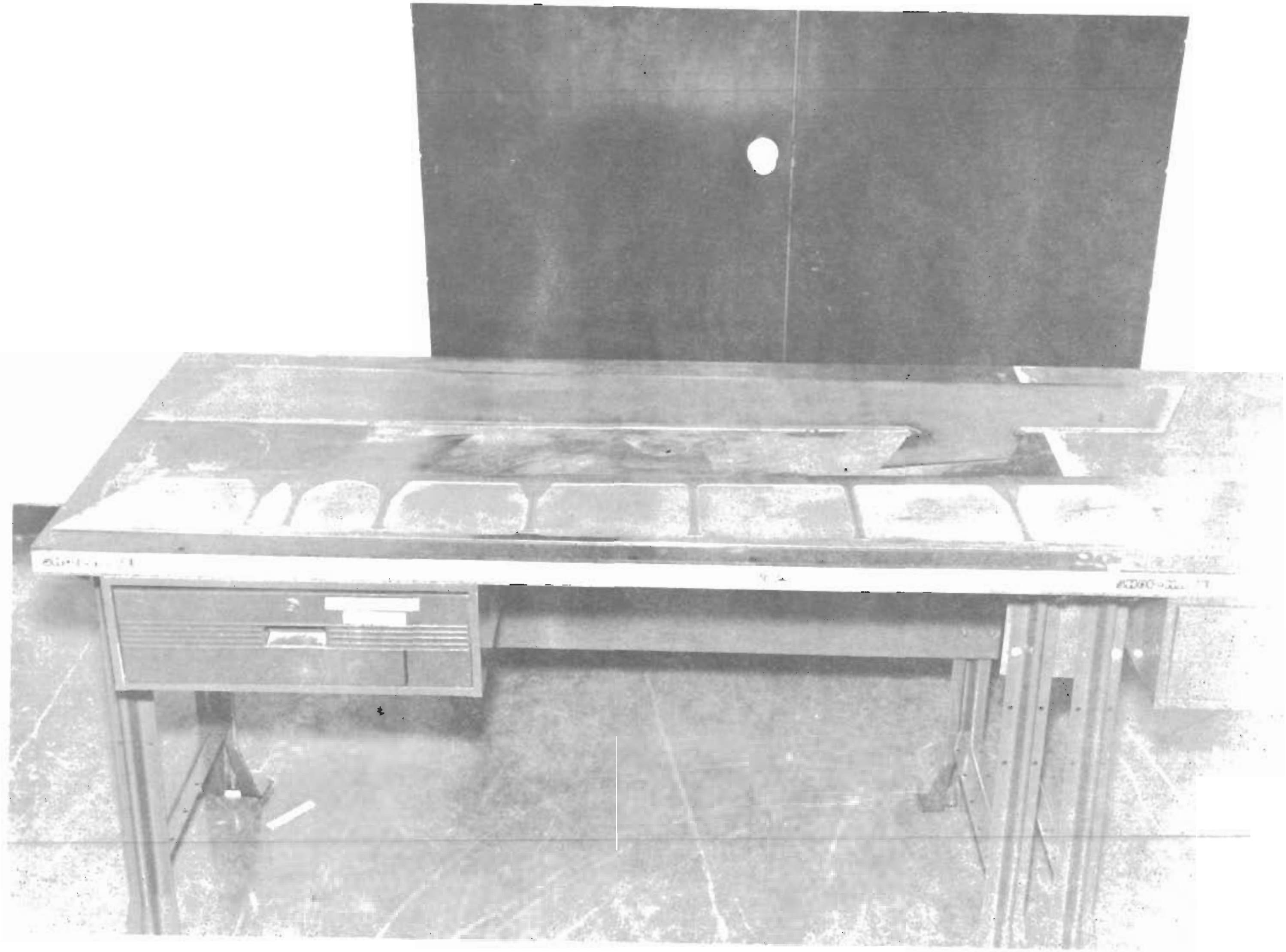

Figure 83 – Beryllium Rudder Front Torque Box Cover Skins

9. Adhesive Bonding

The honeycomb trailing edge assembly for the beryllium rudder is a relatively complex structure which was bonded with FM-61 adhesive, a nitrite pehnolic/epoxy film. The trailing edge assembly detail parts are shown before, during, and after the bonding operation in Figures 84, 85, and 86, respectively. The face skins, doublers, and edging members all are beryllium. The non-perforated honeycomb core is 5052-H39 aluminum with 1/4 inch cell size and .001 inch foil thickness. The aluminum core and the adhesive are the same as those used in the trailing edge assembly of the production rudder for the F-4 aircraft.

Bonding materials and procedures are the same as those used to bond aluminum, except that chemical etching is required for cleaning the beryllium parts prior to bonding. It is most convenient if bonding is performed within 24 hours after the beryllium parts received their final chemical etch, provided the parts are protected from contamination during this time. If this cannot be accomplished, a light chemical etch to remove .0005 from the surface is adequate for cleaning the beryllium prior to bonding. After cleaning, all surfaces to be bonded, except the honeycomb core, were treated with an epoxy resin primer (coupling agent), air dried for 30 minutes, and oven dried at 230-240°F. The parts were then assembled on a contoured base with the FM-61 adhesive film between all faying surfaces. Thereafter, the assembly was placed in a vacuum bag and compressed when the bag pressure was reduced to approximately 10 inches of mercury. While maintaining the vacuum condition, the assembly was placed in an autoclave. Autoclave pressure was increased to approximately 25 psig. and the vacuum bag vented to atmospheric pressure. Temperature in the autoclave was raised to 330-345°F and maintained for one hour before the assembly was allowed to cool. Autoclave pressure was maintained during the cooling cycle. Tests of the composite section and all of the other bonded test specimens, discussed in Section IV, substantiated the adequacy of this bonding process for the beryllium rudder.

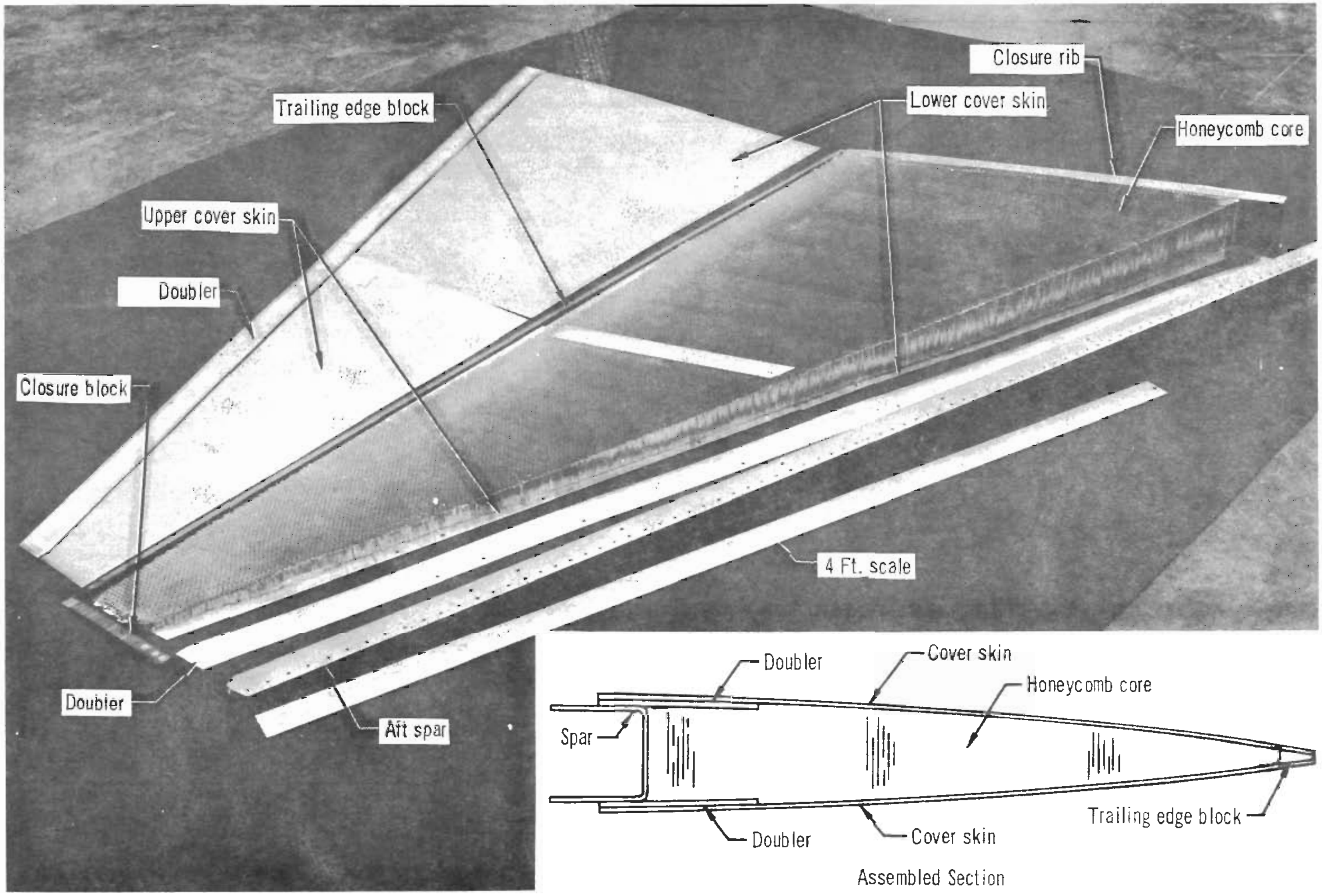
Trailing edge block
Lower cover skin
Closure rib
Honeycomb core
Upper cover skin
Doubler
Closure block
4 Ft. scale
Doubler
Aft spar
Doubler
Cover skin
Honeycomb core
Spar
Trailing edge block
Doubler
Cover skin
Assembled Section

Figure 84- Rudder Trailing Edge Assembly Structural Details

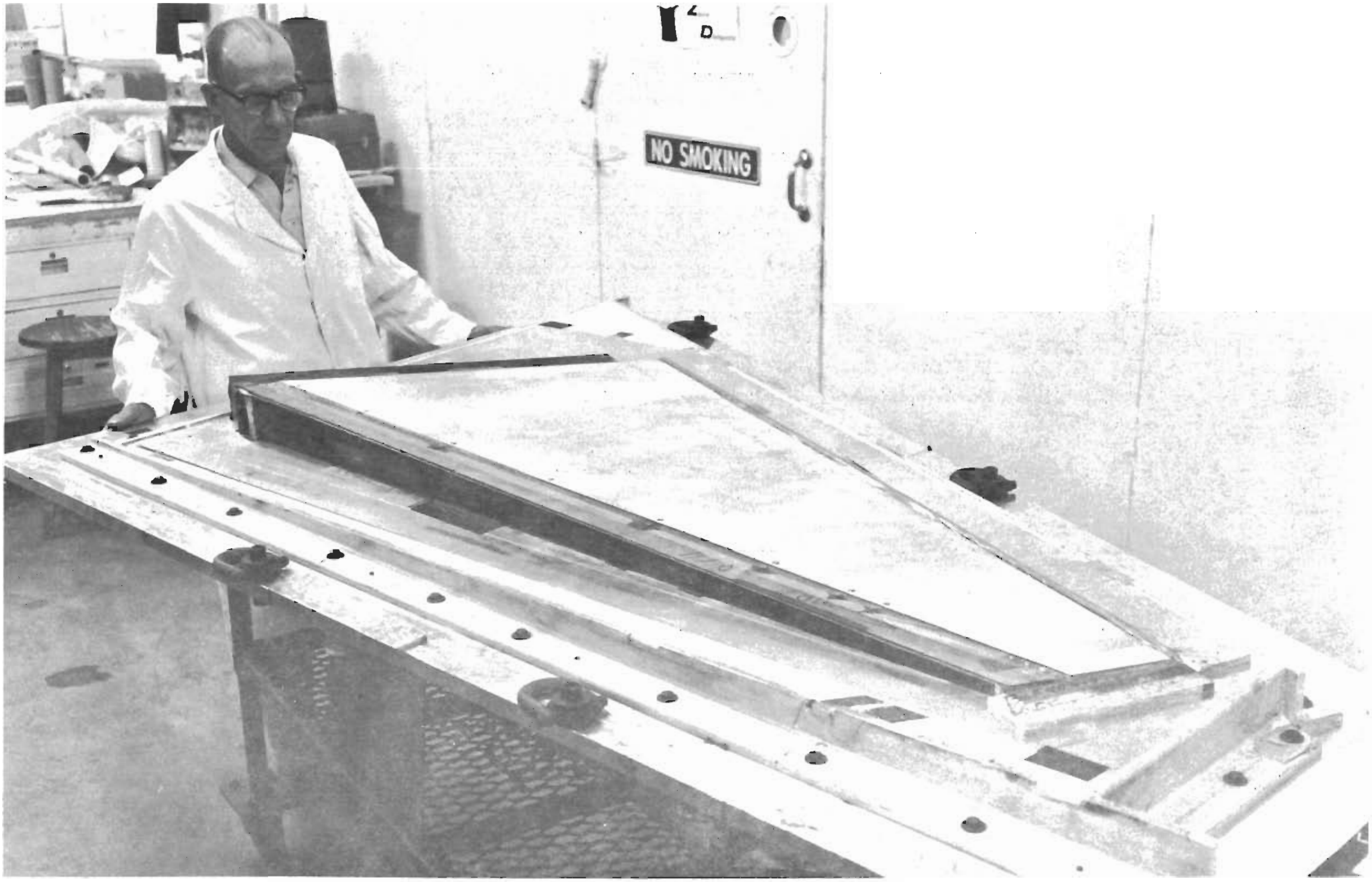

Figure 85- Rudder Trailing Edge Assembly and Bonding Fixture

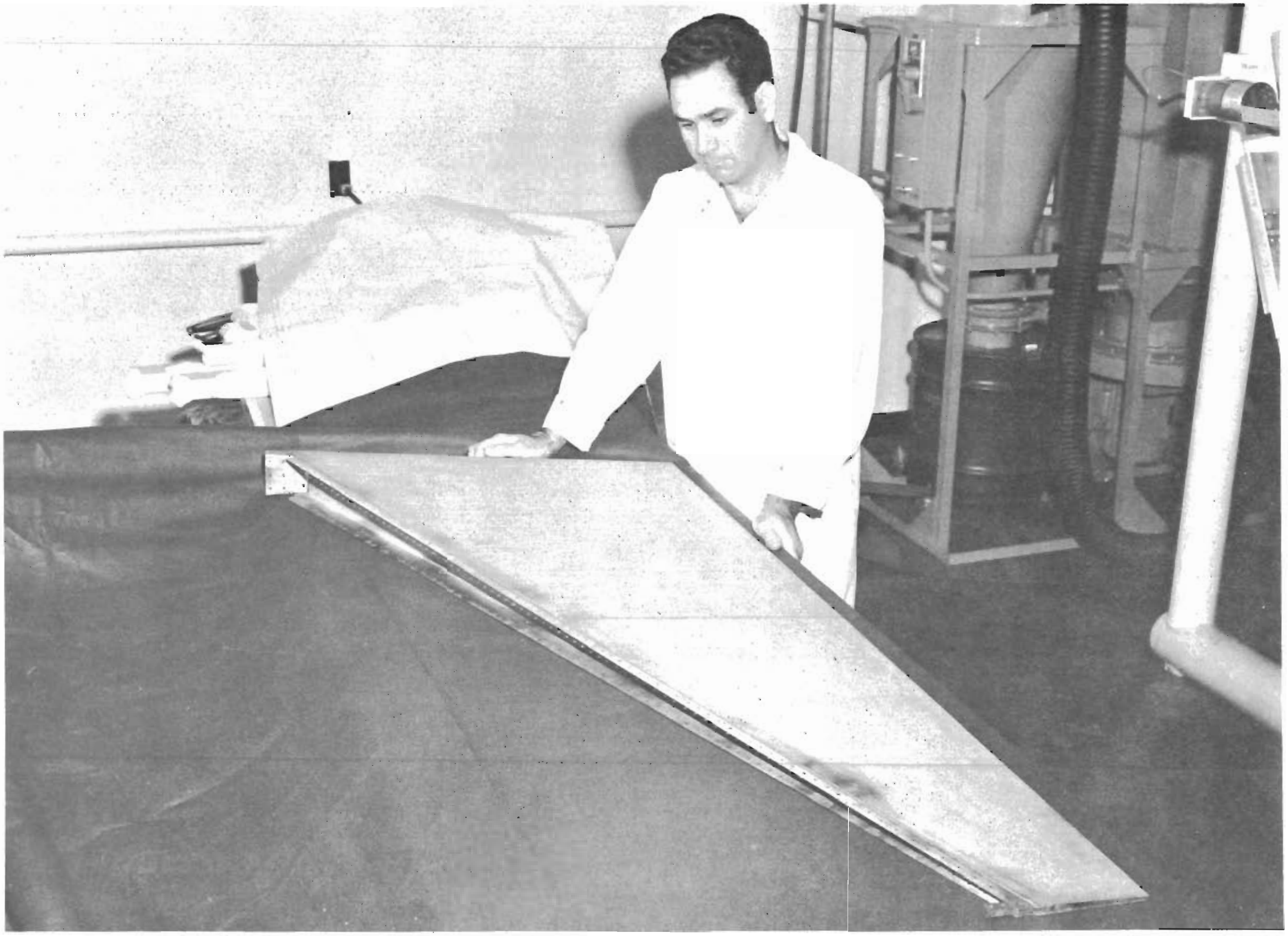

Figure 86- Beryllium Rudder Bonded Trailing Edge Assembly

10. Inspection

Standard aerospace inspection procedures were used on the beryllium detail parts and assemblies. Fluorescent penetrant inspection was used extensively as an aid in locating surface defects introduced in manufacturing. Large or complicated parts were fluorescent penetrant inspected several times in the course of fabrication to eliminate defective parts at the earliest possible time, and to aid in determining the cause of the defects. Fluorescent penetrant inspection is not completely reliable for locating defects on a machined surface since the defect is often smeared over in machining and will not show up until the surface is chemically etched. Therefore, final fluorescent penetrant inspection should be performed after chemical etching.

11. Rudder Assembly

Assembly of the beryllium rudder was accomplished with only minor difficulty. The knowledge and experience gained in Reference 2 contract and in the fabrication of the test specimens, especially the rudder composite section, for this program, proved very helpful. Following is a description of the rudder assembly sequence.

After fabrication, excluding the drilling of fastener holes, the detail rudder parts were assembled in the assembly fixture using clamps as shown in Figure 87. This was accomplished (1) to determine the need for any final machining operations, shimming requirements, or other procedures necessary to insure proper fit of the various rudder parts and (2) to locate and pilot drill fastener holes as shown in Figure 88. After disassembly, the fastener holes and countersink recesses were drilled to size (less .004 inch allowance for chemical etching of beryllium parts). After the drilling operation, the beryllium parts underwent chemical etching and final fluorescent penetrant inspection. Two ribs (see Subsection 5) and two doublers (see Subsection 4) were found to have cracks resulting from machining or drilling operations and were replaced.

After inspection, the trailing edge beryllium skins, the aluminum honeycomb core, the edging members and the aft spar were cleaned and bonded together, in the manner previously described in this section, into the trailing edge assembly (see Figure 86). Upon completion of the bonding operation, a crack was discovered in one of the upper cover skins at the rear spar. The cause of this crack could not be determined. It may have developed when the skin was deformed under bonding pressure (these skins were quite wavy) because of the differing foundation stiffness or because of a mismatch between the aluminum honeycomb core and beryllium spar (refer to Figure 84 for the trailing edge configuration). Because this area of the rudder is only lightly loaded, an external

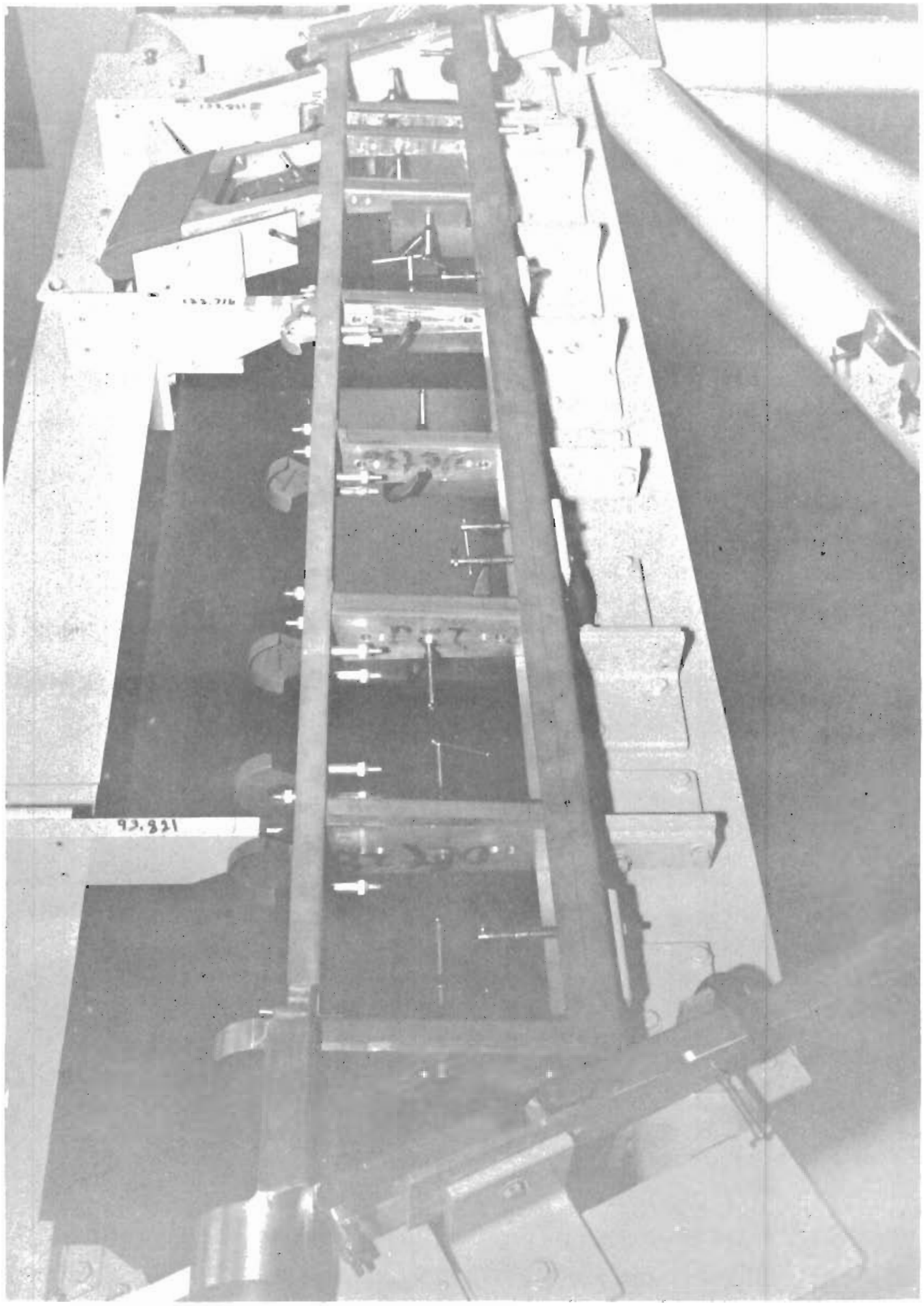
122.716
93.821

Figure 87 – Pre-Fit Assembly of Beryllium Rudder in Assembly Fixture

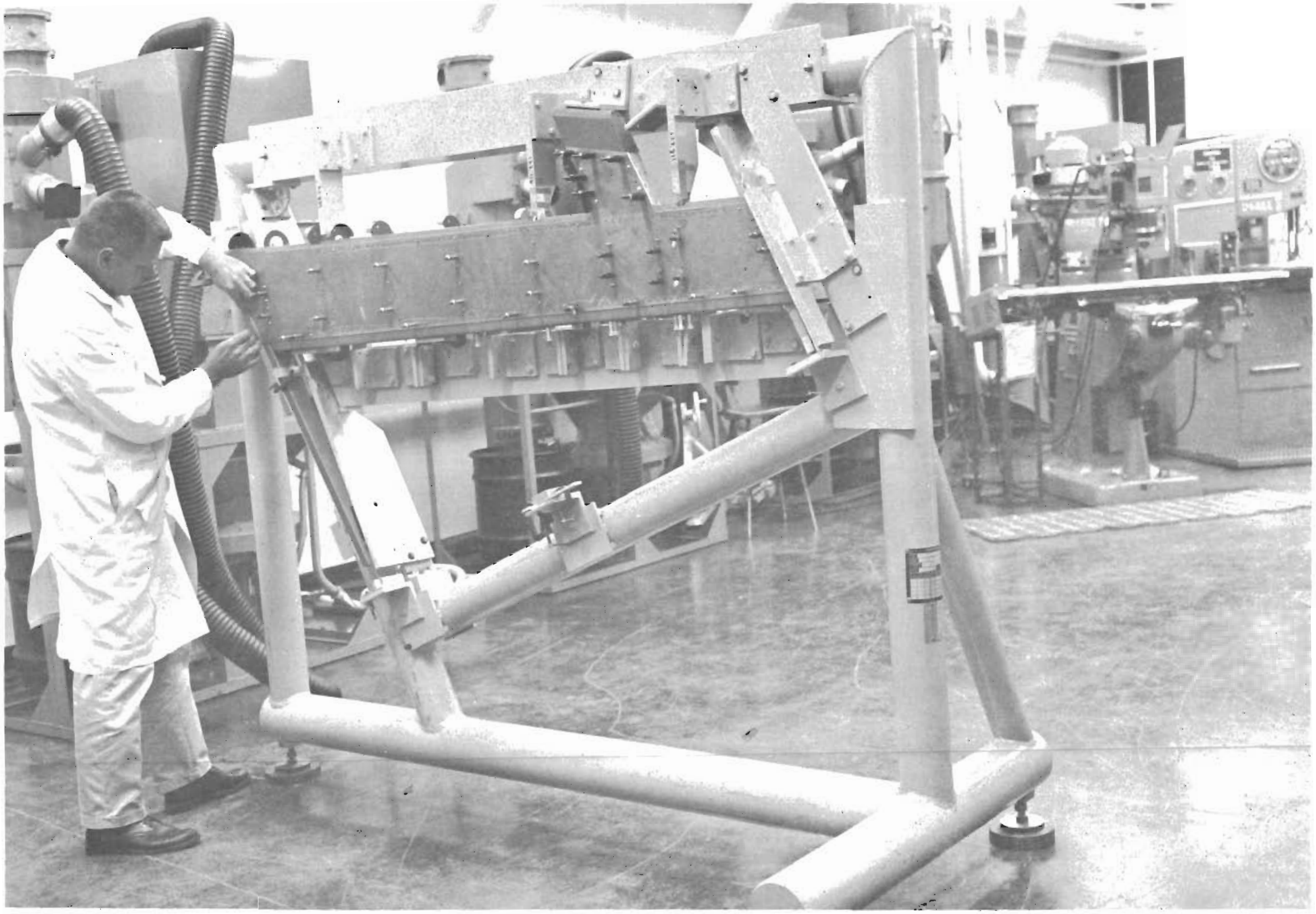

Figure 88 – Locating Fastener Holes in Rudder Front Torque Box

doubler bonded over the area of the skin containing the crack was adequate to completely restore the structural integrity of the assembly. The adequacy of this repair was demonstrated by element testing and is discussed in Section IV.

Final assembly of the beryllium rudder was accomplished using conventional fasteners and installation procedures, except that vibration driven fasteners were not allowed. The front torque box beryllium detail parts shown in Figure 89, the torque tube fitting, the hinge fitting, the balance weight assembly and the leading edge structure were assembled in the fixture and joined with Hi Shear rivets, Hi Loks, Jo Bolts and Cherry rivets. Figure 90 shows the installation of Hi Shear rivets along the front spar. The trailing edge assembly was attached with Hi Shear and Cherry rivets. During assembly, while installing fasteners in the front spar-to-rib shear clip, a portion of one flange of the lower balance weight rib was broken when bumped by the fastener installation tool. An angle splice was fabricated and joined to the rib by both adhesive bonding and mechanical fasteners. With the splice, and the broken section of flange serving as a filler, the rib was secured to the spars and cover skins in a conventional manner. Figure 91 shows the broken rib flange and illustrates the manner in which the angle splice was installed.

Except for the broken flange of the balance weight rib discussed above, the final assembly operation was completed with comparative ease. Assembly of the rudder was greatly facilitated by the positive control of the position of all structural elements afforded by the assembly fixture. Accordingly, hole alignment and subsequent fastener installation was accomplished with little difficulty. Figure 92 shows the final assembly of the beryllium rudder in the assembly fixture. The high degree of accuracy maintained in the fabrication of the forming tools and the care exercised in the forming and chem-milling operations resulted in relatively little mismatching of parts and subsequent shimming requirements. The beryllium rudder, completely assembled, is shown in Figure 93.

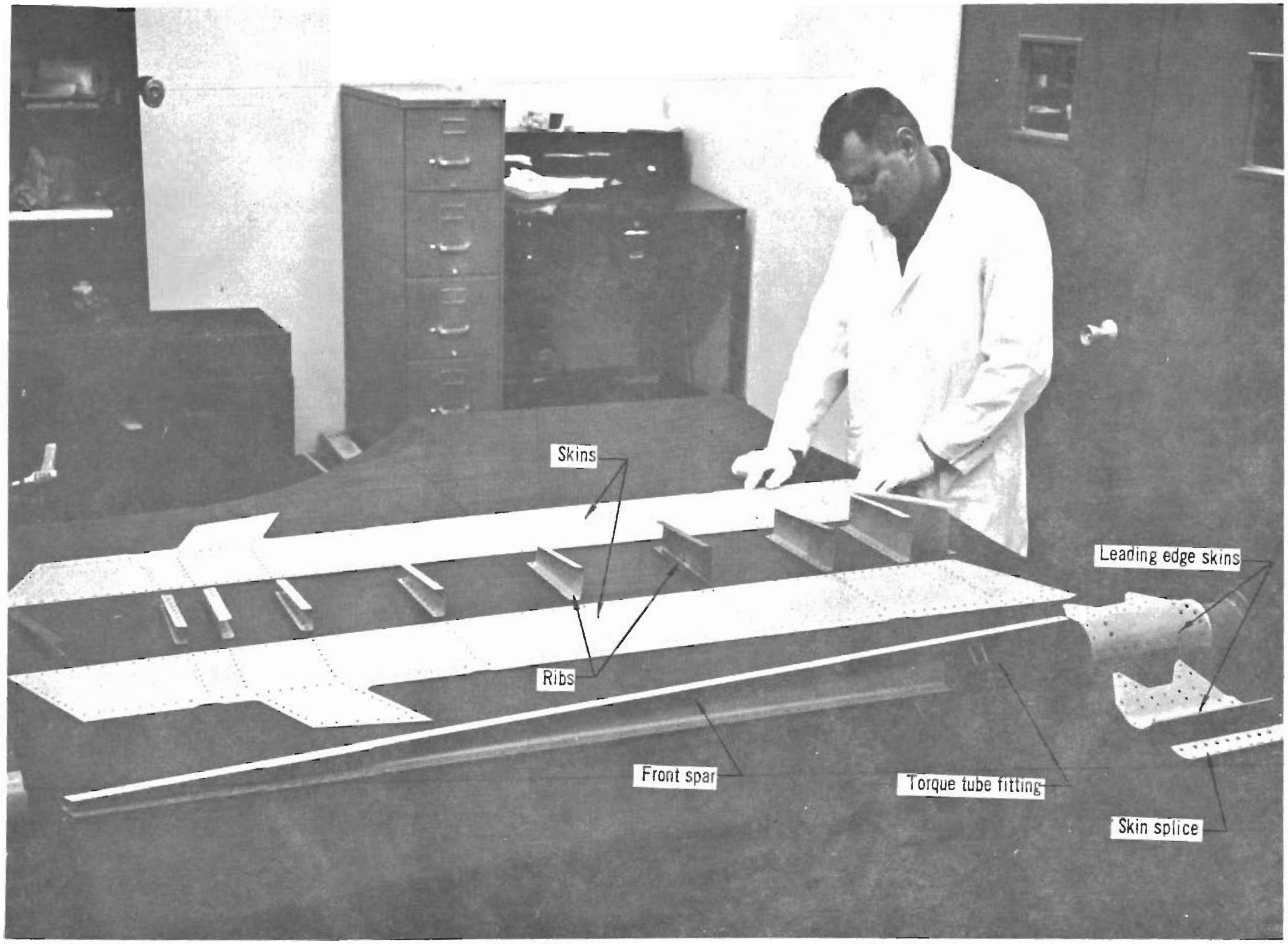
Skins
Ribs
Leading edge skins
Front spar
Torque tube fitting
Skin splice

Figure 89 – Rudder Front Torque Box Detail Parts

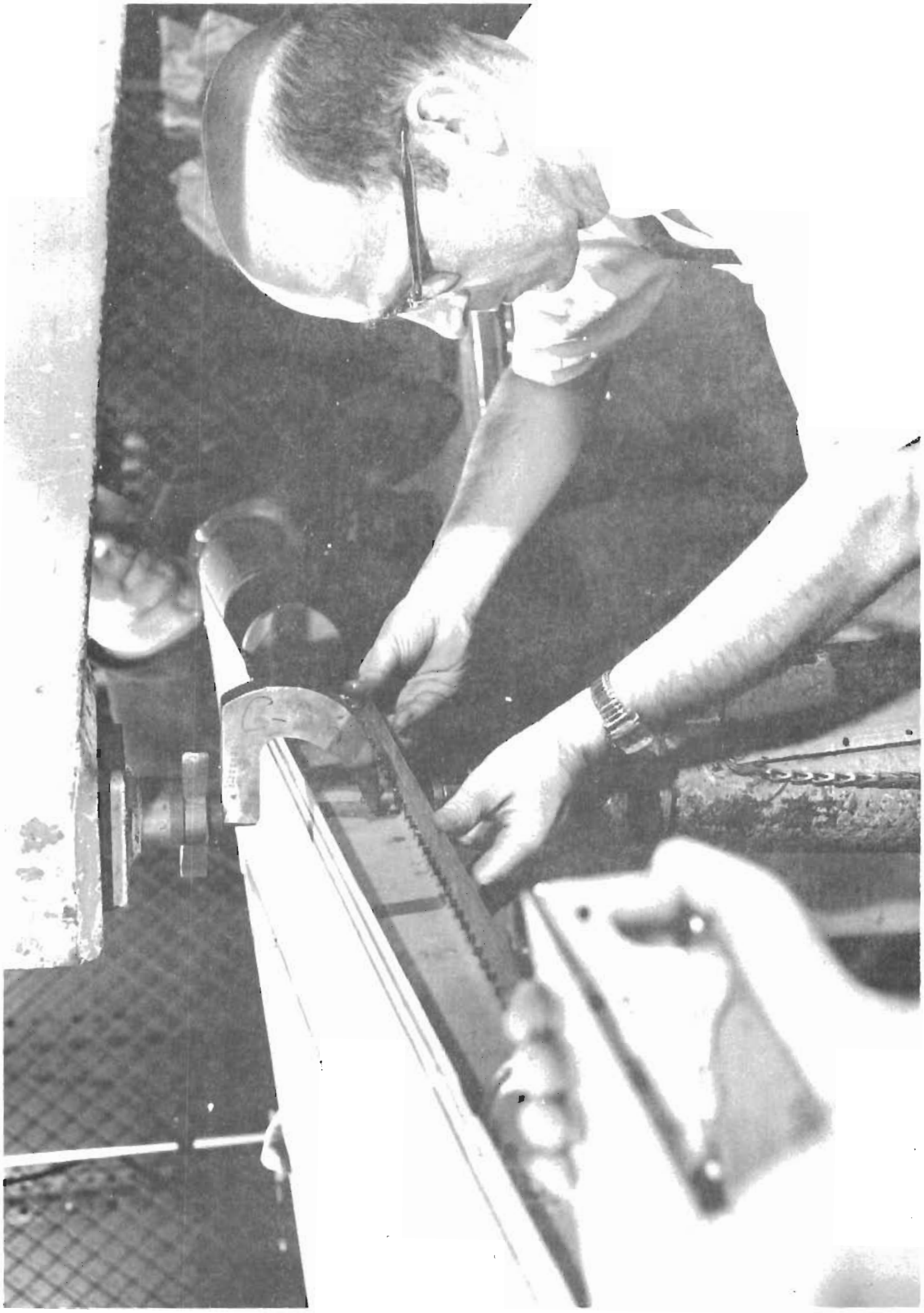

Figure 90 – Rivet Installation Along Front Spar of Beryllium Rudder

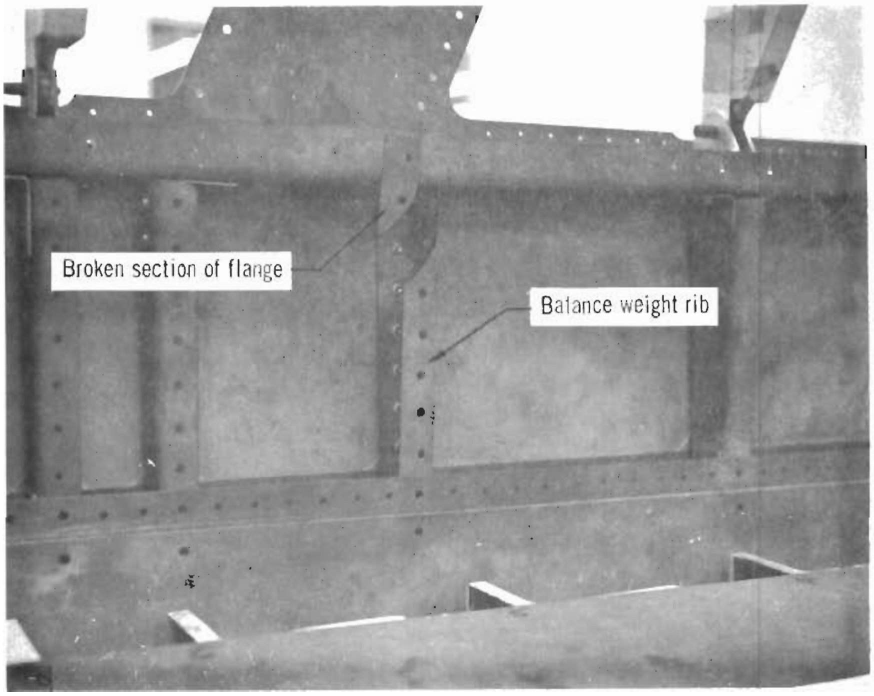
Broken section of flange
Balance weight rib

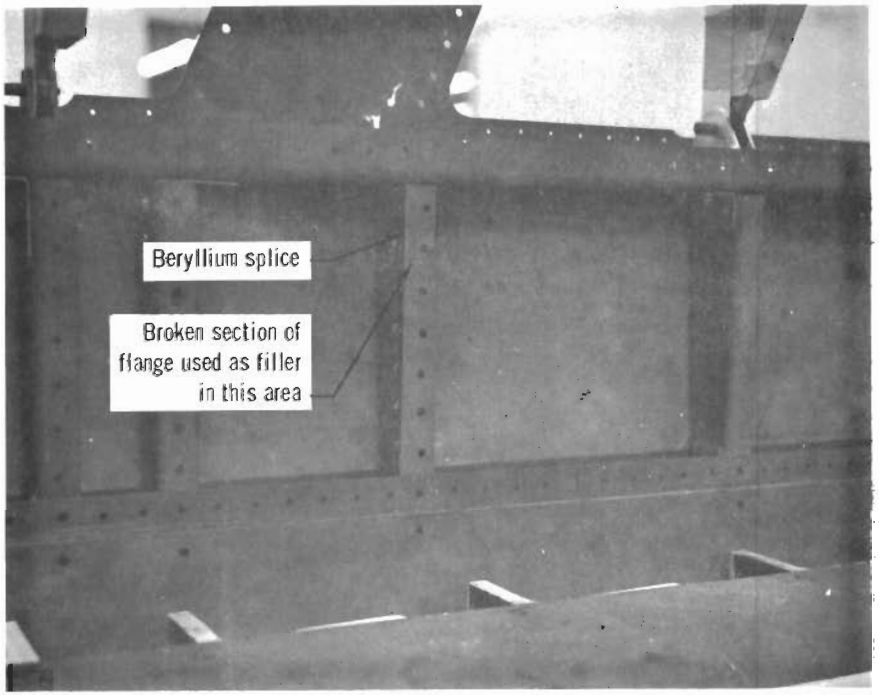
Beryllium splice
Broken section of flange used as filler in this area

Figure 91 – Beryllium Rib with Broken Flange and Repair Splice

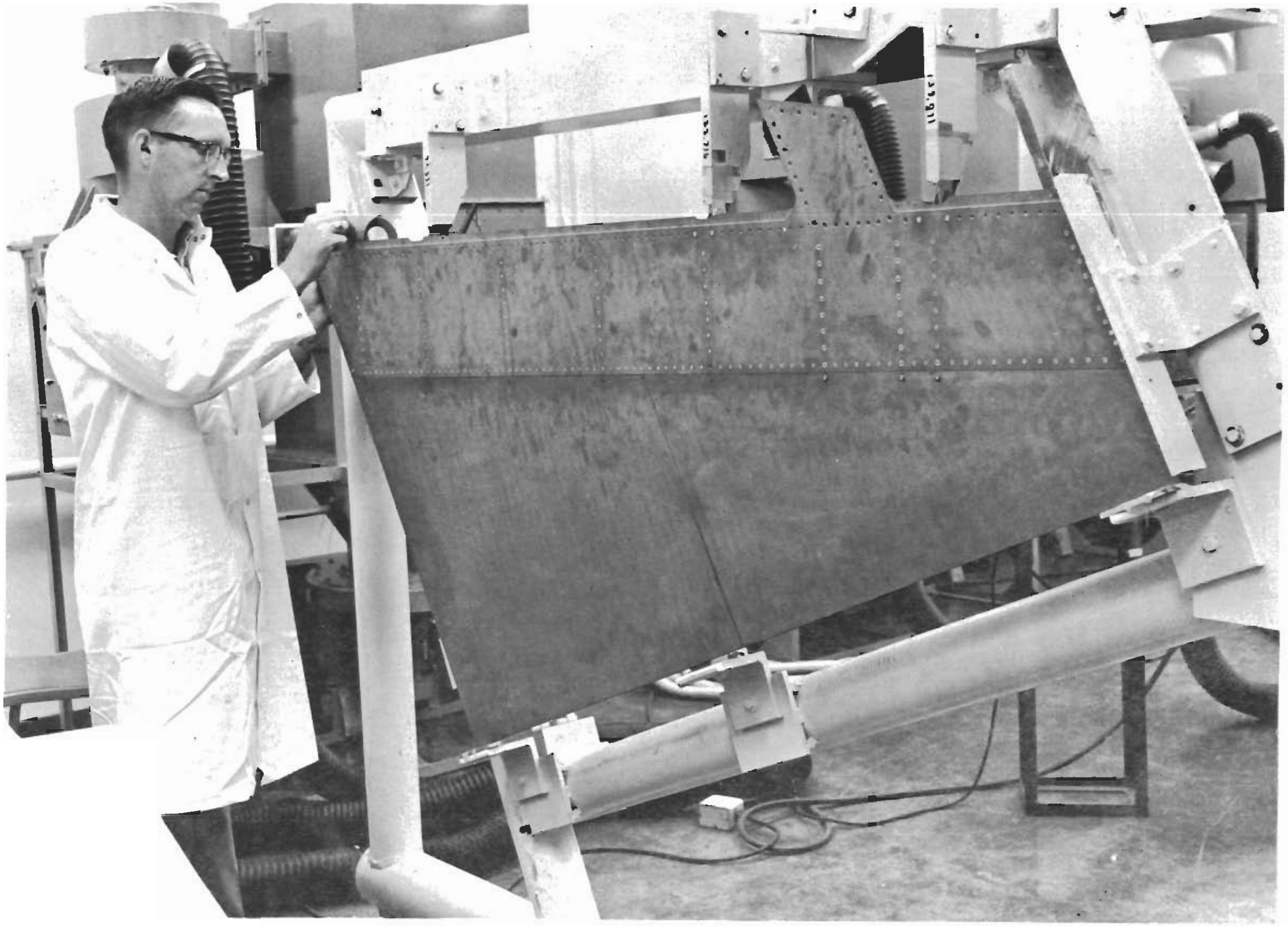

Figure 92 – Final Assembly of Beryllium Rudder

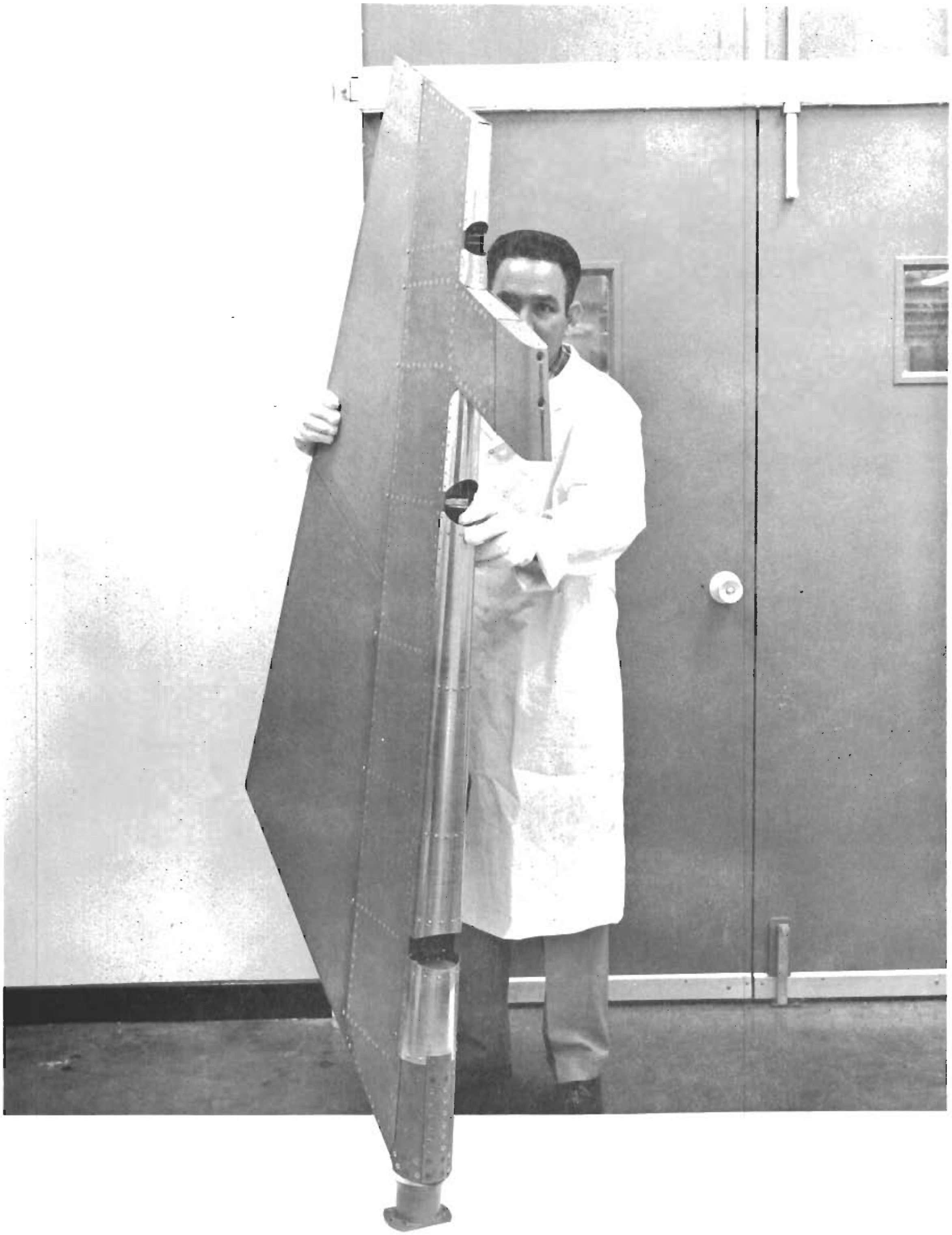

Figure 93 – Completed Beryllium Rudder Assembly

SECTION VI

RUDDER TEST PROGRAM

1. Introduction

The objective of the beryllium rudder ground test program was to substantiate the structural integrity of the rudder assembly and thus to qualify it for flight testing on the F-4 aircraft. Test conditions duplicated as nearly as practical the design loading conditions described in Section III. The tests performed are summarized below in chronological order.

- Test 1 - Fatigue test of the upper balance weight support structure, in which the rudder was subjected to 50,000 cycles of ± 40g's inertial load on the upper balance weight, perpendicular to the symmetry plane of the aircraft. This test was completed with no apparent damage to the beryllium structure.
- Test 2 - Rudder ultimate static test to Condition I loads, in which the rudder was subjected to 150% of the maximum airload, with center of pressure at 30% chord, which produces the maximum torque that the rudder structure can sustain without overpowering the rudder actuator. This test was completed with no apparent damage to the rudder structure.
- Test 3 - Rudder ultimate static test to Condition III loads, in which the rudder and the fin were subjected to 150% of maximum total load on the vertical tail, producing the maximum vertical tail bending and deflections and hence the maximum bending and shear in the rudder due to the compatibility between the rudder and fin structures. This test was completed with no apparent damage to the rudder structure.
- Test 4 - Test 2 above was repeated, with the load allowed to increase beyond the 150% level to provide a direct comparison with the production aluminum rudder which had previously sustained 225% of the

maximum limit load of Test 2. After approximately 205% of the limit load had been applied, a crack occurred at the forward end of the trailing edge lower closure rib. However, the load did not fall off. It was subsequently increased to 250% of the limit and held for 30 seconds, after which the test was discontinued.

The beryllium rudder test program was more stringent than the one undergone by the production aluminum rudder. The successful completion of this test program demonstrated the structural integrity of the rudder and qualified it for eventual flight testing on the parent F-4 aircraft. Following is a description of the tests and a discussion of the test results.

2. Test 1: Fatigue Test of Upper Balance Weight Support Structure

The objective of this test was to demonstrate the structural integrity of the upper balance weight support structure for repeated inertial loading, in accordance with the requirements set forth in Section III. The lower balance weight support structure is identical to that which had already been qualified on the production rudder and, therefore, was not tested. Following is a description of the test set-up and a discussion of the test results.

2.1 Test Set-Up - The set-up for the fatigue test of the beryllium rudder is shown in Figure 94. The rudder was installed in a vertical fin - aft fuselage assembly, with the fin in a horizontal position. Rudder hinge points were connected as in a normal service installation. The fuselage section was bolted to a fixed support at its forward end (fuselage station 515.00). A torsion spring bolted to a support fixture was connected to the control horn attachment of the rudder, as shown in Figure 95, to simulate the actuator back-up stiffness. A large exciter (Model C-10, MC Electronics Co.) was connected by a loading link to the balance weight. The connection was made by bolting through a 1/4 in. (6.35 mm) hole drilled through the balance weight's center of gravity. To reduce inertial loads in the fin, it was restrained during the test with lead weights and a link attached to the tip of the fin and the platform supporting the exciter. The tension pads shown in Figure 94 had been installed for subsequent use in static testing the rudder, but were not used in the fatigue test.

The test load was measured by a 500 lbs. (2224 N) capacity force gage (Model 2103, Endevco Corp.) attached to the loading link and monitored on a voltmeter (Model 320, Balantine Laboratories, Inc.). In addition, an accelerometer (Model 2235C, Endevco Corp.) and a vibration pickup with meter (Models 115 and

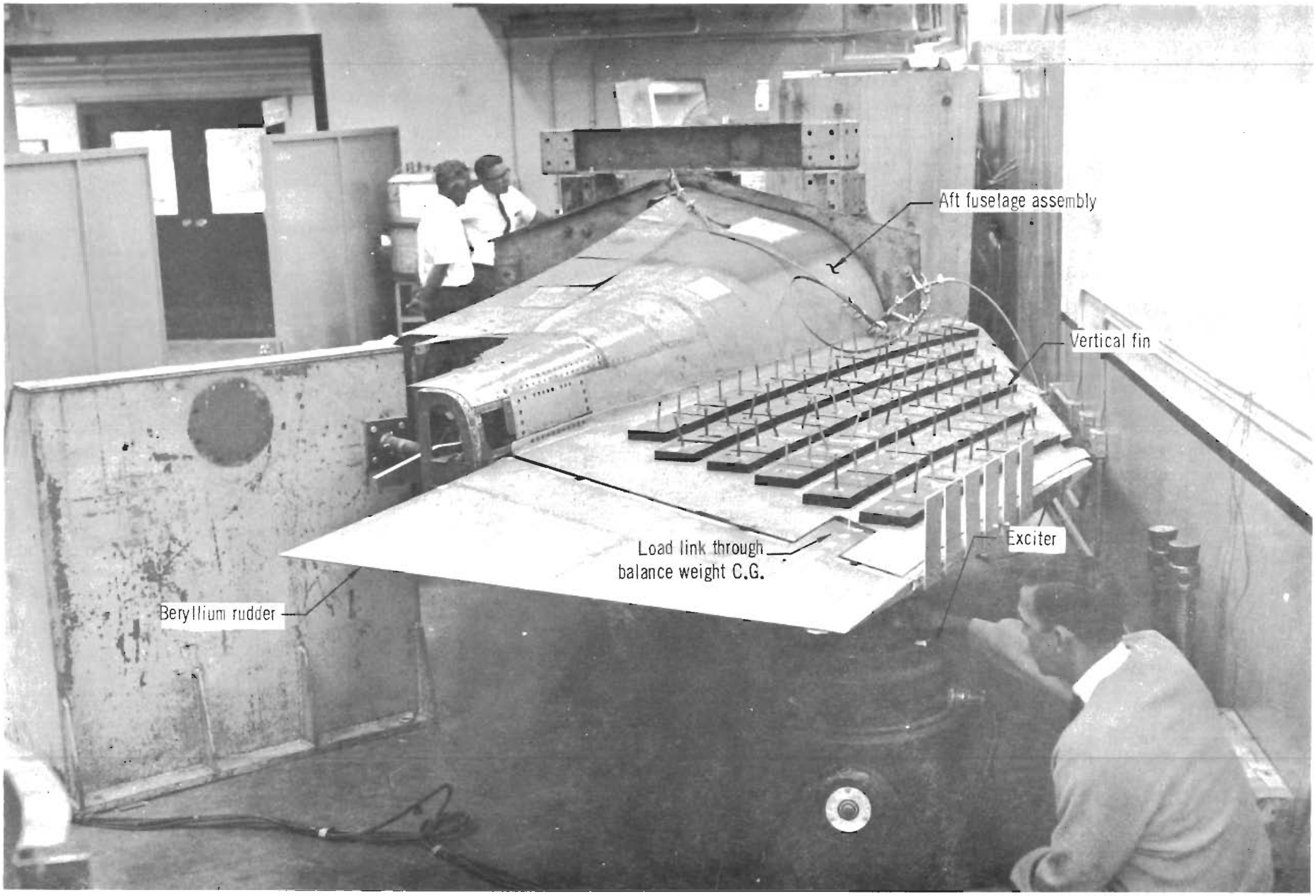
Aft fuselage assembly
Vertical fin
Exciter
Load link through balance weight C.G.
Beryllium rudder

Figure 94 – Set-Up for Balance Weight Support Structure Fatigue Test

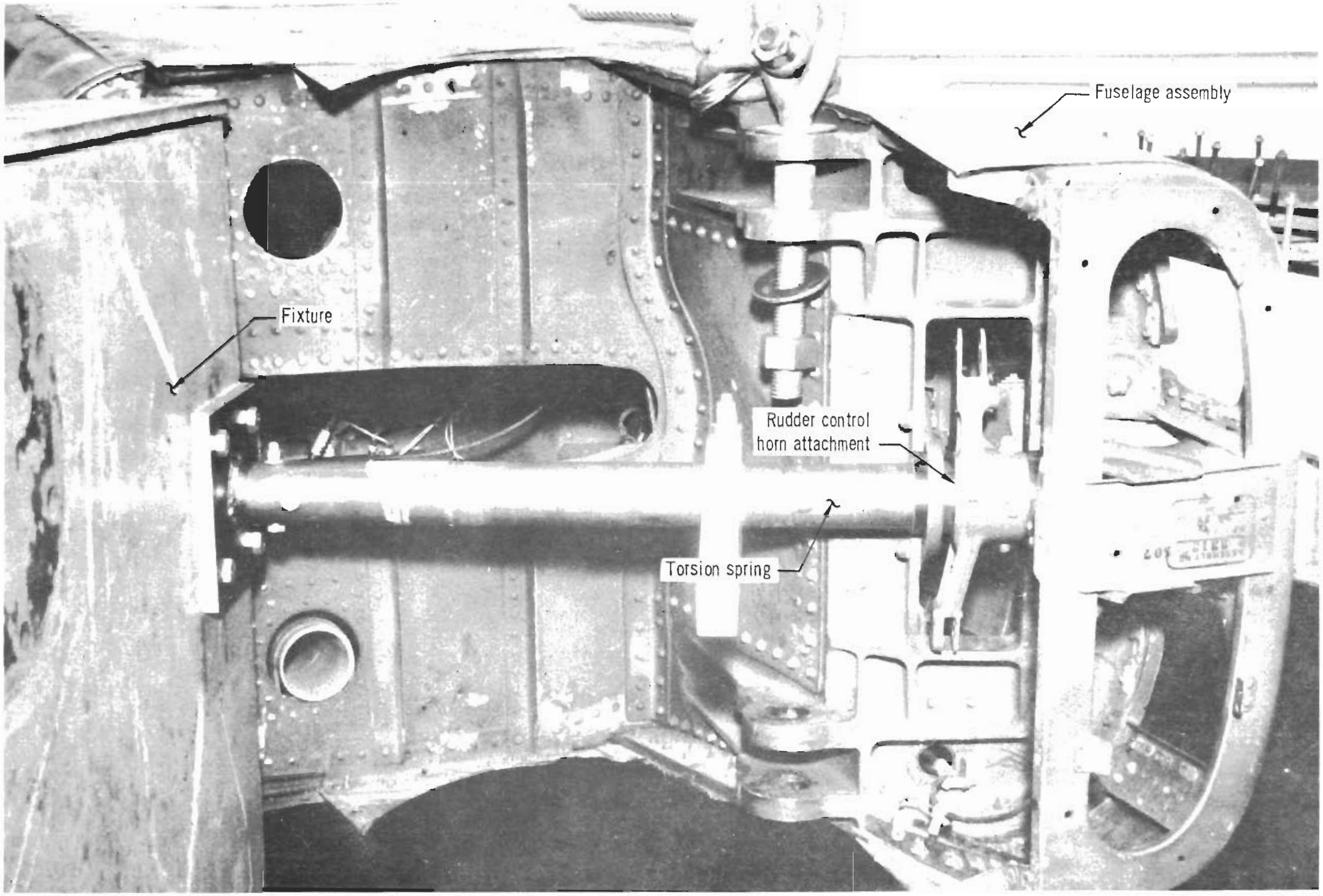
Fuselage assembly
Fixture
Rudder control horn attachment
Torsion spring

Figure 95 – Torsion Spring Installation

M-6, respectively, MB Electronics Co.) were used intermittently during the test to measure the deflection, acceleration and velocity at various positions on the rudder structure. These readings were correlated with the loading frequency to provide a check on the input load.

2.2 Test Procedure and Results - In this test, a 5-cps (Hz) sinusoidal force perpendicular to the symmetry plane of the aircraft and equal to a 40 g's peak load was imparted to the rudder structure at the balance weight center of gravity. This force was applied for 50,000 cycles and was equal to 40 times 8.87 lbs. (4.02 kg) of balance weight; force = 355 lbs. (1579 N). The counter for recording the number of cycles was not activated until this peak load was reached as indicated by the force gage.

A loud sharp noise was heard at 28,275 cycles, and testing was immediately halted. Examination showed the rudder structure to be unharmed, but a rivet failure had occurred. The rivet was one of four aluminum Hi-Shear fasteners used to attach the hinge fitting at station Z_R = 122.72 to the rudder spar flanges (refer to Figure 12, Section III, for hinge location). Figure 96 shows the failed rivet which had fractured at a section in the collar retention groove and also had microscopic cracks in the head-to-shank filler radius. The failure probably resulted from the prying action of the test load which was reacted at that hinge. The failed rivet was replaced with a steel Hi Lok threaded fastener and testing was continued; the other three Hi Shear rivets at this hinge were similarly replaced after the test was completed. The required 50,000 cycles were attained with no further incident. A post-test inspection did not reveal any damage to the beryllium rudder assenbly.

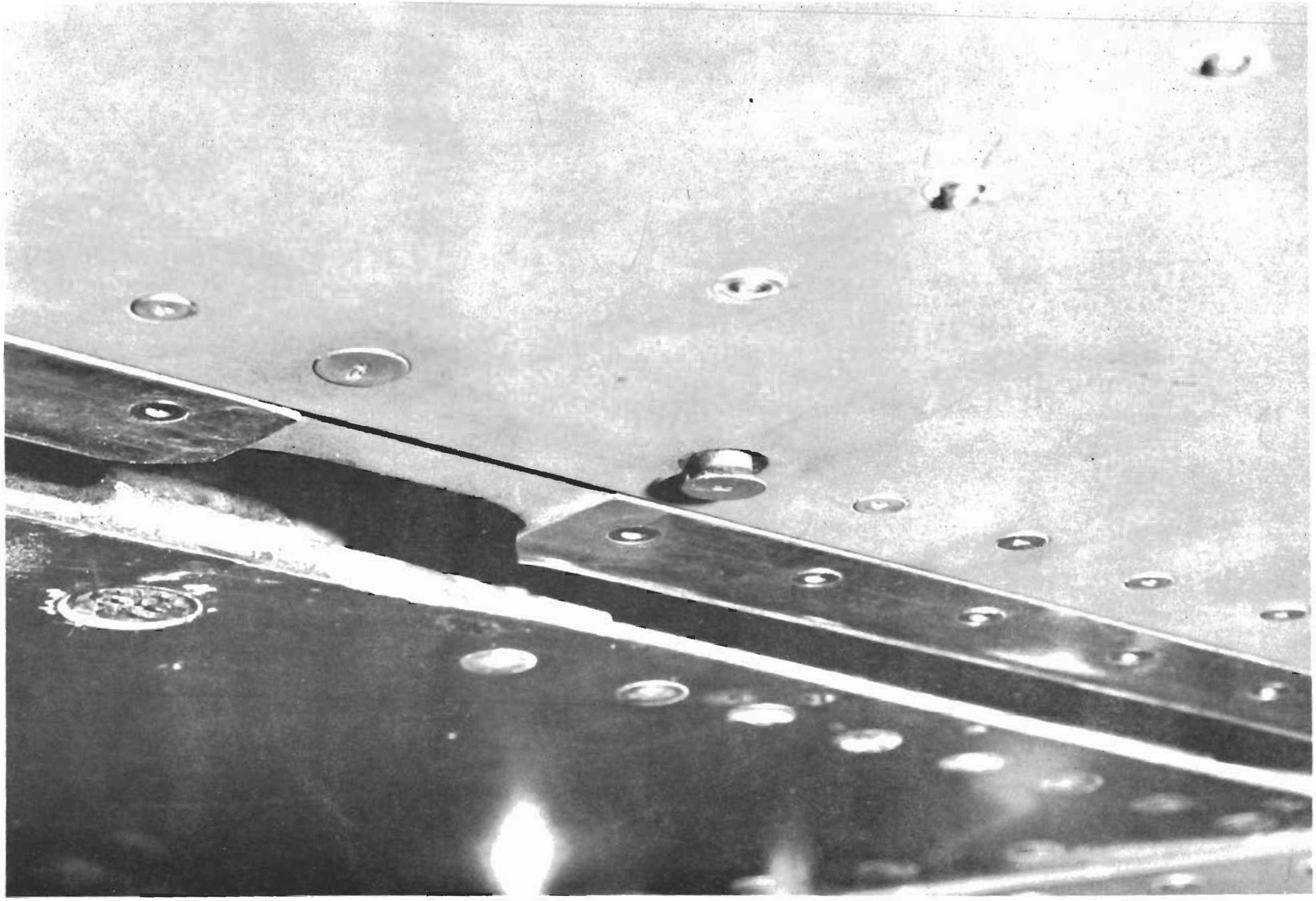

Figure 96 – Rivet Failure During Fatigue Test

3. Test 2: Rudder Ultimate Static Test With Maximum Airload at 30% Chord

The objective of this test was to demonstrate the structural integrity of the rudder structure under airloads producing the full available actuator hinge moment with the airloads center of pressure at 30% chord. The test loads simulated the loads of Design Condition I, described in Section III, and were carried to ultimate (150% of limit). Following is a description of the test set-up and a ciscussion of the test results.

3.1 Test Set-Up - The test set-up is shown in Figure 97. The rudder was installed in a vertical fin - aft fuselage assembly with the tail in a horizontal position. Rudder hinge points were connected as in a normal service installation. The aft fuselage assembly was cantilevered from a fixture, shown in Figure 98, at Fuselage Station 515.00. A fixed length jig assembly simulating the actuator was installed between the rudder and fuselage to maintain the rudder in neutral position during the test.

Neoprene rubber tension pads for applying test loads were bonded to the upper surface of the rudder using EC1300 adhesive (Minnesota Mining and Manufacturing). The rudder, with the tension pads installed, is shown in Figure 99. The pads were linked through a whiffletree loading system to a hydraulic actuator. Loads were controlled by load programmers (made by Research, Inc.) through a calibrated strain link - feedback system. Only the rudder was loaded in this test; the separate tension pad - whiffletree loading system for the fin, shown in Figure 97, was used in Test 3.

Strain gages (Baldwin - Lima - Hamilton, AD-13) were bonded to the rudder at the locations shown schematically in Figure 100. Deflection indicators (rotary potentiometers) were placed on the underside of the rudder at the locations shown schematically in Figure 101. These deflection indicators installed

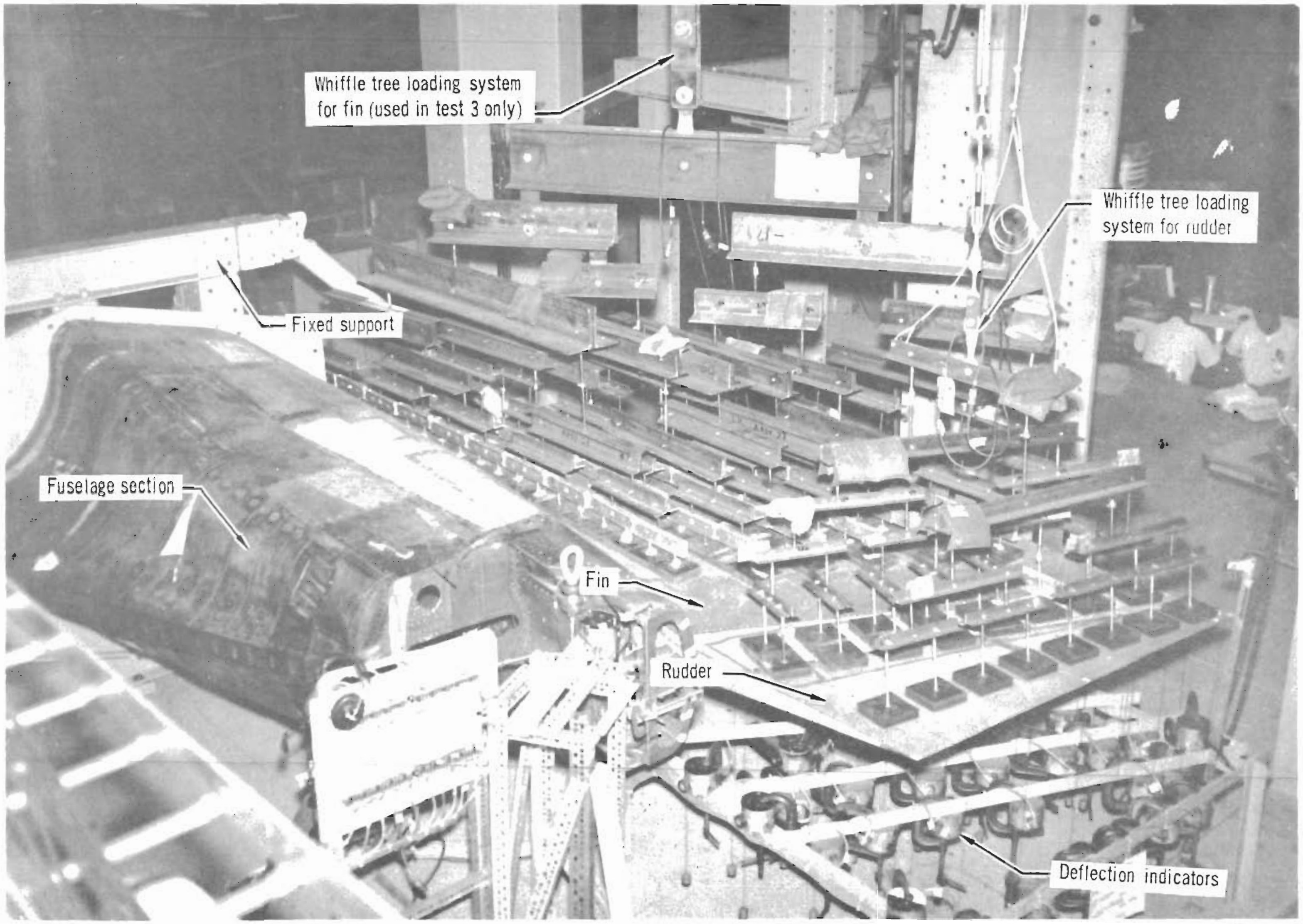
Whiffle tree loading system for fin (used in test 3 only)
Whiffle tree loading system for rudder
Fixed support
Fuselage section
Fin
Rudder
Deflection indicators

Figure 97 – Set-Up for Static Tests of Beryllium Rudder

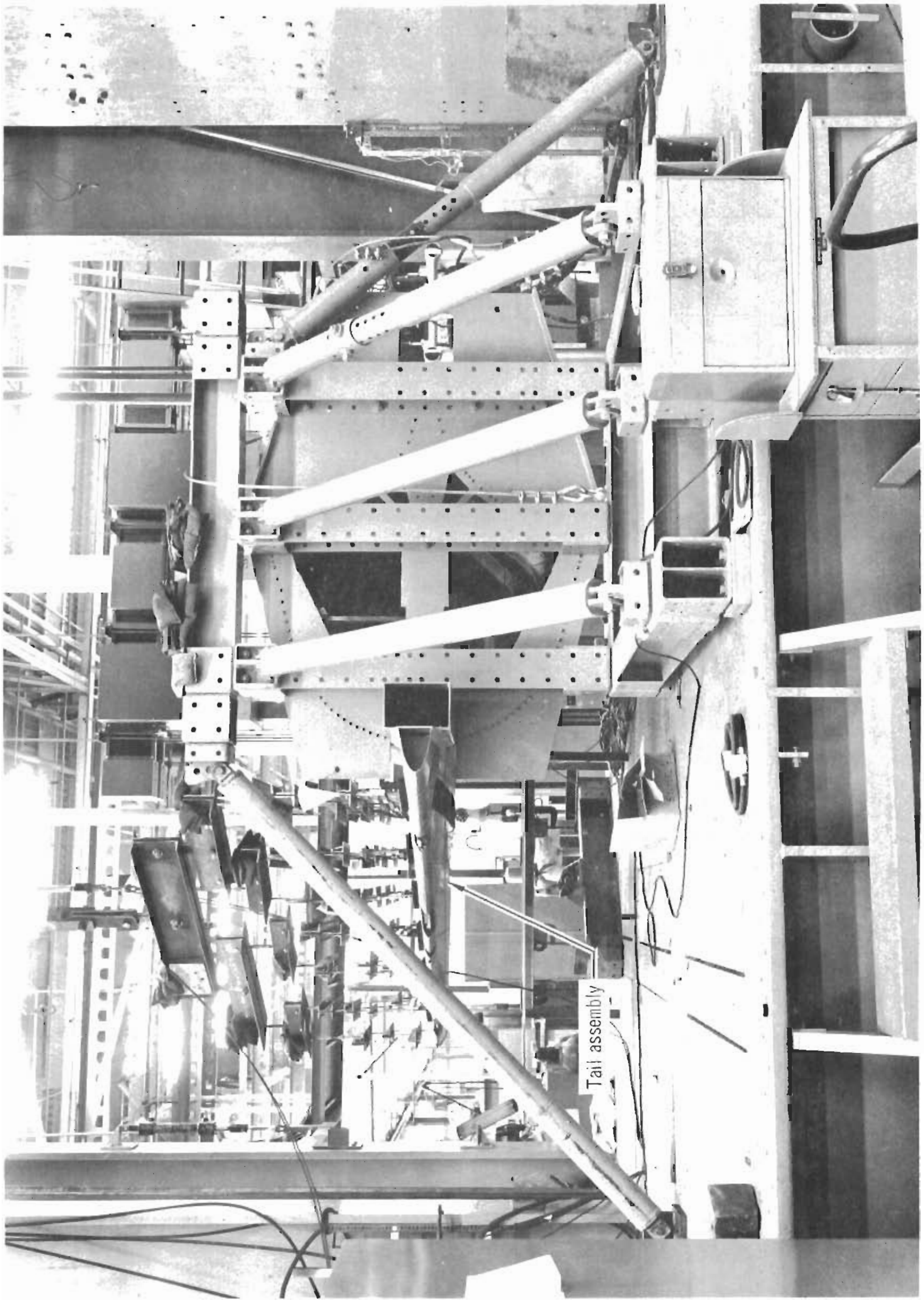
Tail assembly

Figure 98 – Aft Fuselage Support Fixture for Beryllium Rudder Static Tests

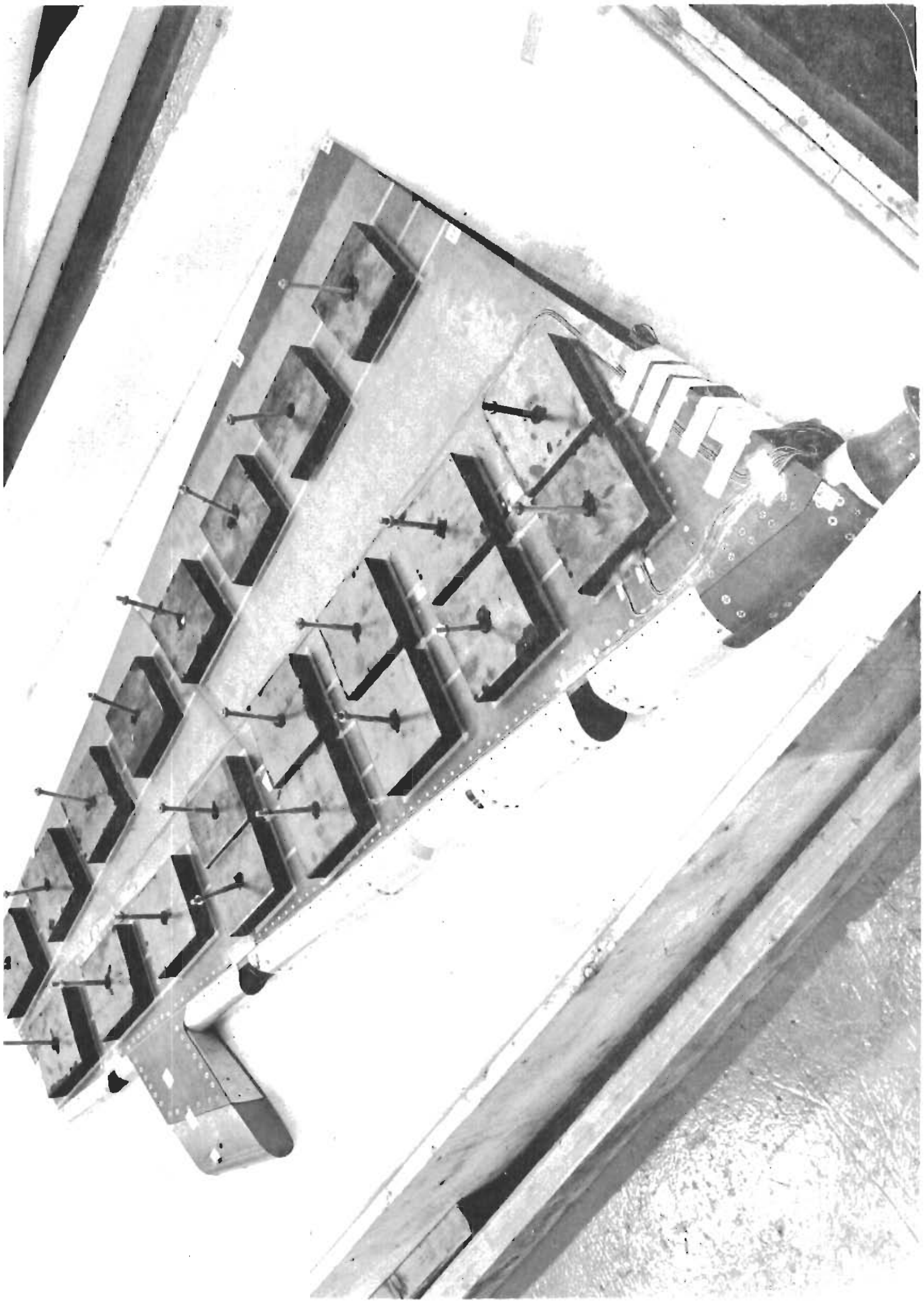

Figure 99 – Beryllium Rudder With Tension Pads Installed

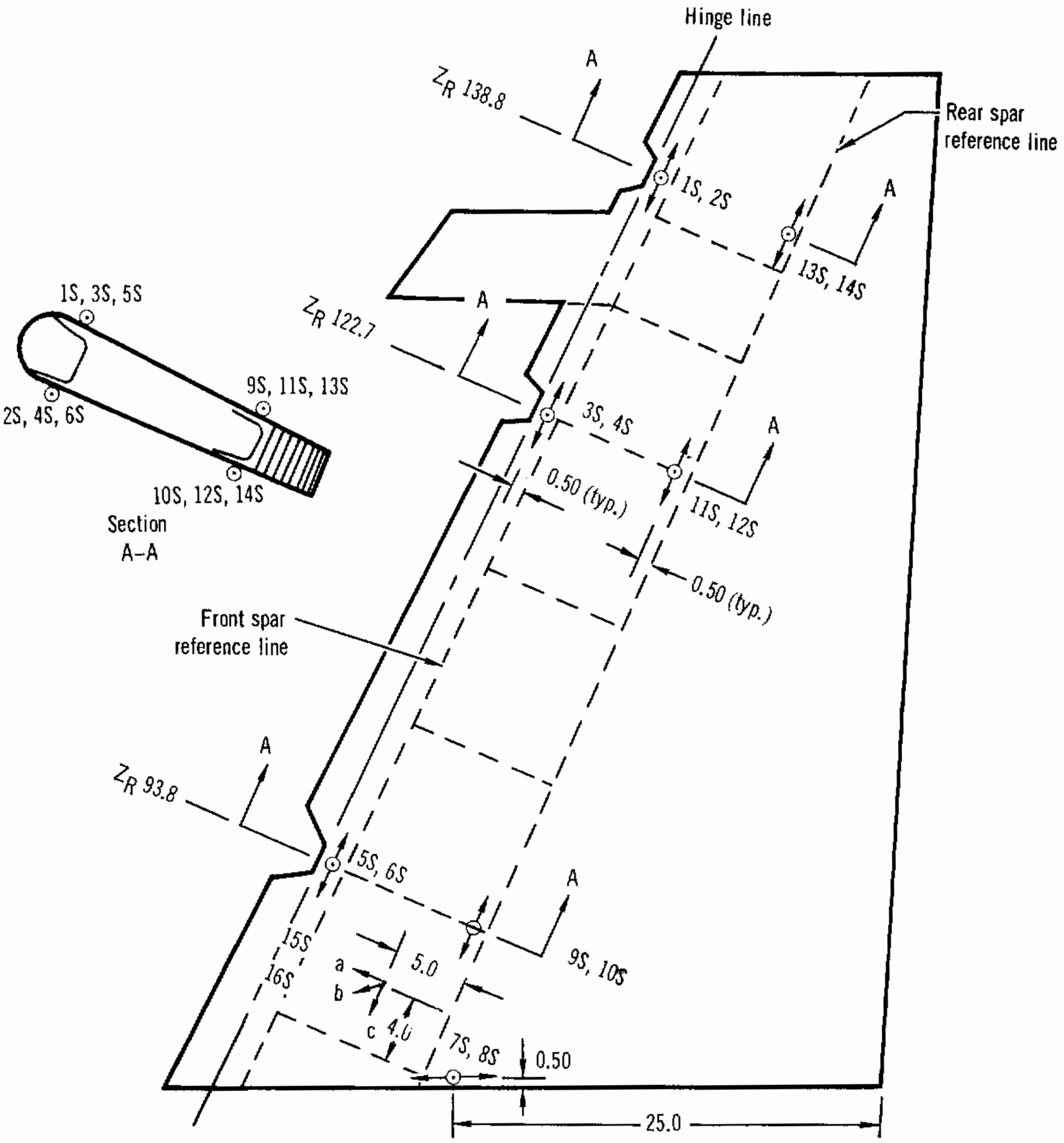
Hinge line
A
Z_R 138.8
Rear spar reference line
1S, 2S
A
13S, 14S
1S, 3S, 5S
A
Z_R 122.7
9S, 11S, 13S
2S, 4S, 6S
3S, 4S
A
0.50 (typ.)
11S, 12S
10S, 12S, 14S
Section A–A
0.50 (typ.)
Front spar reference line
A
Z_R 93.8
5S, 6S
A
15S
16S
a
b
c
5.0
4.0
9S, 10S
7S, 8S
0.50
25.0

Notes: 1. Instrumentation installed on both sides of rudder at locations indicated.

2. —⊙— indicates axis of strain gages.

↗ indicates strain rosette.

3. All instrumentation installed on rudder external surfaces.

Figure 100 – Beryllium Rudder Strain Gage Locations

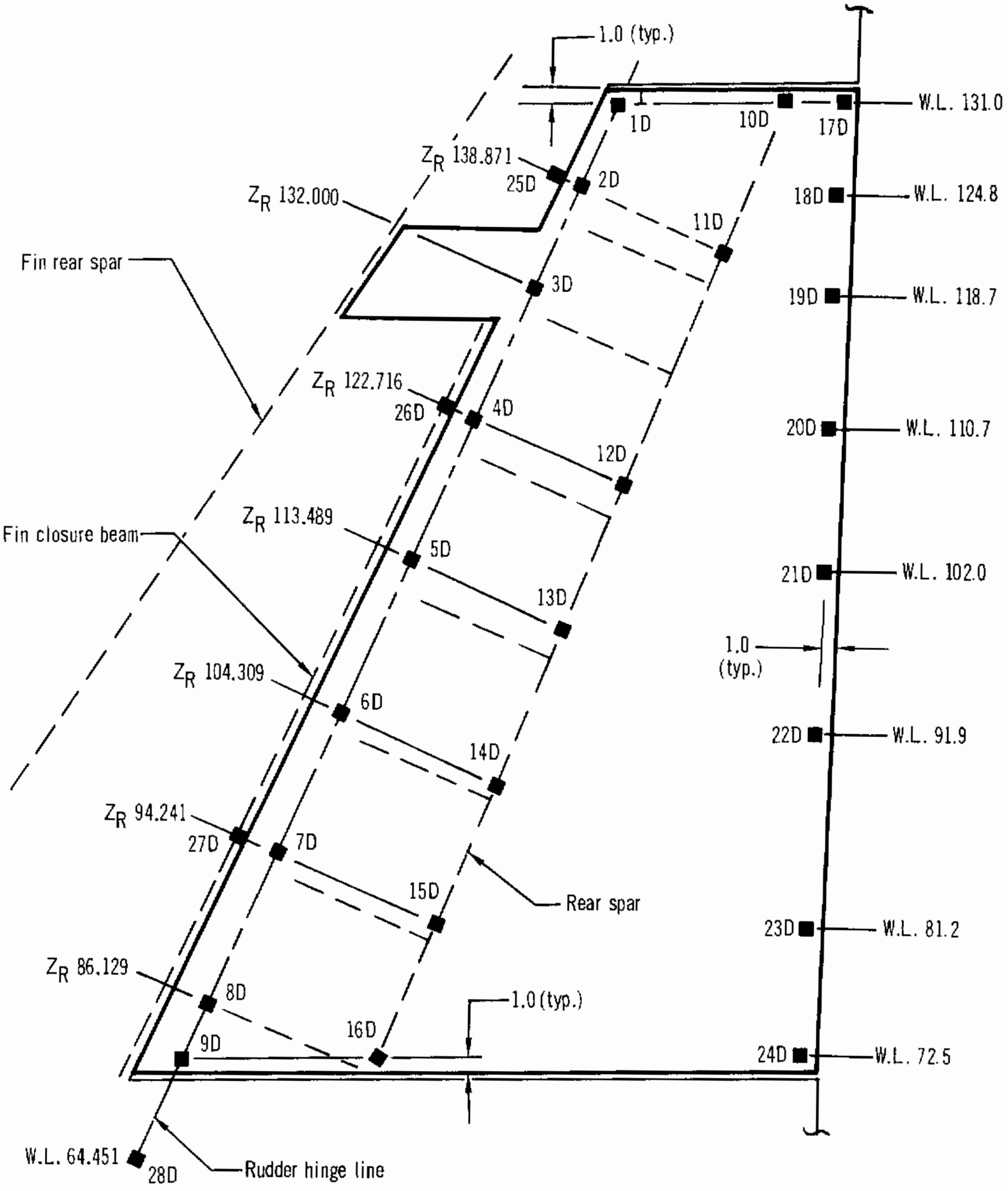
1.0 (typ.)
W.L. 131.0
1D
10D
17D
Z_R 138.871
25D
2D
18D
W.L. 124.8
Z_R 132.000
11D
Fin rear spar
3D
19D
W.L. 118.7
Z_R 122.716
26D
4D
20D
W.L. 110.7
12D
Z_R 113.489
5D
Fin closure beam
21D
W.L. 102.0
13D
1.0
(typ.)
Z_R 104.309
6D
22D
W.L. 91.9
14D
Z_R 94.241
27D
7D
15D
Rear spar
23D
W.L. 81.2
Z_R 86.129
8D
1.0 (typ.)
16D
9D
24D
W.L. 72.5
W.L. 64.451
28D
Rudder hinge line

Figure 101 – Beryllium Rudder Deflection Point Locations

on the rudder are shown in Figure 97. Test data was recorded with the McDonnell Central Data Acquisition System. Strain gage and deflection instrumentation were the same for all static tests.

3.2 Test Procedure and Results - Test loads, simulating rudder airloads, were applied to the tension pads at a maximum rate of 20% of limit load per 30 seconds, in increments of 20% of limit load, up to limit load. From limit to ultimate load, loads were applied in increments of 10% of limit load. Loads were held constant for approximately 30 seconds after each load increment. Figure 102 shows a schematic of the tension pad layout and the maximum loads applied to the rudder in Test 2. Figure 102 presents a comparison of test and design loads for Condition I.

The strain data recorded during the test are shown in Figures 104 through 106. As shown, loads were first applied up to their limit value, then reduced to 20% of limit, and finally increased to 150% of limit (ultimate). As expected, the spanwise spar cap strains are relatively low; the maximum recorded value is 290×10^{-6} in./in. (equivalent to a stress of approximately 12 ksi (83 MN/m^2). The maximum stresses for this loading condition occur in the trailing edge cover skins as a result of the airloads being carried forward to the rudder front torque box and in the drive ribs where the rudder torque is transferred to the torque tube.

Deflection data are presented in Figures 107 through 110. Figure 111 presents a schematic of the rudder with deflections at 150% of design limit load. There was no damage to the rudder during Test 2.

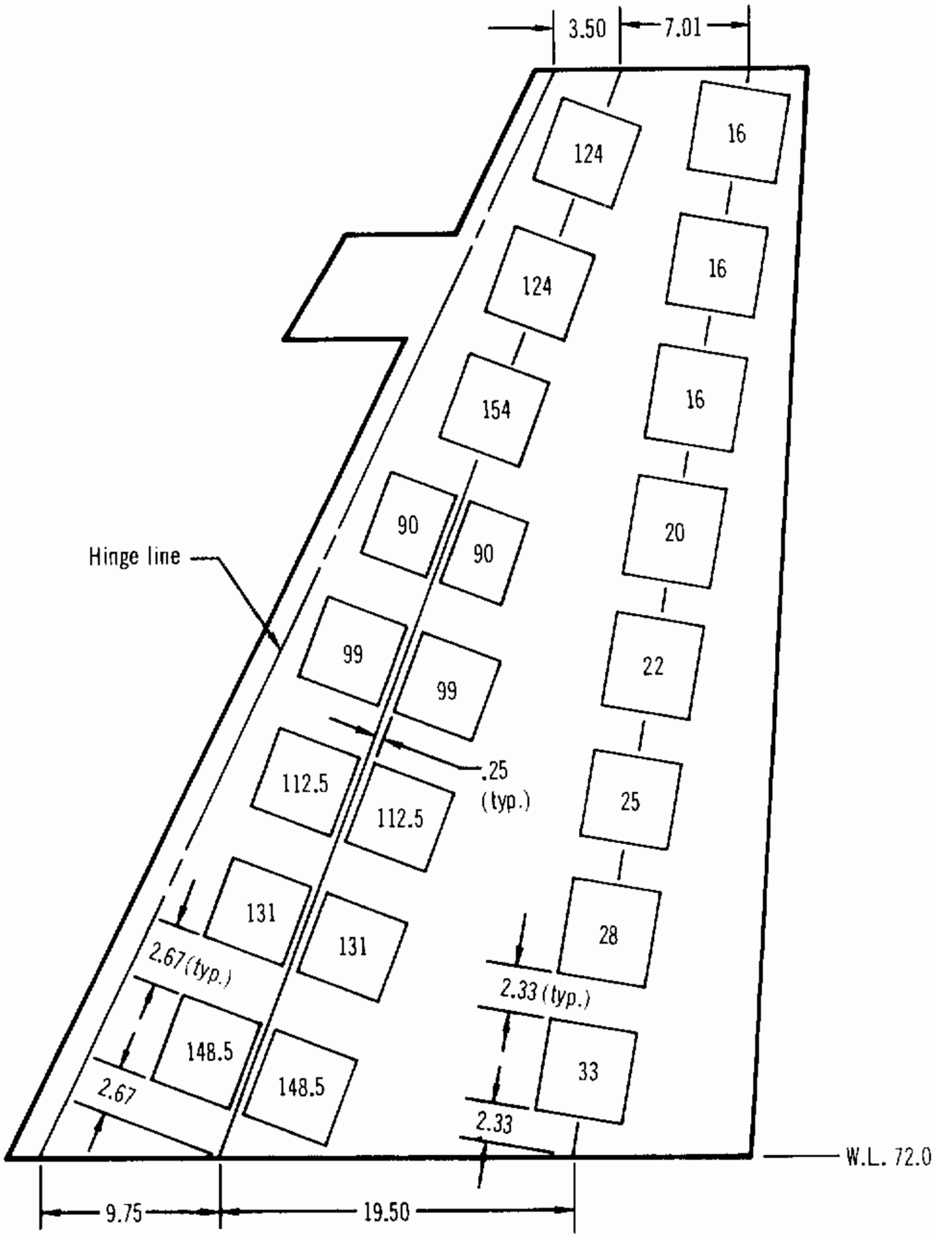
3.50
7.01
124
16
124
16
154
16
90
20
Hinge line
90
99
22
99
.25
(typ.)
112.5
25
112.5
131
28
131
2.67 (typ.)
2.33 (typ.)
148.5
33
148.5
2.67
2.33
W.L. 72.0
9.75
19.50

Notes: 1. ☐ indicates tension pad and load in pounds.

2. All tension pads were 5 inches x 5 inches except two pads with 90 lb. loads. These pads were 4 inches x 5 inches.

3. Ultimate load = 1,740 lbs. Ultimate hinge moment = 13,500 in.-lbs. Center of pressure at 30% chord.

Figure 102 – Rudder Tension Pad Layout and Ultimate Loads for Test 2

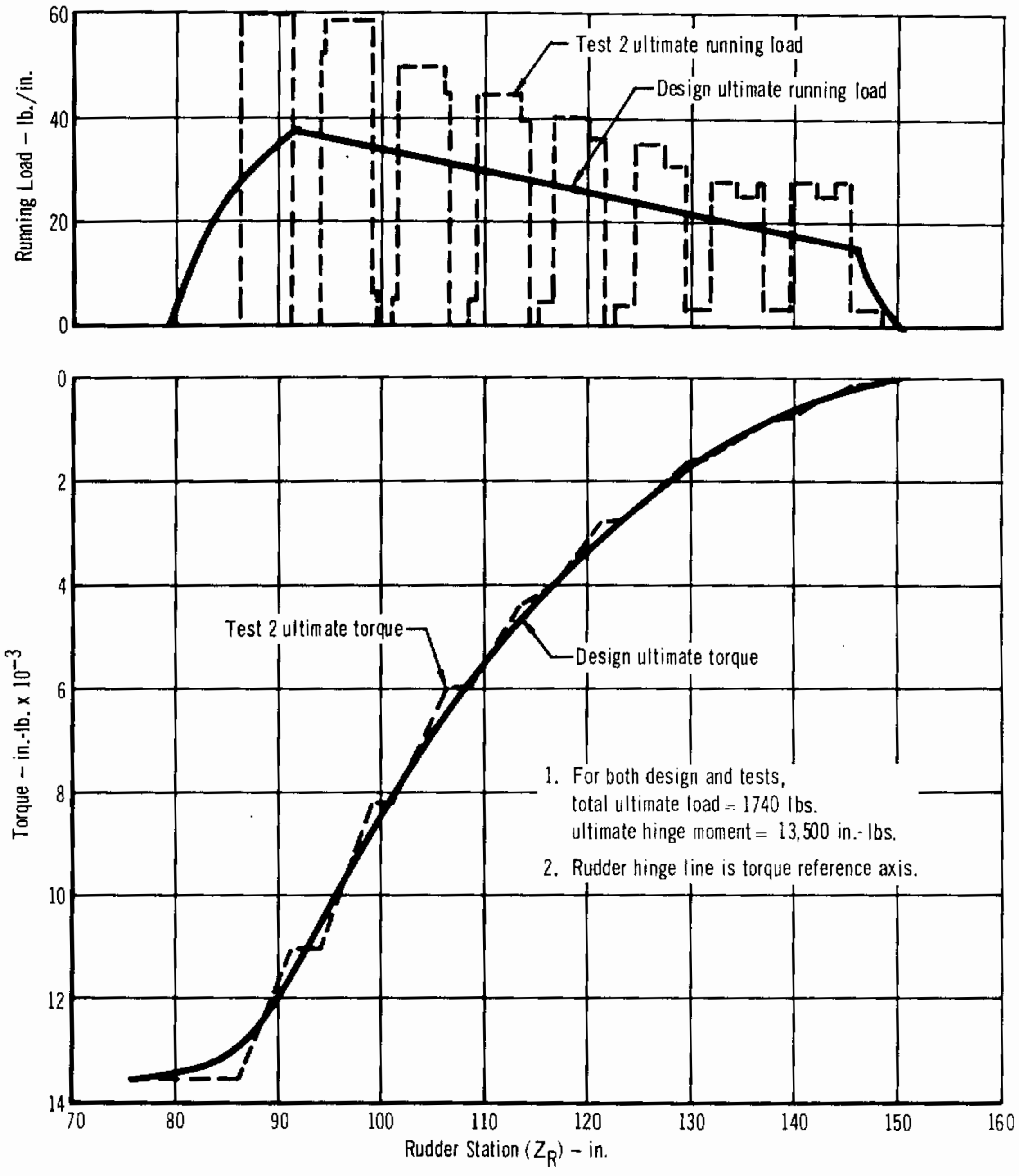

1. For both design and tests,
   total ultimate load = 1740 lbs.
   ultimate hinge moment = 13,500 in.-lbs.
2. Rudder hinge line is torque reference axis.

Figure 103 – Comparison of Test and Design Loads: Design Condition I

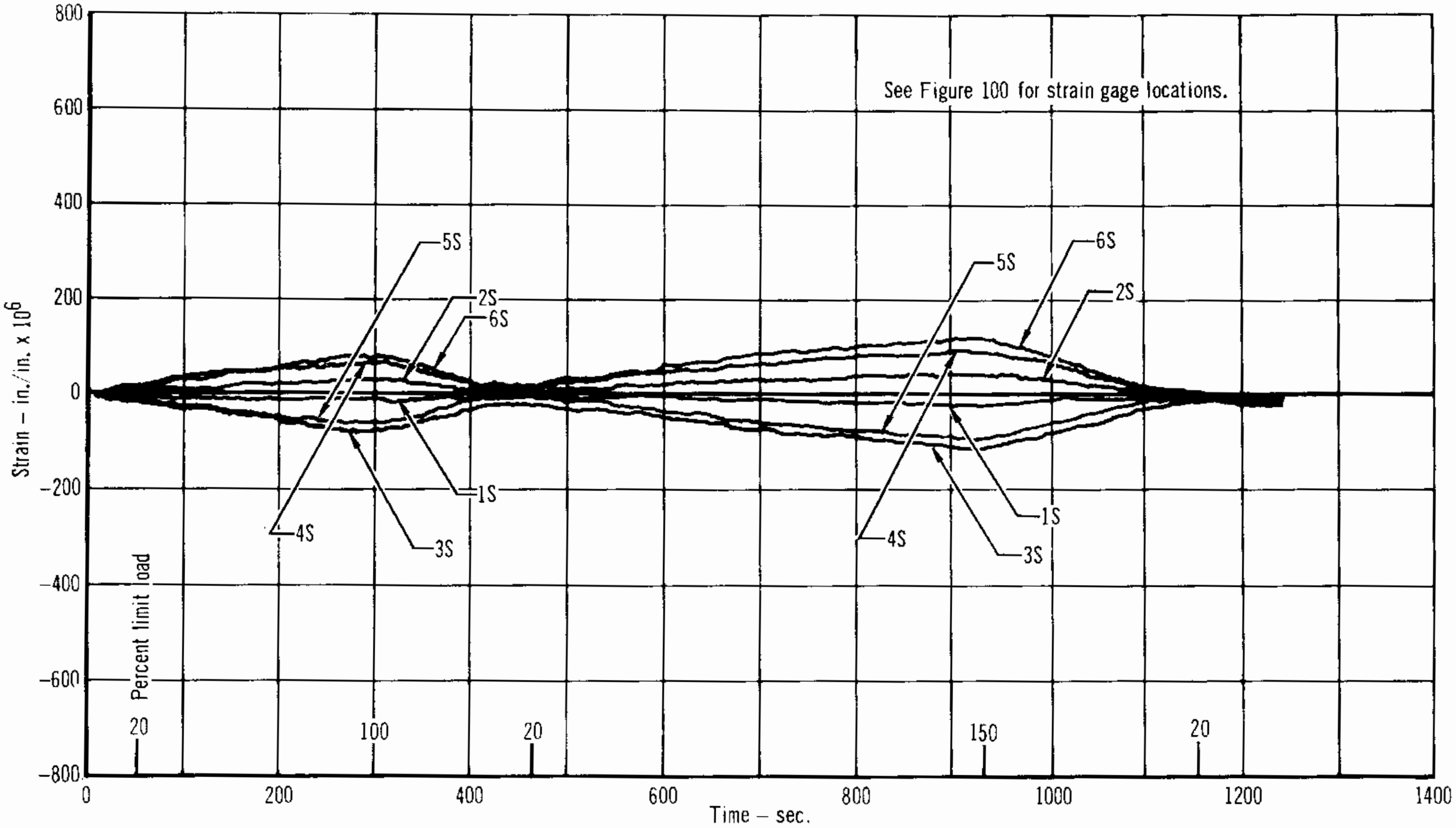

Figure 104 – Front Spar Strains: Test 2

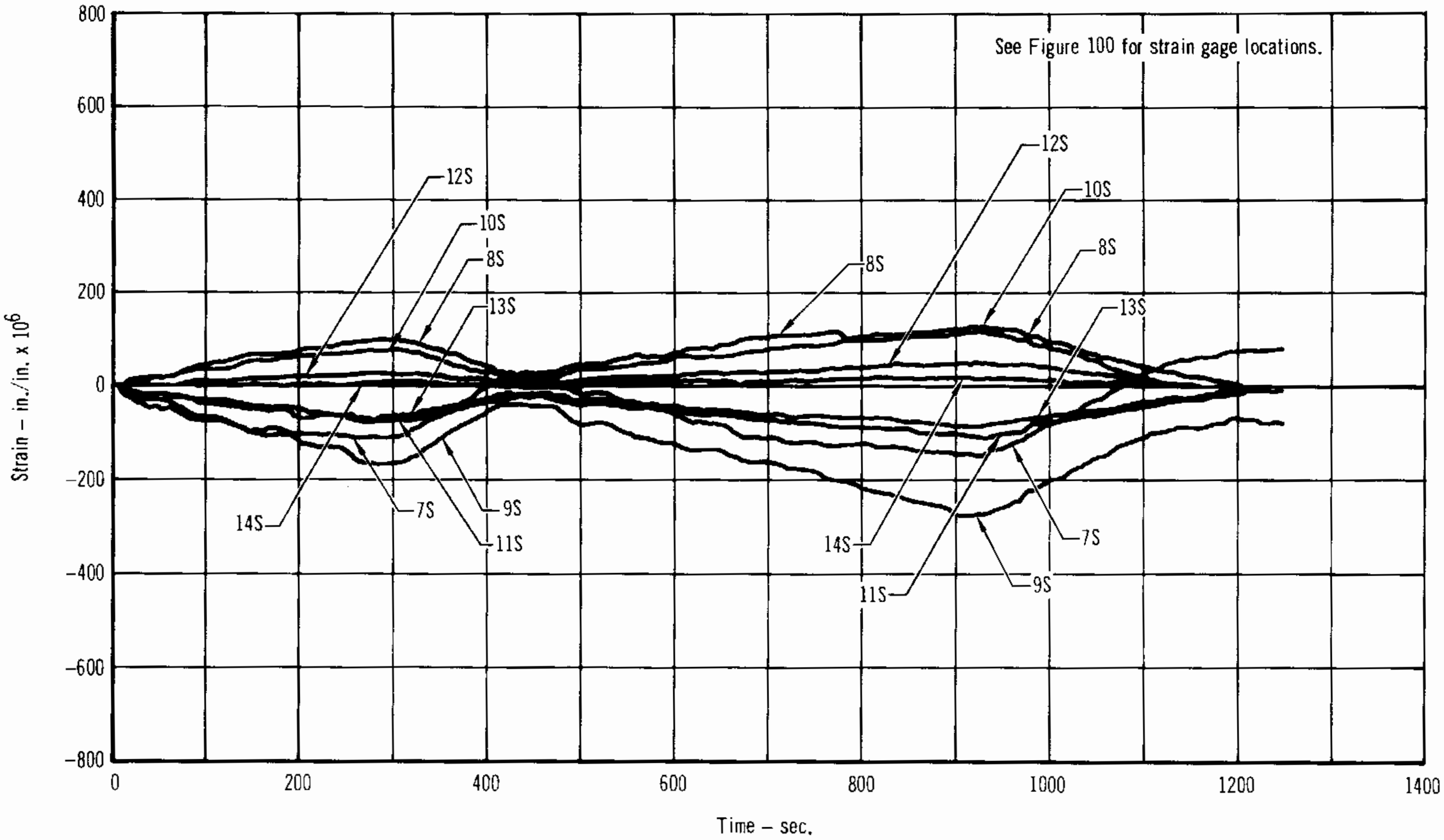

Figure 105 – Rear Spar and Trailing Edge Strains: Test 2

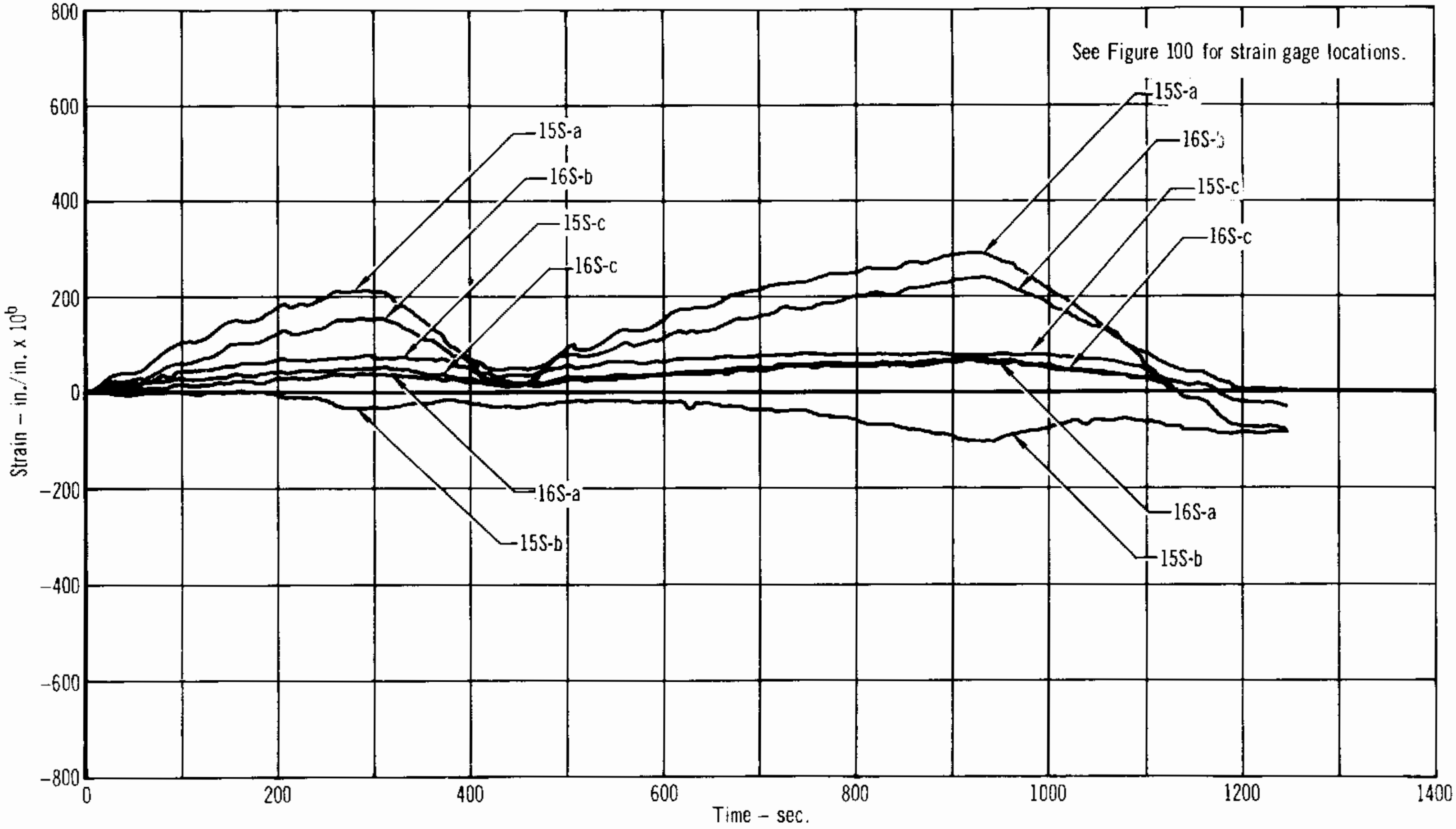

Figure 106 – Forward Cover Skin Strains: Test 2

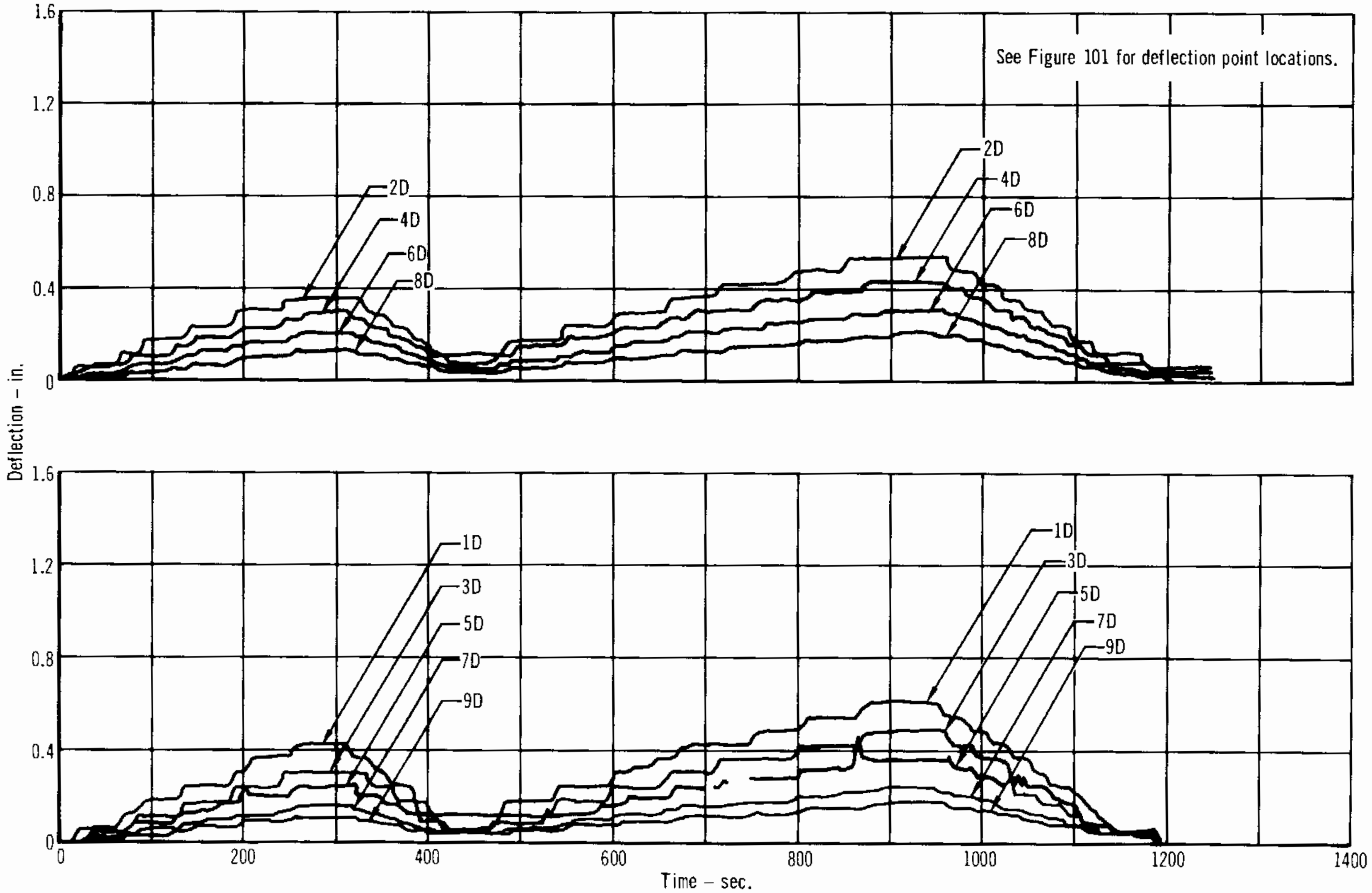

Figure 107 – Front Spar Deflections: Test 2

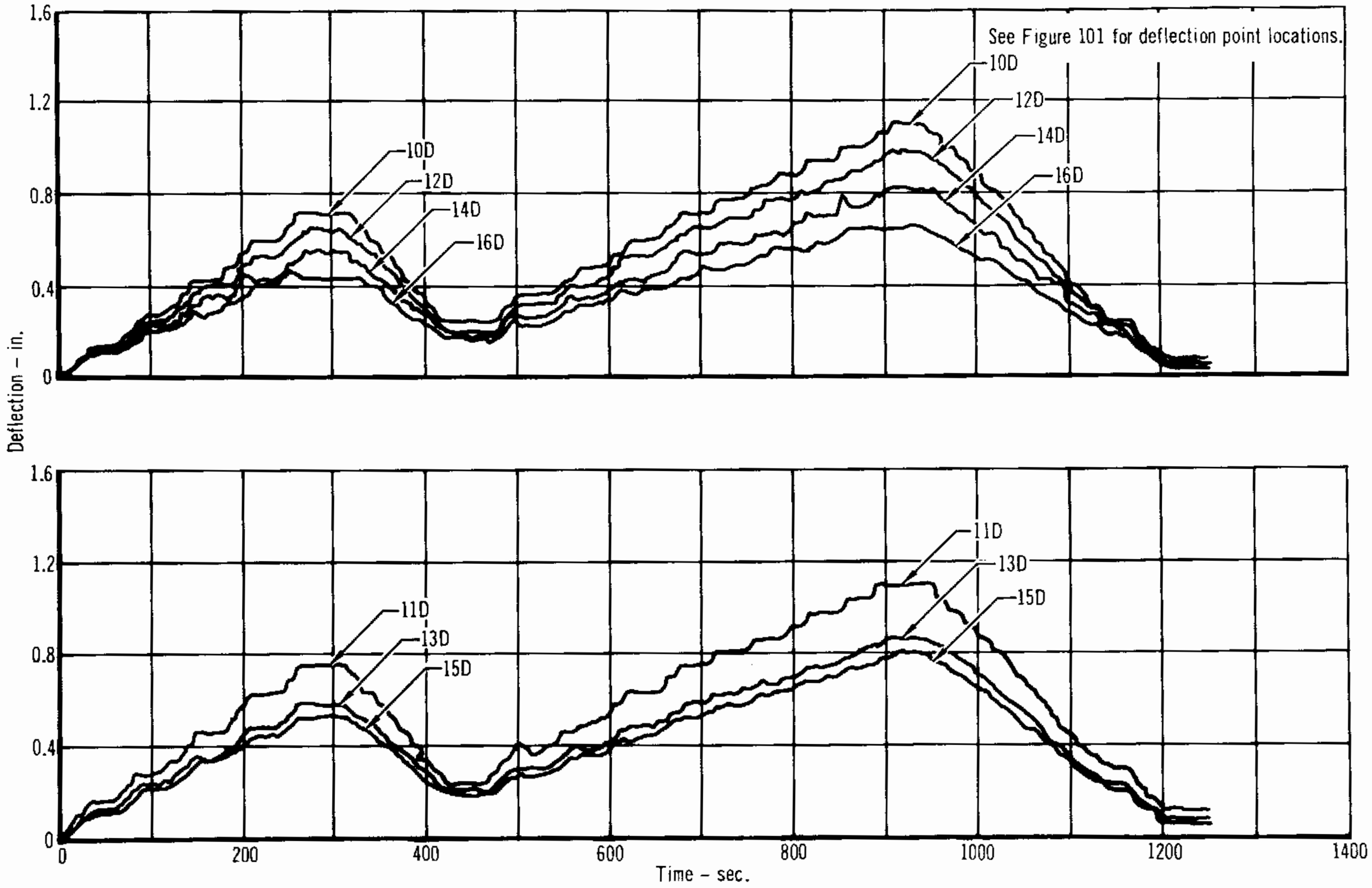

Figure 108 – Rear Spar Deflections: Test 2

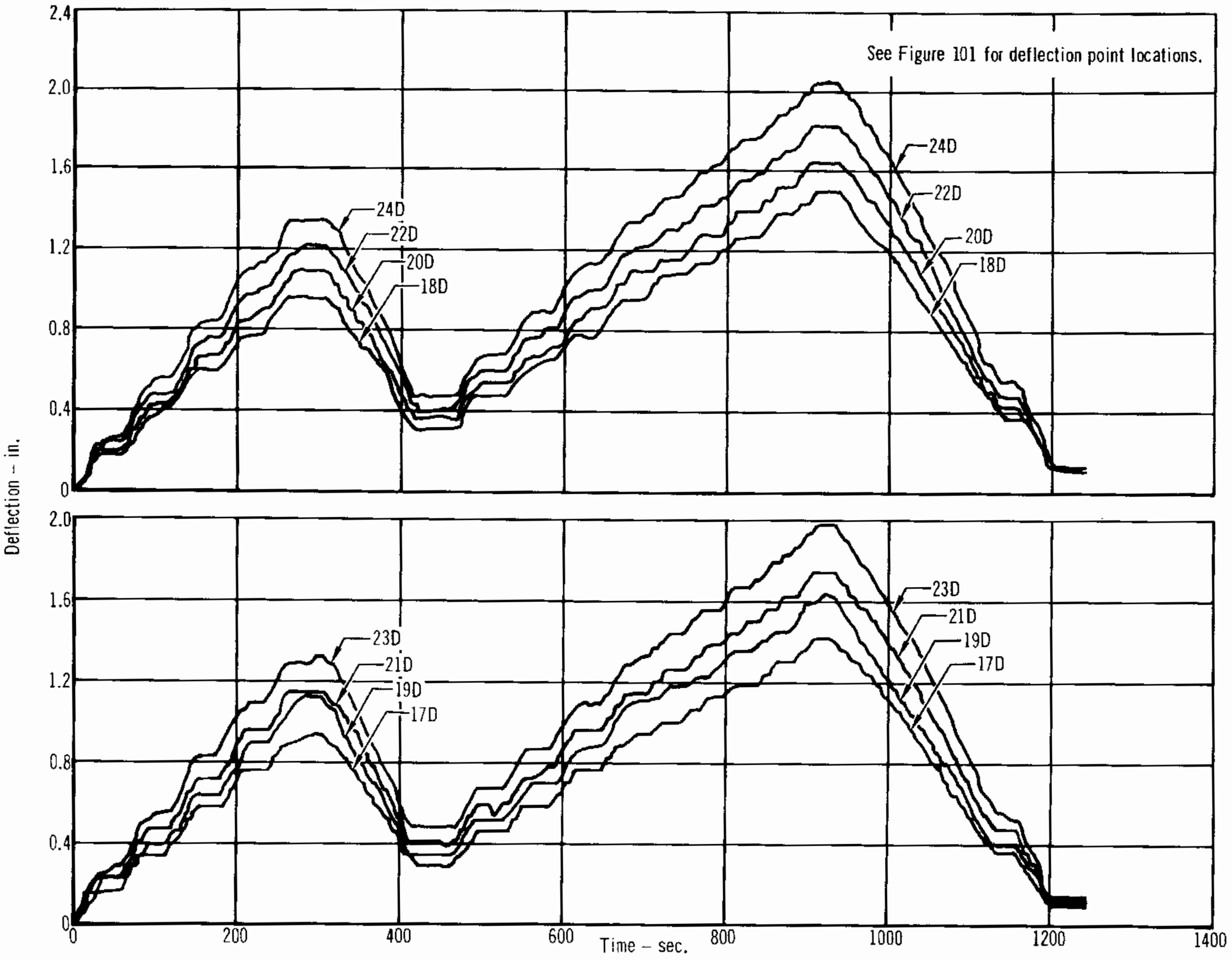

Figure 109 – Trailing Edge Deflections: Test 2

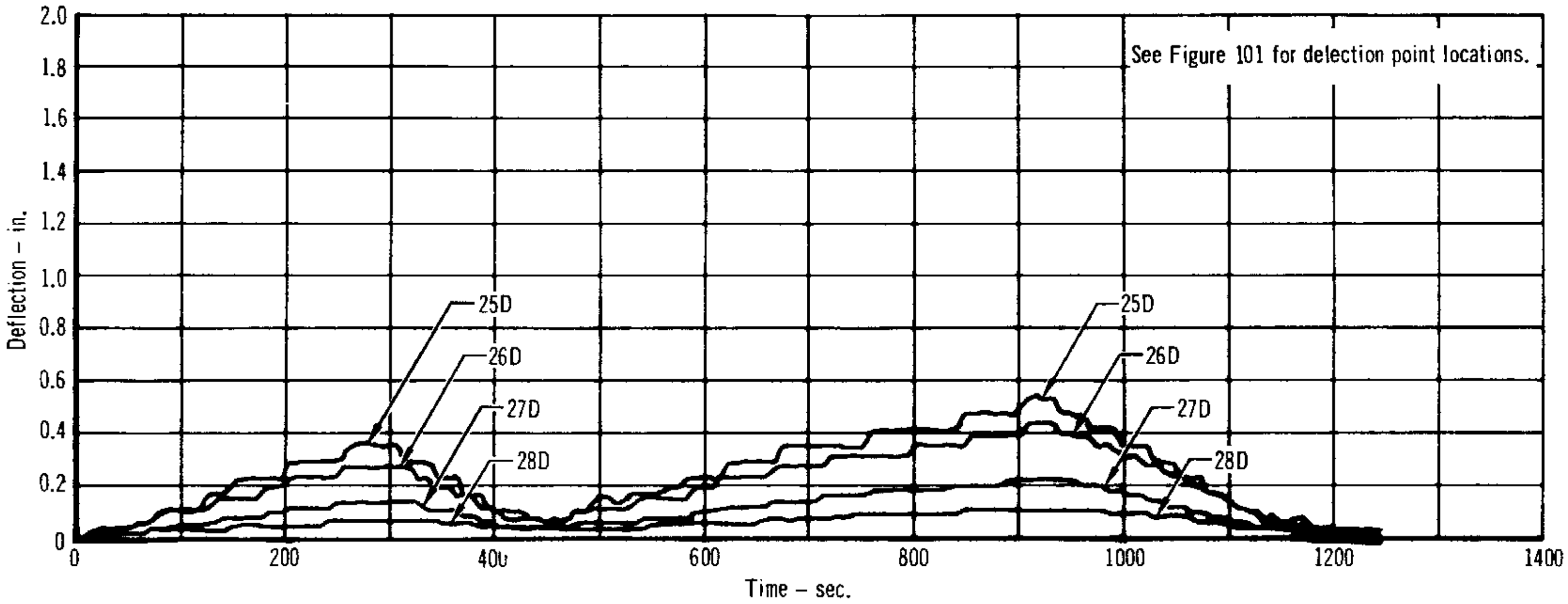

See Figure 101 for delection point locations.

Figure 110 – Hinge Deflections: Test 2

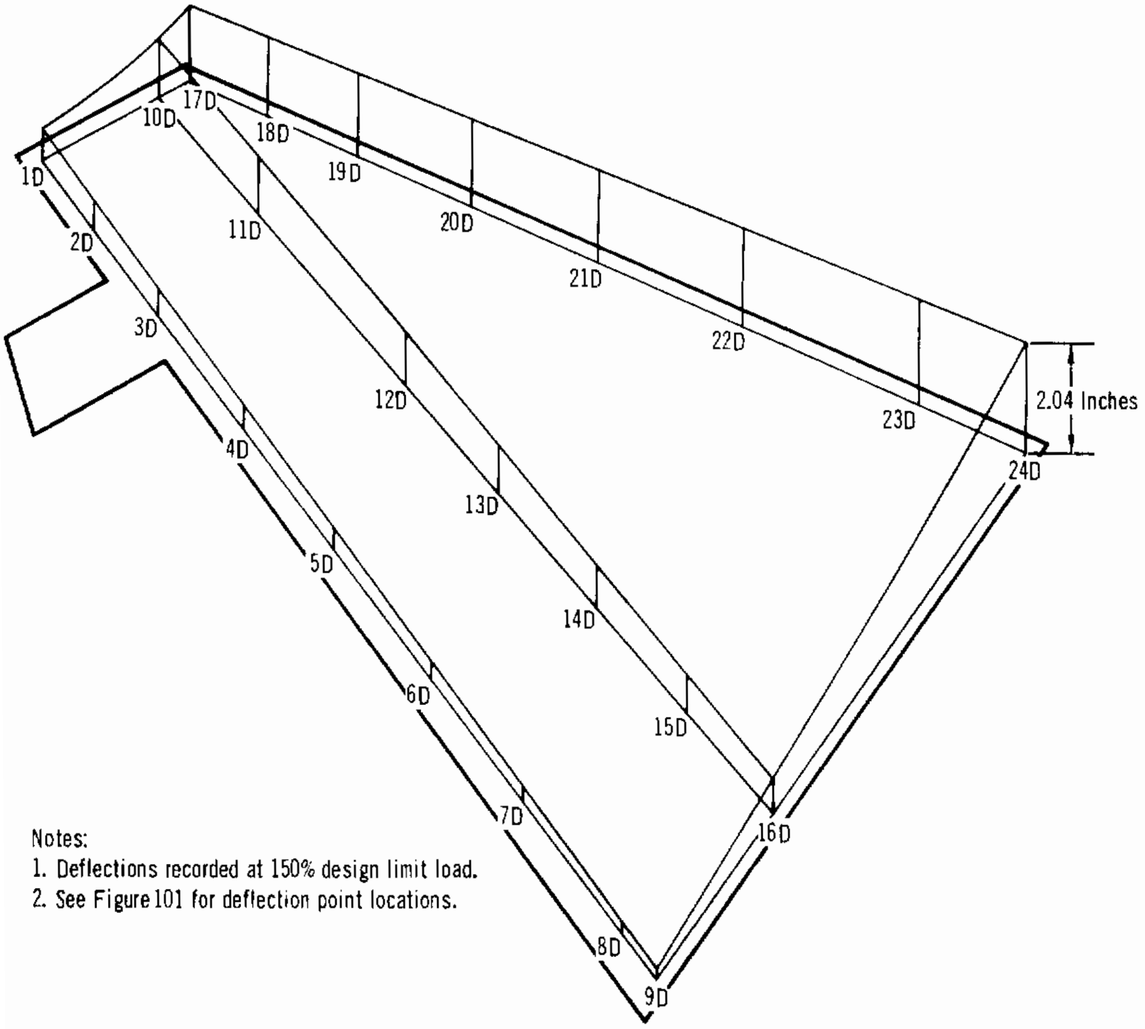
1D
2D
3D
4D
5D
6D
7D
8D
9D
10D
11D
12D
13D
14D
15D
16D
17D
18D
19D
20D
21D
22D
23D
24D
2.04 Inches

Notes:
1. Deflections recorded at 150% design limit load.
2. See Figure 101 for deflection point locations.

Figure 111 – Rudder Deflections: Design Condition I

4. Test 3: Rudder Ultimate Static Test With Maximum Loading on Vertical Tail

The objective of this test was to demonstrate the structural integrity of the rudder assembly for the maximum loading developed on the aircraft vertical tail during rooling pull-out maneuvers. The test loads simulated the load of Design Condition III, described in Section III, and were carried to ultimate.

4.1 Test Set-up - The set-up for this test is shown in Figure 97. The rudder was installed in a vertical fin - aft fuselage assembly with hinge points connected as in a normal service installation. The fuselage assembly was cantilevered from a fixture, at fuselage station 515, with the vertical tail in the horizontal position. For the loading conditions to be duplicated in this test, a jig assembly simulating the rudder actuator was installed between the rudder and fuselage to maintain the rudder in a position four degrees (.07 rad) from neutral in the direction of the applied loads. The tension pad-whiffletree loading systems for both the fin and rudder were used for applying test loads. Loading was applied simultaneously to the fin and rudder and controlled by programmers in conjunction with calibrated strain links.

The instrumentation described in Subsection 3.1 was the same for all static tests. The locations of the strain gages and deflection indicators are shown in Figures 100 and 101, respectively.

4.2 Test Procedure and Results - Test loads, simulating air and inertial loading on the tail assembly, were applied to the fin and rudder tension pads at a maximum rate of 20% of limit load per 30 seconds, in increments of 20% of limit load, up to limit load. From limit to ultimate load, loads were applied in increments of 10% of limit load. Loads were held constant for approximately 30 seconds after each load increment. Schematics of tension pad layouts with maximum test loads are shown for the fin and rudder in Figures 112 and 113, respectively. The rudder, before and after maximum test loads were applied,

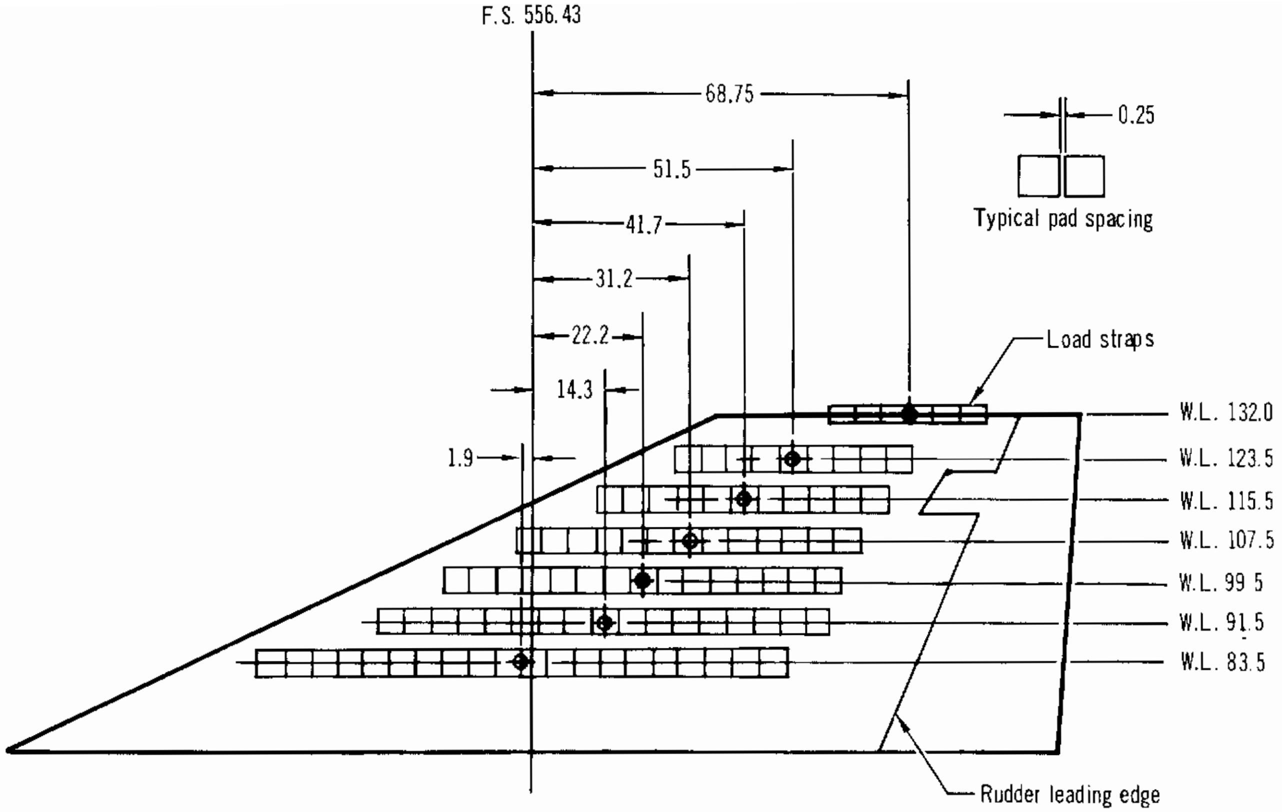
F.S. 556.43
68.75
51.5
41.7
31.2
22.2
14.3
1.9
0.25
Typical pad spacing
Load straps
W.L. 132.0
W.L. 123.5
W.L. 115.5
W.L. 107.5
W.L. 99 5
W.L. 91.5
W.L. 83.5
Rudder leading edge

NOTES: 1) All pads 5 inches x 5 inches.
2) Total ultimate load = 22,213 lbs.
3) Geometric center (⊕) of each row of pads located from F.S. 556.43
4) In a given row, all pad loads are equal.

Row	No. of Pads	Ultimate test load/pad (lb.)
W.L. 132.0	6	485
W.L. 123.5	9	248
W.L. 115.5	11	229
W.L. 107.5	13	217
W.L. 99.5	15	207
W.L. 91.5	17	198
W.L. 83.5	20	263

5) Vertical fin test loads were applied in conjunction with and in the same direction as the rudder loads shown in Figure 113.
6) Vertical fin design and test loads are compared in Figure 116.

Figure 112 – Vertical Fin Tension Pad Layout and Ultimate Loads for Test 3

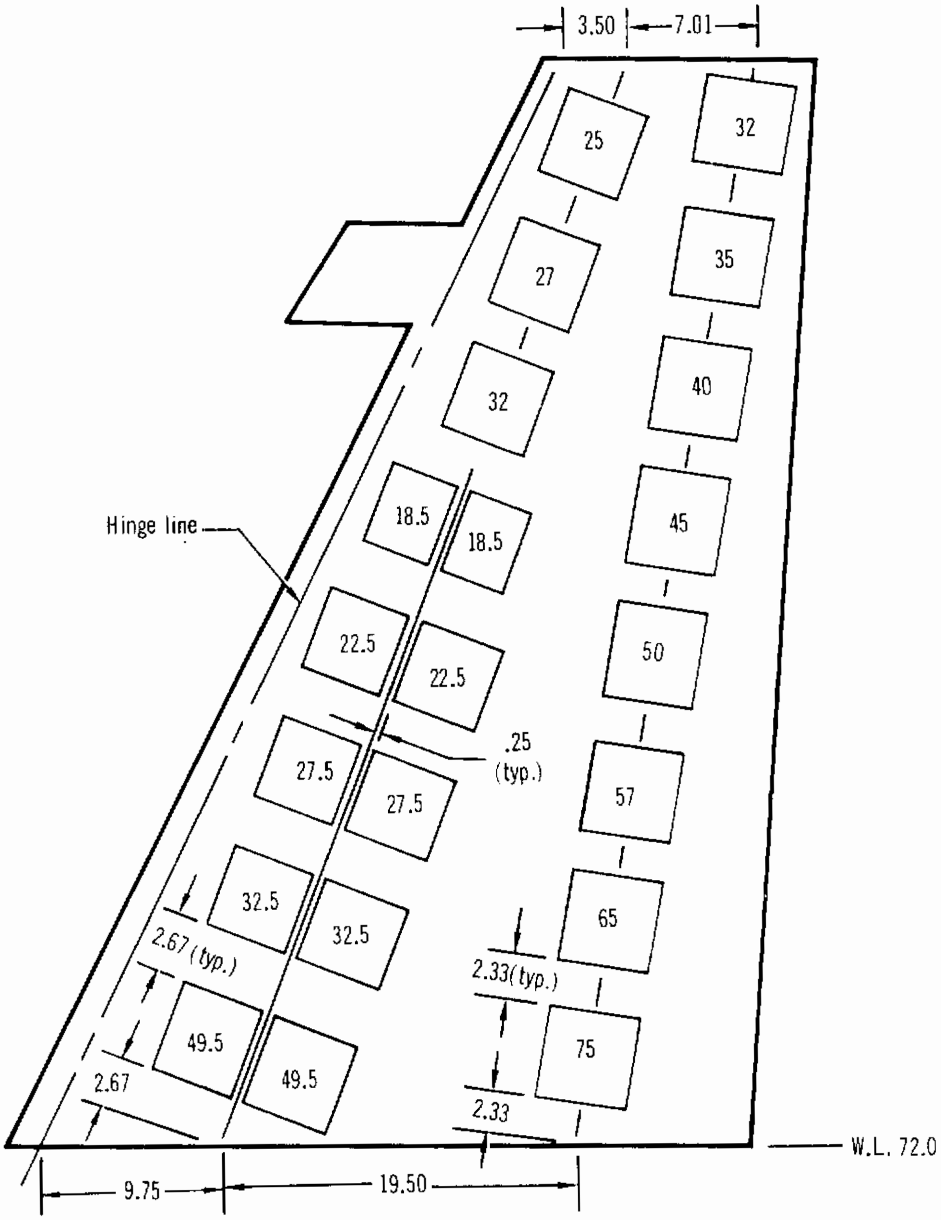
3.50
7.01
25
32
27
35
32
40
18.5
18.5
45
Hinge line
22.5
22.5
50
.25
(typ.)
27.5
27.5
57
32.5
32.5
65
2.67 (typ.)
2.33(typ.)
49.5
49.5
75
2.67
2.33
W.L. 72.0
9.75
19.50

Notes: 1. ☐ indicates tension pad and load in pounds.

2. All tension pads were 5 inches x 5 inches, except two pads with 18.5 lb. loads. These pads were 4 inches x 5 inches.

3. Ultimate load = 784 lb. Ultimate hinge moment = 10,260 in.-lb. Center of pressure at 45% chord.

4. These loads were applied in conjunction with and in the same direction as the vertical fin loads shown in Figure 112.

Figure 113 – Rudder Tension Pad Layout and Ultimate Loads for Test 3

is shown in Figures 114 and 115, respectively. Comparisons of test and design (Condition III) loads for the fin and rudder are shown in Figures 116 and 117.

The strain data recorded during the test are presented in Figures 118 through 120. Nearly all of the strain in the structure was caused by bending loads. This is indicated by the nearly equal magnitudes and reverse directions of the strains for any two opposite gages at a section of the rudder. As predicted, the maximum strain (785×10^{-6} in./in.) occurred in the front spar at the lower hinge (station Z_R=93.82). The stress associated with this strain is approximately 33 ksi (228 MN/m^2) and represents only 65% of the calculated crippling strength capability of the spar cap. In the design of the front spar, the conservative assumption was made that all bending was carried by the front spar (see design and analysis discussion, Section III). As shown by the data, however, the corresponding strain in the aft spar at this station is 370×10^{-6} in./in., and the stress associated with this strain is approximately 15.5 ksi (107 MN/m^2). Because the rear spar carries some of the bending loads which the front spar was designed for, the front spar has a reserve bending strength capability for this ultimate loading condition. The maximum total moment carried by the front and rear spars in combination, as determined by the strain data and the physical characteristics of the spars, is approximately 24,000 in.-lbs. (2712 m-N). This is in reasonable agreement with maximum ultimate design moment of 28,000 in.-lbs. (3164 m-N) shown in Figure 18, Section III, and indicates a certain degree of conservatism in the redundant analysis.

The deflection data recorded during this test are presented in Figures 121 through 124. Figure 125 presents a schematic of the rudder with maximum recorded deflections. As a result of the conservatism previously discussed, the curvature of the deflected hinge line was less pronounced than that used in design. A comparison of the deflected hinge line used in design with that developed from the test data (taking out fuselage station) is shown in Figure 126.

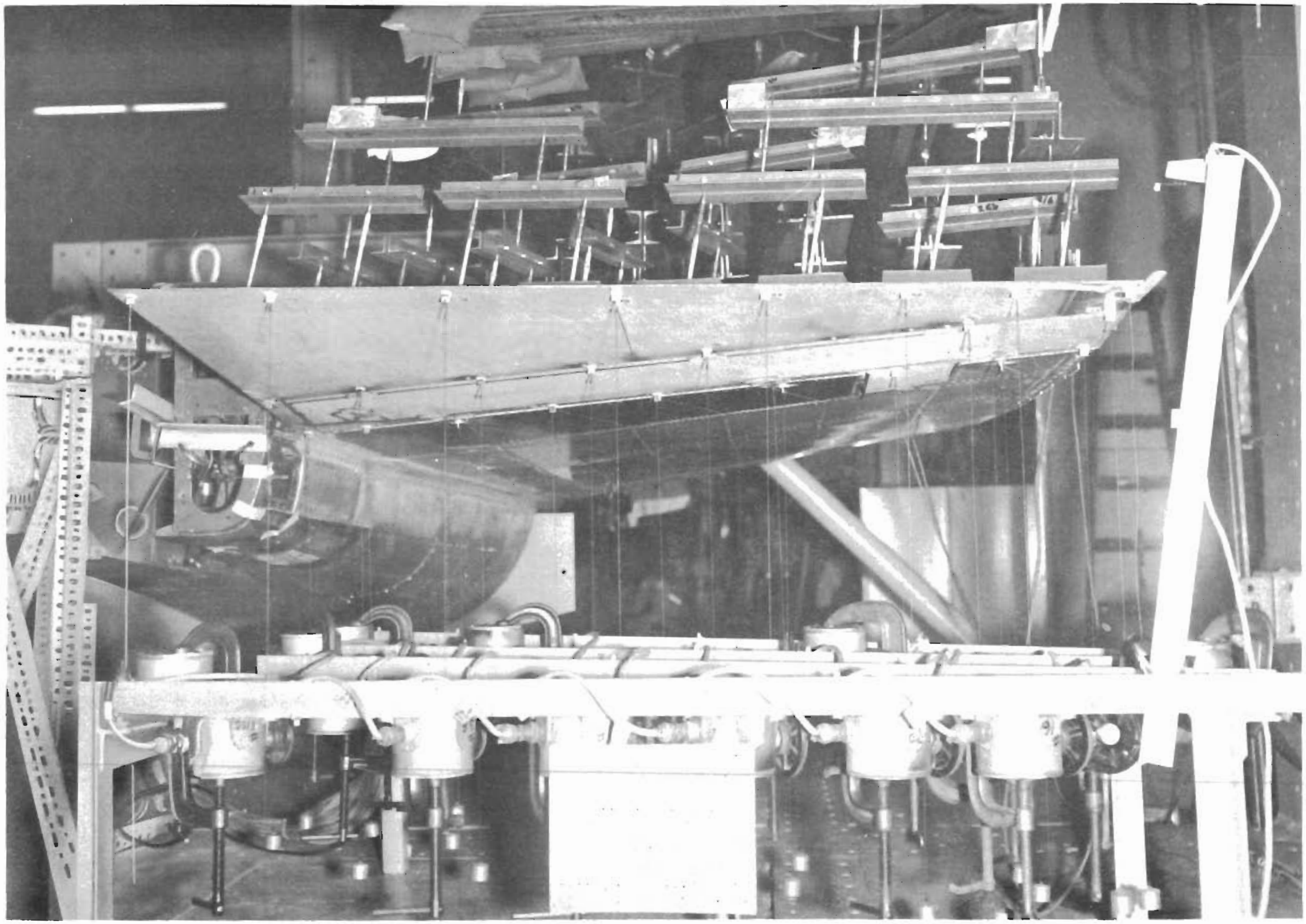

Figure 114 – Beryllium Rudder Prior to Loading

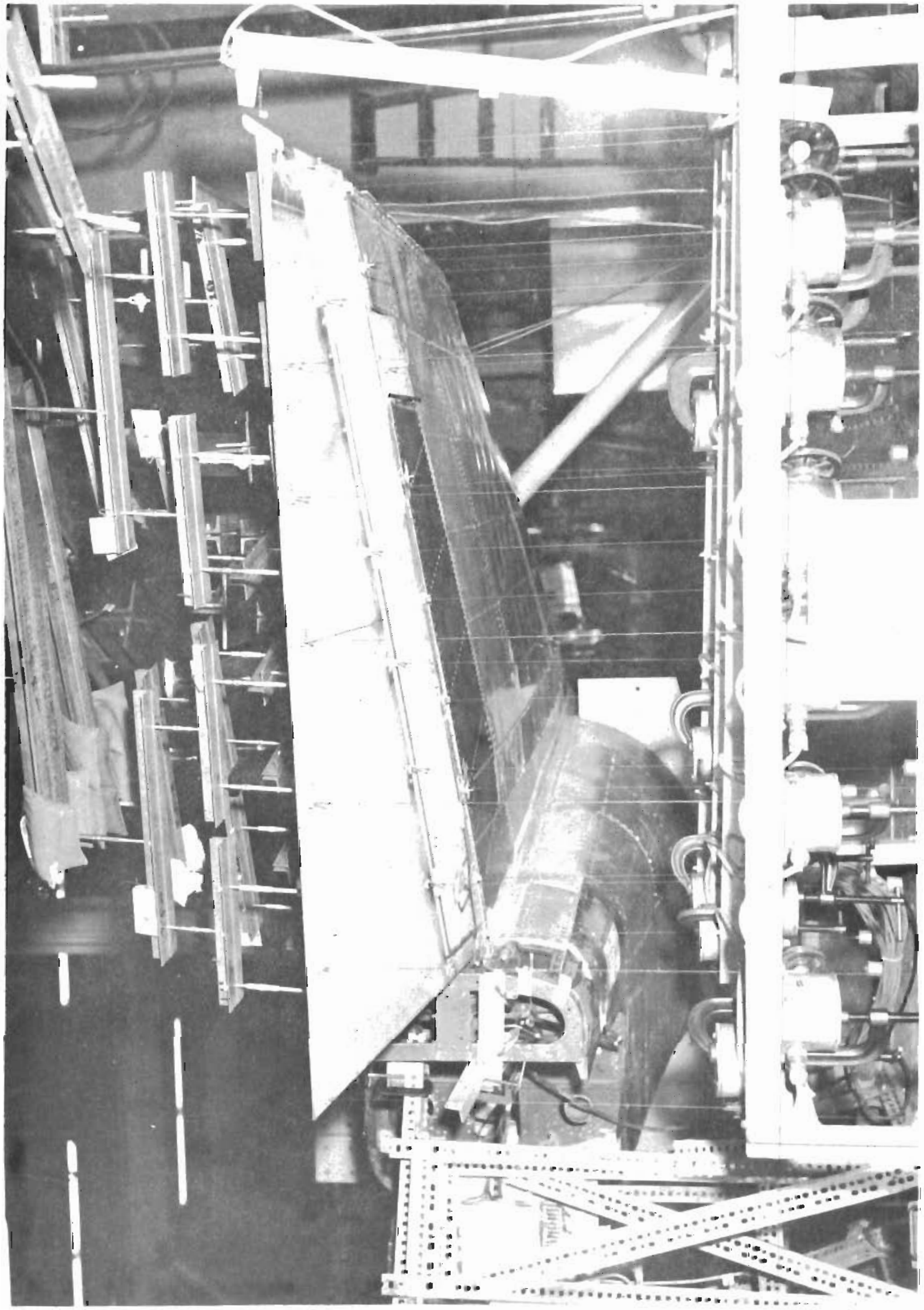

Figure 115 – Beryllium Rudder with Condition III Ultimate Loads Applied

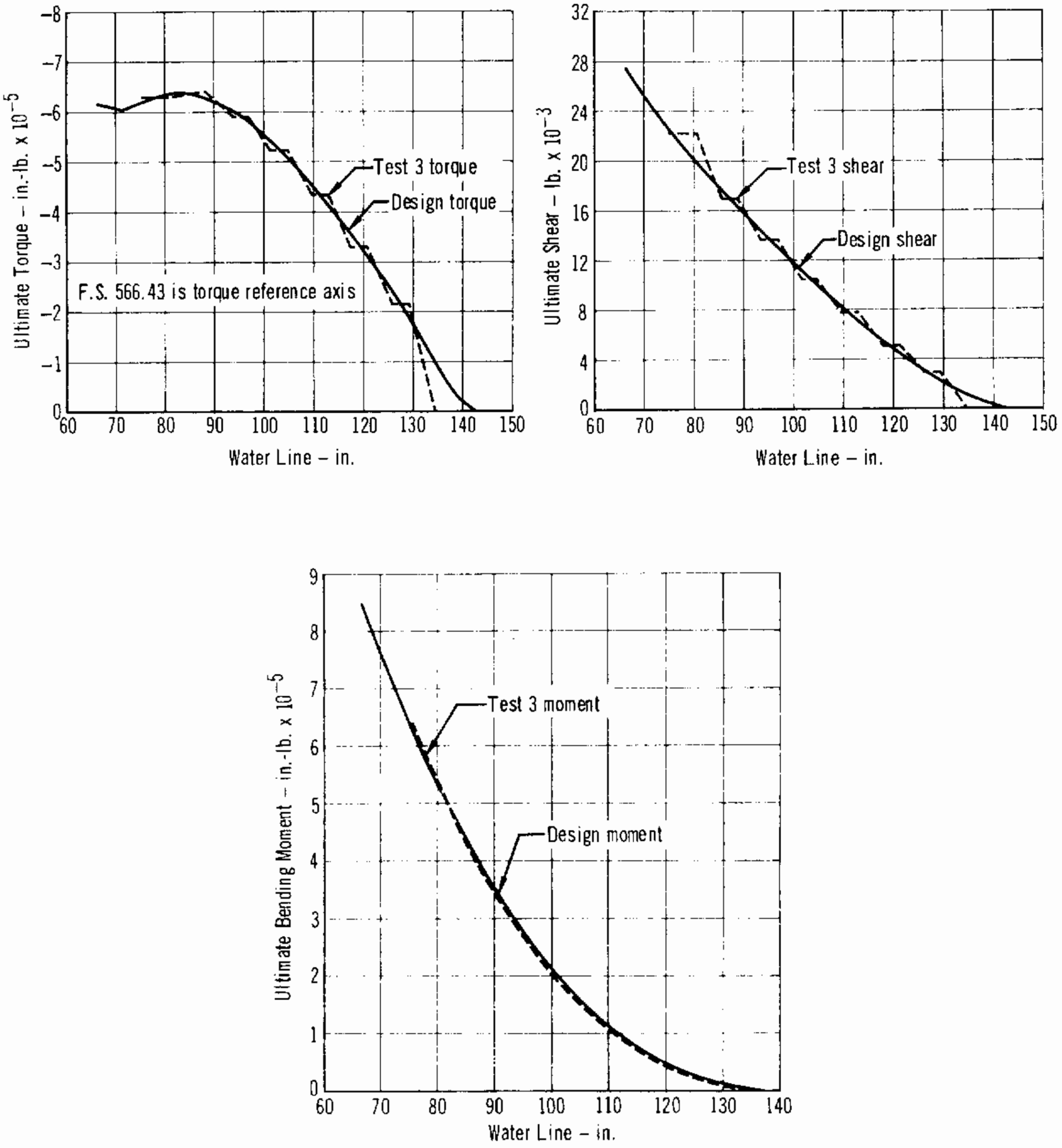

Figure 116 – Comparison of Fin Test and Design Loads: Design Condition III

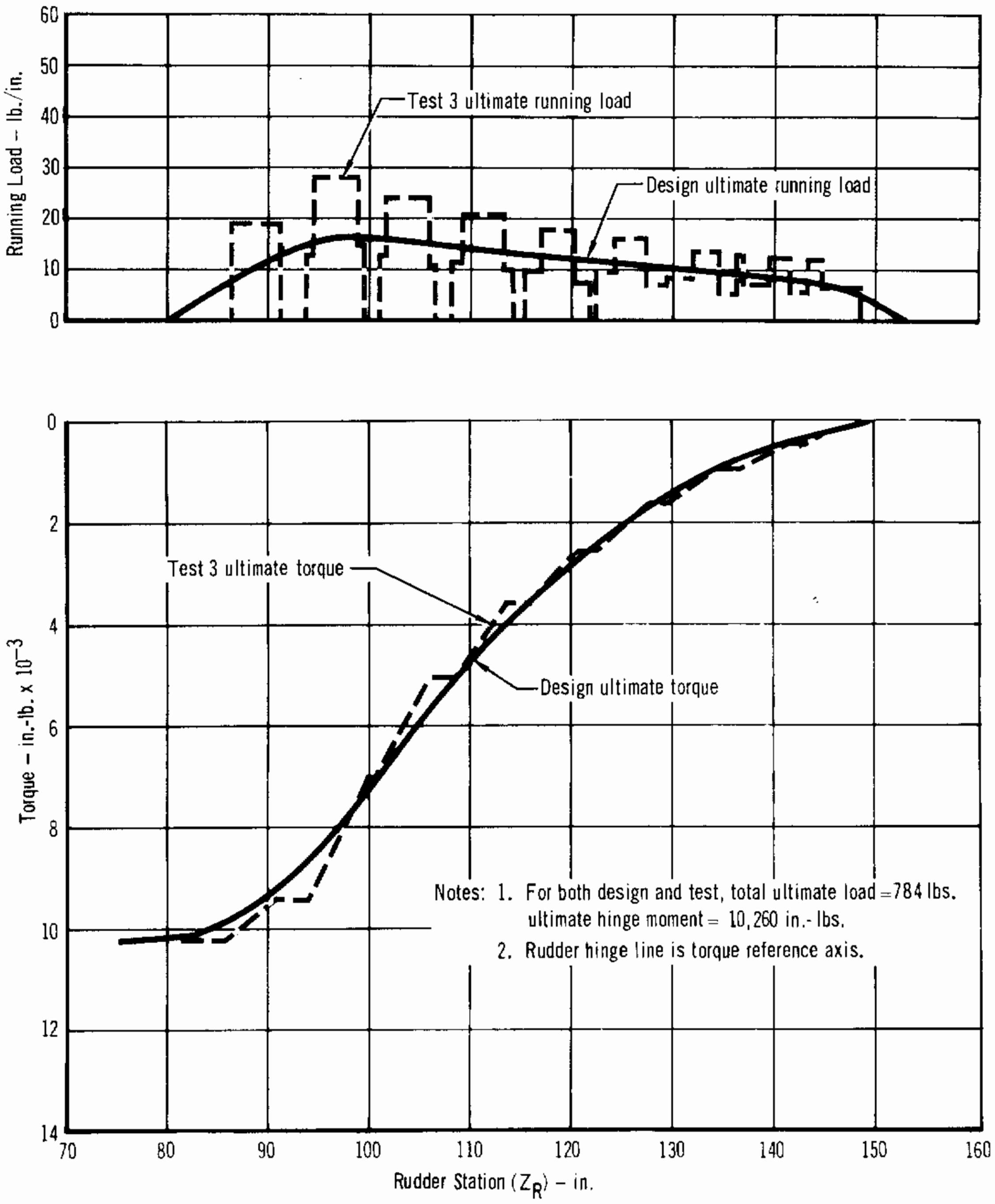

Notes: 1. For both design and test, total ultimate load = 784 lbs. ultimate hinge moment = 10,260 in.-lbs.

2. Rudder hinge line is torque reference axis.

Figure 117 – Comparison of Rudder Test and Design Loads: Design Condition III

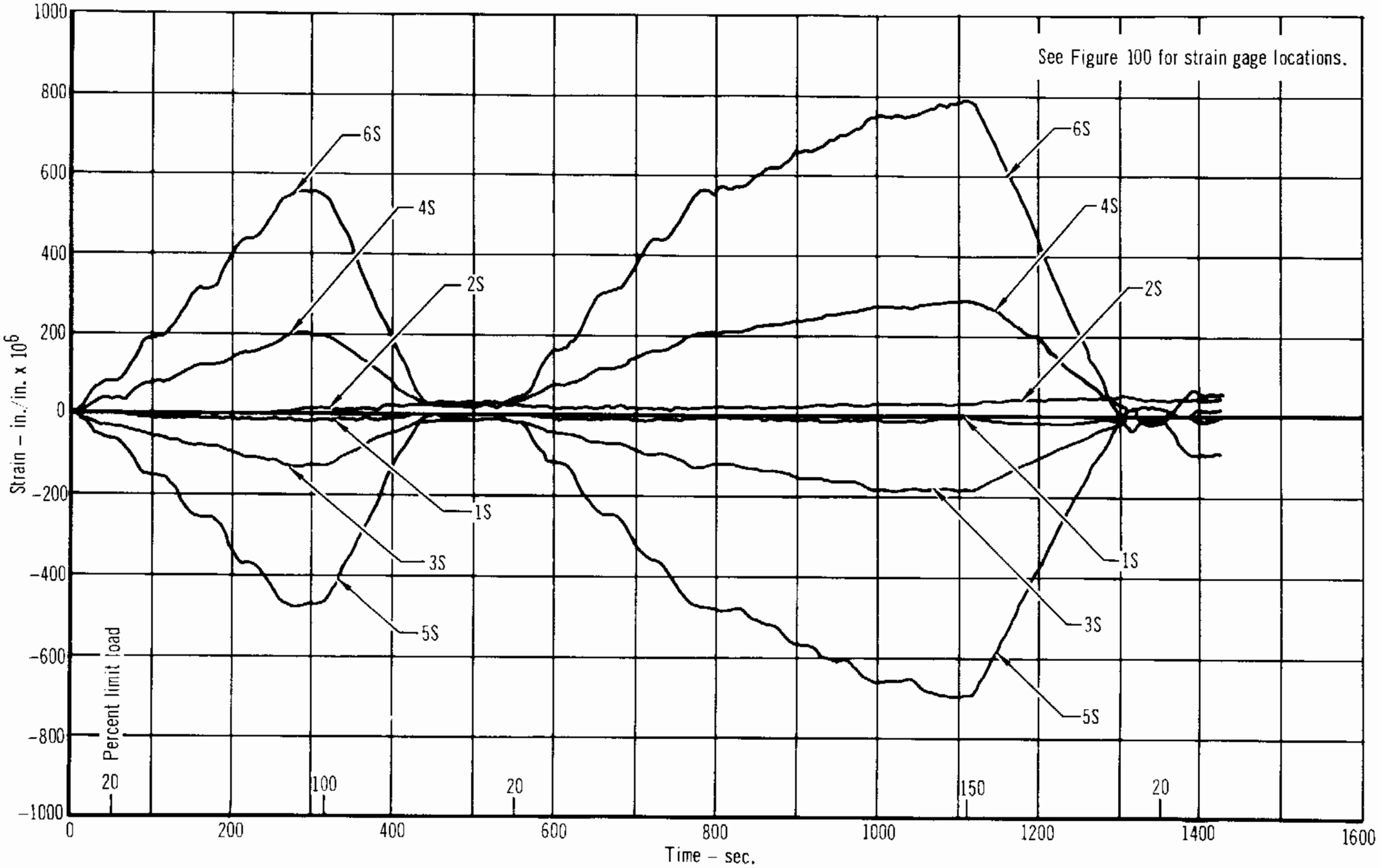

Figure 118 – Front Spar Strains: Test 3

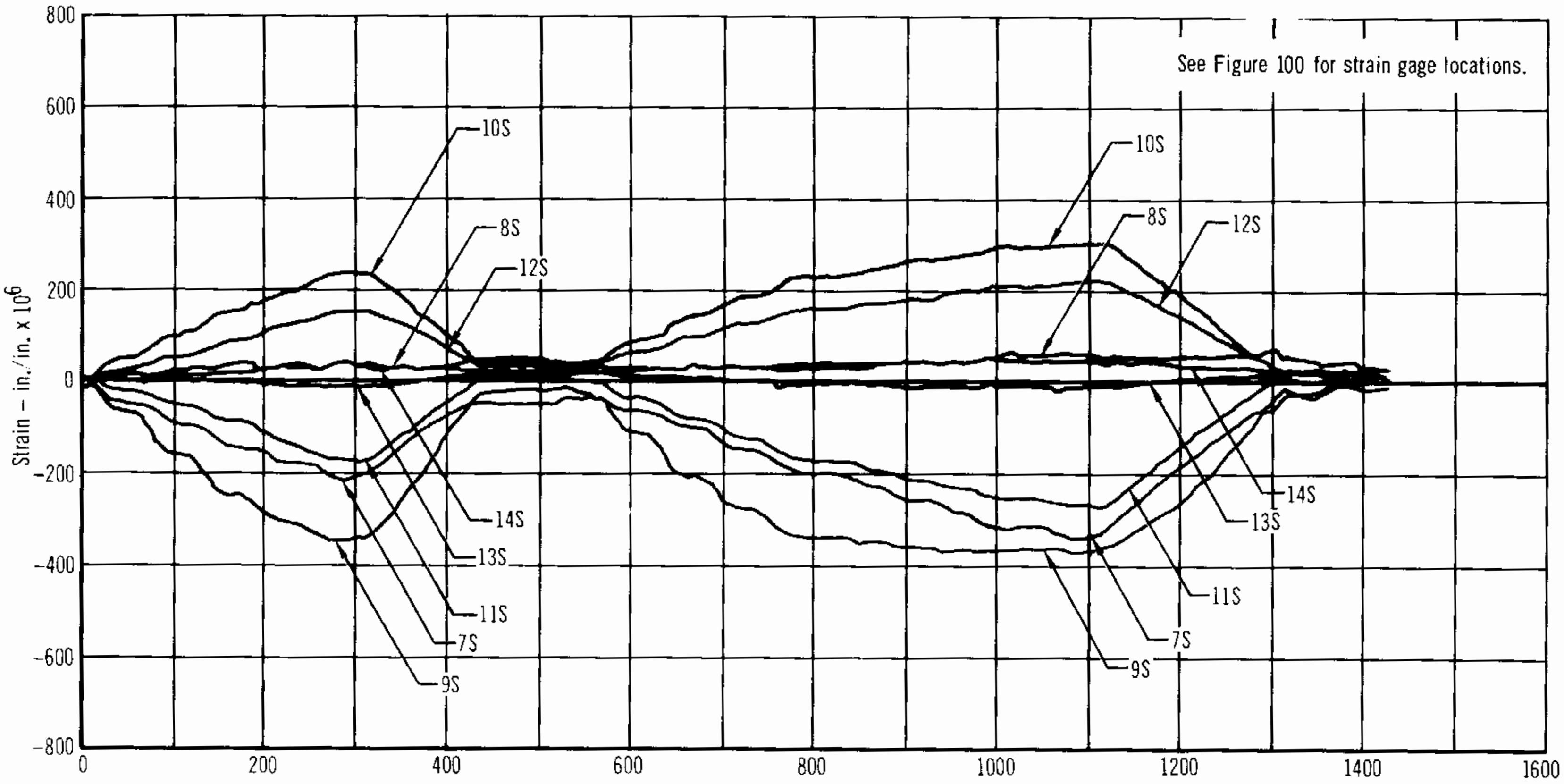

Figure 119 – Rear Spar and Trailing Edge Strains: Test 3

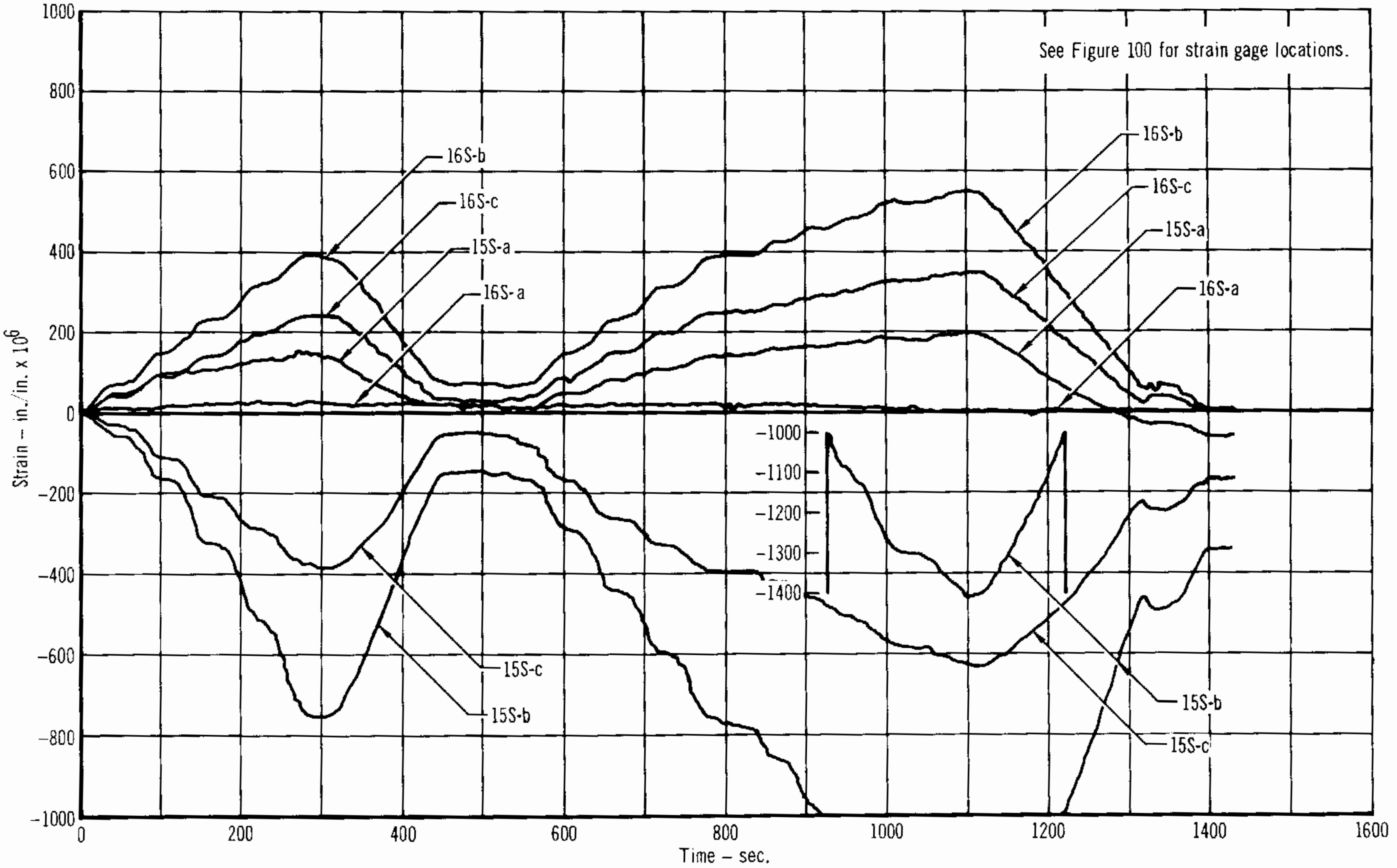

Figure 120 – Forward Cover Skin Strains: Test 3

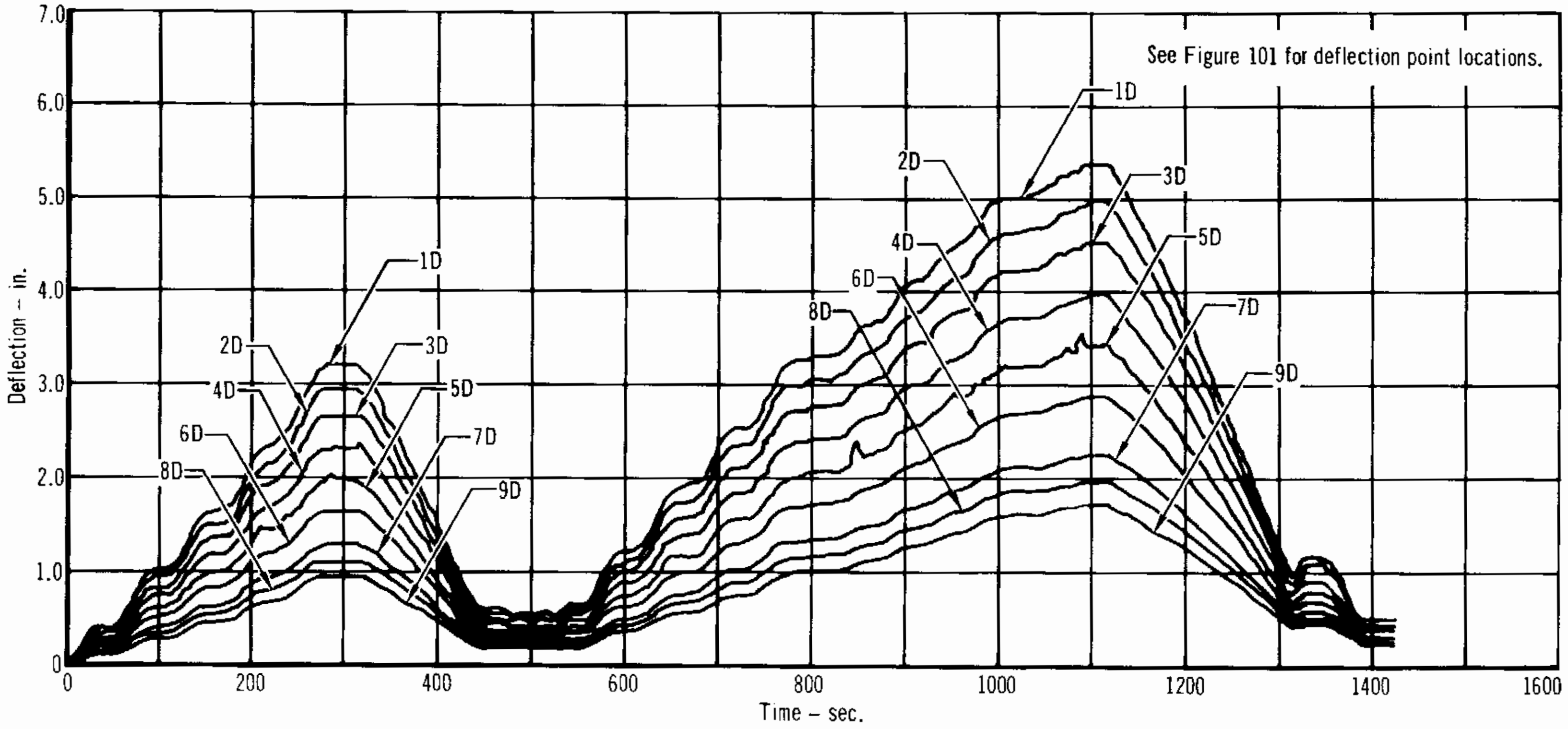

See Figure 101 for deflection point locations.

Figure 121 – Front Spar Deflections: Test 3

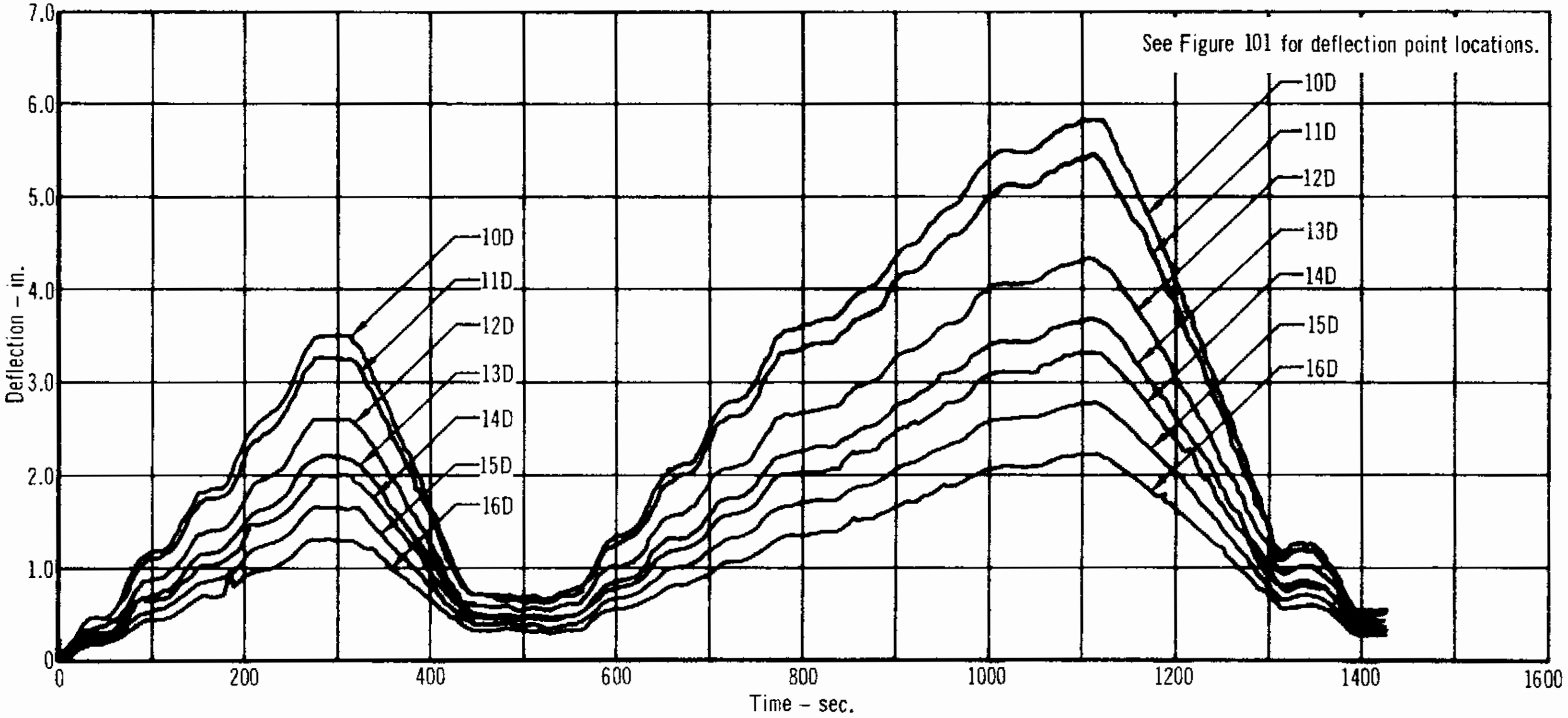

See Figure 101 for deflection point locations.

Figure 122 – Rear Spar Deflections: Test 3

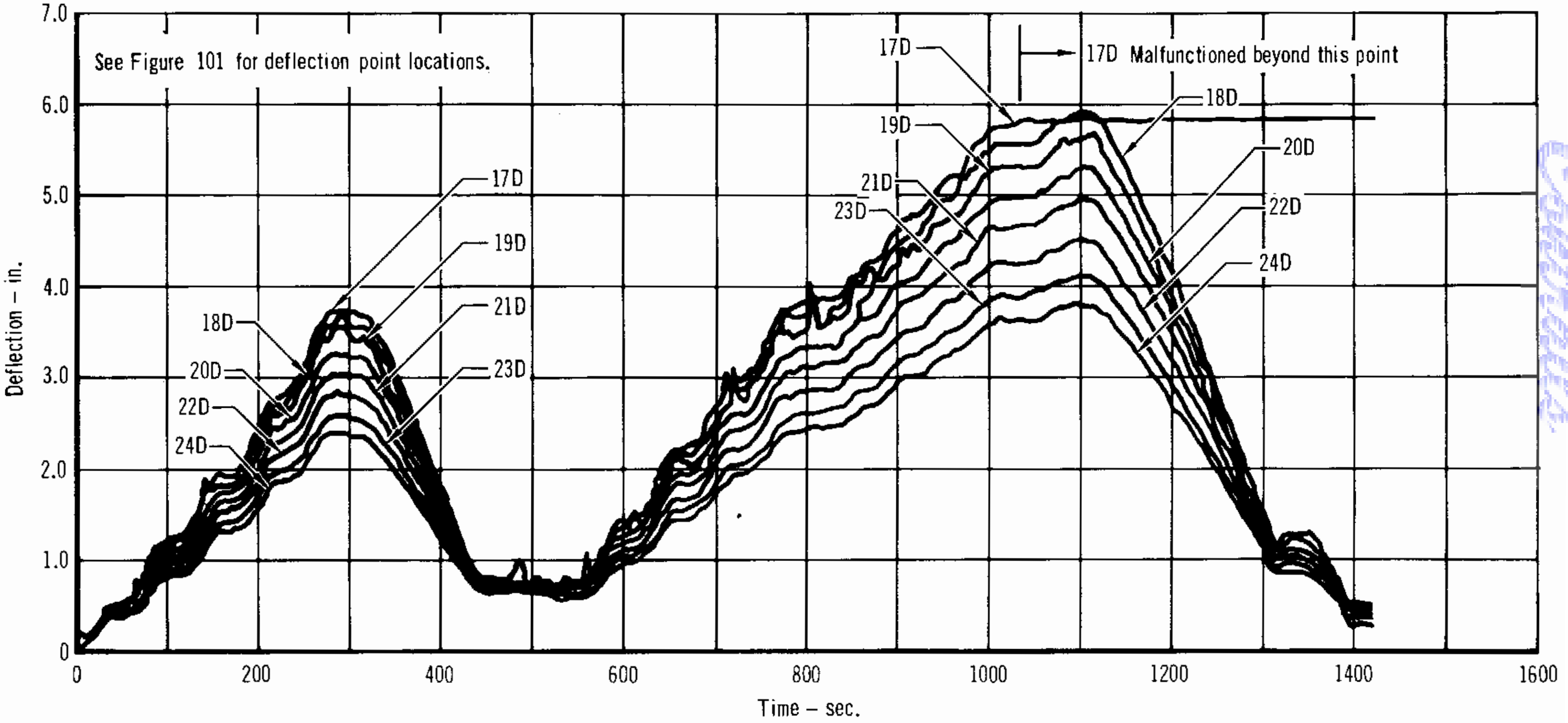

Figure 123 – Trailing Edge Deflections: Test 3

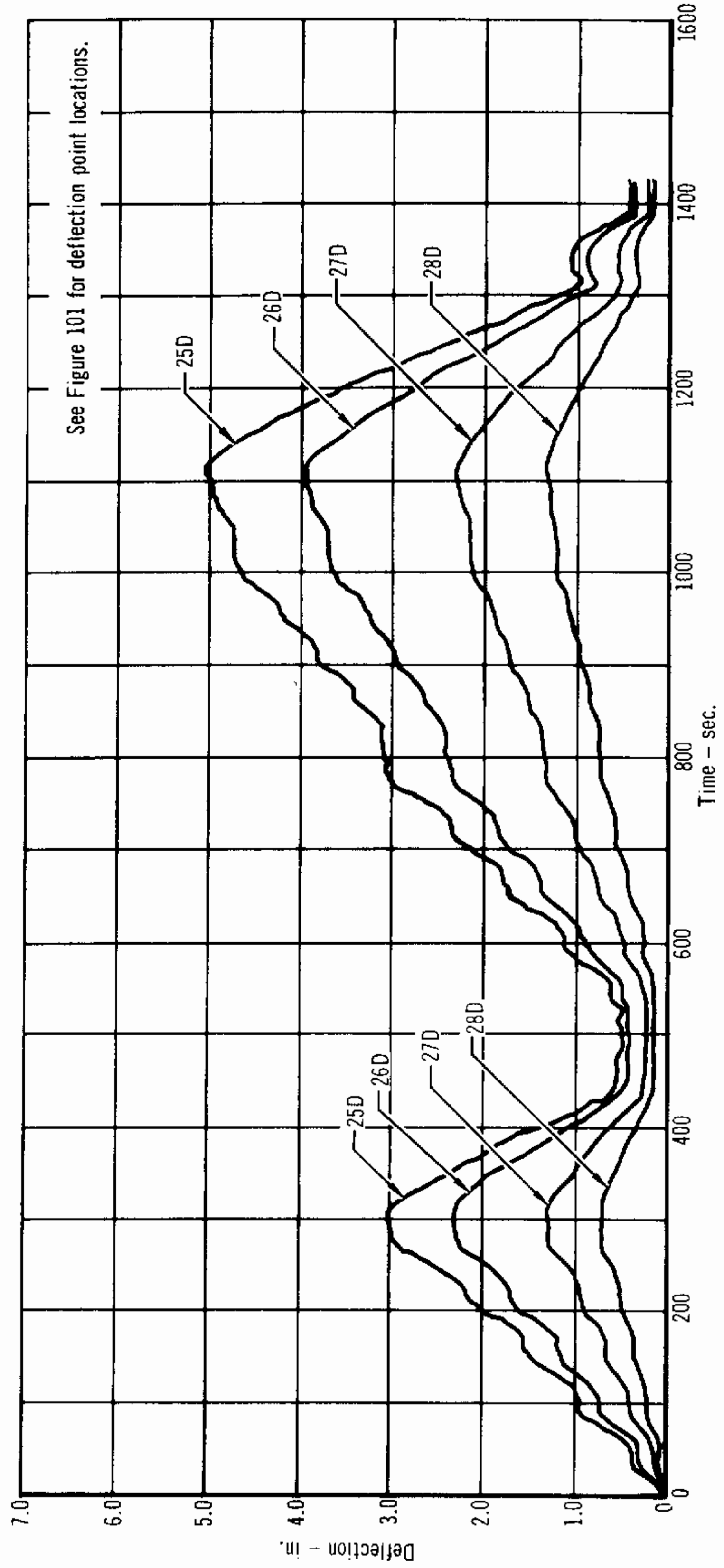

Figure 124 – Hinge Deflections: Test 3

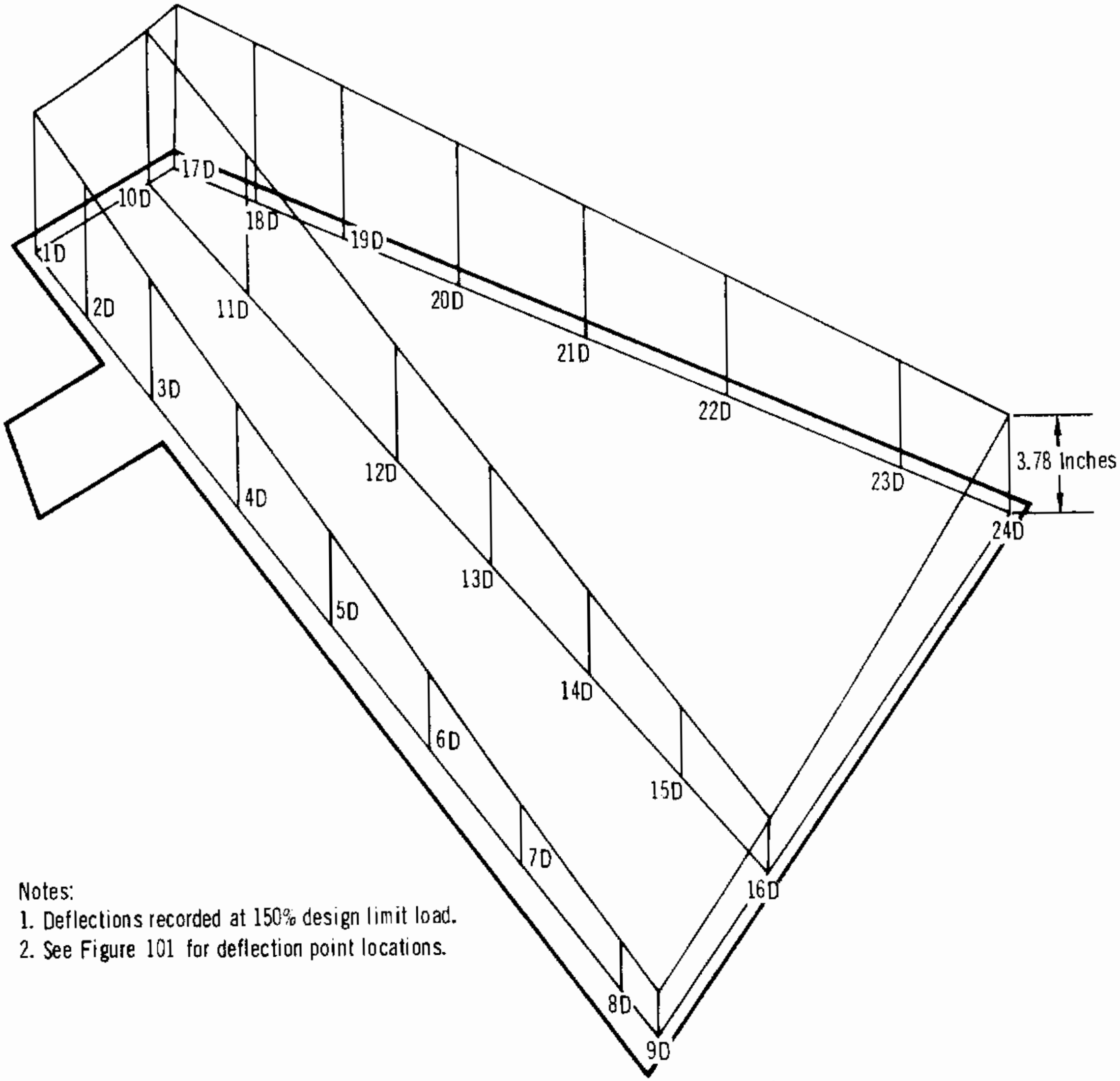
1D
2D
3D
4D
5D
6D
7D
8D
9D
10D
11D
12D
13D
14D
15D
16D
17D
18D
19D
20D
21D
22D
23D
24D
3.78 Inches

Notes:
1. Deflections recorded at 150% design limit load.
2. See Figure 101 for deflection point locations.

Figure 125 – Rudder Deflections: Design Condition III

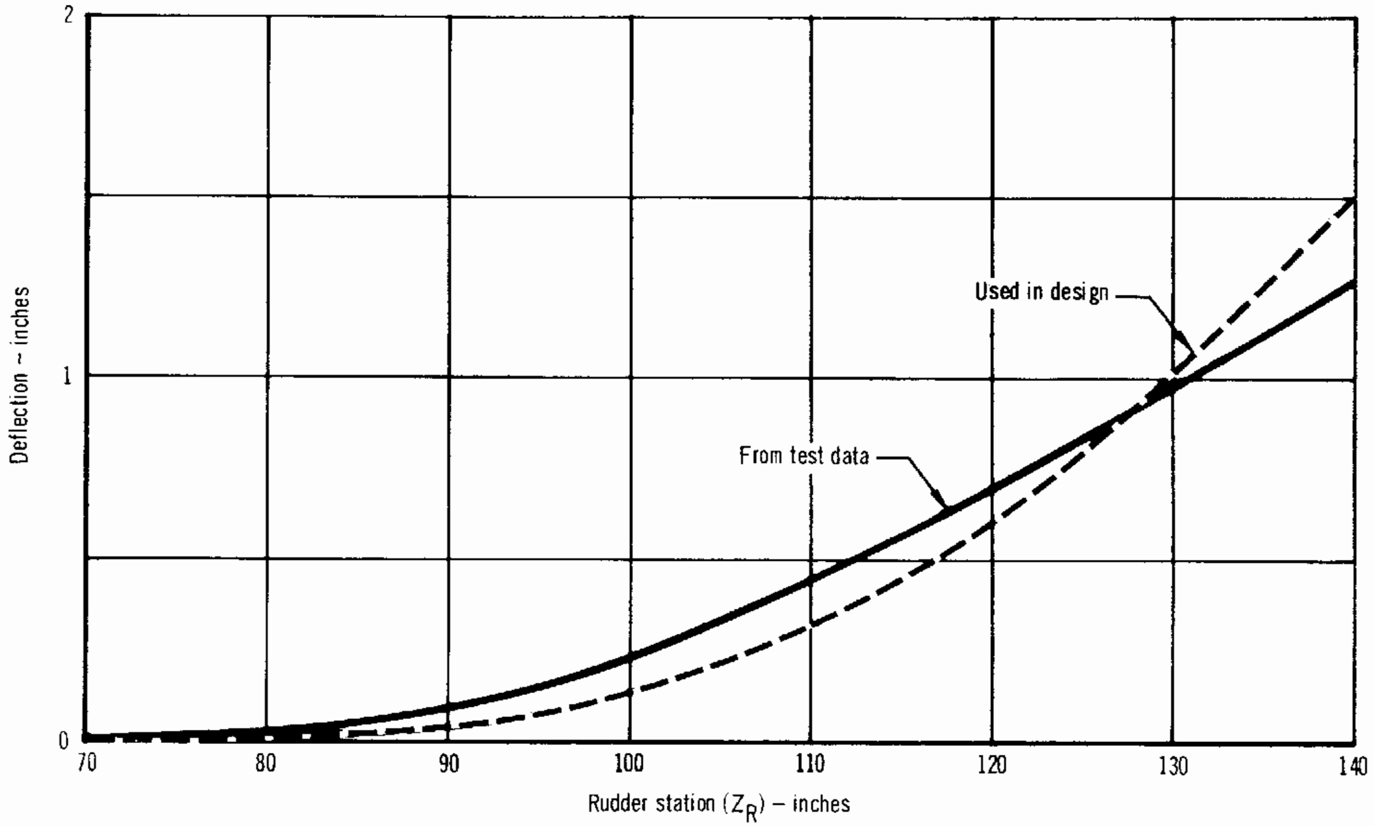

Figure 126 – Deflected Hinge Line: Design Condition III

There was no damage to the beryllium rudder at the conclusion of Test 3. It should be noted that at that point in the test program, with the successful completion of the fatigue test and the two ultimate load static tests, the beryllium rudder was structurally qualified for flight use.

5. Test 4: Same as Test 2, With Loading Carried Beyond Ultimate

The objective of this test was to provide a direct strength comparison with the production aluminum rudder which had sustained 225% of Design Condition I limit load without catastrophic failure. In Test 4, therefore, the beryllium rudder was subjected to Design Condition I loading in a manner identical with that described for Test 2, but with loads increased incrementally beyond ultimate (150% of limit). The test set-up and instrumentation were identical with those described previously in Sebsection 3.1.

5.1 Test Procedure and Results - Only the rudder was loaded in this test. Test loads were applied at a maximum rate of 20% of limit load per 30 seconds, in increments of 20% of limit load, up to limit load. From limit load to the conclusion of the test, loads were applied in increments of 10% of limit load. Loads were held for approximately 30 seconds after each load increment.

When the loads on the rudder reached approximately 205% of limit, a sharp noise was heard. However, the load did not fall off, and the test was continued, with incremental load increases of 10% of limit load, as before. After the rudder had sustained 250% of design limit load (1.67 times loads shown in Figure 102) for 30 seconds, testing was discontinued. It was felt that testing beyond that point would be of little significance at the conclusion of an already sucessful test program.

During the post-test examination, a small crack was discovered in the web of the trailing edge lower closure rib where that rib connects to the closure rib of the front torque box at the rear spar line. As shown in Figure 127, the crack passes through a fastener hole, an area of high stress concentration. The crack very likely was caused by the shear load transferred from the trailing edge assembly at the rib joint. No other damage to the rudder structure was found.

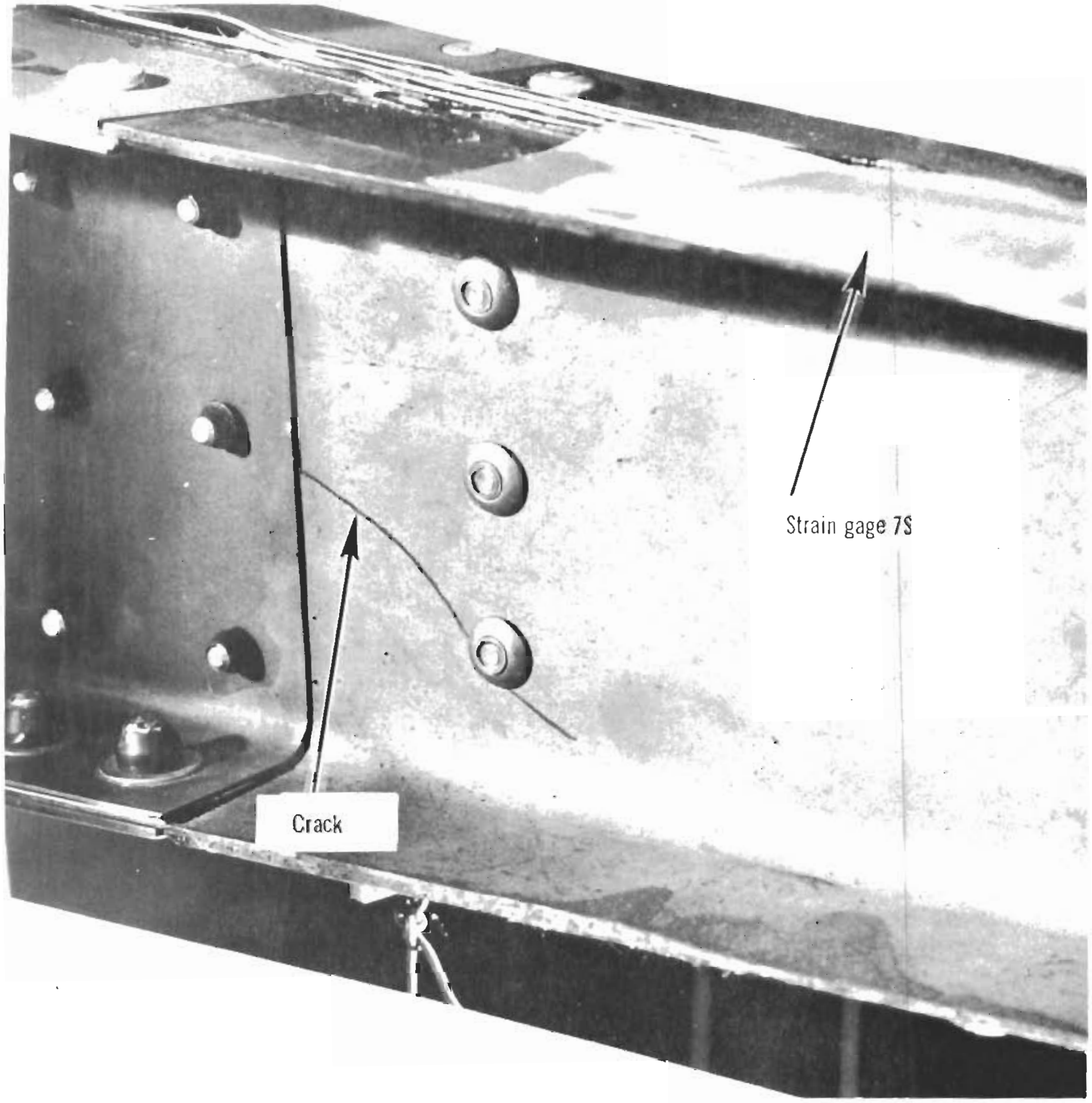
Strain gage 7S
Crack

Figure 127 – Crack in Trailing Edge Lower Closure Rib of Beryllium Rudder

The strain data recorded during the test are shown in Figures 128 through 130. Note the reaction of strain gages 7S and 8S, approximately 760 seconds after the start of testing. These gages are located adjacent to the area of the cracked web on the outer surface of the rib caps. This test time corresponds to the occurrence of the noise after 205% of design limit load has been applied to the rudder. This confirms the statement that the crack occurred at this load level. Deflection data for this test are shown in Figures 131 through 134. The load-deflection relationships are as expected, with no unusual occurrences.

The ability of the beryllium rudder to sustain 250% of Design Condition I limit load without catastrophic failure demonstrates a strength capability for this condition comparable to that of the production aluminum rudder. Moreover, the beryllium rudder sustained this load after being fatigue tested and twice static tested to design ultimate loads - a ground test program more stringent than any undergone by its aluminum counterpart.

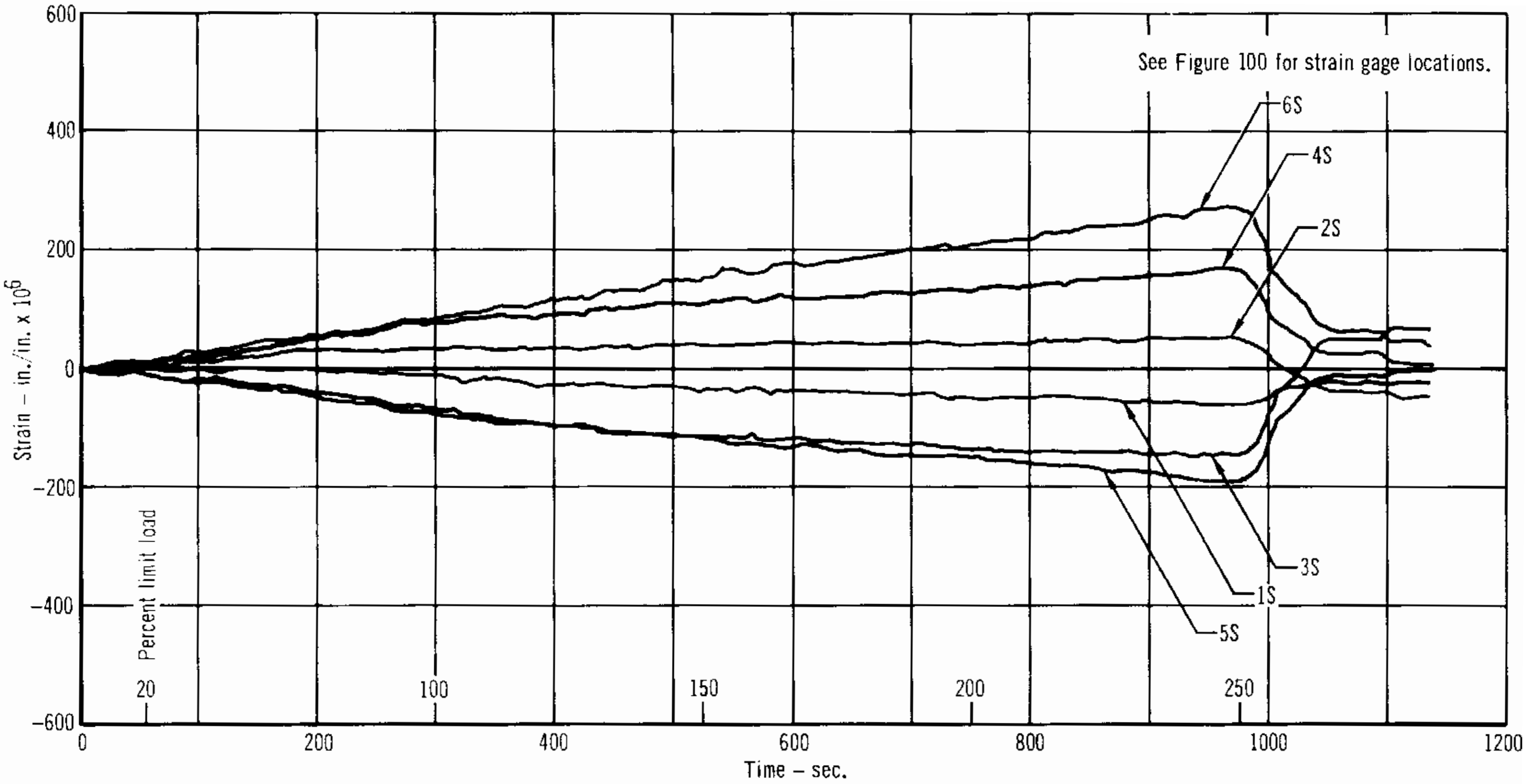

Figure 128 – Front Spar Strains: Test 4

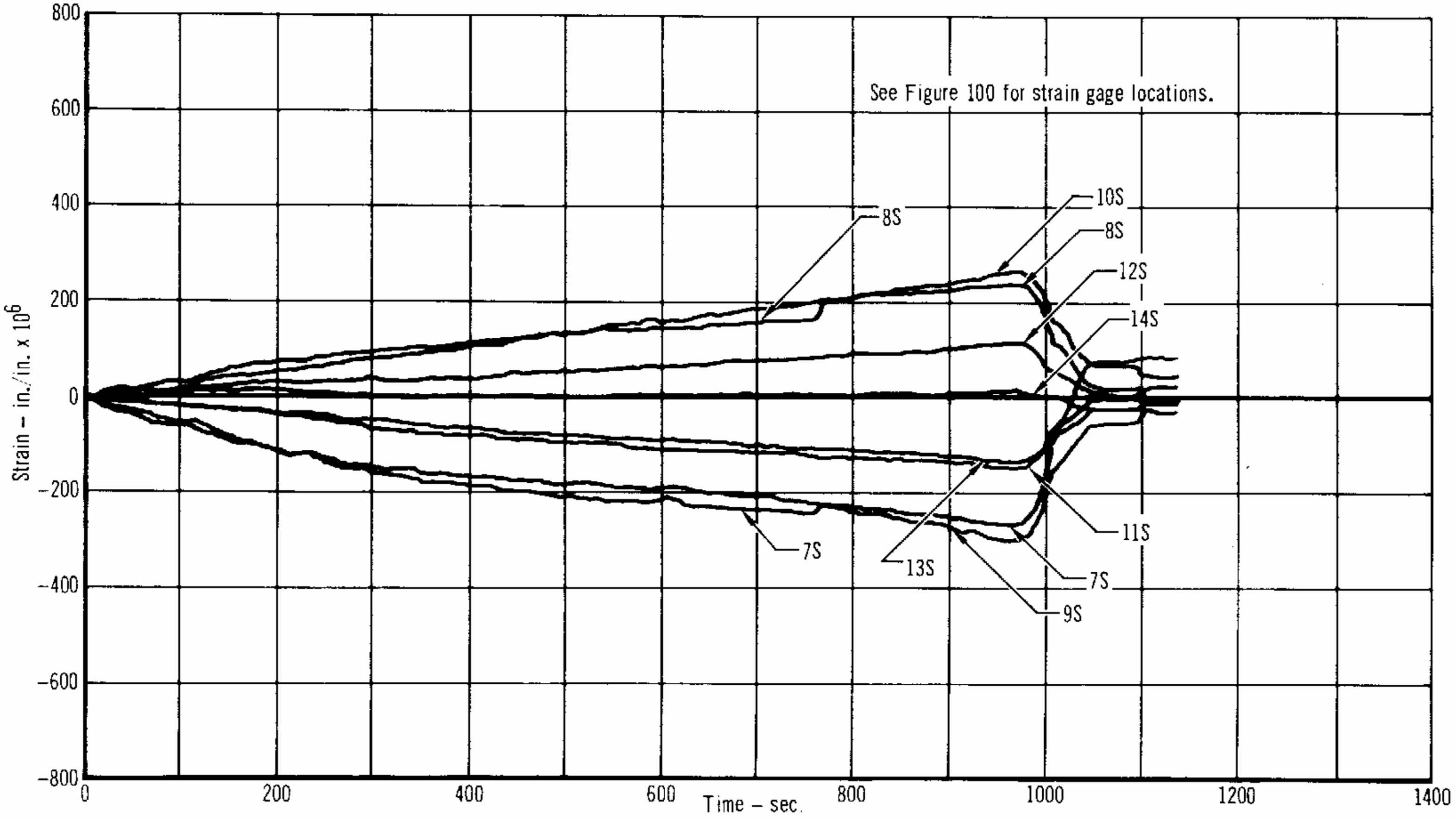

Figure 129 – Rear Spar and Trailing Edge Strains: Test 4

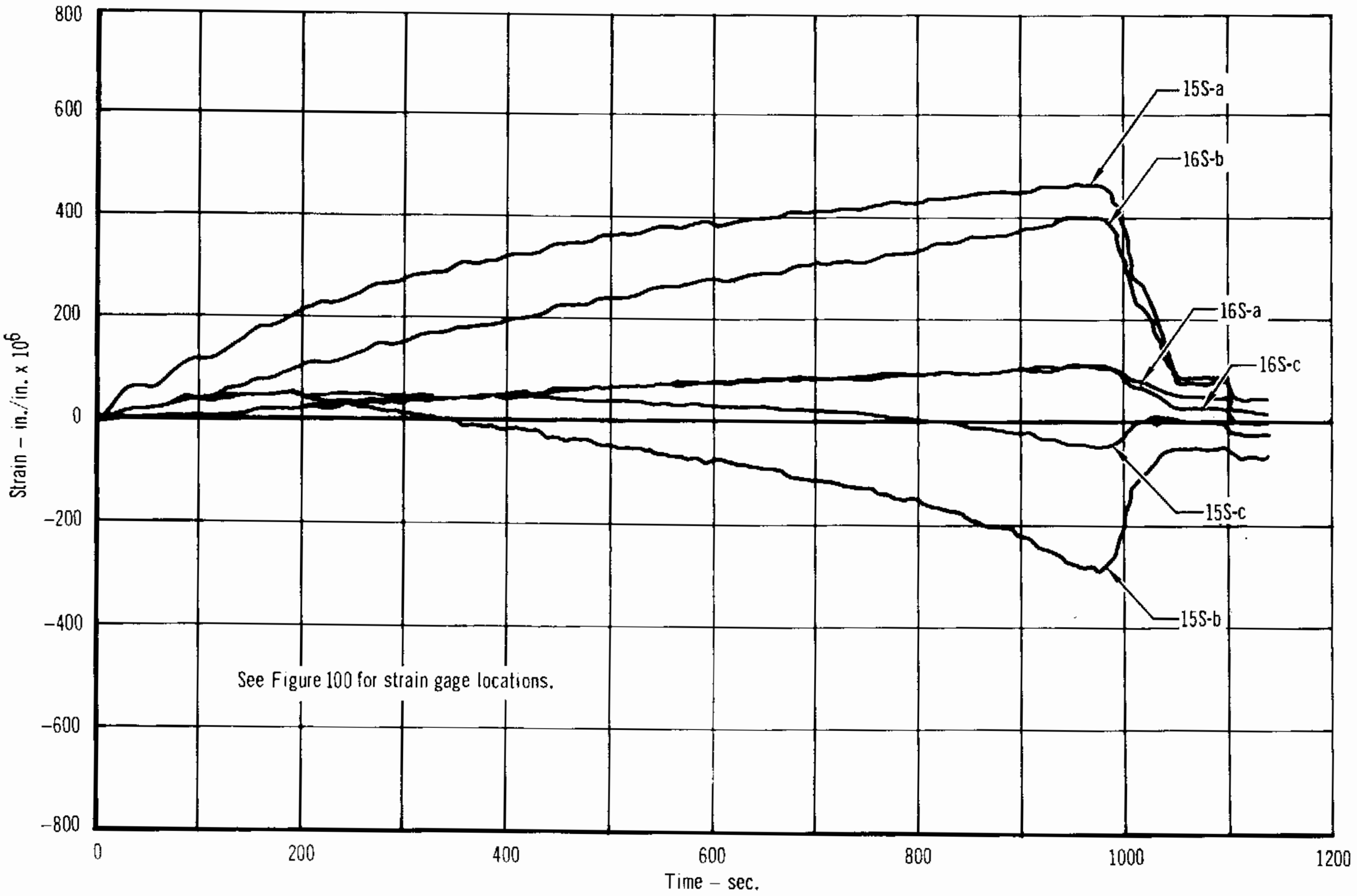

Figure 130 – Forward Cover Skin Strains: Test 4

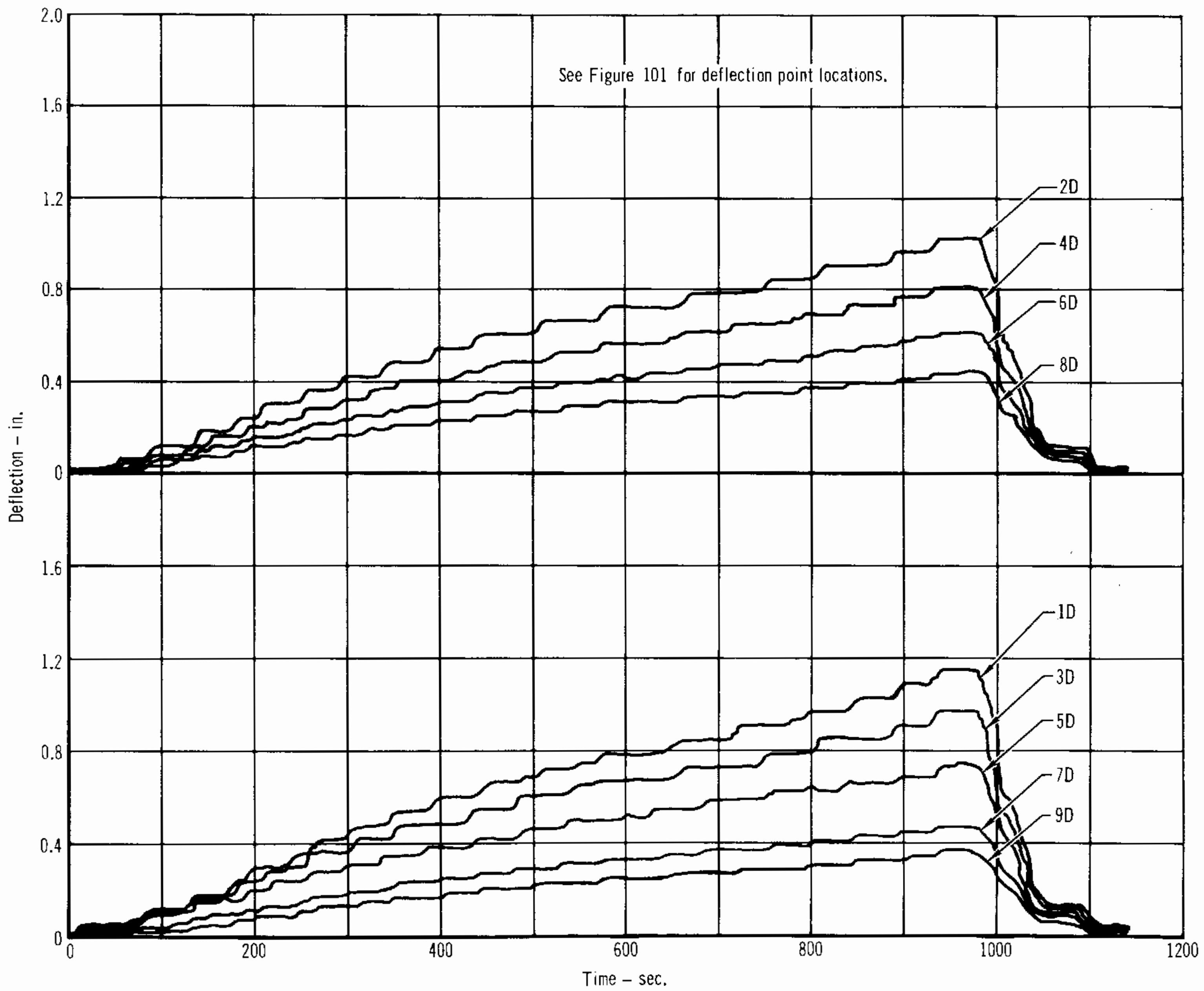

See Figure 101 for deflection point locations.

Figure 131 – Front Spar Deflections: Test 4

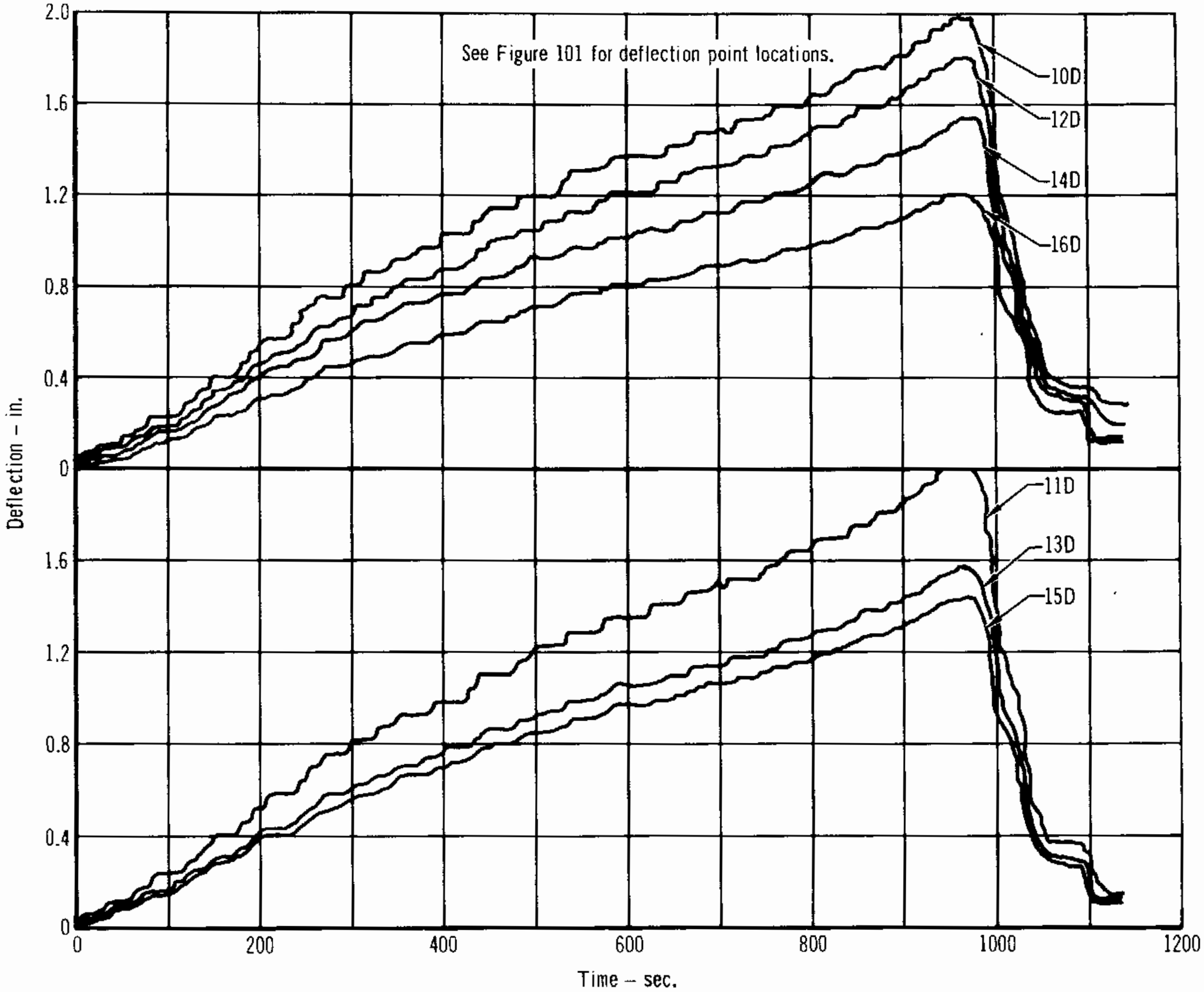

Figure 132 – Rear Spar Deflections: Test 4

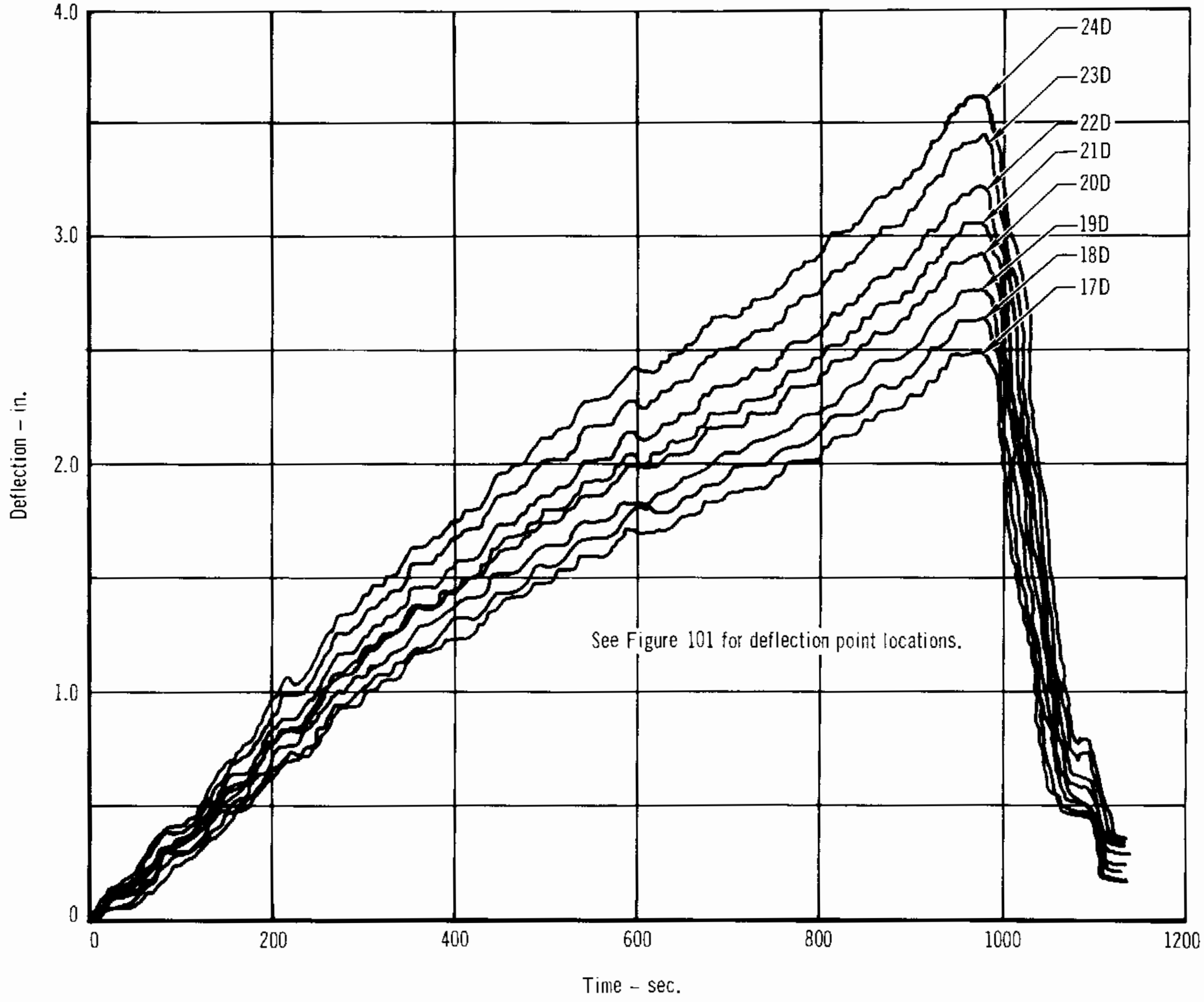

Figure 133 – Trailing Edge Deflections: Test 4

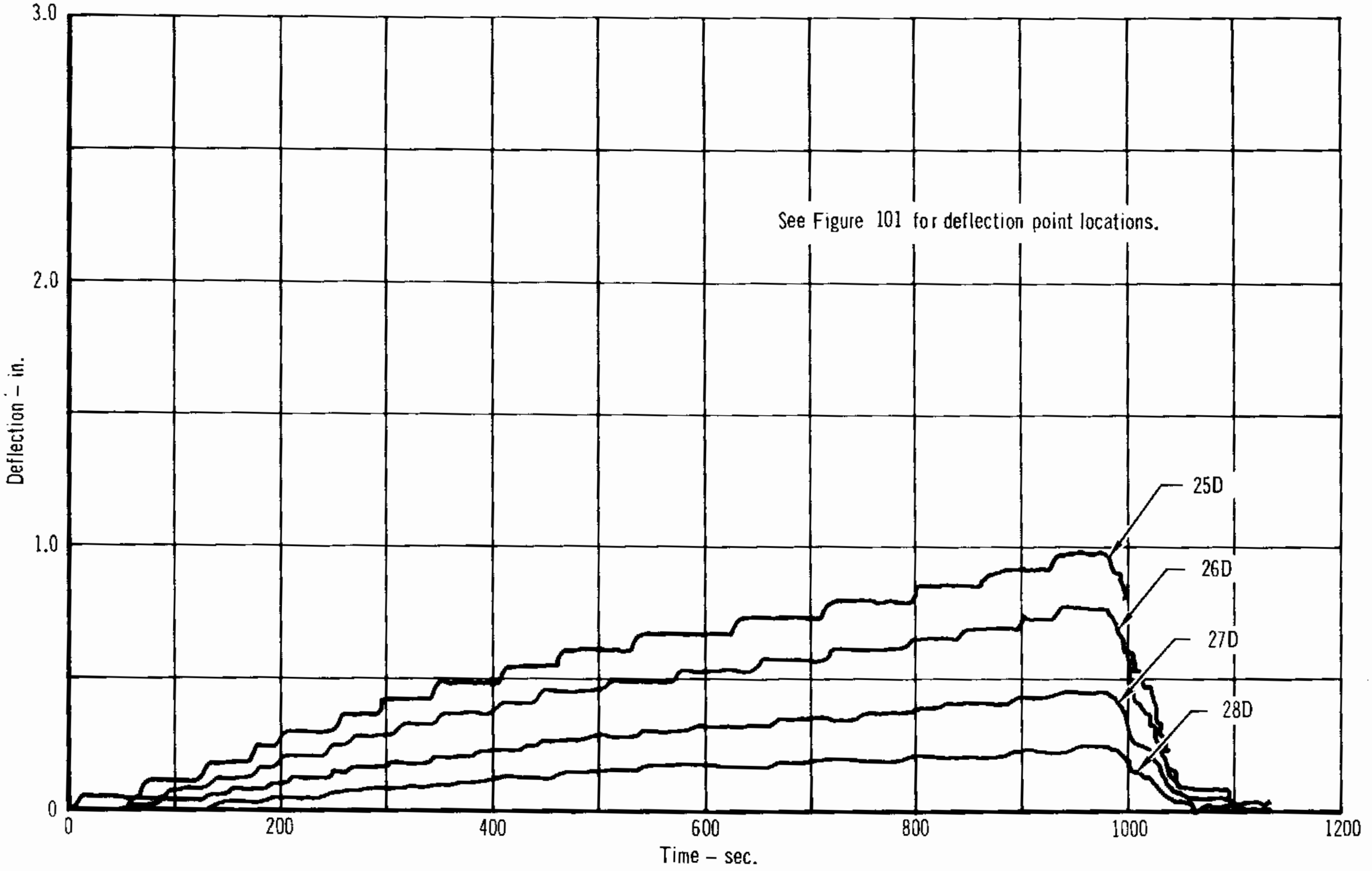

See Figure 101 for deflection point locations.

Figure 134 – Hinge Deflections: Test 4

SECTION VII

REFERENCES

1. Contract No. AF33(615)-2974, "Design, Fabrication, Testing, and Evaluation of Beryllium Structures for Flight Vehicles," 15 June 1965.

2. Air Force Report AFFDL-TR-67-38, "Design, Fabrication and Test of an Aerospace Plane Beryllium Wing-Box," March 1967.

3. "Beryllium in Aerospace Structures," The Brush Beryllium Company.

4. Cozzone, F. P. and Melcon, M. A., "Non-Dimensional Buckling Curves - Their Development and Application," Journal of Aeronautical Sciences, pp. 511-517, October 1946.

5. Kuhn, Paul, Peterson, James R., and Levin, L. Ross, "A Summary of Diagonal Tension Part I, Methods of Analysis," National Advisory Committee for Aeronautics, TN-2661, Washington, D.C., May 1952.

6. Chance Vought Corporation, Burns, A. Bruce, and Terry, E. L., "Summary of Shear Panel Design Procedures," Structures Development Memo 119, Dallas, Texas, November 1959.

7. ASD Technical Report 61-192, "Strength, Efficiency, and Design Data for Beryllium Structures," February 1962.

8. Gerard, George, and Becker, Herbert, "Handbook of Structural Stability, Part I - Buckling of Flat Plates," National Advisory Committee for Aeronautics, Technical Note 3781, July 1957.

9. McDonnell Report 339, "Structure Handbook."

APPENDIX

DETAIL DRAWINGS

Composite Section Drawing

No. 404-005, "Rudder Composite Section" (3 sheets)

Beryllium Rudder Drawings

No. 404-100, "Rudder Installation Beryllium Rudder"

No. 404-101, "Rudder Assembly"

No. 404-102, "Structure Assembly Beryllium Rudder"

No. 404-103, "Trailing Section Assembly - Rudder Honeycomb (2 sheets)

No. 404-104, "Forward Spar Assembly"

No. 404-105, "Fitting - Rudder Torque Tube Upper"

No. 404-106, "Hinge - Rudder"

No. 404-107, "Rib Assembly Rudder Upper Balance Weight"

No. 404-108, "Rib Assembly"

No. 404-109, "Rib Assembly"

No. 404-110, "Ribs - Rudder Assembly"

No. 404-111, "Ribs - Rudder Assembly"

No. 404-112, "Ribs - Rudder Assembly"

No. 404-113, "Skins - Torque Box Upper & Lower"

No. 404-114, "Fitting - Rudder Leading Edge Rib"

No. 404-115, "Leading Edge Rib - Rudder"

No. 32-24004, "Support Assembly - Balance Weight & Horn"

DETAIL-55
ASS'Y A-A
DETAIL-53
BASE PLATE

DETAIL -5 ASS'Y B14 △6
DO NOT INSTALL INSTRUMENTATION PRIOR TO BONDING.
ALL FASTENER HOLES IN -25, -39 & -43 WILL BE DRILLED FULL SIZE & -25, -39 & -43 WILL BE FINAL ETCHED PRIOR TO BONDING. THERE WILL BE NO DRILLING OR ETCHING ON -5 ASS'Y AFTER BONDING. ETCH CLEANING PRIOR TO ATTACHING LOADING PADS OR INSTRUMENTATION AFTER BONDING IS PERMITTED

	3M85 / COLLAR	NW	3M117		
FE	3M91	DR	3M83		
PZ	3M2668		3M88 / COLLAR		
PV	3M2678	EH	3M90		
BB	MS20426AD	BJ	MS20470AD	LZ	NAS1097AD
CODE	RIVET	CODE	RIVET	CODE	RIVET

BASIC CODE | DIA DASH NO. AND LOCATION OF MFD HEAD
SHT PREPARATION | LENGTH DASH NO.
F = FAR SIDE
D2C = DIMPLE SHTS 1 & 2, CSINK LWR SHT
DC = DIMPLE TOP SHT, CSINK LWR SHT
D = DIMPLE
CC = CSINK - DOUBLE FLUSH HD
C = CSINK
N = NEAR SIDE
R = REF RIVET
☐ = INSTALL. RIVET
AC 5 N / D 2 MS20601AD5–2 RIVET INSTALL. RIVET DIMPLE ALL SHTS INSTALL NEAR SIDE
NO. OF EQUAL SPACES
NAS523 RIVET CODE

19 ALL BERYLLIUM PARTS ARE PRIOR TO FINAL ETCH EXCEPT AS NOTED.

△18 STOCK FOR -55 TO BE MADE AT MAC MAKE WHATEVER SIZE THAT IS NECESSARY FOR MACHINING

17. ODD DASH NO'S SHN. EVEN DASH NO'S. OPP.

△16 CORE SHALL BE IN ACCORDANCE WITH MMS 701 EXCEPT THAT THE FOIL SHALL BE NON-PERFORATED

15. ALL STEEL PARTS MAY BE MARKED WITH STEEL STAMPS. DO NOT MARK ANY BERYLLIUM PARTS USE TAGS TO IDENTIFY BERYLLIUM.

14. BREAK ALL SHARP EDGES. (STEEL PARTS ONLY)

13. MACHINE FINISH 125 OR BETTER - ALL MACHINED PARTS.

12. HOLE SIZES FOR FASTENERS IN BERYLLIUM PARTS ARE AS FOLLOWS:

FASTENER	DIA. BEFORE ETCH	DIA AFTER ETCH
DR 5	.162 +.005 -.000	.165 +.006 -.000
DR 6	.196 +.005 -.000	.199 +.006 -.000
PV 4	.140 +.002 -.000	.143 +.003 -.000
PV 5	.173 +.003 -.000	.176 +.004 -.000
PZ 4	.140 +.002 -.000	.143 +.003 -.000
EH 4	.122 +.004 -.000	.125 +.005 -.000
FE 4	.122 +.004 -.000	.125 +.005 -.000
FE 5	.153 +.003 -.000	.156 +.004 -.000
NW 3	.095 +.003 -.000	.098 +.004 -.000

11. MAX MISMATCH BETWEEN FAYING SURFACES, WHEN AT LEAST ONE PIECE IS BERYLLIUM, IS TO BE .010. IF MISMATCH EXCEEDS .010 CONSULT ENGINEERING FOR DISPOSITION PRIOR TO INSTALLING FASTENERS.

△10 PARTS TO BE STRAIGHT AT THEIR BEND TANGENT LINE WITHIN .005 IN ANY 5 INCH LENGTH.

9. INSTRUMENTATION REQUIRED FOR THE TEST OF THIS COMPOSITE IS AN INTREGAL PART OF THIS ASSY. AND MUST BE INSTALLED DURING FABRICATION AND ASSEMBLY. DEPT. 253 IS TO FURNISH AND INSTALL THE INSTRUMENTATION.

△8 HEAT TREAT TO 7178-T6 PER MAC PS 15529.

△7 PEEL SHIM STOCK ON ASSY AS REQ.

△6 BOND ALL PARTS OF THIS ASS'Y PER MAC PS 14044 TYPE I USE FM61 FILM ADHESIVE AND BR 227A PRIMER.
CLEANING PROCEDURE FOR BERYLLIUM PARTS PRIOR TO BONDING:
a. VAPOR DEGREASE PER MAC PS 12020.
b. ALKALINE CLEAN PER MAC PS 12030 TYPE I WITH NO CURRENT.
c. IMMERSE IN STANDARD ACID ETCH SOLUTION 155° ± 5° FOR ONE (1) MIN. (SULFURIC ACID - SODIUM DICHROMATE.)
d. RINSE THOROUGHLY. CHECK FOR WATER BREAK FREE SURFACE REPEAT ABOVE ETCHING OPERATION IF WATER BREAK APPEARS. HANDLE CLEAN PARTS ONLY WITH CLEAN WHITE COTTON GLOVES.
e. AIR DRY AT 300°F FOR 30 MIN.
f. APPLY PRIMER WITHIN 4 HRS.
X-RAY ASSEMBLY AFTER BONDING AND EXAMINE FOR VOIDS OR BOND FAILURE. THERE WILL BE NO OTHER TEST PERFORMED ON THIS ASSY. THERE WILL BE NO CONTROL SPECIMENS.

5. INSTALL FASTENERS PER MAC PS 19000.

4. DO NOT VIBRATION DRIVE ANY FASTENERS IN THIS ASSY.

3. FINAL ETCH ALL BERYLLIUM PARTS .003-.004 TOTAL THICKNESS.

2. CHEM MILL BERYLLIUM PARTS PER MAC PROCESS BULLETIN 10-67.

1. FABRICATE BERYLLIUM PARTS PER MAC PS 14104 EXCEPT FOR TOL ON FINAL ETCH. (SEE NOTE 3.)

NOTES:

	-7	-5	-3	-1	PART NUMBER	PART NAME				
	3				3M26785-2	RIVET				
	57				3M26784-2	RIVET				
	12				3M26684-1	RIVET				
	9				3M88-5	COLLAR				
	153				3M88-4	COLLAR				
	3				3M90-5-2					
	72				3M90-4-3					
	57				3M90-4-2					
	6				3M91-5-2	HI-SHEAR				
	24				3M91-4-2	HI-SHEAR				
				6	3M83-5-1	JO-BOLT				
				8	3M83-5-2	JO-BOLT				
				26	3M83-5-3	JO-BOLT				
			7		3M83-5-4	JO-BOLT				
			8		3M83-5-5	JO-BOLT				
			1		MS20002C5	WASHER				
			3		AN960-516	WASHER				
			118		AN960-10	WASHER				
			2		AN960-10L	WASHER				
			28		NAS679A3W	NUT				
			1		AN45-5A	EYE BOLT				
			3		AN5-5A	BOLT				
			41		AN3-6A	BOLT				
			21		AN3-5A	BOLT				
			2		AN3-3A	BOLT				
			3		NAS333CF4	BOLT				
			1		-67	BASE	.125X5.55X8.20	STEEL	MMS 202	B10
			1		-65	TAB	.125X1.60X3.50	STEEL	MMS 202	A11
△7				2	-63	SHIM	.062X.55X2.40	5052-H39	LAM. SHIM	B12
△7				2	-61	SHIM	.062X1.05X2.40	5052-H39	LAM SHIM	E12
△7			2		-59	SHIM	.062X1.25X8.33	5052-H39	LAM SHIM	C9
			1		-57	SPACER	.100X1.57X10.90	2024-T3 ALC	QQ-A-362 COND T3	A11
△18		1			-55	FITTING	.190X.50X23.76	PLASTIC LAMINATE	PS14034 TYPE I CLASS D	B20
			2		-53	JIG RIB	.125X2.370X2.305	STEEL	MMS-202	B11
△7			2		-51	SHIM	.062X1.25X1.90	5052-H39	LAM SHIM	C9
△7			2		-49	SHIM	.062X1.25X1.57	5052-H39	LAM SHIM	C9
△7			1		-47	SHIM	.062X1.57X10.30	5052-H39	LAM. SHIM	B10
			1		-45	SPACER	.100X1.57X10.90	2024-T3 ALC	QQ-A-362 COND. T3	B10
		2			-43	SKIN	.020X17.48X23.76	BERYLLIUM	MMS-191	C20
△16		1			-41	CORE	1.62X16.00X23.76	5052-H39	.001 FOIL X 1/4 CELL	A24
		2			-39	DOUBLER	.029X1.75X23.68	BERYLLIUM	MMS-191	E20
			1		-37	CHANNEL	.040X4.21X13.50	4130 STL	MIL-S-6758 COND. D	B11
△8	3				-35	RIB	.025X3.80X4.10	7178-0 ALC	MIL-A-9183 COND. O	D16
	3				-33	CLIP	.032X1.15X1.55	7178-T6 ALC	MIL-A-9183 COND. T6	C15
	3				-31	CLIP	.032X1.50X1.95	7178-T6 ALC	MIL-A-9183 COND. T6	D15
△10	3				-29	RIB	.036X3.64X6.10	BERYLLIUM	MMS-191	C15
	1				-28	SKIN	.084X8.95X31.80	BERYLLIUM	MMS-191	C14
	1				-27	SKIN	.084X8.95X31.80	BERYLLIUM	MMS-191	C14
△10		1			-25	REAR SPAR	.029X4.94X31.80	BERYLLIUM	MMS-191	E21
			1		-23	CHANNEL	.080X4.78X13.50	4130 STL	MIL-S-6758 COND. D	D11
△10	1				-21	FWD. SPAR	.054X5.03X31.80	BERYLLIUM	MMS-191	C16
	1				-19	SKIN	.025X5.25X22.00	7178-T6 ALC	MIL-A-9183 COND. T6	D15
△7				4	-17	SHIM	.032X.76X.84	5052-H39	LAM. SHIM	B12
△7				2	-15	SHIM	.062X.76X1.52	5052-H39	LAM. SHIM	B12
			2		-13	SPACER	.125X1.00X10.93	2024-T3 ALC	QQ-A-362 COND. T3	D9
			1		-12	JIG SKIN	.125X9.75X13.50	STEEL	MMS 202	A11
			1		-11	JIG SKIN	.125X9.75X12.50	STEEL	MMS 202	B11
△7			1		-9	SHIM	.062X1.00X10.93	5052-H39	LAM. SHIM	D9
				1	-7	RUDDER ASSY				D14
	1				-5	TRAILING EDGE				E14
				2	-3	JIG ASSY				E11

△6 -1

MCDONNELL

DRAWN J. ANDREWS E. PARK
J. Andreano
L KOCH
RCK

RUDDER COMPOSITE SECTION

76301 J 404-005
SCALE FULL
SHEET 1 OF 3

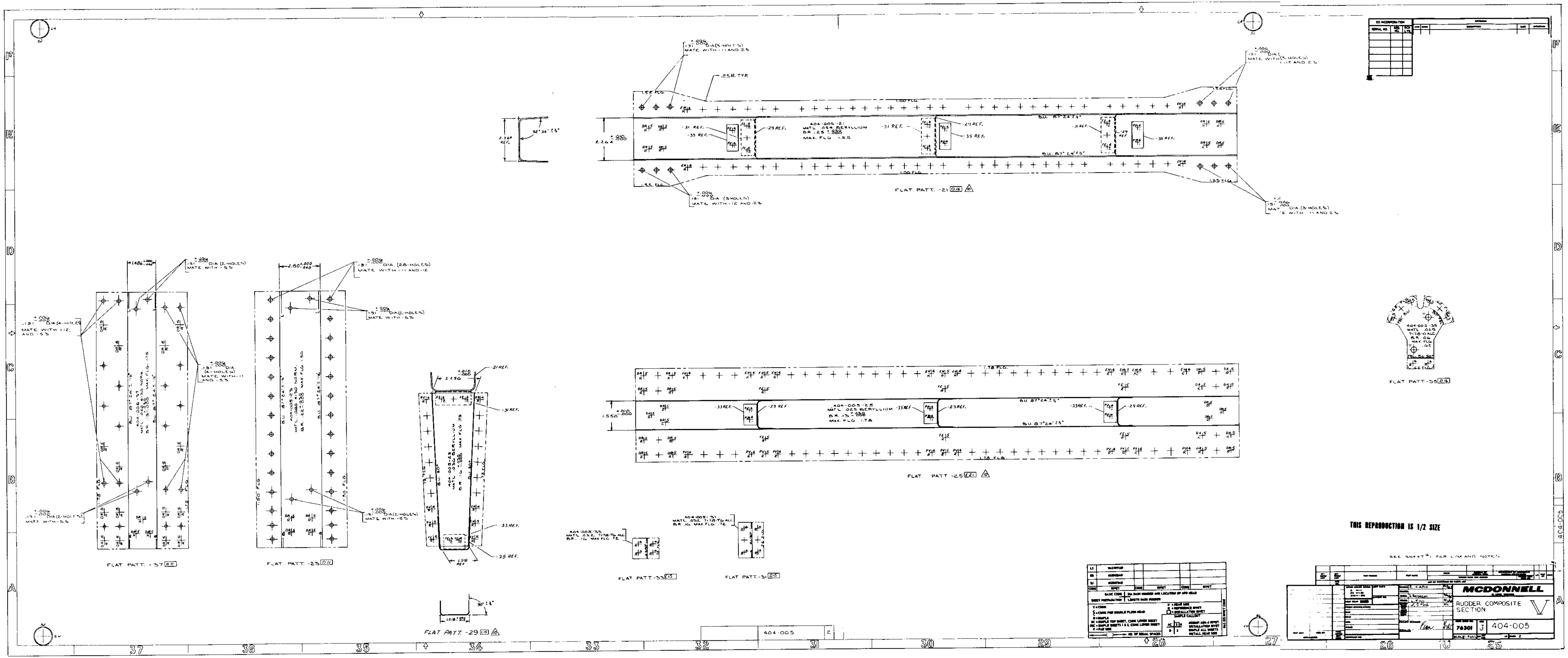

.191 +.006 -.000 DIA (3-HOLES) MATE WITH -11 AND 23
.25R. TYP.
1.55 FLG.
1.00 FLG.
92° 36' ±½°
2.264 REF.
2.264 +.010 -.000
-31 REF.
-35 REF.
-29 REF.
404-005-21
MATL .054 BERYLLIUM
BR .25 +.030 -.000
MAX. FLG 1.55
B.U. 87°24' ±½°
.191 +.006 -.000 DIA (3-HOLES) MATE WITH -12 AND 23
.191 +.006 -.000 DIA (3-HOLES) MATE WITH -11 AND 23
FLAT PATT. -21 D16 10
1.486 +.000 -.040
.191 +.006 -.000 DIA (2-HOLES) MATE WITH -53
.191 +.006 -.000 DIA (4-HOLES) MATE WITH -12, AND -53
.191 +.006 -.000 DIA (4-HOLES) MATE WITH -11 AND -53
404-005-37
MATL .040 4130 NORM.
B.R. .13 +.030 -.000 MAX. FLG. 1.75
B.U. 87°24' ±½°
1.75 FLG.
.191 +.006 -.000 DIA (2-HOLES) MATE WITH -53
FLAT PATT. -37 B11
2.150 +.000 -.040
.191 +.006 -.000 DIA. (28-HOLES) MATE WITH -11 AND -12
.191 +.006 -.000 DIA (2-HOLES) MATE WITH -53
404-005-23
MATL .080 4130 NORM.
B.R. .22 +.030 -.000 MAX. FLG. 1.50
1.50 FLG.
FLAT PATT. -23 D11
2.256 +.010 -.000
.21 REF.
.31 REF.
404-005-29
MATL .036 BERYLLIUM
B.R. .16 +.030 -.000 MAX. FLG .79
B.U. 90°
.79 FLG.
.33 REF.
.25 REF.
1.518 REF.
30° ±½°
FLAT PATT. -29 C16 10
1.550 +.010 -.000
1.78 FLG.
-33 REF.
-29 REF.
404-005-25
MATL .025 BERYLLIUM
B.R. .13 +.030 -.000
MAX. FLG. 1.78
BU 87°24' ±½°
FLAT PATT -25 E21 10
404-005-33
MATL .032 7178-T6 ALC
BR .16 MAX FLG .72
FLAT PATT. -33 C15
404-005-31
MATL .032 7178-T6 ALC
BR .16 MAX FLG. .72
FLAT PATT. -31 D15
404-005-35
MATL .025
7178-0 ALC.
B.R. .06
MAX. FLG.
.62
FBL. BU 90°
.62 FLG.
FLAT PATT -35 D16
THIS REPRODUCTION IS 1/2 SIZE
SEE SHEET #1 FOR L/M AND NOTES
CODE
RIVET
BASIC CODE
SHEET PREPARATION
LENGTH DASH NUMBER
C = CSINK
D = DIMPLE
P = PAD SIDE
SAMPLE CALLOUT
INSTALLATION RIVET
NO. OF EQUAL SPACES
E. FARK
MCDONNELL
RUDDER COMPOSITE SECTION
V
76301
J
404-005
SCALE-FULL
2
404-005
F
E
D
C
B
A
37
36
35
34
33
32
31
30
29
28
27
26
25

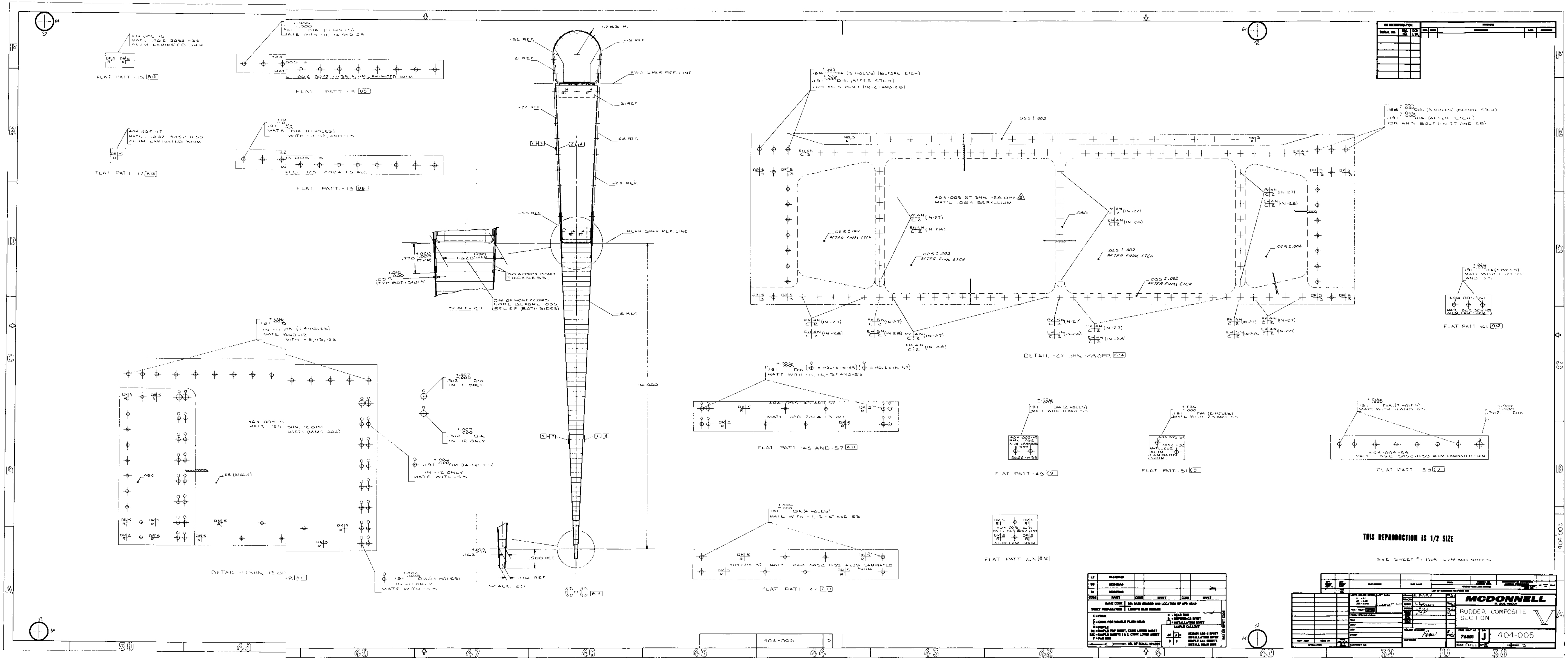
FLAT PATT -15 B12
404-005-15 MAT'L .062 5052 H39 ALUM LAMINATED SHIM
FLAT PATT -9 D5
.191 +.006 -.000 DIA. (11 HOLES) MATE WITH -11, -12 AND -23
404-005-9 MAT'L .062 5052-H39 ALUM LAMINATED SHIM
FLAT PATT -17 B12
404-005-17 MAT'L .032 5052-H39 ALUM LAMINATED SHIM
FLAT PATT -13 D8
404-005-13 MAT'L .125 7024 T3 ALC
-35 REF
-21 REF
-31 REF
-27 REF
-23 REF
-25 REF
-33 REF
-5 REF
.1283 R.
FWD SPAR REF LINE
REAR SPAR REF LINE
SCALE 2:1
.010 APPROX BOND THICKNESS
DIM OF HONEYCOMB CORE BEFORE .035 RELIEF (BOTH SIDES)
.035 (TYP BOTH SIDES)
.770
1.620
12.000
.500 REF
.116 REF
.162 +.000 -.010
C-C
.188 +.005 -.000 DIA (3 HOLES) (BEFORE ETCH)
.191 +.006 -.000 DIA. (AFTER ETCH)
FOR AN3 BOLT (IN -27 AND -28)
.055 ± .002
404-005-27 SHN. -28 OPP. 2
MAT'L .064 BERYLLIUM
.025 ± .002 AFTER FINAL ETCH
.080
DETAIL -27 SHN. -28 OPP. C14
.191 +.006 -.000 DIA (3 HOLES) MATE WITH -11, -27, -21 AND -23
404-005-61 MAT'L .062 5052-H39
FLAT PATT -61 D12
.191 +.006 -.000 DIA. (14 HOLES) IN -11 AND -12 MATE WITH -9, -13, -23
404-005-11 MAT'L .125 SHN. -12 OPP. STEEL (MMS 202)
.080
.125 (STOCK)
.312 +.007 -.000 DIA IN -11 ONLY
.312 +.007 -.000 DIA. IN -12 ONLY
.191 +.006 -.000 DIA (14 HOLES) IN -12 ONLY MATE WITH -53
.191 +.006 -.000 DIA (14 HOLES) IN -11 ONLY MATE WITH -53
DETAIL -11 SHN. -12 OPP. A11
.191 +.006 -.000 DIA (4 HOLES IN -45) (4 HOLES IN -57) MATE WITH -11, -12, -37 AND -55
404-005-45 AND 57 MAT'L .100 2024 T3 ALC
FLAT PATT -45 AND -57 A11
.191 +.006 -.000 DIA (4 HOLES) MATE WITH -11, -12, -57 AND 53
404-005-47 MAT'L .062 5052 H39 ALUM LAMINATED SHIM
FLAT PATT -47 C11
.191 +.006 -.000 DIA (2 HOLES) MATE WITH -11 AND -53
404-005-49 MAT'L .062 ALUM LAMINATED SHIM 5052-H39
FLAT PATT -49 C9
.191 +.006 -.000 DIA (2 HOLES) MATE WITH -11 AND -53
404-005-51 5052-H39 MAT'L .062 ALUM LAMINATED SHIM
FLAT PATT -51 C9
404-005-63 MAT'L .063 5052 H39 ALUM. LAM. SHIM
FLAT PATT -63 B12
.191 +.006 -.000 DIA (7 HOLES) MATE WITH -11 AND -53
.312 +.007 -.000 DIA
404-005-59 MAT'L .062 5052-H39 ALUM LAMINATED SHIM
FLAT PATT -59 C2
THIS REPRODUCTION IS 1/2 SIZE
SEE SHEET #1 FOR L/M AND NOTES
MCDONNELL
ST. LOUIS, MISSOURI
RUDDER COMPOSITE SECTION
V
E. PARK
S. ANDREWS
76301
J
404-005
SCALE FULL
SHEET 3
404-005

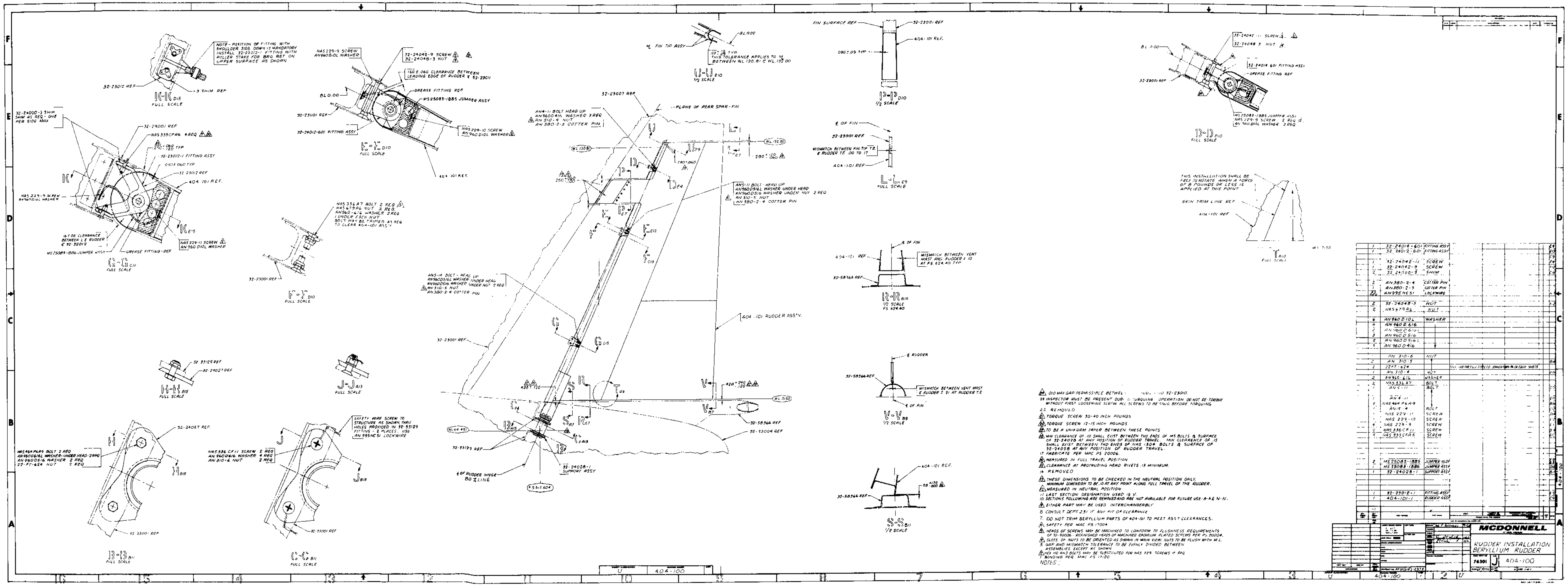
K-K D15 FULL SCALE
32-23012 REF
.3 SHIM REF
NOTE - POSITION OF FITTING WITH SHOULDER SIDE DOWN IS MANDATORY INSTALL 32-23012-1 FITTING WITH ROLLER STAKE FOR BRG RET. ON UPPER SURFACE AS SHOWN
32-24000-3 SHIM SHIM AS REQ - ONE PER SIDE MAX
32-24001 REF
NAS333CFA6 4 REQ
32-23012-1 FITTING ASSY
404-101 REF
NAS 229-9 SCREW
MS25083-1886 JUMPER ASSY
GREASE FITTING REF
NAS 229-11 SCREW
AN960 D10L WASHER
G-G C11 FULL SCALE
NAS 229-9 SCREW
AN960D10L WASHER
32-24042-9 SCREW
32-24048-3 NUT
.160 ± .060 CLEARANCE BETWEEN LEADING EDGE OF RUDDER ℄ 32-23011
GREASE FITTING REF
MS25083-1885 JUMPER ASSY
BL 0.00
32-23001 REF
32-24012-601 FITTING ASSY
NAS 229-10 SCREW
AN960 D10L WASHER
F-F D10 FULL SCALE
404-101 REF.
NAS 336 A7 BOLT 2 REQ
NAS 679 A6 NUT 2 REQ
AN960-616 WASHER 2 REQ
1 UNDER EACH NUT
BOLT MAY BE TRIMMED AS REQ TO CLEAR 404-101 ASS'Y
32-23001 REF
F-F D10 FULL SCALE
H-H B15 FULL SCALE
32-33129 REF
32-24027 REF
J-J A13 FULL SCALE
32-24027 REF.
NAS464 P6A9 BOLT 2 REQ
AN960D616L WASHER - UNDER HEAD - 2 REQ
AN960D616 WASHER 2 REQ
22-FT-624 NUT 2 REQ
32-33001 REF
B-B B11 FULL SCALE
NAS 336 CF11 SCREW 2 REQ
AN 960D616 WASHER 4 REQ
AN 310-6 NUT 2 REQ
SAFETY WIRE SCREW TO STRUCTURE AS SHOWN THRU HOLES PROVIDED IN 32-33129 FITTING - 2 PLACES. USE AN 995NC51 LOCKWIRE
32-33001 REF
C-C B11 FULL SCALE
FIN TIP ASSY
BL 0.00
.03 ± .03 TYP THIS TOLERANCE APPLIES TO ℄ BETWEEN WL 130.81 & WL 132.00
U-U E10 1/2 SCALE
32-23007 REF
PLANE OF REAR SPAR - FIN
AN4-11 BOLT HEAD UP
AN960416L WASHER 3 REQ
AN 310-4 NUT
AN 380-2-3 COTTER PIN
AN5-11 BOLT HEAD UP
AN960D516L WASHER UNDER HEAD
AN960D516 WASHER UNDER NUT 2 REQ
AN 310-5 NUT
AN 380-2-4 COTTER PIN
AN5-14 BOLT - HEAD UP
AN960D516L WASHER UNDER HEAD
AN960D516 WASHER UNDER NUT 2 REQ
AN 310-5 NUT
AN 380-2-4 COTTER PIN
404-101 RUDDER ASS'Y.
32-23001 REF
32-33129 REF
℄ OF RUDDER HINGE 80% LINE
32-24028-1 SUPPORT ASSY
FS 517.604
32-58366 REF
32-33004 REF
FIN SURFACE REF
32-23001 REF
404-101 REF
P-P D10 1/2 SCALE
℄ OF FIN
32-23001 REF
MISMATCH BETWEEN FIN TIP T.E. & RUDDER T.E. .00 TO .17
404-101 REF
L-L E9 FULL SCALE
℄ OF FIN
MISMATCH BETWEEN VENT MAST AND RUDDER ± .10 AT FS 624.40 TYP
404-101 REF
32-58366 REF
R-R B10 1/2 SCALE FS 624.40
℄ RUDDER
32-58366 REF
MISMATCH BETWEEN VENT MAST & RUDDER ± .31 AT RUDDER T.E.
℄ OF FIN
V-V B9 1/2 SCALE
404-101 REF.
32-58366 REF
S-S B11 1/2 SCALE
BL 0.00
32-24042-11 SCREW
32-24048-3 NUT
32-24014-601 FITTING ASSY
GREASE FITTING REF
32-23001 REF
MS25083-1885 JUMPER ASSY
NAS 229-9 SCREW 2 REQ
AN 960D10L WASHER 2 REQ
D-D D10 FULL SCALE
THIS INSTALLATION SHALL BE FREE TO ROTATE WHEN A FORCE OF 8 POUNDS OR LESS IS APPLIED AT THIS POINT
SKIN TRIM LINE REF.
404-101 REF
T-T B10 FULL SCALE
WL 7.50
16
15
14
13
12
11
10
9
8
7
6
5
4
3
F
E
D
C
B
A

NOTES:
1 BONDING PER MAC PS 17120
2 HEX HD AN3 BOLTS MAY BE SUBSTITUTED FOR NAS 229 SCREWS IF REQ
3. GAP AND MISMATCH TOLERANCE TO BE EVENLY DIVIDED BETWEEN ASSEMBLIES EXCEPT AS SHOWN
4 SLOTS OF NUTS TO BE ORIENTED AS SHOWN IN MAIN VIEW. NUTS TO BE FLUSH WITH M.L.
5 HEADS OF SCREWS MAY BE MACHINED TO CONFORM TO FLUSHNESS REQUIREMENTS OF 32-90006 - REFINISHED HEADS OF MACHINED CADMIUM PLATED SCREWS PER PS 20004.
6 SAFETY PER MAC PS 17004
7. DO NOT TRIM BERYLLIUM PARTS OF 404-101 TO MEET ASSY CLEARANCES.
8 CONSULT DEPT. 231 IF ANY FIT OR CLEARANCE
9 EITHER PART MAY BE USED INTERCHANGEABLY
10 SECTIONS FOLLOWING ARE REMOVED AND ARE NOT AVAILABLE FOR FUTURE USE: A-A & N-N.
11 LAST SECTION DESIGNATION USED IS V.
12 MEASURED IN NEUTRAL POSITION
13 THESE DIMENSIONS TO BE CHECKED IN THE NEUTRAL POSITION ONLY. MINIMUM DIMENSION TO BE .10 AT ANY POINT ALONG FULL TRAVEL OF THE RUDDER.
14 REMOVED
15 CLEARANCE AT PROTRUDING HEAD RIVETS .13 MINIMUM.
16 MEASURED IN FULL TRAVEL POSITION
17 FABRICATE PER MAC PS 20006.
18 MIN CLEARANCE OF .10 SHALL EXIST BETWEEN THD ENDS OF MS BOLTS & SURFACE OF 32-24028 AT ANY POSITION OF RUDDER TRAVEL. MIN CLEARENCE OF .15 SHALL EXIST BETWEEN THD ENDS OF NAS 1304 BOLTS & SURFACE OF 32-24028 AT ANY POSITION OF RUDDER TRAVEL.
19 TO BE A UNIFORM TAPER BETWEEN THESE POINTS
20 TORQUE SCREW 12-15 INCH POUNDS
21 TORQUE SCREW 30-40 INCH POUNDS
22 REMOVED
23 INSPECTOR MUST BE PRESENT DURING TORQUING OPERATION DO NOT RE-TORQUE WITHOUT FIRST LOOSENING SCREW. ALL SCREWS TO BE SNUG BEFORE TORQUING
24 .010 MAX GAP PERMISSIBLE BETWEEN [illegible] 32-23010.

1	32-24014-601	FITTING ASSY	E4
1	32-24012-601	FITTING ASSY	E13
			C9
1	32-24042-11	SCREW	F4
1	32-24042-9	SCREW	F12
2	32-24000-3	SHIM	E16
2	AN380-2-4	COTTER PIN	
1	AN380-2-3	COTTER PIN	
A/R	AN995NC51	LOCKWIRE	
2	32-24048-3	NUT	F12
2	NAS679A6	NUT	
6	AN960D10L	WASHER	
6	AN960D616		
2	AN960D616L		
3	AN960D516		
2	AN960D516L		
1	AN960D416		
	AN 310-6	NUT	
2	AN 310-5		B14
2	22FT-624		
1	AN 310-4	NUT	
2	AN960-616	WASHER	
2	NAS336A7	BOLT	
1	AN5-11	BOLT	
1	AN4-11		E11
2	NAS464P6A9		B16
1	AN5-14	BOLT	C12
1	NAS 229-11	SCREW	D14
1	NAS 229-10	SCREW	E12
4	NAS 229-9	SCREW	E11
2	NAS336CF11	SCREW	B14
4	NAS333CFA6	SCREW	E15
2	MS25083-1885	JUMPER ASSY	
1	MS25083-1886	JUMPER ASSY	D16
1	32-24028-1	SUPPORT ASSY	B11
1	32-23012-1	FITTING ASSY	E15
1	404-101-1	RUDDER ASSY	C9

MCDONNELL

RUDDER INSTALLATION
BERYLLIUM RUDDER

76301 J 404-100

AF33(616)-2374

404-100

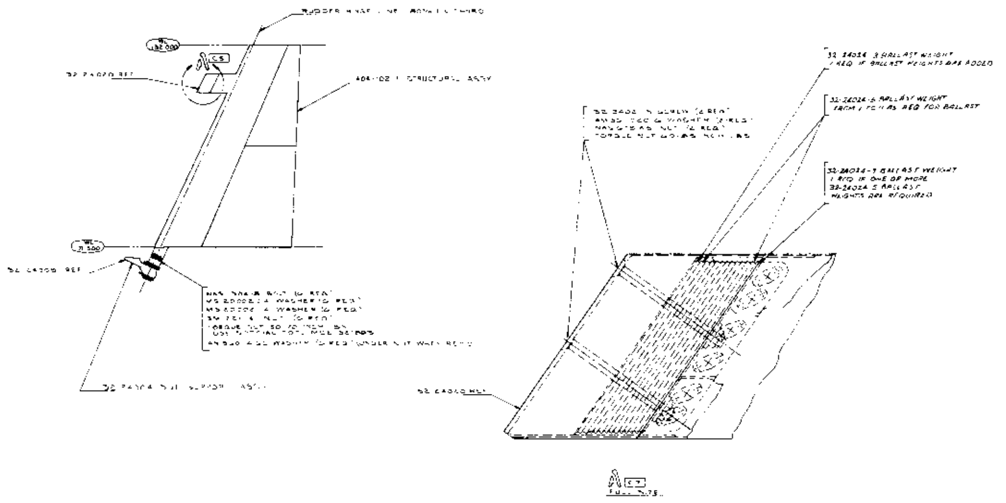
RUDDER HINGE LINE ROTATE THRU
WL 132.000
32-24020 REF
C5
404-102-1 STRUCTURAL ASSY
WL 71.500
32-24005 REF
NAS 1304-8 BOLT (6 REQ)
MS 20002C4 WASHER (6 REQ)
MS 20002-4 WASHER (6 REQ)
3M221-4 NUT (6 REQ)
TORQUE NUT 50-70 INCH LBS
USE TYPICAL TORQUE SETUPS
AN 960-416L WASHER (6 REQ) UNDER NUT WHEN REQ'D
32-24004-301 SUPPORT ASSY
32-24021-3 SCREW (2 REQ)
AN 960-C6 WASHER (2 REQ)
NAS 679 A5 NUT (2 REQ)
TORQUE NUT 40-45 INCH LBS
32-24024-3 BALLAST WEIGHT
1 REQ IF BALLAST WEIGHTS ARE ADDED
32-24024-5 BALLAST WEIGHT
FROM 1 TO 11 AS REQ FOR BALLAST
32-24024-3 BALLAST WEIGHT
1 REQ IF ONE OR MORE
32-24024-5 BALLAST
WEIGHTS ARE REQUIRED
32-24020 REF
C5
FULL SIZE

NOTE
1 MARK PN PER MAC PS 1302
2 DO NOT STEEL STAMP
3 TORQUE FASTENERS PER MAC PS 16000

QTY ASSY	QTY ASSY	QTY ASSY	QTY ASSY	PART NUMBER	PART NAME
			6	NAS 1304-8	BOLT
			6	3M221-4	NUT
			2	AN 960-C616	WASHER
			7	NAS 679 A5	NUT
			6	MS 20002 C4	WASHER
			6	MS 20002-4	WASHER
			6	AN 960-416L	WASHER
			AS REQ	32-24024-5	BALLAST WT.
			AS REQ	32-24024-3	BALLAST WT.
			2	32-24021-3	SCREW
			1	32-24004-301	SUPPORT ASSY
			1	404-102-1	STRUCTURAL ASSY

LIST OF MATERIALS OR PARTS LIST

MCDONNELL
ST. LOUIS, MISSOURI

RUDDER ASSY

SIZE J
CODE IDENT NO. 76301
404-1C1

CONTRACT NO. AF 33(615)1974

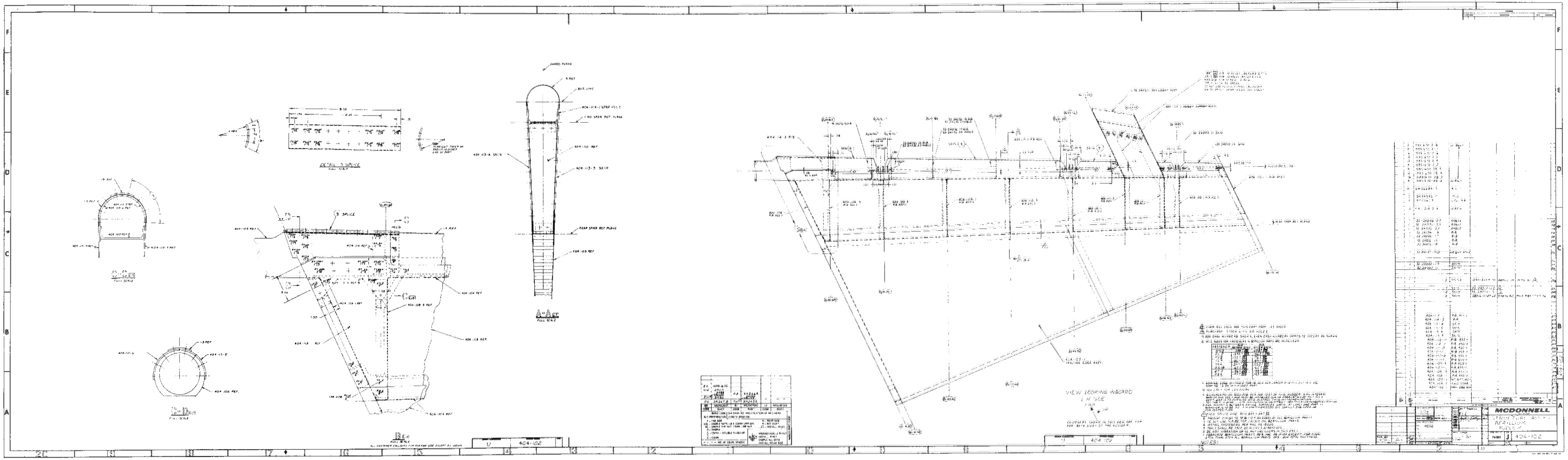
DETAIL SPLICE
FULL SCALE
A-A
FULL SCALE
404-113-5 SKIN
REAR SPAR REF PLANE
VIEW LOOKING INBOARD
NOTES:
FASTENER
MCDONNELL
STRUCTURAL ASSY
BERYLLIUM
RUDDER
76301
J
404-102

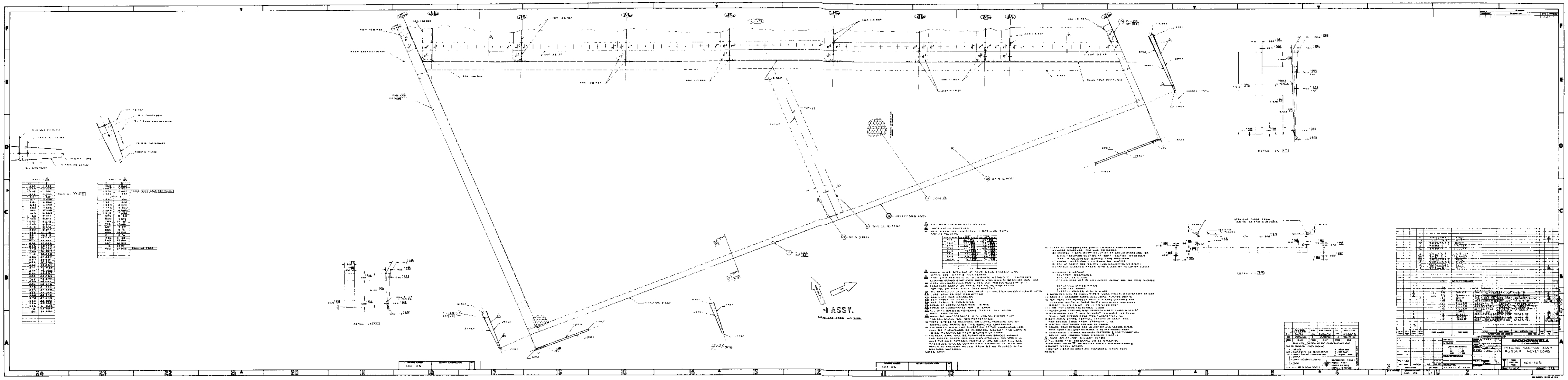
-1 ASSY.
MCDONNELL
TRAILING SECTION ASSY
RUDDER HONEYCOMB
404-105

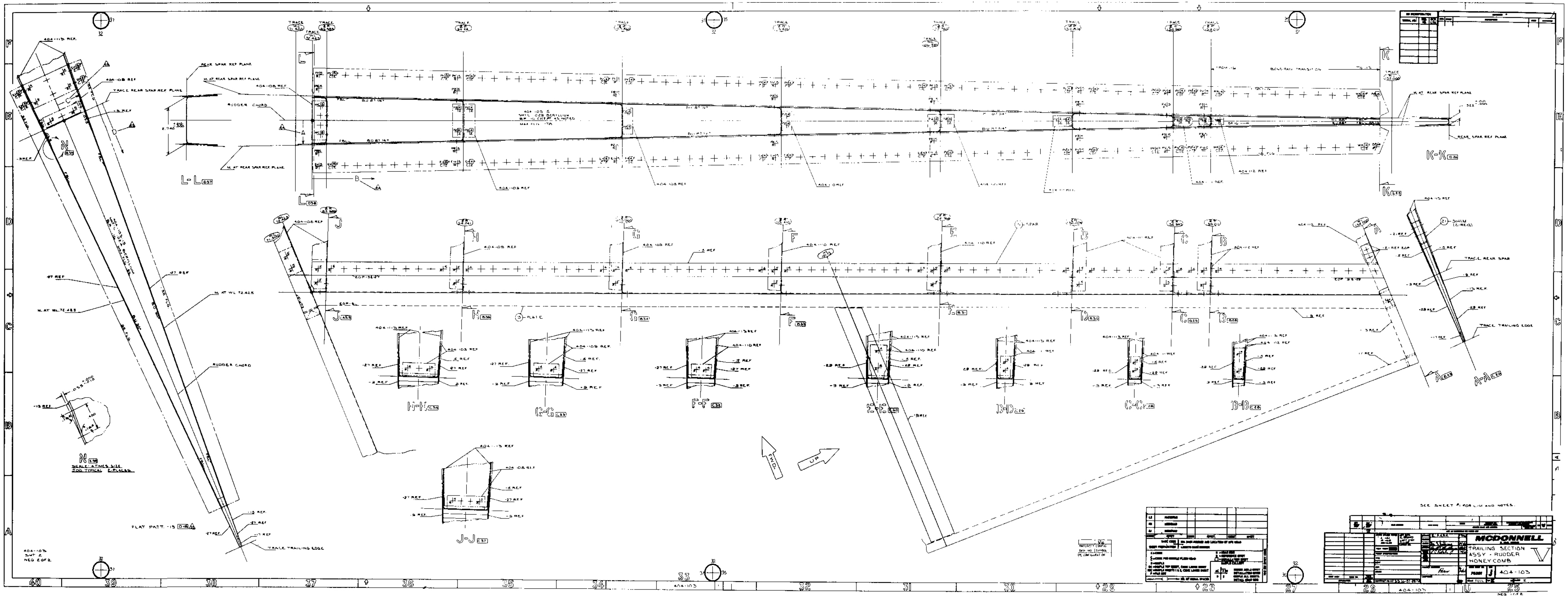
404-113 REF
404-108 REF
TRACE REAR SPAR REF PLANE
REAR SPAR REF PLANE
RUDDER CHORD
L-L
K-K
J-J
H-H
G-G
F-F
E-E
D-D
C-C
B-B
A-A
N
SCALE: 4 TIMES SIZE
TRACE TRAILING EDGE
FLAT PATT. -13
FWD
UP
404-103
SHT 2
NEG 1 OF 2
SEE SHEET 1 FOR L/M AND NOTES.
MCDONNELL
TRAILING SECTION
ASSY - RUDDER
HONEYCOMB
V
J
404-103
FULL
NEG 1 OF 2

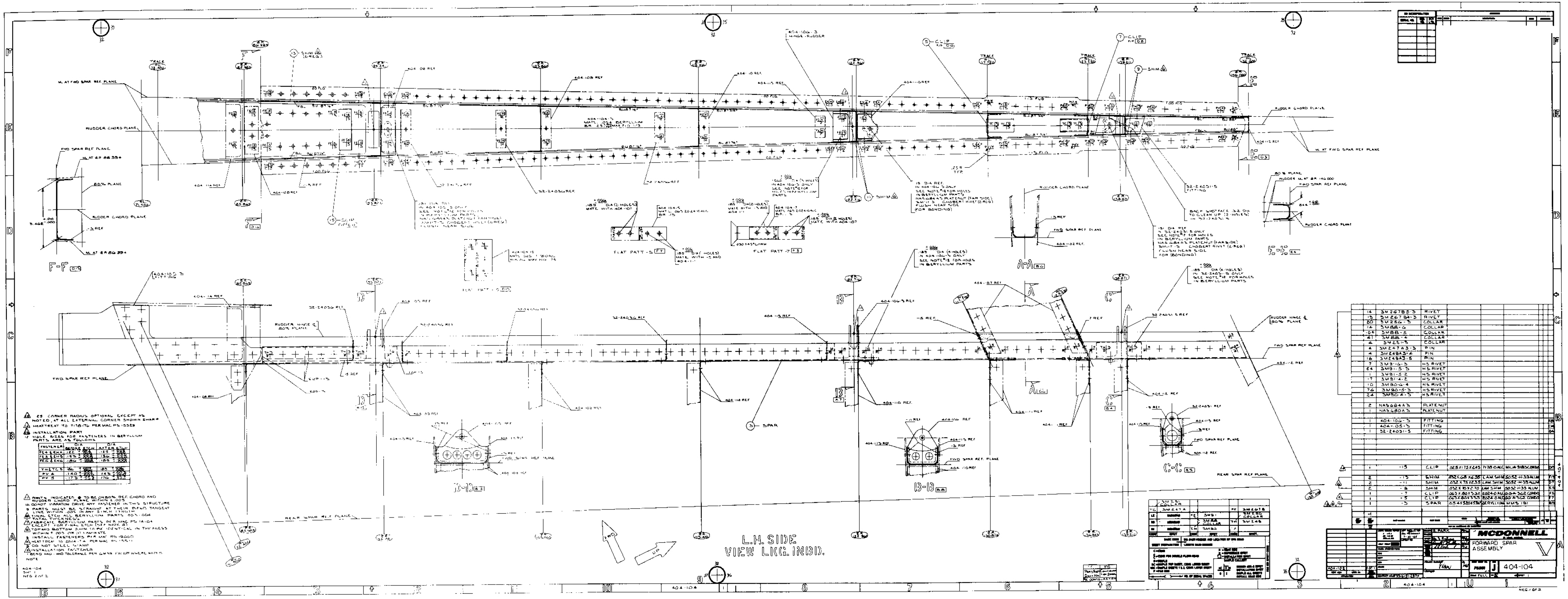

15 .25 CORNER RADIUS OPTIONAL EXCEPT AS NOTED, AT ALL EXTERNAL CORNER SHOWN SHARP

14 HEATTREAT TO 7178-T6 PER MAC PS 15529

13 INSTALLATION PART

12 HOLE SIZES FOR FASTENERS IN BERYLLIUM PARTS ARE AS FOLLOWS

FASTENER	DIA BEFORE ETCH	DIA AFTER ETCH
FE4 & EH4	.122 [illegible]	.125 [illegible]
FE5 & EH5	.153 [illegible]	.156 [illegible]
FE6 & EH6	.186 [illegible]	.189 [illegible]
THETC5	.186 [illegible]	.189 [illegible]
PV 4	.140 [illegible]	.143 [illegible]
PV 5	.173 [illegible]	.176 [illegible]

11 POINTS INDICATED ● TO BE ON 80% REF. CHORD AND RUDDER CHORD PLANE WITHIN ±.005

10. DO NOT VIBRATION DRIVE ANY FASTENER IN THIS STRUCTURE

9 PARTS MUST BE STRAIGHT AT THEIR BEND TANGENT LINE WITHIN .005 IN ANY 5 INCH LENGTH

8 FINAL ETCH ALL BERYLLIUM PARTS .003-.004 TOTAL THICKNESS

7 FABRICATE BERYLLIUM PARTS PER MAC PS 14104 EXCEPT FOR FINAL ETCH (SEE NOTE 8)

6 TOP AND BOTTOM SHIM TO BE IDENTICAL IN THICKNESS WITHIN ±.005 OR (1) LAMINATE

5 INSTALL FASTENERS PER MAC PS 19000

4 HEATTREAT TO 2024-T4 PER MAC PS 15511

3 DO NOT STEEL STAMP

2 INSTALLATION FASTENER

1 BEND RAD. AND TOLERANCE PER GM 98 EXCEPT WHERE NOTED

NOTE

404-104
SHT 1
NEG 2 OF 2

14	3M267B5-3	RIVET				
13	3M267B4-3	RIVET				
20	3M256-3	COLLAR				
14	3M88-6	COLLAR				
104	3M88-5	COLLAR				
41	3M88-4	COLLAR				
4	3M251-3	COLLAR				
4	3M247A3-3	PIN				
4	3M249A3-4	PIN				
16	3M249A3-5	PIN				
7	3M91-6-3	HS RIVET				
64	3M91-5-3	HS RIVET				
1	3M91-5-2	HS RIVET				
17	3M91-4-2	HS RIVET				
10	3M90-6-4	HS RIVET				
76	3M90-5-3	HS RIVET				
24	3M90-4-3	HS RIVET				
2	NAS684A3	PLATE NUT				
1	NAS680A3	PLATE NUT				
1	404-106-3	FITTING				
1	404-105-3	FITTING				
1	32-24031-5	FITTING				
1	-15	CLIP	.025 X 1.75 X 2.45	7178-0 ALC	MIL-A-9180 COND	
2	-13	SHIM	.032 X .68 X 2.38	LAM. SHIM	5052-H-39 ALUM	
2	-11	SHIM	.032 X .75 X 2.35	LAM. SHIM	5052-H-39 ALUM	
2	-9	SHIM	.032 X .70 X 2.70	LAM SHIM	5052-H39 ALUM	
1	-7	CLIP	.063 X .80 X 3.32	2024-0 ALC	QQ-A-362 COND	
1	-5	CLIP	.063 X .80 X 3.55	2024-0 ALC	QQ-A-362 COND	
1	-3	SPAR	.054 X 3.20 X 55.56	BERYLLIUM	MMS 191	

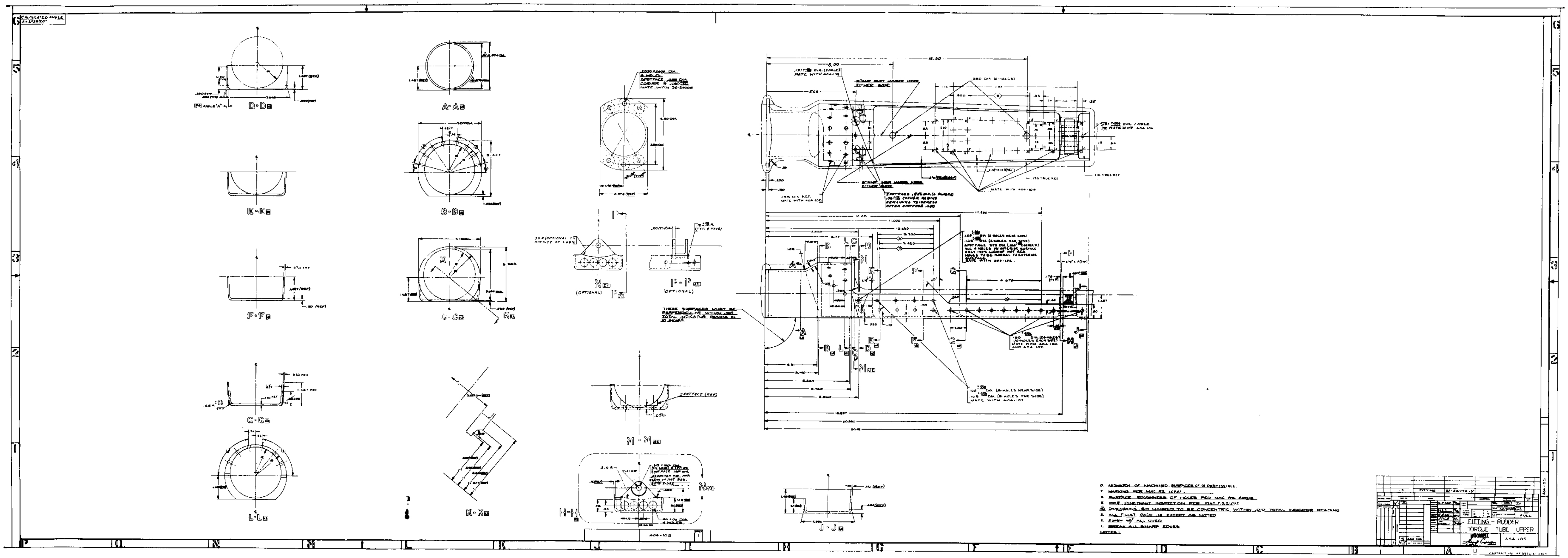
CALCULATED ANGLE
D-D
A-A
B-B
E-E
F-F
C-C
G-G
K
N
(OPTIONAL)
P-P
(OPTIONAL)
THESE SURFACES MUST BE PERPENDICULAR WITHIN .010 TOTAL INDICATOR READING IN 10 INCHES
STAMP PART NUMBER HERE EITHER SIDE
MATE WITH 404-104
MATE WITH 404-103
16.50
8.00
17.430
20.380
C-C
L-L
K-K
M-M
H-H
J-J
SPOTFACE (REF)
404-105
-3
FITTING
32-24039-3F
FULL
FITTING - RUDDER
TORQUE TUBE UPPER
404-105
CONTRACT NO. AF 33(G)51-2374

8. MISMATCH OF MACHINED SURFACES OF .01 PERMISSIBLE.
7. MARKING PER MAC P.S. 16001.
6. SURFACE ROUGHNESS OF HOLES PER MAC PS 20018
5. 100% PENETRANT INSPECTION PER MAC P.S. 21202
4. DIMENSIONS SO MARKED TO BE CONCENTRIC WITHIN .010 TOTAL INDICATOR READING.
3. ALL FILLET RADII .16 EXCEPT AS NOTED
2. FINISH 125 ALL OVER
1. BREAK ALL SHARP EDGES
NOTES:

CALCULATED ANGLES
A : 2° 21′ 55″

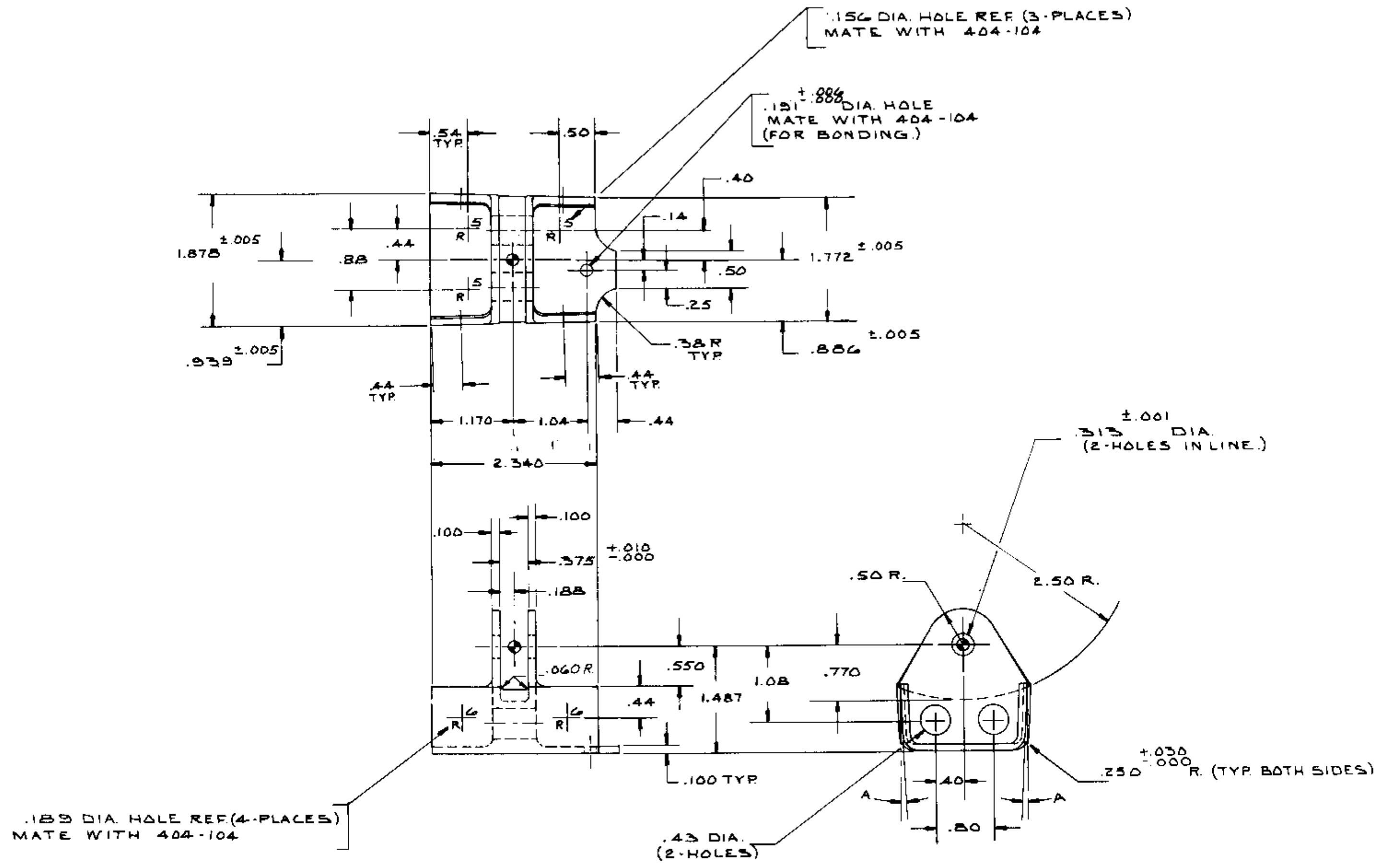
.156 DIA. HOLE REF (3-PLACES)
MATE WITH 404-104
.151 +.006 -.000 DIA. HOLE
MATE WITH 404-104
(FOR BONDING.)
.54 TYP
.50
.40
.14
1.878 ±.005
.88
.44
5 R
5 R
5 R
.50
.25
1.772 ±.005
.939 ±.005
.38 R TYP
.886 ±.005
.44 TYP
.44 TYP
1.170
1.04
.44
2.340
.313 ±.001 DIA.
(2-HOLES IN LINE.)
.100
.100
.375 +.010 -.000
.188
.50 R.
2.50 R.
.060 R
.550
.44
1.487
1.08
.770
6 R
6 R
.100 TYP
.250 +.030 -.000 R. (TYP. BOTH SIDES)
A
A
.40
.80
.189 DIA. HOLE REF (4-PLACES)
MATE WITH 404-104
.43 DIA.
(2-HOLES)

7. PENETRANT INSPECTION PER MAC PS. 21202.
6. SURFACE ROUGHNESS OF HOLES PER MAC PS 20018.
5. DO NOT STEEL STAMP.
4. SURFACE ROUGHNESS $\sqrt{}$ 125 OR BETTER, ALL OVER.
3. MACHINE FINISH PER MAC PS 23041.
2. BREAK ALL SHARP EDGES PER PS 23041.
1. MACHINED FILLET RADII TO BE .13 EXCEPT AS SHOWN.
NOTES:

QTY REQD/ ASSY	QTY REQD/ ASSY	PART NUMBER	PART NAME	STOCK	MATERIAL OR MATERIAL CODE	GOVERNMENT OR COMMERCIAL MATERIAL SPECIFICATION	I/R	UNIT WT	ZONE
		-3	HINGE	2.00 X 2.10 X 2.70	7075-T6 AL AL	QQ-A-282 COND-T6			

FIND NO.	LIST OF MATERIALS OR PARTS LIST

NEXT ASSY	USED ON	FINAL ARTICLE QTY REQD
404-102		1 OF-3

APPLICATION

LIMITS UNLESS NOTED
.X = ±.1
.XX = ±.03
.XXX = ±.010

LOFT DATA

LAYOUT NO.

HEAT TREAT NOTED

FINISH SPECIFICATIONS
MAC 32-90000
USAF
USN
OTHER

CONTRACT NO. AF33(615)-2974

DRAWN E. FARK 7/26
TRACED
CHECK J.K.H. 12/8/65
STRESS Donald E. Muehlberger 12/10/65
GROUP ENGR E.C. Koch 12/10
ELEC ENGR
MECH ENGR
PROJECT ENGINEER 12/14/65
CUSTOMER

MCDONNELL
ST. LOUIS, MISSOURI

HINGE — RUDDER

CODE IDENT NO. 76301
SIZE D
404-106
SCALE FULL
WT ACT CAL LB
SHEET 1

MAC 1190D (REV 22 APR 63)

404-106

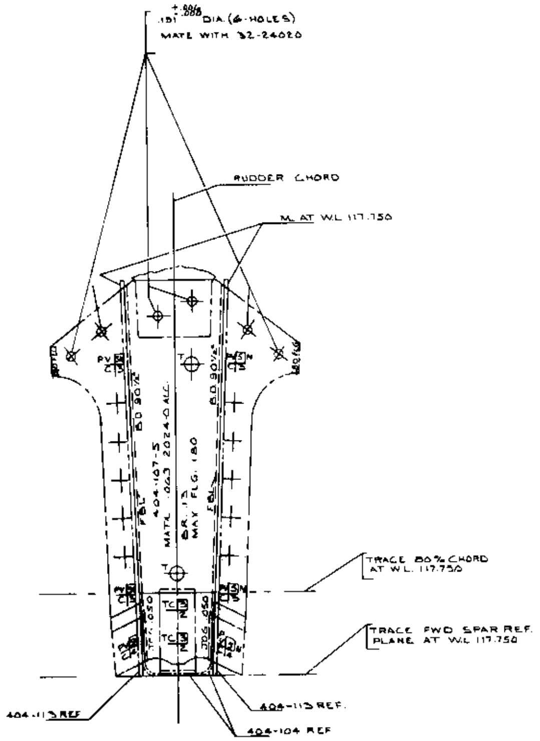
.151 +.006 -.000 DIA. (6-HOLES)
MATE WITH 32-24020
RUDDER CHORD
ML AT W.L. 117.750
PV
C
404-107-5
MATL .063 2024-0 ALC.
BR. 13
MAX FLG. 180
B.D. 90½°
FBL
T
TC
.050
JOG
TRACE 80% CHORD AT W.L. 117.750
TRACE FWD SPAR REF. PLANE AT W.L. 117.750
404-113 REF
404-113 REF.
404-104 REF

FLAT PATT. -5 D7

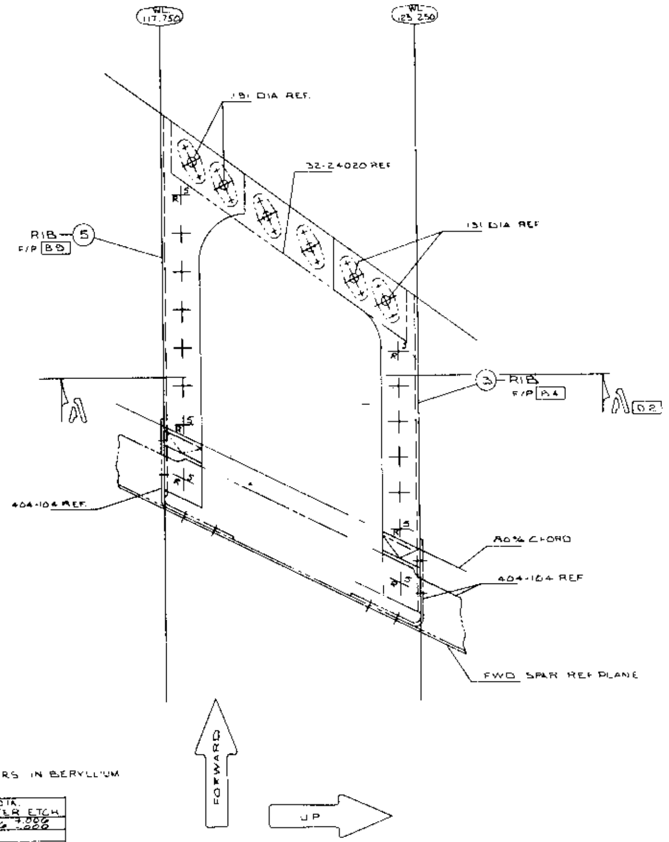
WL 117.750
WL 123.250
.151 DIA REF.
32-24020 REF
.151 DIA REF
RIB 5
F/P B9
3 RIB
F/P A4
A
A D2
404-104 REF.
80% CHORD
404-104 REF
FWD SPAR REF PLANE
FORWARD
UP

-1 ASSY
VIEW LKG INBD.

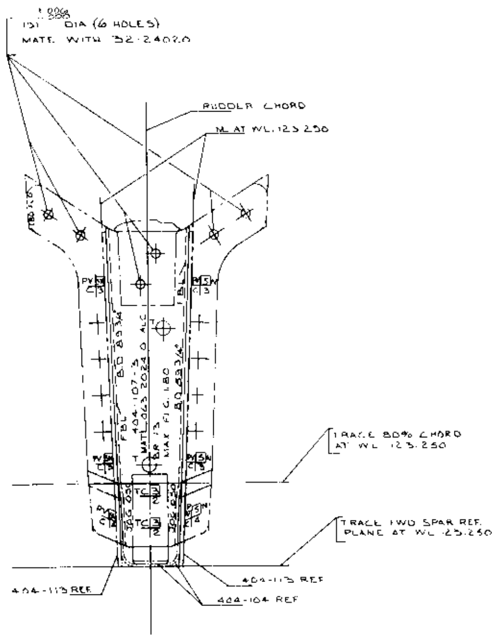
.151 +.006 -.000 DIA (6 HOLES)
MATE WITH 32-24020
RUDDER CHORD
ML AT WL 123.250
PV
C
404-107-3
MATL .063 2024-0 ALC
BR. 13
MAX FLG. 180
B.D. 89¾°
B.D. 83¾°
FBL
T
TC
JOG .030
TRACE 80% CHORD AT WL 123.250
TRACE FWD SPAR REF. PLANE AT WL 123.250
404-113 REF
404-113 REF
404-104 REF

FLAT PATT -3 C6

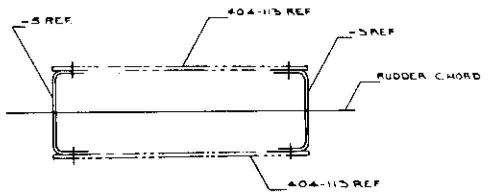
-5 REF
404-113 REF
-3 REF
RUDDER CHORD
404-113 REF

A-A C5

10 HOLE SIZES FOR FASTENERS IN BERYLLIUM PARTS ARE AS FOLLOWS:

FASTENER	DIA BEFORE ETCH	DIA. AFTER ETCH
PV5	$.175^{+.003}_{-.000}$	$.176^{+.006}_{-.000}$

9 HOLE SIZE FOR 3M247A3 HI-LOCKS TO BE $.189^{+.004}_{-.000}$ IN ALUM. PARTS.

8. INSTALL FASTENERS PER MAC PS 19000

7 HEAT TREAT TO 2024-T4 PER MAC PS 15511.

6 INSTALLATION FASTENERS

5 MARKING PER MAC PS 16001

4. ALL JOGGLES PER GM51.

3 ALL BEND RADII PER GM33.

2. FABRICATE PER MAC PS 20006.

1. BREAK ALL SHARP EDGES

NOTE

LZ		PV	3M267B		
			3M251 COLLAR		
		TC	3M247A3		
CODE	RIVET	CODE	RIVET	CODE	RIVET

BASIC CODE | NAS DASH NUMBER AND LOCATION OF MFD HEAD
SHEET PREPARATION | LENGTH DASH NUMBER

C = CSNK
D = DIMPLE
DC = DIMPLE TOP SHEET, CSNK LOWER SHEET
F = FAR SIDE
N = NEAR SIDE
R = REFERENCE RIVET
☐ = INSTALLATION RIVET
SAMPLE CALLOUT
NO. OF EQUAL SPACES
NAS 523 RIVET CODE

	4	3M251-3	COLLAR						
	4	3M247A3-2	PIN						
	4	3M267B5-4	RIVET						
	26	3M267B5-3	RIVET						
	1	-5	RIB	.063X5.50X8.62	2024-0ALC	QQ-A-362 COND-0			D7
	1	-3	RIB	.063X5.25X7.60	2024-0ALC	QQ-A-362 COND-0			C6
	-1								

404-107

404-102		1 OF -1
NEXT ASSY	USED ON	
APPLICATION		

LOFT DATA
LOFT 4045
J HS 850 AMF
9-8-65

CONTRACT NO. AF33(615) 2974

DRAWN E. FARK

MCDONNELL
ST. LOUIS, MISSOURI

RIB ASSY. RUDDER
UPPER BALANCE
WEIGHT.

CODE IDENT NO. 76301
SIZE J
404 107
SCALE FULL
SHEET 1

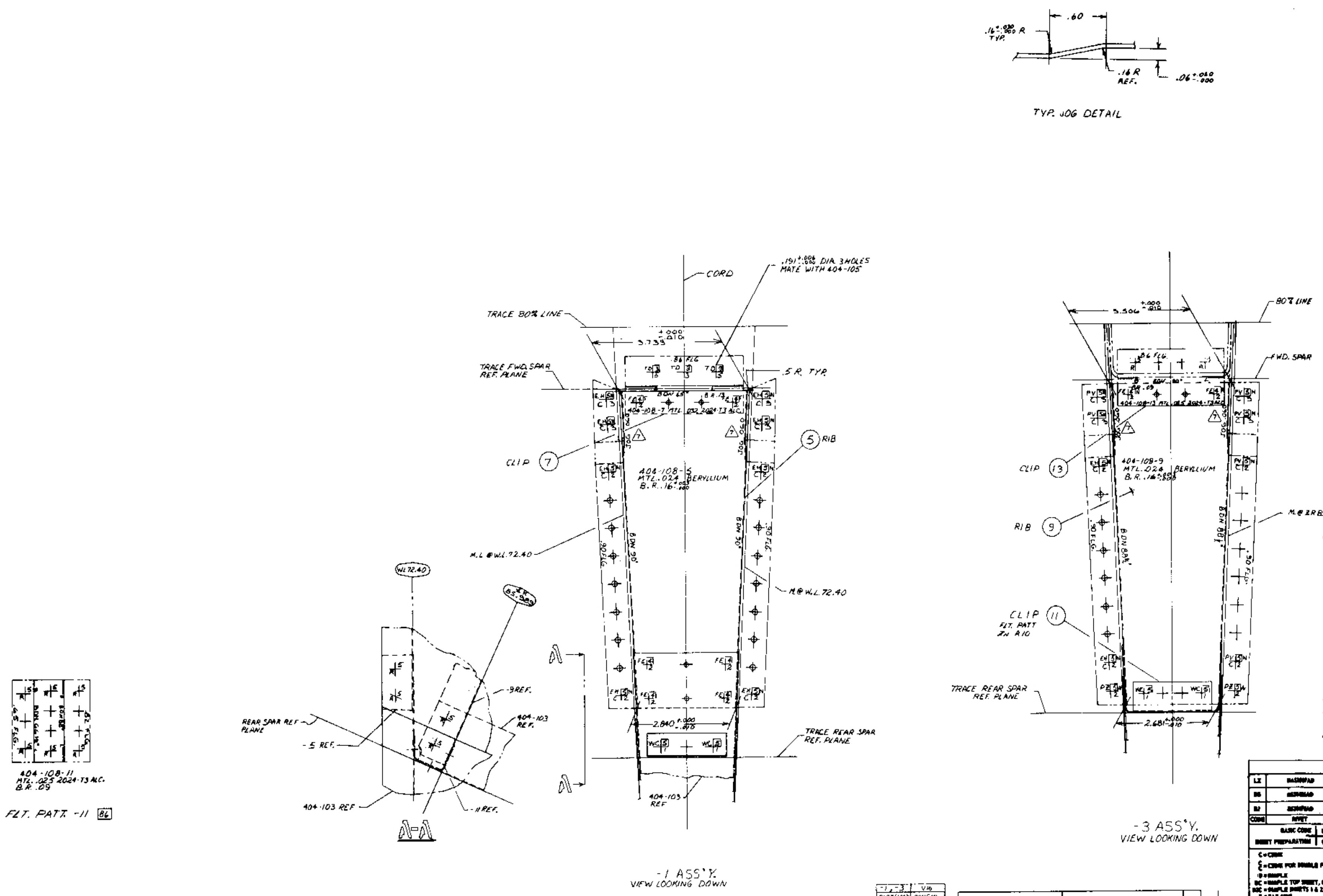
.16 +.030 -.000 R TYP.
.60
.16 R REF.
.06 +.020 -.000
TYP. JOG DETAIL
CORD
.191 +.006 -.000 DIA. 3 HOLES MATE WITH 404-105
TRACE 80% LINE
3.739 +.000 -.010
TRACE FWD. SPAR REF. PLANE
.5 R. TYP.
.86 FLG
404-108-7 MTL .032 2024-T3 ALC.
CLIP 7
5 RIB
404-108-5 MTL .024 BERYLLIUM B.R. .16 +.003 -.000
JOG .060
BDN 90°
.90 FLG.
M.L @ W.L. 72.40
M @ W.L. 72.40
WL 72.40
ZR 85.989
-9 REF.
404-103 REF.
REAR SPAR REF. PLANE
-5 REF.
404-103 REF
-11 REF.
A
A-A
2.840 +.000 -.010
TRACE REAR SPAR REF. PLANE
404-103 REF
-1 ASS'Y. VIEW LOOKING DOWN
404-108-11 MTL .025 2024-T3 ALC. B.R. .09
FLT. PATT. -11
5.506 +.000 -.010
80% LINE
FWD. SPAR
404-108-13 MTL .025 2024-T3 ALC.
CLIP 13
404-108-9 MTL .024 BERYLLIUM B.R. .16 +.003 -.000
RIB 9
BDN 88°
BDN 88½°
CLIP 11 FLT. PATT ZN A10
TRACE REAR SPAR REF. PLANE
2.681 +.000 -.010
M @ ZR 85.989
-3 ASS'Y. VIEW LOOKING DOWN

8. .25 CORNER RADIUS OPTIONAL, EXCEPT AS NOTED, AT ALL EXTERNAL CORNER SHOWN SHARP.

7. TOLERANCE ON JOGGLE DEPTH TO BE +.020 -.000.

6. HOLE SIZES FOR FASTENERS IN BERYLLIUM PARTS ARE AS FOLLOWS.

FASTENER	DIA. BEFORE ETCH	DIA. AFTER ETCH
FE5 & EH5	.153 +.002 -.000	.156 +.002 -.000
FE4	.122 +.002 -.000	.125 +.002 -.000
PV5 & WS	.173 +.002 -.000	.176 +.002 -.000
WC5	.173 +.002 -.000	.176 +.002 -.000

5. DO NOT VIBRATION DRIVE ANY FASTENER IN THIS STRUCTURE.
4. PARTS TO BE STRAIGHT AT THEIR BEND TANGENT LINE WITHIN .005 IN ANY 5 INCH LENGTH.
3. INSTALL FASTENERS PER MAC PS 19000.
2. FINAL ETCH ALL BERYLLIUM PARTS .003-.004 TOTAL THICKNESS.
1. FABRICATE BERYLLIUM PARTS PER MAC PS 14104 EXCEPT FOR FINAL ETCH. (SEE NOTE 2)

NOTES:

	WC	3M266M	3M256 COLLAR
LX	EH	3M90	TD 3M247A
		3M88 COLLAR	PW 3M267B
	FE	3M91	PZ 3M266B
CODE	RIVET	CODE	RIVET

-3	-1						
	4	3M90-5-3	PIN				
4		3M267B5-3	RIVET				
	3	3M256C3	COLLAR				
	1	3M247A3-3	PIN				
	2	3M247A3-5	PIN				
4	10	3M88-4	COLLAR				
4	10	3M91-4-2	PIN				
8	18	3M90-5-2	PIN				
8	22	3M88-5	COLLAR				
2		3M266B52	RIVET				
8		3M267B5-2	RIVET				
4	3	3M266M5P-1	RIVET				
1		-13	CLIP	.025×1.51×3.07	2024-T3 ALC.	QQ-A-362 COND. T3	C6
1		-11	CLIP	.025×2.26×2.29	2024-T3 ALC.	QQ-A-362 COND. T3	B6
1		-9	RIB	.024×5.08×8.89	BERYLLIUM	MMS-191	B6
	1	-7	CLIP	.032×1.59×3.40	2024-T3 ALC.	QQ-A-362 COND. T3	C8
	1	-5	RIB	.024×5.40×9.10	BERYLLIUM	MMS-191	C7

8 2 1 (-9)
8 2 1 (-5)

SEE DCN

-1, -3	V16		
PART/ASS'Y DASH NO.	CONFIG SYMBOL		
M. CONFIGURATION			

404-102 1ST -3
404-102 1ST -1

LAYOUT NO. 404-601

HEAT TREAT NONE

CONTRACT NO. AF 33(615)-2374

MCDONNELL

RIB ASS'Y
WL 72.400 & ZR 85.869

V

76301 J 404-108

SCALE FULL

404-108

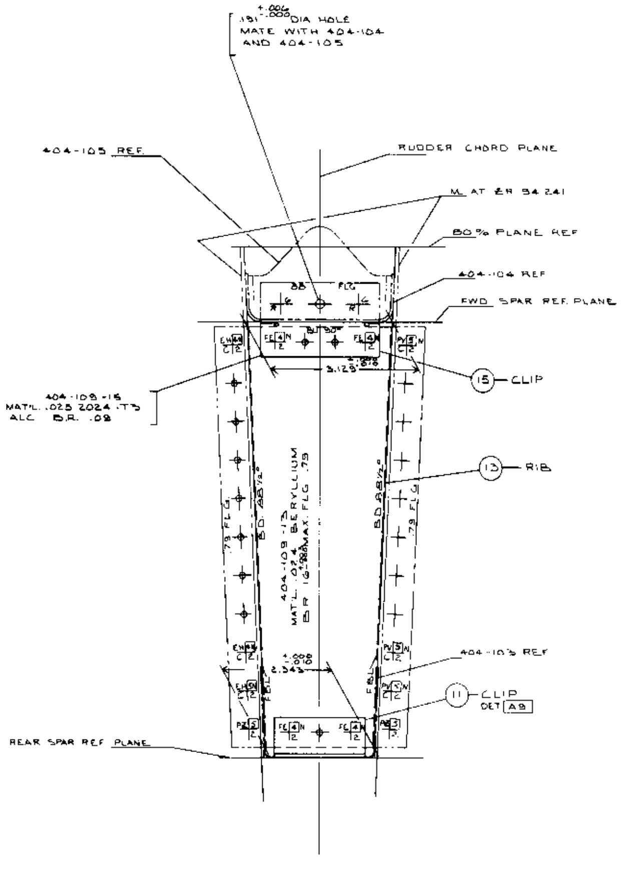
.191 +.006 -.000 DIA HOLE
MATE WITH 404-104
AND 404-105
404-105 REF.
RUDDER CHORD PLANE
ML AT ZR 94.241
80% PLANE REF
404-104 REF
FWD. SPAR REF. PLANE
BB FLG
BL 90°
3.129 ±.010
15 CLIP
404-109-15
MAT'L .025 2024-T3
ALC B.R. .09
13 RIB
.79 FLG.
BD. 88½°
404-109-13
MAT'L .024 BERYLLIUM
B.R. 16 MAX. FLG. .79
2.343 +.008 -.010
404-103 REF
11 CLIP
DET A9
REAR SPAR REF PLANE

-3 ASSY
VIEW LKG DN.

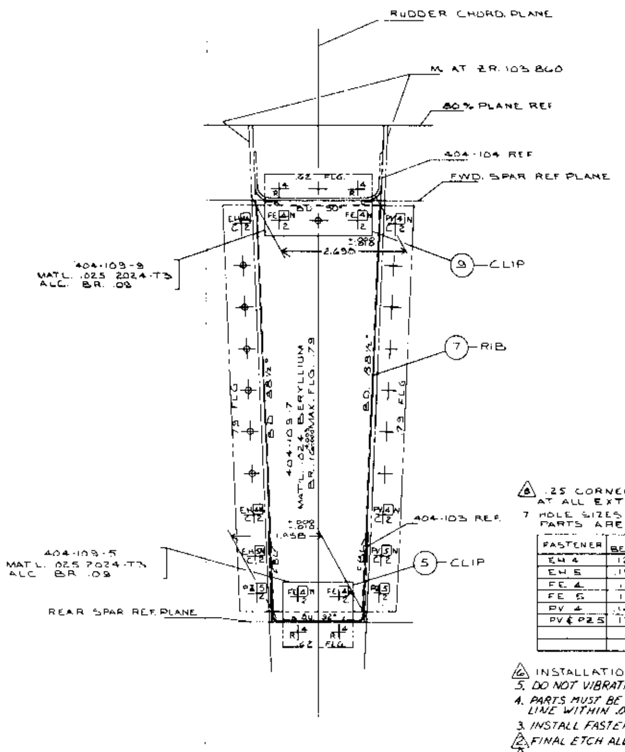
RUDDER CHORD PLANE
ML AT ZR 103.860
80% PLANE REF
404-104 REF
FWD. SPAR REF PLANE
.82 FLG.
BL 90°
2.690 ±.010
9 CLIP
404-109-9
MAT'L .025 2024-T3
ALC. BR. .09
7 RIB
.79 FLG
BD. 88½°
404-109-7
MAT'L .024 BERYLLIUM
BR. 16 MAX. FLG. .79
1.858 +.008 -.010
404-103 REF.
5 CLIP
404-109-5
MAT'L .025 2024-T3
ALC BR .09
REAR SPAR REF. PLANE
.62 FLG.

-1 ASSY
VIEW LKG DN.

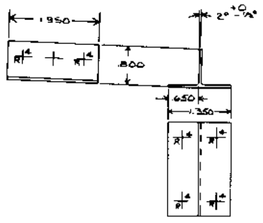
1.950
2° +0 -½°
.800
.650
1.350

DETAIL -11 B7
MATL 1M5462
7178-T6 AL.AL.

8. .25 CORNER RADIUS OPTIONAL, EXCEPT AS NOTED, AT ALL EXTERNAL CORNER SHOWN SHARP.

7. HOLE SIZES FOR FASTENERS IN BERYLLIUM PARTS ARE AS FOLLOWS.

FASTENER	DIA. BEFORE ETCH	DIA. AFTER ETCH
EH 4	.122 $^{+.004}_{-.000}$	.125 $^{+.003}_{-.000}$
EH 5	.153 $^{+.005}_{-.000}$	.156 $^{+.006}_{-.000}$
FE 4	.122 $^{+.004}_{-.000}$	.125 $^{+.003}_{-.000}$
FE 5	.153 $^{+.005}_{-.000}$	.156 $^{+.006}_{-.000}$
PV 4	.140 $^{+.003}_{-.000}$	.143 $^{+.003}_{-.000}$
PV & PZ 5	.173 $^{+.003}_{-.000}$	.176 $^{+.003}_{-.000}$

6. INSTALLATION FASTENER

5. DO NOT VIBRATION DRIVE ANY FASTENER IN THIS STRUCTURE

4. PARTS MUST BE STRAIGHT AT THEIR BEND TANGENT LINE WITHIN .005 IN ANY 5 INCH LENGTH.

3. INSTALL FASTENERS PER MAC P.S. 19000

2. FINAL ETCH ALL BERYLLIUM PARTS .003-.004 TOTAL THICKNESS

1. FABRICATE BERYLLIUM PARTS PER MAC PS 14104 EXCEPT FOR FINAL ETCH. (SEE NOTE 2)

NOTES

	-3	-1						
6	10	1	3M267B-5-2	RIVET				
6		8	3M267B-4-2	RIVET				
6	1	1	3M88-5	COLLAR				
6	16	13	3M88-4	COLLAR				
6	2	2	3M266B5-2	RIVET				
6	7	5	3M91-4-2	H.S. RIVET				
6	1	1	3M90-5-2	H.S. RIVET				
6	9	8	3M90-4-2	H.S. RIVET				
	1		-15	CLIP	.025X1.60X2.65	2024-T3ALC	QQ-A-362 COND T3	C7
8 2 1	1		-13	RIB	.024X4.65X8.70	BERYLLIUM	MMS 191	C7
	1		-11	CLIP	1M5462 X2.00	7178T6 AL	MIL-A-9186 COND T6	B7
		1	-9	CLIP	.025X1.35X2.35	2024-T3ALC	QQ-A-362 COND T3	C5
8 2 1		1	-7	RIB	.024X4.20X8.45	BERYLLIUM	MMS 191	C5
		1	-5	CLIP	.025X1.40X1.60	2024-T3ALC	QQ-A-362 COND T3	B5

CODE	RIVET	CODE	RIVET	CODE	RIVET
LZ	NAS1097AD	EH	3M90	PZ	3M266B
BB	MS20426AD		3M88 COLLAR	PV	3M267B
BJ	MS20470AD	FE	3M91		

BASIC CODE | DIA DASH NUMBER AND LOCATION OF MFD HEAD
SHEET PREPARATION | LENGTH DASH NUMBER

C = CSNK
C̶ = CSNK FOR DOUBLE FLUSH HEAD
D = DIMPLE
DC = DIMPLE TOP SHEET, CSNK LOWER SHEET
DDC = DIMPLE SHEETS 1 & 2, CSNK LOWER SHEET
F = FAR SIDE
N = NEAR SIDE
R = REFERENCE RIVET
☐ = INSTALLATION RIVET
NO. OF EQUAL SPACES

SAMPLE CALLOUT
AC 5 N / D 2
MS20601 AD5-2 RIVET INSTALLATION RIVET DIMPLE ALL SHEETS INSTALL NEAR SIDE

MAC 323 RIVET CODE

V6
MULTI DASH CONFIG
DASH NO. SYMBOL
& CONFIGURATION

404-109

404-102 | 1OF-3
404-102 | 1OF-1
APPLICATION

LOFT 2809
E. FARK
CONTRACT NO. AF 33(615)-2974

MCDONNELL

RIB ASS'Y
ZR 94.241 & ZR 103.86
V

76301 | J | 404-109
SCALE FULL

404-109

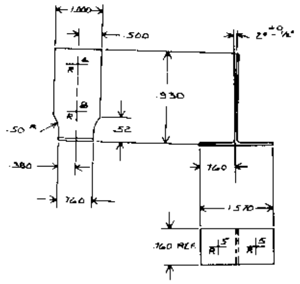

1.000
.500
2°+0/-1/2°
.930
.50 R
.52
.380
.760
.760
1.510
.760 REF

DETAIL -5 B4
MAT'L. 1M5462
7178-T6 AL.AL.

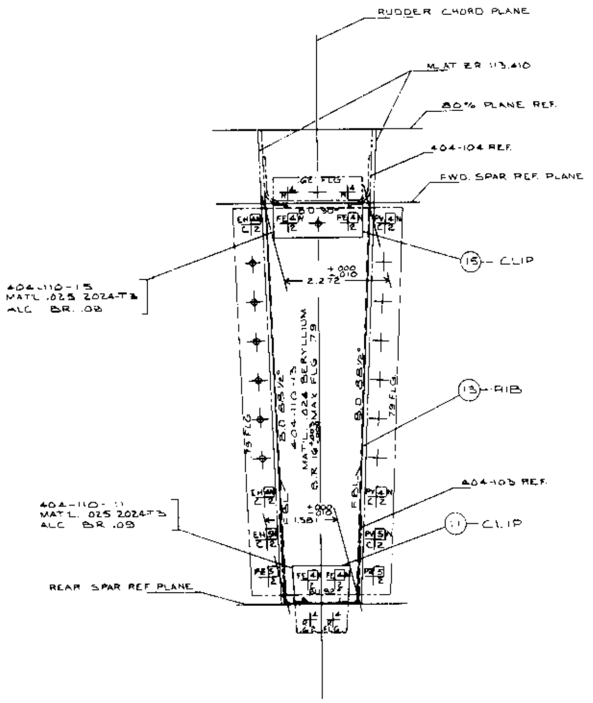

RUDDER CHORD PLANE
M.L AT ZR 113.410
80% PLANE REF.
404-104 REF.
FWD. SPAR REF. PLANE
15 - CLIP
404-110-15
MAT'L .025 2024-T3
ALC BR. .08
2.272 +.000/-.010
13 - RIB
404-110-13
MAT'L .024 BERYLLIUM
B.R. .16 MAX FLG .79
B.O. 88 1/2°
.79 FLG
404-103 REF.
11 - CLIP
404-110-11
MAT'L .025 2024-T3
ALC BR .09
1.581 +.000/-.010
REAR SPAR REF PLANE

-3 ASSY
VIEW LKG. DN.

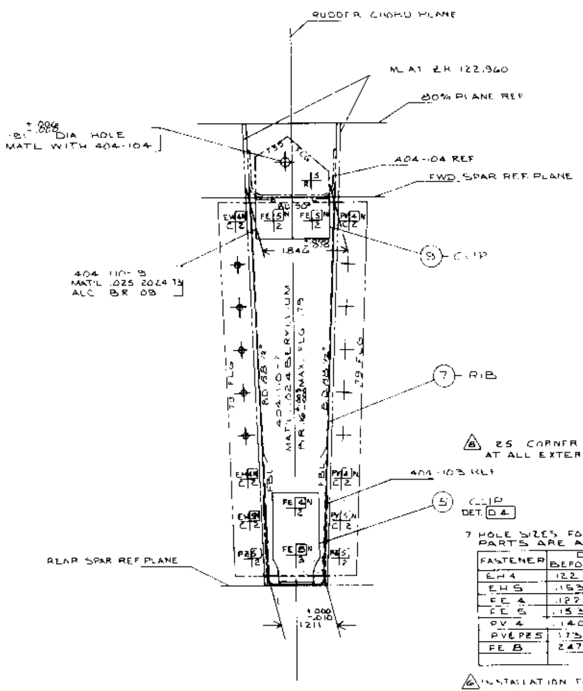

RUDDER CHORD PLANE
M.L AT ZR 122.960
80% PLANE REF
.81 +.006/-.000 DIA HOLE
MATL WITH 404-104
404-104 REF
FWD. SPAR REF PLANE
9 - CLIP
404-110-9
MAT'L .025 2024 T3
ALC BR .09
1.846
7 - RIB
404-110-7
MAT'L .024 BERYLLIUM
B.R. .16 MAX FLG .79
B.O. 88 1/2°
.79 FLG
404-103 REF
5 CLIP
DET. D4
REAR SPAR REF PLANE
1.211 +.000/-.010

-1 ASSY
VIEW LKG. DN.

NOTES.

1. FABRICATE BERYLLIUM PARTS PER MAC PS 14104 EXCEPT FOR FINAL ETCH (SEE NOTE 2.)
2. FINAL ETCH ALL BERYLLIUM PARTS .003 .004 TOTAL THICKNESS
3. INSTALL FASTENERS PER MAC PS 19000
4. PARTS MUST BE STRAIGHT AT THEIR BEND TANGENT LINE WITHIN .005 IN ANY 5 INCH LENGTH.
5. DO NOT VIBRATION DRIVE ANY FASTENER IN THIS STRUCTURE
6. INSTALLATION FASTENER
7. HOLE SIZES FOR FASTENERS IN BERYLLIUM PARTS ARE AS FOLLOWS.

FASTENER	DIA BEFORE ETCH	DIA AFTER ETCH
EH 4	.122 +.004/-.000	.125 +.003/-.000
EH 5	.153 +.003/-.000	.156 +.004/-.000
FE 4	.127 +.004/-.000	.125 +.003/-.000
FE 5	.153 +.003/-.000	.156 +.004/-.000
PV 4	.140 +.003/-.000	.143 +.003/-.000
PV & PZ 5	.173 +.003/-.000	.176 +.004/-.000
FE 8	.247 +.003/-.000	.250 +.003/-.000

8. .25 CORNER RADIUS OPTIONAL, EXCEPT AS NOTED AT ALL EXTERNAL CORNER SHOWN SHARP.

QTY -3	QTY -1	PART NUMBER	PART NAME	SIZE	MATERIAL	SPEC	ZONE
	1	3M91-8-3	HS RIVET				
	1	3M88-8	COLLAR				
1	1	3M267B 5-2	RIVET				
8	7	3M267B-4-2	RIVET				
1	3	3M88-5	COLLAR				
13	8	3M88-4	COLLAR				
	2	3M91-5-2	HS RIVET				
5	1	3M91-4-2	HS RIVET				
1	1	3M90-5-2	HS RIVET				
8	7	3M90-4-2	HS RIVET				
2	2	3M266B5-2	RIVET				
1		-15	CLIP	.025X1.30X2.00	2024 T3 ALC	QQ-A-362 COND-T3	E7
1		-13	RIB	.024X3.80X8.20	BERYLLIUM	MMS 191	C7
1		-11	CLIP	.025X1.30X1.45	2024 T3 ALC	QQ-A-362 COND-T3	B7
	1	-9	CLIP	.025X1.10X2.20	2024 T3 ALC	QQ-A-362 COND-T3	E5
	1	-7	RIB	.024X3.40X7.90	BERYLLIUM	MMS 191	C5
	1	-5	CLIP	1M5462 X1.60	7178-T6 AL	MIL-A-9186 COND-T6	B5
-3	-1						

LZ	[illegible]	PV	3M267B	PZ	3M266B
[illegible]	[illegible]		3M88 COLLAR		3M88 COLLAR
[illegible]	[illegible]	FE	3M91	FH	3M90
CODE	RIVET	CODE	RIVET	CODE	RIVET

404-110

404-102
404-102

CONTRACT NO AF 33(657)-2974

LOFT 2809

DRAWN E. FARK

MCDONNELL
ST. LOUIS, MISSOURI

RIBS-RUDDER ASSY
Z.R. 113.410 AND
Z.R. 122.960

CODE IDENT NO. 76301
SIZE J
404-110
SCALE FULL

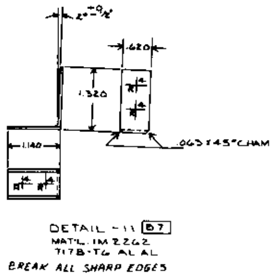
2° +0 -1/2°
.620
1.320
1.140
.063 x 45° CHAM

DETAIL -11 B7
MAT'L. 1M 2262
7178-T6 AL AL
BREAK ALL SHARP EDGES

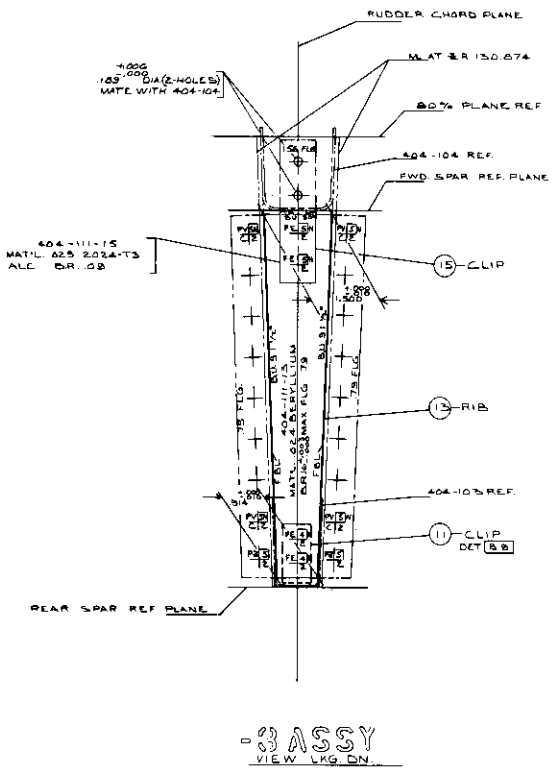
RUDDER CHORD PLANE
℄ AT ZR 130.874
.189 +.006 -.000 DIA.(2-HOLES) MATE WITH 404-104
80% PLANE REF
404-104 REF.
FWD. SPAR REF. PLANE
404-111-15
MAT'L .025 2024-T3
ALC. B.R. .08
15 CLIP
1.500 +.000 -.010
B.D. 91 1/2°
B.D. 91 1/2°
.75 FLG.
.79 FLG.
404-111-13
MAT'L .024 BERYLLIUM
B.R.16 +.003 -.000 MAX FLG .79
FBL
13 RIB
.914 +.000 -.010
404-103 REF.
11 CLIP DET B8
REAR SPAR REF PLANE
PV 5 N C 2
FE 5 N 2
FE 4 N 2
PZ 5 2

-3 ASSY
VIEW LKG. DN.

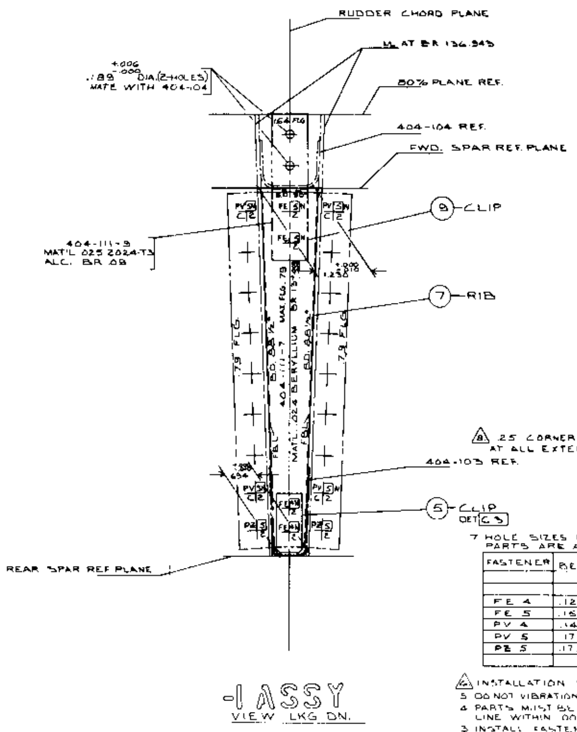
RUDDER CHORD PLANE
℄ AT ZR 136.943
.189 +.006 -.000 DIA.(2-HOLES) MATE WITH 404-104
80% PLANE REF.
404-104 REF.
FWD. SPAR REF. PLANE
9 CLIP
404-111-9
MAT'L .025 2024-T3
ALC. BR .08
1.250 +.000 -.010
7 RIB
.79 FLG.
.79 FLG.
404-111-7
MAT'L .024 BERYLLIUM
MAX FLG .79
B.D. 88 1/2°
FBL
.694 +.000 -.010
404-103 REF.
5 CLIP DET C3
REAR SPAR REF PLANE
PV 5 N C 2
FE 5 N 2
FE 4 N 2
PZ 5 2

-1 ASSY
VIEW LKG. DN.

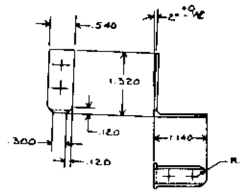
.540
2° +0 -1/2°
1.320
.120
.300
.120
1.140
R.

DETAIL -5 B4
MAT'L. 1M 2262
7178-T6 AL.AL.
BREAK ALL SHARP EDGES

B .25 CORNER RADIUS OPTIONAL, EXCEPT AS NOTED, AT ALL EXTERNAL CORNER SHOWN SHARP

7 HOLE SIZES FOR FASTENERS IN BERYLLIUM PARTS ARE AS FOLLOWS:

FASTENER	DIA. BEFORE ETCH	DIA. AFTER ETCH
FE 4	.122 +.004 -.000	.125 +.003 -.000
FE 5	.153 +.003 -.000	.156 +.006 -.000
PV 4	.140 +.003 -.000	.143 +.003 -.000
PV 5	.173 +.003 -.000	.176 +.004 -.000
PZ 5	.173 +.003 -.000	.176 +.004 -.000

6 INSTALLATION FASTENER

5 DO NOT VIBRATION DRIVE ANY FASTENER IN THIS STRUCTURE.

4 PARTS MUST BE STRAIGHT AT THEIR BEND TANGENT LINE WITHIN .005 IN ANY 5 INCH LENGTH

3 INSTALL FASTENERS PER MAC PS 19000

2 FINAL ETCH ALL BERYLLIUM PARTS .003-.004 TOTAL THICKNESS.

1 FABRICATE BERYLLIUM PARTS PER MAC PS 14104 EXCEPT FOR FINAL ETCH (SEE NOTE 2)

NOTES.

2	2	3M266B-5-2	RIVET				
16	16	3M267B-5-2	RIVET				
2	2	3M88-5	COLLAR				
2	2	3M88-4	COLLAR				
2	2	3M91-5-2	H.S RIVET				
2	2	3M91-4-2	H.S RIVET				
1		-15	CLIP	.025X.850X3.00	2024-T3 ALC	QQ-A-362 COND T3	C7
1		-13	RIB	.024X3.00X7.70	BERYLLIUM	MMS 191	C7
1		-11	CLIP	1M2262 X.650	7178-T6 AL	MIL-A-9186 COND T6	B7
	1	-9	CLIP	.025X.850X3.10	2024-T3 ALC	QQ-A-362 COND T3	C5
	1	-7	RIB	.024X2.80X7.65	BERYLLIUM	MMS 191	C5
	1	-5	CLIP	1M2262 X.550	7178-T6 AL	MIL-A-9186 COND T6	B5
-3	-1						

6 (3M266B-5-2, 3M267B-5-2, 3M88-5, 3M88-4, 3M91-5-2, 3M91-4-2)

B 2 1 (-15, -13, -11)

B 2 1 (-9, -7, -5)

LZ	NAS1097AD	PV	3M267B	PZ	3M266B
			3M88 COLLAR		
		FE	3M91		
CODE	RIVET	CODE	RIVET	CODE	RIVET

BASIC CODE | DASH NUMBER AND LOCATION OF MFG HEAD
SHEET PREPARATION | LENGTH DASH NUMBER

C = CSINK
N = NEAR SIDE
R = REFERENCE RIVET
☐ = INSTALLATION RIVET
D = DIMPLE
DC = DIMPLE TOP SHEET, CSINK LOWER SHEET
DDC = DIMPLE SHEETS 1 & 2, CSINK LOWER SHEET
F = FAR SIDE
NO. OF EQUAL SPACES

SAMPLE CALLOUT
AC 3 N / D 2
INSTALLATION RIVET
DIMPLE ALL SHEETS
INSTALL NEAR SIDE

MAC 333 RIVET CODE

404-111

PART/ASSY DASH NO. | CONFIG SYMBOL

NEXT ASSY	USED ON	
404-102		1 OF-3
404-102		1 OF-1

APPLICATION

LOFT DATA: LOFT 2809

CONTRACT NO. AF 33(615)-2974

DRAWN E. FARK

CHECK B.S.A.

MCDONNELL
ST. LOUIS, MISSOURI

RIBS - RUDDER ASSY.
ZR 136.943 AND
ZR 130.874

CODE IDENT NO. 76301 | SIZE J | 404-111

SCALE FULL | SHEET 1

404-111

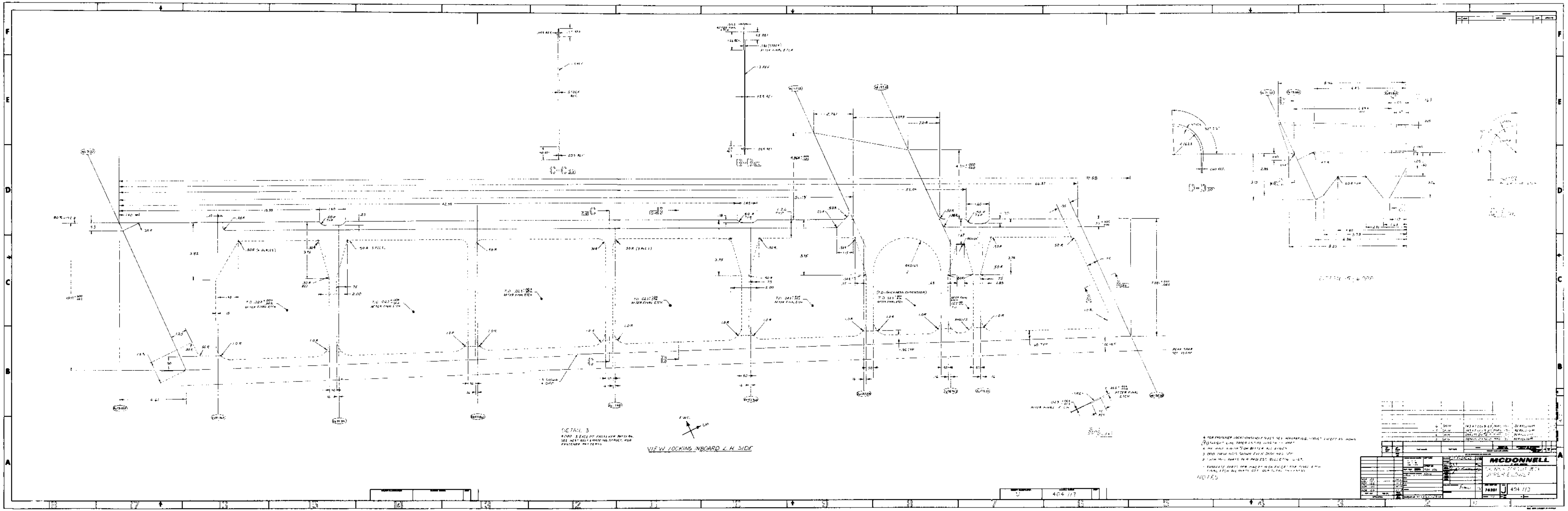
VIEW LOOKING INBOARD L.H. SIDE
DETAIL 3
FWD
UP
NOTES
MCDONNELL
76301
J
404 113
SKIN
BERYLLIUM

CALCULATED ANGLES
A: 1° 17' 53"

SYM	ZONE	REVISIONS DESCRIPTION	DATE	APPROVED

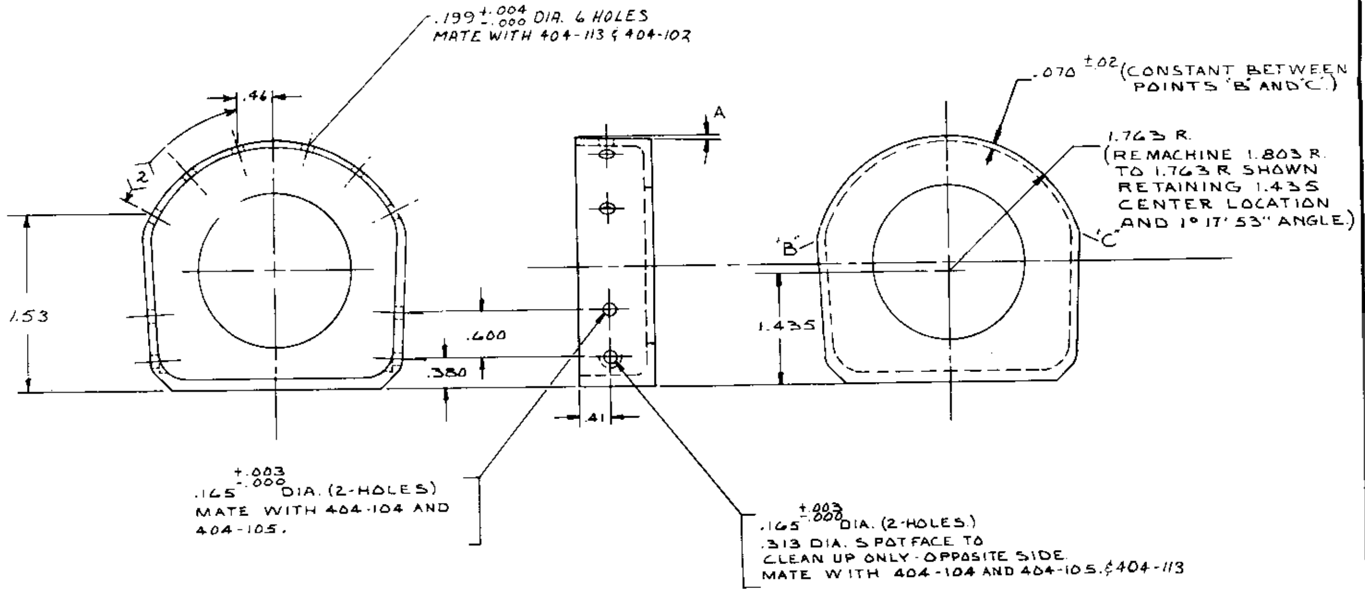
.199 +.004 -.000 DIA. 6 HOLES
MATE WITH 404-113 & 404-102
.46
2
1.53
.600
.380
.41
A
.070 ±.02 (CONSTANT BETWEEN POINTS 'B' AND 'C'.)
1.763 R.
(REMACHINE 1.803 R. TO 1.763 R SHOWN RETAINING 1.435 CENTER LOCATION AND 1° 17' 53" ANGLE.)
'B'
'C'
1.435
.165 +.003 -.000 DIA. (2-HOLES) MATE WITH 404-104 AND 404-105.
.165 +.003 -.000 DIA. (2-HOLES.)
.313 DIA. SPOTFACE TO CLEAN UP ONLY - OPPOSITE SIDE.
MATE WITH 404-104 AND 404-105. & 404-113

7. USE 32-24037-5 FINISH MACHINED PART WITHOUT HOLES AND REWORK AS SHOWN. ALL MACHINING DIMENSIONS NOT SHOWN ARE SAME AS 32-24037-5.
6. PART TO BE STRAIGHT WITHIN .016.
5. 100% PENETRANT INSPECTION PER MAC P.S. 21202.
4. ALL MACHINED SURFACES 250
3. MARKING PER MAC P.S. 16001.
2. SURFACE INSPECTION IN ACCORDANCE WITH MAC P.S. 23030.
1. BREAK ALL SHARP EDGES.

NOTES.

QTY REQD/ASSY	QTY REQD/ASSY	FIND NO.	PART NUMBER	PART NAME	STOCK / VENDOR NAME AND ADDRESS	MATERIAL OR MATERIAL CODE	GOVERNMENT OR COMMERCIAL MATERIAL SPECIFICATION / VENDOR CODE IDENT NO.	I/S	UNIT WT	ZONE
			-3	FITTING (MACH)	32-24037-5/7					

LIST OF MATERIALS OR PARTS LIST

NEXT ASSY	USED ON	FINAL ARTICLE QTY REQD
404-102		1 OF-3

APPLICATION

LIMITS UNLESS NOTED
.X = ±.1
.XX = ±.03
.XXX = ±.010

HEAT TREAT NOTED

LOFT DATA

LAYOUT NO.

FINISH SPECIFICATIONS
MAC 32-90000
USAF
USN
OTHER

CONTRACT NO. AF 33(615)-2974

DRAWN	E. FARK	9/65
TRACED		
CHECK	J. J. Andrews	12/7/65
STRESS		12/9/65
GROUP ENGR	L C Koch	12/9
ELEC ENGR		
MECH ENGR		
PROJECT ENGINEER	Finn	12/11/65
CUSTOMER		

MCDONNELL
ST. LOUIS, MISSOURI

FITTING - RUDDER
LEADING EDGE RIB.

CODE IDENT NO. 76301
SIZE C
404-114
SCALE FULL
WT ACT CAL
LB
SHEET

MAC 1180C (REV 23 APR 62)

DRAWING NUMBER 404-114

DATE PRINTED

404-114

EO INCORPORATION		
SERIAL NO.	SEQ. NO.	DCN LTR.

REVISIONS				
SYM	ZONE	DESCRIPTION	DATE	APPROVED

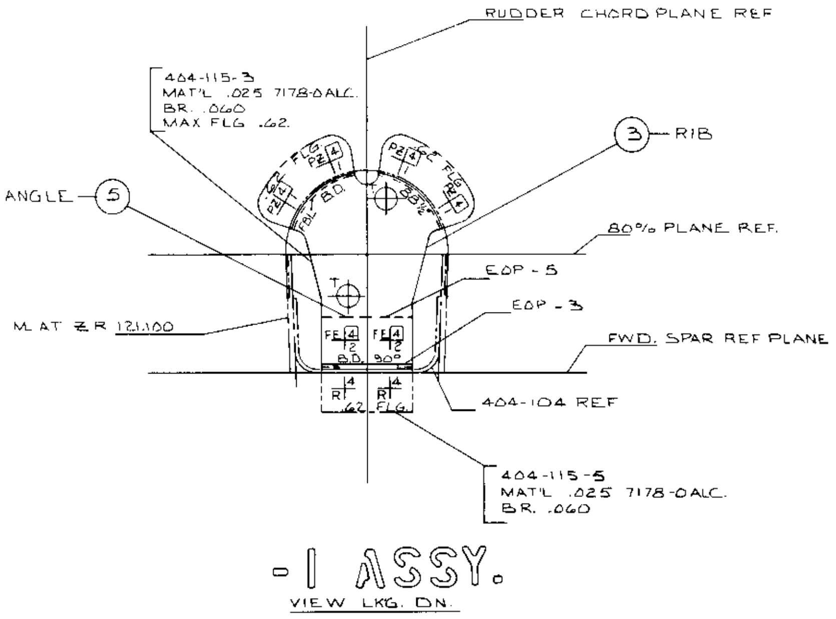
RUDDER CHORD PLANE REF
404-115-3
MAT'L .025 7178-0 ALC.
BR. .060
MAX FLG .62
3 RIB
ANGLE 5
80% PLANE REF.
EOP - 5
EOP - 3
M.L. AT ZR 121.100
FWD. SPAR REF PLANE
404-104 REF
404-115-5
MAT'L .025 7178-0 ALC.
BR. .060
FLG
PE 4
BD
FE 4
R 4
.62
80°
90°
FLG

-1 ASSY.

VIEW LKG. DN.

△7. INSTALLATION FASTENERS

6. NOMINAL EDGE DISTANCE FOR 1/8 INCH DIA. AND LARGER RIVETS EXCEPT HI-SHEAR = (2 DIA + .06) SHOP TOLERANCE ±.09 EXCEPT AS SHOWN.

5. BREAK ALL SHARP EDGES.

4. USE .25 RADIUS ON ALL CORNERS SHOWN ROUNDED.

3. MARKING PER MAC. PS. 16001.

2. BEND RADII PER 6M39.

△1. HEAT TREAT TO 7178-T6 PER MAC PS. 15529.

NOTE:

PART/ASSY DASH NO	V16
CONFIG. SYMBOL	
ML CONFIGURATION	

CODE	RIVET	CODE	RIVET	CODE	RIVET
L2	NAS1097AD	P2	3M266B		
BB	MS20426AD		3M88 COLLAR		
AJ	MS20470AD	FE	3M91		

NAS 523 RIVET CODE

BASIC CODE | DIA DASH NUMBER AND LOCATION OF MFD HEAD
SHEET PREPARATION | LENGTH DASH NUMBER

C = CSINK
C = CSINK FOR DOUBLE FLUSH HEAD
D = DIMPLE
DC = DIMPLE TOP SHEET, CSINK LOWER SHEET
DDC = DIMPLE SHEETS 1 & 2, CSINK LOWER SHEET
F = FAR SIDE
N = NEAR SIDE
R = REFERENCE RIVET
☐ = INSTALLATION RIVET
NO. OF EQUAL SPACES

SAMPLE CALLOUT
AC 5 N
D 2
MS20601 AD5-2 RIVET
INSTALLATION RIVET
DIMPLE ALL SHEETS
INSTALL NEAR SIDE

	QTY REQD/ASSY	QTY REQD/ASSY	PART NUMBER	PART NAME	STOCK	MATERIAL OR MATERIAL CODE	GOVERNMENT OR COMMERCIAL MATERIAL SPECIFICATION			ZONE
△7		4	3M266B-4-1	RIVET						
		2	3M88-4	COLLAR						
△7		2	3M91-4-2	H.S. RIVET						
△1		1	-5	ANGLE	.025 X 1.30 X 1.30	7178-0 ALC.	MIL-A-9183 COND-0			B5
		1	-3	RIB	.025 X 3.05 X 3.10	7178-0 ALC.	MIL-A-9183 COND-0			B4
		1								

LIST OF MATERIALS OR PARTS LIST

404-115

NEXT ASSY	USED ON	
404-102		1 OF -1

APPLICATION

UNITS UNLESS NOTED
.X = ±.1
.XX = ±.03
.XXX = ±.010

LOFT DATA LOFT 2801
J. HASSKAMP
8-11-65

LAYOUT NO.

HEAT TREAT (NOTED)

FINISH SPECIFICATIONS

MAC

USAF

USN

OTHER

CONTRACT NO. AF 33(615)-2974

DRAWN E. FARK
CHECK
PROJECT ENGINEER
CUSTOMER

MCDONNELL
ST. LOUIS, MISSOURI

LEADING EDGE
RIB - RUDDER

CODE IDENT NO. 76301

404-115

SCALE FULL

SHEET 1

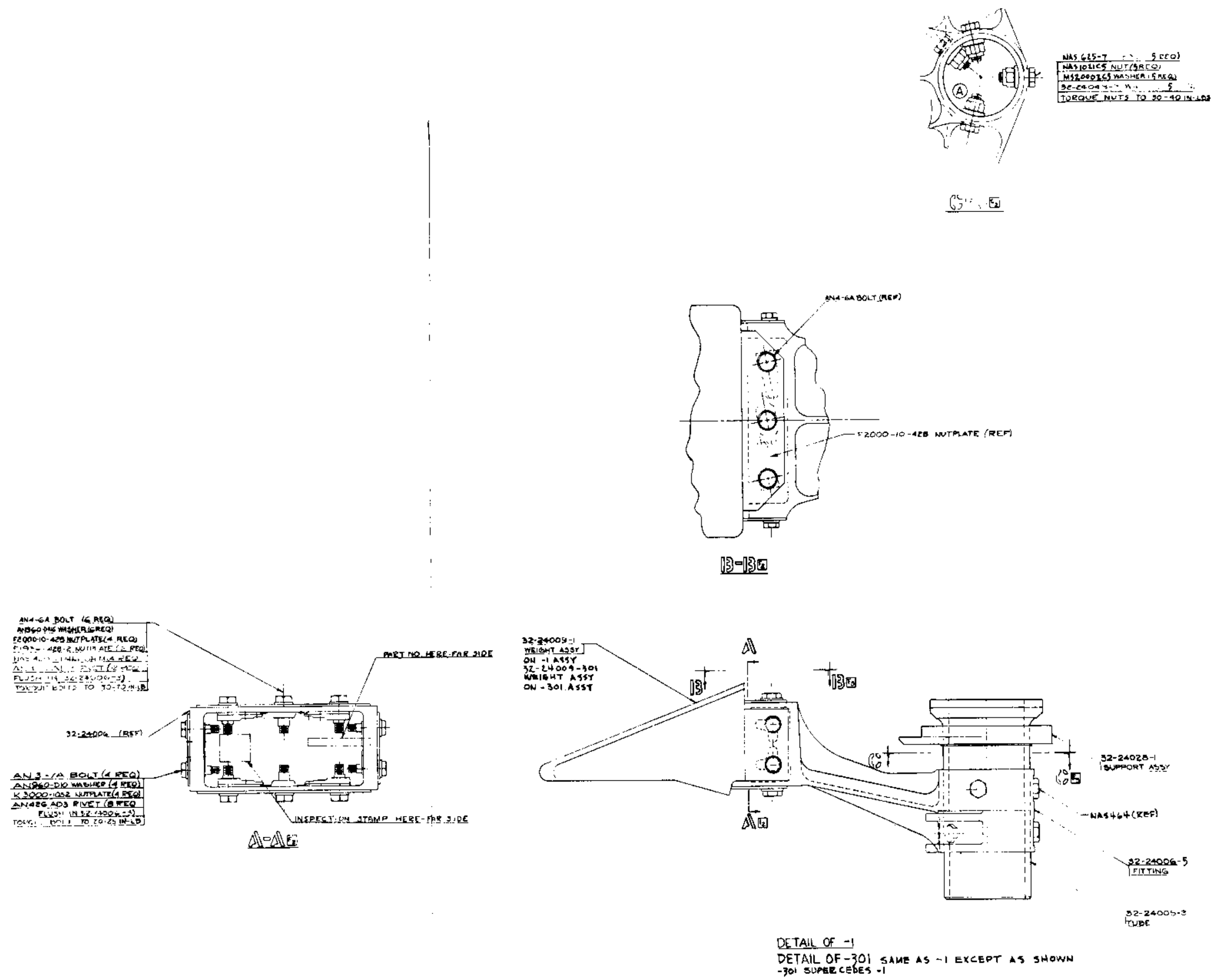
NAS 625-7 [illegible] (5 REQ)
NAS1021C5 NUT (5 REQ)
MS20002C5 WASHER (5 REQ)
32-24043-5 WASHER (5 REQ)
TORQUE NUTS TO 30-40 IN-LBS
Ⓐ
C-C E2
AN4-6A BOLT (REF)
F2000-10-428 NUTPLATE (REF)
B-B E2
AN4-6A BOLT (6 REQ)
AN960-D416 WASHER (6 REQ)
F2000-10-428 NUTPLATE (4 REQ)
F1934-428-2 NUTPLATE (2 REQ)
NAS463Y-004 SHIM (4 REQ)
AN426AD3 RIVET (12 REQ)
FLUSH IN 32-24006-5)
TORQUE BOLTS TO 50-70 IN-LB
PART NO. HERE-FAR SIDE
32-24006 (REF)
AN3-7A BOLT (4 REQ)
AN960-D10 WASHER (4 REQ)
K3000-1032 NUTPLATE (4 REQ)
AN426AD3 RIVET (8 REQ)
FLUSH IN 32-24006-5)
TORQUE BOLT TO 20-25 IN-LB
INSPECTION STAMP HERE-FAR SIDE
A-A E2
32-24009-1
WEIGHT ASSY
ON -1 ASSY
32-24009-301
WEIGHT ASSY
ON -301 ASSY
A
B
B E2
A E2
C
C E5
32-24028-1
SUPPORT ASSY
NAS464 (REF)
32-24006-5
FITTING
32-24005-3
TUBE

DETAIL OF -1

DETAIL OF -301 SAME AS -1 EXCEPT AS SHOWN
-301 SUPERCEDES -1

4	4	NAS463Y-004	SHIMS			I2
4	4	AN960-D10	WASHER			I2
6	6	AN960-D416	WASHER			I6
2	2	F1934-428-2	NUT, ANCHOR	KAYNAR MFG CO, PICO-RIVERA, CALIF. [illegible]	75537	I2
4	4	F2000-10-428	"	"	"	E6
4	4	K3000-1032	NUT, ANCHOR	KAYNAR MFG CO, PICO-RIVERA, CALIF. [illegible]	75537	I2
5	5	NAS1021C5	NUT			E5
4	4	AN3-7A	BOLT			
5	5	NAS625-7	BOLT			
6	6	AN4-6A	BOLT			
5	5	MS20002C5	WASHER			
6	6	32-24043-5	WASHER			E5
1	1	32-24028-1	SUPPORT ASSY			E7
	1	32-24009-1	WEIGHT ASSY			G2
1	1	32-24006-5	FITTING			E2
1	1	32-24005-3	TUBE			E2
1		32-24009-301	WEIGHT ASSY			
-301	-1	PART NO.	NAME			

-1		-301	
SUPERSEDED UNIT	EFF. NOTE	SUPERSEDING UNIT	EFF. NOTE
SUPERSEDENCE TABLE			

4. INSTALL FASTENERS PER MAC PS. 19000.
3. LAST SECTION LETTER USED C-C
2. NOMINAL EDGE DISTANCE FOR 3/32 DIA. RIVETS = .26; SHOP TOL [illegible]
1. MARKING PER MAC PS. 16001

NOTES

32-24004

32-011007
HANCOCK
32-90006
FULL
32-24001
32-24001

SUPPORT ASSY –
BALANCE WEIGHT & HORN

McDONNELL
Aircraft Corporation

32-24004

DRAWN BY N.A.I.

UNCLASSIFIED
Security Classification

DOCUMENT CONTROL DATA - R&D

(Security classification of title, body of abstract and indexing annotation must be entered when the overall report is classified)

1. ORIGINATING ACTIVITY *(Corporate author)*
THE MCDONNELL COMPANY
ST. LOUIS, MISSOURI

2a. REPORT SECURITY CLASSIFICATION
UNCLASSIFIED

2b. GROUP
N/A

3. REPORT TITLE
Design, Fabrication, and Ground Testing of the F-4 Beryllium Rudder

4. DESCRIPTIVE NOTES *(Type of report and inclusive dates)*
Final Report June 1965 - January 1967

5. AUTHOR(S) *(Last name, first name, initial)*
Finn, Joseph M.
Koch, Leland C.
Muehlberger, Donald E.

6. REPORT DATE
April 1967

7a. TOTAL NO. OF PAGES

7b. NO. OF REFS

8a. CONTRACT OR GRANT NO. AF33(615)-2974

b. PROJECT NO. 1368

c. Task No. 136806

d.

9a. ORIGINATOR'S REPORT NUMBER(S)

9b. OTHER REPORT NO(S) *(Any other numbers that may be assigned this report)*
N/A

10. AVAILABILITY/LIMITATION NOTICES

Each transmittal of this document outside the agencies of the U. S. Government must have prior approval of the Air Force Flight Dynamics Laboratory, FDTS, Research and Technology Division, W-PAFB, Ohio 45433

11. SUPPLEMENTARY NOTES
None

12. SPONSORING MILITARY ACTIVITY
Flight Dynamics Laboratory (FDTS)
Research and Technology Division
Wright-Patterson AFB, Ohio 45433

13. ABSTRACT

A program was performed for the advancement of structural beryllium technology through the design, fabrication, test and evaluation of a load-carrying aircraft component to demonstrate a potential for increased capability and efficiency through use of beryllium. The component selected for the performance of this program was the rudder of the McDonnell F-4 aircraft. The beryllium rudder was designed, analyzed, fabricated, and successfully ground tested to the same loading conditions and criteria that apply to the production aluminum rudder. An extensive element test program was conducted to obtain material properties and design data not previously available, and formulate design criteria for beryllium structures. The beryllium rudder weighs 37.59 lbs. (17.05 kg) as compared to 63.03 lbs. (28.59 kg) for the production aluminum rudder and is completely interchangeable with it.

Upon completion of fabrication, the beryllium rudder was installed on the F-4 vertical fin and aft fuselage assembly and subjected to one fatigue test and three static tests. Prior to conducting the static tests, the beryllium rudder upper balance weight was successfully fatigue tested for 50,000 cycles under a fully reversed loading corresponding to 40 g's on the balance weight as required by the aircraft detail specification.

Distribution of this abstract is unlimited.

DD FORM 1 JAN 64 **1473**

UNCLASSIFIED
Security Classification

14. KEY WORDS	LINK A		LINK B		LINK C	
	ROLE	WT	ROLE	WT	ROLE	WT
Airframes, Aircraft Structures, Structural Design, Beryllium, Beryllium Fabrication, Airframe Component Production, Light Weight Alloys						

INSTRUCTIONS

1. ORIGINATING ACTIVITY: Enter the name and address of the contractor, subcontractor, grantee, Department of Defense activity or other organization *(corporate author)* issuing the report.

2*a*. REPORT SECURITY CLASSIFICATION: Enter the overall security classification of the report. Indicate whether "Restricted Data" is included. Marking is to be in accordance with appropriate security regulations.

2*b*. GROUP: Automatic downgrading is specified in DoD Directive 5200.10 and Armed Forces Industrial Manual. Enter the group number. Also, when applicable, show that optional markings have been used for Group 3 and Group 4 as authorized.

3. REPORT TITLE: Enter the complete report title in all capital letters. Titles in all cases should be unclassified. If a meaningful title cannot be selected without classification, show title classification in all capitals in parenthesis immediately following the title.

4. DESCRIPTIVE NOTES: If appropriate, enter the type of report, e.g., interim, progress, summary, annual, or final. Give the inclusive dates when a specific reporting period is covered.

5. AUTHOR(S): Enter the name(s) of author(s) as shown on or in the report. Enter last name, first name, middle initial. If military, show rank and branch of service. The name of the principal author is an absolute minimum requirement.

6. REPORT DATE: Enter the date of the report as day, month, year; or month, year. If more than one date appears on the report, use date of publication.

7*a*. TOTAL NUMBER OF PAGES: The total page count should follow normal pagination procedures, i.e., enter the number of pages containing information.

7*b*. NUMBER OF REFERENCES: Enter the total number of references cited in the report.

8*a*. CONTRACT OR GRANT NUMBER: If appropriate, enter the applicable number of the contract or grant under which the report was written.

8*b*, 8*c*, & 8*d*. PROJECT NUMBER: Enter the appropriate military department identification, such as project number, subproject number, system numbers, task number, etc.

9*a*. ORIGINATOR'S REPORT NUMBER(S): Enter the official report number by which the document will be identified and controlled by the originating activity. This number must be unique to this report.

9*b*. OTHER REPORT NUMBER(S): If the report has been assigned any other report numbers *(either by the originator or by the sponsor)*, also enter this number(s).

10. AVAILABILITY/LIMITATION NOTICES: Enter any limitations on further dissemination of the report, other than those imposed by security classification, using standard statements such as:

(1) "Qualified requesters may obtain copies of this report from DDC."

(2) "Foreign announcement and dissemination of this report by DDC is not authorized."

(3) "U. S. Government agencies may obtain copies of this report directly from DDC. Other qualified DDC users shall request through
________________________________."

(4) "U. S. military agencies may obtain copies of this report directly from DDC. Other qualified users shall request through
________________________________."

(5) "All distribution of this report is controlled. Qualified DDC users shall request through
________________________________."

If the report has been furnished to the Office of Technical Services, Department of Commerce, for sale to the public, indicate this fact and enter the price, if known.

11. SUPPLEMENTARY NOTES: Use for additional explanatory notes.

12. SPONSORING MILITARY ACTIVITY: Enter the name of the departmental project office or laboratory sponsoring *(paying for)* the research and development. Include address.

13. ABSTRACT: Enter an abstract giving a brief and factual summary of the document indicative of the report, even though it may also appear elsewhere in the body of the technical report. If additional space is required, a continuation sheet shall be attached.

It is highly desirable that the abstract of classified reports be unclassified. Each paragraph of the abstract shall end with an indication of the military security classification of the information in the paragraph, represented as *(TS)*, *(S)*, *(C)*, or *(U)*.

There is no limitation on the length of the abstract. However, the suggested length is from 150 to 225 words.

14. KEY WORDS: Key words are technically meaningful terms or short phrases that characterize a report and may be used as index entries for cataloging the report. Key words must be selected so that no security classification is required. Identifiers, such as equipment model designation, trade name, military project code name, geographic location, may be used as key words but will be followed by an indication of technical context. The assignment of links, roles, and weights is optional.